Journal of Amino Acids

Bioactive Peptides in Cancer: Therapeutic Use and Delivery Strategies

Guest Editors: Paola Stiuso, Michele Caraglia, Giuseppe De Rosa, and Antonio Giordano

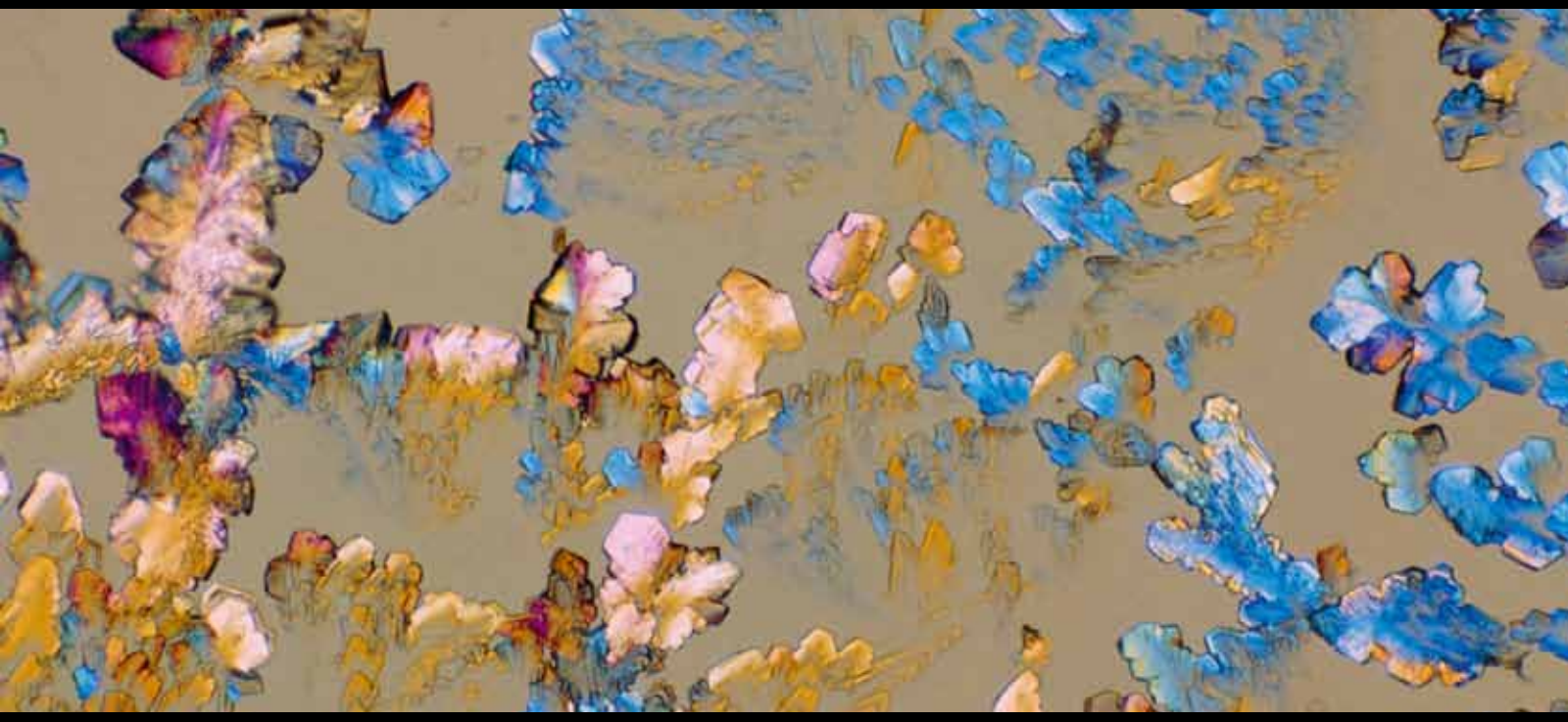

Bioactive Peptides in Cancer: Therapeutic Use and Delivery Strategies

Journal of Amino Acids

Bioactive Peptides in Cancer: Therapeutic Use and Delivery Strategies

Guest Editors: Paola Stiuso, Michele Caraglia, Giuseppe De Rosa, and Antonio Giordano

Editorial Board

Contents

Bioactive Peptides in Cancer: Therapeutic Use and Delivery Strategies, Paola Stiuso, Michele Caraglia, Giuseppe De Rosa, and Antonio Giordano
Volume 2013, Article ID 568953, 2 pages

DTNQ-Pro, a Mimetic Dipeptide, Sensitizes Human Colon Cancer Cells to 5-Fluorouracil Treatment, Isabel Gomez-Monterrey, Pietro Campiglia, Ilaria Scognamiglio, Daniela Vanacore, Alessandra Dicitore, Angela Lombardi, Michele Caraglia, Ettore Novellino, and Paola Stiuso
Volume 2013, Article ID 509056, 7 pages

Amino Acid Derivatives as New Zinc Binding Groups for the Design of Selective Matrix Metalloproteinase Inhibitors, Mariateresa Giustiniano, Paolo Tortorella, Mariangela Agamennone, Antonella Di Pizio, Armando Rossello, Elisa Nuti, Isabel Gomez-Monterrey, Ettore Novellino, Pietro Campiglia, Ermelinda Vernieri, Marina Sala, Alessia Bertamino, and Alfonso Carotenuto
Volume 2013, Article ID 178381, 12 pages

Potential Anticarcinogenic Peptides from Bovine Milk, Giacomo Pepe, Gian Carlo Tenore, Raffaella Mastrocinque, Paola Stusio, and Pietro Campiglia
Volume 2013, Article ID 939804, 7 pages

Design, Synthesis, and Evaluation of New Tripeptides as COX-2 Inhibitors, Ermelinda Vernieri, Isabel Gomez-Monterrey, Ciro Milite, Paolo Grieco, Simona Musella, Alessia Bertamino, Ilaria Scognamiglio, Stefano Alcaro, Anna Artese, Francesco Ortuso, Ettore Novellino, Marina Sala, and Pietro Campiglia
Volume 2013, Article ID 606282, 7 pages

Urotensin-II Ligands: An Overview from Peptide to Nonpeptide Structures, Francesco Merlino, Salvatore Di Maro, Ali Munaim Yousif, Michele Caraglia, and Paolo Grieco
Volume 2013, Article ID 979016, 15 pages

The Antitumor Peptide CIGB-552 Increases COMMD1 and Inhibits Growth of Human Lung Cancer Cells, Julio R. Fernández Massó, Brizaida Oliva Argüelles, Yelaine Tejeda, Soledad Astrada, Hilda Garay, Osvaldo Reyes, Livan Delgado-Roche, Mariela Bollati-Fogolín, and Maribel G. Vallespí
Volume 2013, Article ID 251398, 13 pages

Cancer Treatment Using Peptides: Current Therapies and Future Prospects, Jyothi Thundimadathil
Volume 2012, Article ID 967347, 13 pages

Hindawi Publishing Corporation
Journal of Amino Acids
Volume 2013, Article ID 568953, 2 pages
http://dx.doi.org/10.1155/2013/568953

Editorial

Bioactive Peptides in Cancer: Therapeutic Use and Delivery Strategies

Paola Stiuso,[1] Michele Caraglia,[1] Giuseppe De Rosa,[2] and Antonio Giordano[3]

[1] *Department of Biochemistry Biophysics and General Pathology, Second University of Naples, Via L. De Crecchio 7, 80138 Napoli, Italy*
[2] *Department of Pharmacy, University of Naples Federico II, Via Montesano, 80131 Naples, Italy*
[3] *Sbarro Institute for Cancer Research and Molecular Medicine, Temple University, Philadelphia, PA 19122, USA*

Correspondence should be addressed to Paola Stiuso; paola.stiuso@unina2.it

Received 11 April 2013; Accepted 11 April 2013

Human cancer is one of the most important causes of death in western and industrialized countries. In advanced stages, therapeutic opportunities are still limited due to the difficulty to target specifically only cancer cells sparing healthy ones. Cancer often has specific molecular alterations of signal transduction pathway or of other molecules linked to the proliferation and wide spreading of tumour cells. Several peptides have been isolated from natural products and/or physiological sources and several of them have biological activity on cancer cells. This special issue addresses the role of these natural peptides and of their synthetic derivatives in cancer therapy, alone or in combination with other anticancer agents.

One of the most interesting peptides of natural origin is Urotensin-II (U-II) originally isolated from the goby urophysis and subsequently identified in humans. It binds a specific receptor (UTR) that mediates a very strong contraction of vessel muscle cells. In particular, since the modulation of the U-II system offers a great potential for therapeutic strategies related to the treatment of several diseases, like cardiovascular diseases, the research of selective and potent ligands at UTR is more fascinating. Finally, it was recently reported by several groups a potential role of U-II and its receptor in the regulation of cancer biology. The paper by F. Merlino et al. discusses peptide and nonpeptide U-II and UTR structures that have led to a more rational and detectable design and synthesis of new molecules with high affinity for UTR. Other peptides with anticancer properties are peptide hormones acting on the pituitary axis in the treatment of endocrinological cancers such as breast and prostate cancer and peptides acting on neuroendocrine receptors such as somatostatin and BN/GRP (bombesin/gastrin-releasing peptide). The paper by J. Thundimadathil discussed the role of luteinizing hormone-releasing hormone (LHRH) agonists and antagonists and on the possible action of somatostatin analogues as radioisotope or cytotoxic drug carriers in the treatment of somatostatin receptor expressing tumours. Finally, the possible use of peptides in cancer vaccine or anti-angiogenic strategies is also described.

Food is another important source for proteins and peptides with potential anticancer activity. Bovine milk is an important component of the human diet, and it contains several proteins formed by two major families: caseins (insoluble) and whey proteins (soluble). The latter are β-lactoglobulin, α-lactalbumin, bovine serum albumin, and lactoferrin while the predominant forms of the caseins in ruminant milk are αS1, αS2, β, and κ. The paper by Pepe et al. describes the main evidences on the anticancer activity of some of these proteins on human cancer cell cultures. Another important function of certain peptides in cancer cell biology is the potential interference with the oxidative processes that are, in turn, strictly implicated in the occurrence and progression of cancer. In this light, cyclooxygenase (COX) is a key enzyme in the biosynthetic pathway leading to the formation of prostaglandins, which are mediators of inflammation and oxidative stress. It exists mainly in

two isoforms COX-1 and COX-2, with the latter being more expressed in cancer cells than in normal counterparts. Therefore, agents that inhibit COX-2 while sparing COX-1 represent a new attractive therapeutic development and offer a new perspective for a further use of COX-2 inhibitors. The paper by Vernieri et al. describes the design of new tripeptide inhibitors of COX-2 with, in some cases, a potent and selective inhibitory activity of the enzymatic function of COX-2. These peptides are, therefore, promising as anticancer agents. Another peptide that has demonstrated to be a strong modulator of the stress response is a quinone-based mimetic dipeptide, named DTNQ-Pro. It has been previously reported to induce differentiation of growing Caco-2 cells through inhibition of heat shock proteins (HSPs) 70 and 90. The paper by Gomez-Monterrey et al. has evaluated whether a decrease of stress proteins induced by DTNQ-Pro in Caco-2 cells could sensitize them to treatment with 5-fluorouracil (5-FU). The pretreatment of Caco-2 with DTNQ-Pro increases lipid peroxidation and decreases expression of p38 mitogen-activated protein kinase (MAPK) and FOXO3a. At the same experimental conditions, an increase of the 5-FU-induced growth inhibition of Caco2 cells was recorded. These effects could be due to enhanced DTNQ-Pro-induced membrane lipid peroxidation that, in turn, causes the sensitization of cancer cells to the cytotoxicity mediated by 5-FU. Again the modulation of oxidative stress by a peptide could be a way to sensitize cancer cells to cytotoxic antitumour agents such as 5-FU. Similarly, the second-generation peptide (CIGB-552) described in the paper by Fernández Massò et al. increases the levels of COMMD1, a protein involved in copper homeostasis, sodium transport, and NF-κB signaling pathway. These effects were recorded together with the decrease of the antioxidant capacity of cancer cells paralleled by proteins and lipids peroxidation. This study provides new insights into the mechanism of action of the peptide CIGB-552, which could be relevant in the design of future anticancer therapies.

Tumour microenvironment is becoming even more important in the regulation and sustainment of cancer cell growth. In this light, matrix metalloproteinases (MMPs) are important medicinal targets for cancer invasion and metastasis, where they showed to have a dual role, inhibiting or promoting important processes involved in the pathology. MMPs contain a zinc (II) ion in the protein active site. Tortorella et al. have designed small-molecule inhibitors of these metalloproteins that bind directly to the active site containing metal ions. In this paper, they describe the synthesis and preliminary biological evaluation of amino acid derivatives as new zinc binding groups (ZBGs). The incorporation of selected metal-binding functions in more complex biphenyl sulfonamide moieties allows the identification of a compound able to interact selectively with different MMP enzymatic isoforms. These results disclose new potential strategies to inhibit cancer metastasization processes.

In conclusion, the present special issue represents, in our opinion, an exciting, insightful observation into the state of the art, as well as emerging future topics, in this important interdisciplinary field. Peptides and proteins of natural sources and their synthetic derivatives can represent an important armamentarium with still unexplored potentials in the treatment of human cancers. The research in this specific field is strongly warranted in order to optimize cancer therapy and in order to increase the hopefully requests of the cancer patients.

Paola Stiuso
Michele Caraglia
Giuseppe De Rosa
Antonio Giordano

Hindawi Publishing Corporation
Journal of Amino Acids
Volume 2013, Article ID 509056, 7 pages
http://dx.doi.org/10.1155/2013/509056

Research Article

DTNQ-Pro, a Mimetic Dipeptide, Sensitizes Human Colon Cancer Cells to 5-Fluorouracil Treatment

Isabel Gomez-Monterrey,[1] Pietro Campiglia,[2] Ilaria Scognamiglio,[3] Daniela Vanacore,[3] Alessandra Dicitore,[4] Angela Lombardi,[3] Michele Caraglia,[3] Ettore Novellino,[1] and Paola Stiuso[3]

[1] *Department of Pharmaceutical and Toxicological Chemistry, University of Naples Federico II, Naples, Italy*
[2] *Department of Pharmaceutical Sciences, University of Salerno, Fisciano, Salerno, Italy*
[3] *Department of Biochemistry, Biophysics and General Pathology, Second University of Naples, Naples, Italy*
[4] *Italian Institute for Auxology, IRCC, 20145 Milan, Italy*

Correspondence should be addressed to Paola Stiuso; paola.stiuso@unina2.it

Received 1 February 2013; Accepted 27 March 2013

Academic Editor: Giuseppe De Rosa

The resistance of growing human colon cancer cells to chemotherapy agents has been correlated to endogenous overexpression of stress proteins including the family of heat shock proteins (HSPs). Previously, we have demonstrated that a quinone-based mimetic dipeptide, named DTNQ-Pro, induced differentiation of growing Caco-2 cells through inhibition of HSP70 and HSP90. In addition, our product induced a HSP27 and vimentin intracellular redistribution. In the present study, we have evaluated whether a decrease of stress proteins induced by DTNQ-Pro in Caco-2 cells could sensitize these cells to treatment with 5-fluorouracil (5-FU) cytotoxicity. The pretreatment of Caco-2 with 500 nM of DTNQ-Pro increases lipid peroxidation and decreases expression of p38 mitogen-activated protein kinase (MAPK) and FOXO3a. At the same experimental conditions, an increase of the 5-FU-induced growth inhibition of Caco-2 cells was recorded. These effects could be due to enhanced DTNQ-Pro-induced membrane lipid peroxidation that, in turn, causes the sensitization of cancer cells to the cytotoxicity mediated by 5-FU.

1. Introduction

Adenocarcinoma cells, such as colorectal cancer (CRC) cells, are remarkably resistant to radiation or chemotherapy-induced damage. As a consequence, the tumours are hard to treat and often proliferate rapidly, even under conditions that may adversely affect normal cells. For several years, 5-fluorouracil (5-FU), a pyrimidine antimetabolite, has been the drug of choice for the treatment of CRC as well as head and neck, pancreatic, and breast carcinomas. 5-FU is known to block DNA synthesis by the inhibition of thymidylate synthase (TS), which is regulated by cell cycle proteins controlled by phosphorylation [1]. Unfortunately, many of the schedules based upon 5-FU alone or in combination with other agents become ineffective during the course of the treatment due to the occurrence of drug resistance to 5-FU. Between several survival pathways activated in cancer cells to antagonize the antiproliferative activities of antineoplastic agents [2–4]. The mechanisms underlying the survival advantage can also be partially related to the increased expression of stress proteins [5, 6]. In fact, in contrast to normal cells, the basal levels of inducible heat shock proteins (HSPs) are frequently higher in tumour cells [7, 8]. The high expression of members of the HSP family in CRC cells has been associated with both metastases and resistance to chemotherapy. Moreover, in experimental models, HSP27 and HSP70 have been shown to increase tumorigenicity of cancer cells, and HSP depletion can induce a spontaneous regression of the tumour [9–11]. Recent data provide direct evidence on the association between HSP27 protein expression levels and 5-FU sensitivity in Caco-2 cells. In fact, the suppression of HSP27 expression in these cells may promote 5-FU sensitivity by inducing apoptosis, despite the acceleration in 5-FU metabolism [12].

HSP27 has been also implicated in a wide range of cell functions including cell protection, differentiation, and cell proliferation [13–15]. Moreover, HSPs are often associated with specific lipids or particular membrane areas (such as lipid rafts). In this light, changes of membrane physical state alter HSP gene expression [16–18]. The correlation between HSPs and control of cell proliferation is demonstrated by the fact that they are targets of important cell growth regulators such as mitogen-activated protein kinases (MAPKs) [19]. Moreover, the latter can be modulated by HSP multichaperone complex that protects MAPKs from proteasome-mediated degradation [20]. In addition, it has been reported that the inhibition of the multichaperone complex can sensitize cancer cells to agents raised against ERK-mediated pathways [21].

In mammalian cells, there are three well-characterized subfamilies of MAPKs: the extracellular signal-regulated kinases (ERK), the c-Jun N-terminal kinases (JNK, also known as the stress-activated protein kinases), and the p38 MAPK kinases. Each MAPK is activated through a specific phosphorylation cascade. ERK pathway is activated in response to growth factors, conferring a survival advantage on cells [22]. In contrast, JNK and p38 MAPK are activated in response to a variety of environmental stressors and inflammatory cytokines, which are frequently associated with the induction of apoptosis [23, 24]. Moreover, it was demonstrated that the p38 MAPK-Hsp27 axis plays an essential role in cancer stem cells-mediated Cis-platinum resistance in oral cancer [25]. Therefore, the development of specific modulators of HSP expression could be desirable either to shed further light on the functional roles of these important proteins in cell survival and in cell death or to further develop new clinically useful antitumour drugs.

In our previous report [26], we have demonstrated that DTNQ-Pro, a quinone-based pentacyclic derivative, modulated cellular redox status inducing cell cycle arrest and differentiation and, finally, driving cells to programmed cell death. Moreover, after 48 h of DTNQ-Pro treatment a decrease of mitochondrial superoxide anion induced by manganese superoxide dismutase (MnSOD) was recorded in Caco-2 cells. This effect was followed by a subsequent decrease of HSP70 expression and an increased membrane lipid peroxidation. The oxidative damage of the membrane induced a redistribution of both HSP27 and vimentin and forced Caco-2 cells to differentiate into enterocytes. On the other hand, the second treatment with DTNQ-Pro activated the apoptotic pathway. The ability of DTNQ-Pro to shift the undifferentiated Caco-2 cells to differentiated enterocytes and then undergo a process of programmed cell death strongly suggests that this compound should be additionally investigated for its potential use in new combination chemotherapy for colon cancer. The goal of the present study was to determine if the pretreatment with DTNQ-Pro can modulate the cytotoxic response of Caco2 cells to fluorouracil (5-FU) and assess the potential mechanisms underlying such modulation. In this report, we showed that increased Caco-2 cell differentiation by pretreatment with DTNQ-Pro enhanced the cytotoxic response of human colon carcinoma cells to 5-FU by modulating the expression of molecules that are associated with either drug sensitivity or resistance.

2. Material and Methods

2.1. Cell Cultures. Human colon adenocarcinoma Caco-2 cells (American Type Culture Collection, Rockville, MD, USA) were grown at 37°C in h-glucose MEM containing: 1% (by vol) nonessential amino acids and supplemented with 10% (by vol) decomplemented fetal bovine serum (FBS) (Flow, McLean, VA, USA), 100 $U \cdot mL^{-1}$ penicillin, 100 $mg \cdot mL^{-1}$ streptomycin, 1% L-glutamine, and 1% sodium pyruvate. Cells were grown in six multiwell plates (17–21 passages) in a humidified atmosphere of 95% air/5% CO_2 at 37°C. After incubation for 4 h in Dulbecco's modified Eagle's medium (DMEM) with 10% FBS, the cells were washed with 1% phosphate-buffered saline (PBS) to remove unattached dead cells and were incubated with 500 nM concentration of DTNQ-Pro for 48 h (D-Caco-2). All experiments were performed in triplicate.

2.2. Evaluation of Growth Inhibition of D-Caco-2 Cells. We assessed the sensitivity of the to 5-FU using a microplate colorimetric assay that measures the ability of viable cells to transform a soluble tetrazolium salt (MTT) [27] to an insoluble purple formazan precipitate. D-Caco-2 cells were plated at the appropriate density in 96-well microtitre plates. After 4 h, cells were exposed to different concentration (0–200 μM) of 5-FU for 48 h. 50 mL of MTT (1 $mg \cdot mL^{-1}$) and 200 mL of medium were added to the cells in each well. After a 4 h incubation at 37°C, the medium was removed; then the formazan crystals were solubilized by adding 150 mL of DMSO and by mixing it in an orbital shaker for 5 min. Absorbance at 550 nm was measured using a plate reader. Experiments were performed in triplicate. The percent inhibition of the treated cells was calculated by the following formula:

$$\% \text{ Inhibition} = \frac{A_{550} \text{ treated}}{A_{550} \text{ CTR}}. \quad (1)$$

2.2.1. Alkaline Phosphatase (ALP) Activity Evaluation. ALP activity was used as marker of the degree of differentiation of D-Caco-2 cells. Attached and floating cells were washed and lysed with 0.25% sodium deoxycholate, essentially as described by Herz et al. [28]. ALP activity was determined using Sigma Diagnostics ALP reagent (no. 245). Total cellular protein content of the samples was determined in a microassay procedure as described by Bradford [29] using the Coomassie protein assay reagent kit (Pierce). ALP activity was calculated as units of activity per milligram of protein.

2.3. Lipid Peroxidation Assay. Lipid peroxidation was evaluated using an analytical quantitative methodology. It relies upon the formation of a coloured adduct produced by the stechiometric reaction of aldehydes with thiobarbituric acid (TBA). The thiobarbituric acid reactive substances (TBARS) assay was performed on membranes extracted from cells,

using an icecold lysis buffer (50 mM Tris, 150 mM NaCl, 10 mM EDTA, 1% Triton) supplemented with a mixture of protease inhibitors. The homogenate was centrifuged at 1200 g for 10 min in order to separate cytosol (supernatants) from membranes (pellet). The pellet was dissolved in 50 mM Tris, 150 mM NaCl, and 10 mM EDTA, and the protein content of the samples was determined by Bio-Rad assay (Bio-Rad Laboratories, San Diego, CA, USA). Aliquots (10 mL) of the membrane preparation were added to 2 mL of TBA-trichloroacetic acid (TCA) (15% TCA, 0.3% TBA in 0.12 N HCl) solution at 100°C for 30 min. The reaction was stopped by cooling the sample in cold water, and, after a centrifugation at 15 000 g for 10 min, the chromogen (TBARS) was quantified by spectrophotometry at a wavelength of 532 nm. The amount of TBARS was expressed as $mM \cdot mg^{-1}$ proteins. All data are the mean ± SD of three experiments.

2.4. Western Blot Assay. The effects of DTNQ-Pro on expression of HSP90, p38, p38, and FOXO3a were determined by Western blots. The cells lysates were prepared using an ice-cold lysis buffer (50 mM Tris, 150 mM NaCl, 10 mM EDTA, 1% Triton) supplemented with a mixture of protease inhibitors containing antipain, bestatin, chymostatin, leupeptin, pepstatin, phosphoramidon, pefabloc, EDTA, and aprotinin (Boehringer, Mannheim, Germany). Equivalent protein samples were resolved on 8%–12% sodium dodecyl sulphate-polyacrylamide gels and transferred to nitrocellulose membranes (Bio-Rad, Germany). For immunodetection, membranes were incubated overnight with specific antibodies at the concentrations recommended by the manufacturer. All antibodies were diluted in Tris buffered saline/Tween 20–1% milk powder. This step was followed by incubation with the corresponding horseradish peroxidase conjugated antibody (anti-mouse IgG 1 : 2000, anti-rabbit IgG 1 : 6000, Biosource, Germany). Bands were analysed by enhanced chemiluminescence (ECL kit, Amersham, Germany).

3. Results

3.1. Cytotoxic Effects Induced by 5-FU on Growing D-Caco-2 Cells. Previously, we have shown the biochemical events elicited by DTNQ-Pro, a mimetic peptide, in growing human colon adenocarcinoma cells. Undifferentiated Caco-2 treated for 48 h with 500 nM DTNQ-Pro presented an increased membrane lipid peroxidation and a redistribution of both HSP27 and vimentin [26]. Moreover, growing Caco-2 cells differentiate into enterocytes. Here the effect of conventional cytotoxic agent 5-FU was studied on exponentially growing pretreated DTNQ-Pro Caco-2 cell lines (D-Caco-2). Cells were treated for 48 h with 500 nM DTNQ-Pro and, thereafter, different concentrations of 5-FU (0–200 μM) were added to the cells for 48 h. In exponentially growing cells, pretreatment with DTNQ-Pro potentiated the cell growth inhibition observed with 5-FU alone (Figure 1). As shown in Table 1, for growing Caco-2 cells, the concentration of 5-FU (46 μM) that induced 50% of growth inhibition (IC:50) was reduced about 30-fold in D-Caco-2 (1.2 μM). All successive experiments were performed on Caco-2 cell, treated for 48 h with 500 nM DTNQ-Pro (D-Caco-2).

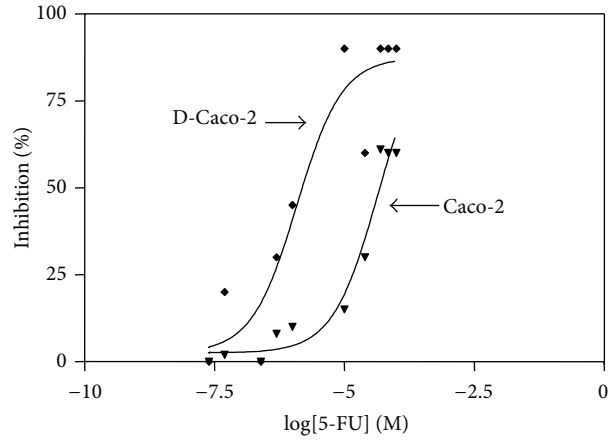

Figure 1: Sensitivity of the D-Caco-2 cells the to 5-FU. Both Caco-2 and D-Caco-2 cells were plated in 96-well microtitre plates at the density of 3×10^3 cells/plate. After 4 h, cells were exposed to different concentration (0–200 μM) of 5-FU for 48 h. The percentage of inhibition was calculated with the formula reported in methods. Experiments were performed in triplicate.

Table 1: IC50 5-FU values (micromolar) in growing human colon carcinoma cell lines with or without DTNQ-Pro pretreatment. Values represent means ± SEM ($n = 8$), $P < 0.05$.

	IC:50 on Caco-2	IC:50 on D-Caco-2
5-FU	46 μM	1.2 μM

3.2. 5-FU Increases Cell Cycle Arrest and D-Caco-2 Differentiation. 5-FU is an antimetabolite known to specifically block cells in S phase. To elucidate whether 5-FU treatment of D-Caco-2 determined cell cycle perturbation, we analysed the percentage cell cycle by FACS analysis. Cell cycle analysis of Caco-2 and D-Caco-2 cells revealed a percentage of cells of 54 ± 4 and 42 ± 6% in G0/G1 phase, 35 ± 5 and 47 ± 5% in S phase, and 11 ± 1% and 11 ± 2% in G2/M phase, respectively (Figure 2). The additional treatment of the cells with 500 nM 5-FU showed a significant ($P < 0.014$) accumulation of D-Caco-2 cells (56%) in S phase if compared to Caco-2 (45%) and a concomitant G0/G1 phase decrease (33%) if compared to Caco-2 cells (44%). As cell division arrest is one of the biological effects required for cell differentiation [30], we determined the effect of DTNQ-Pro on D-Caco-2 differentiation. In Figure 3(b) it is shown that ALP activity, as a marker of differentiation into enterocytes, correlated to postconfluent phase [31]. ALP activity was about 3-fold increased ($P < 0.001$) only in D-Caco-2 cells treated with 500 nM 5-FU while it remained unaltered in the other cases.

3.3. Lipid Peroxidation and Catalase Activity in D-Caco-2 Cells after 5-FU Treatment. In Figure 3 we reported the values of both TBARS, as lipid peroxidation markers [32], and catalase activity, as scavenger enzyme, in both Caco-2 and D-Caco2 cells treated with 500 nM 5-FU. The incubation of Caco-2 cells with 5-FU determined a statistically significant decrease of TBARS values ($P < 0.0015$) with a concomitant increase of the catalase activity ($P < 0.0124$). In the D-Caco-2 the basal

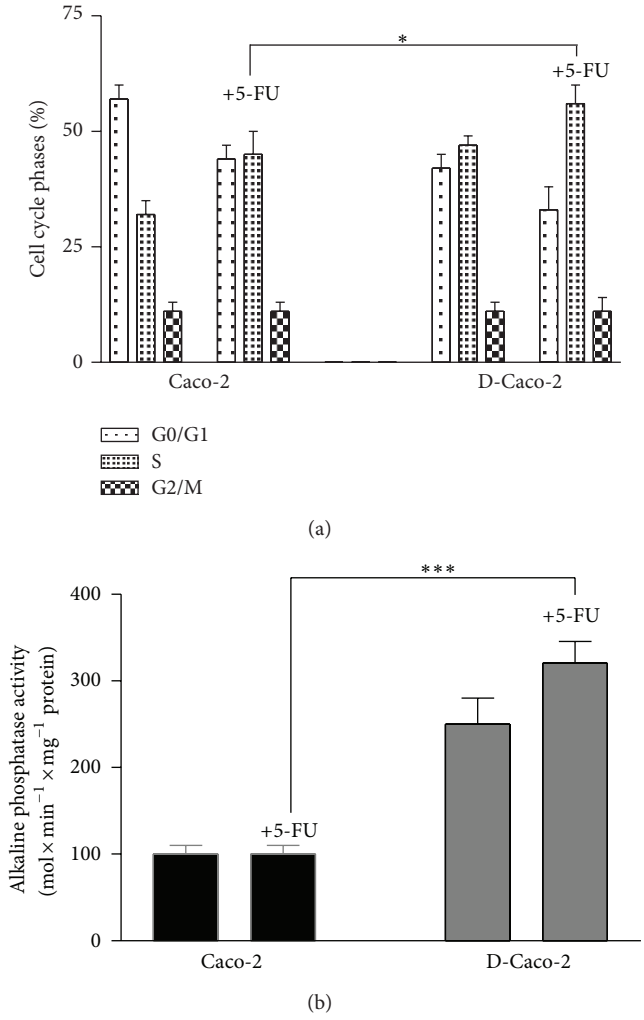

Figure 2: (a) Effects of 5-FU on the distribution of Caco-2 and D-Caco-2 cells populations. Data represent the percentage of cells in each phase of the cell cycle. Cell cycle distribution was determined by DNA flow cytometric analysis. Samples from preconfluent Caco-2 and D-Caco2 cells was analysed after 48 h of treatment with 500 nM 5-FU. Numbers indicate percentage of cells in G0/G1, S and G2/M phases. Data are representative of four separate analyses. (b) Differentiation effects of 5-FU of Caco-2 and D-Caco-2. The differentiation was assessed by measurement of ALP activity after 48 h of culture with 500 nM of 5-FU. Summary data shown are means ± SEM ($n = 4$; $^{***}P < 0.001$).

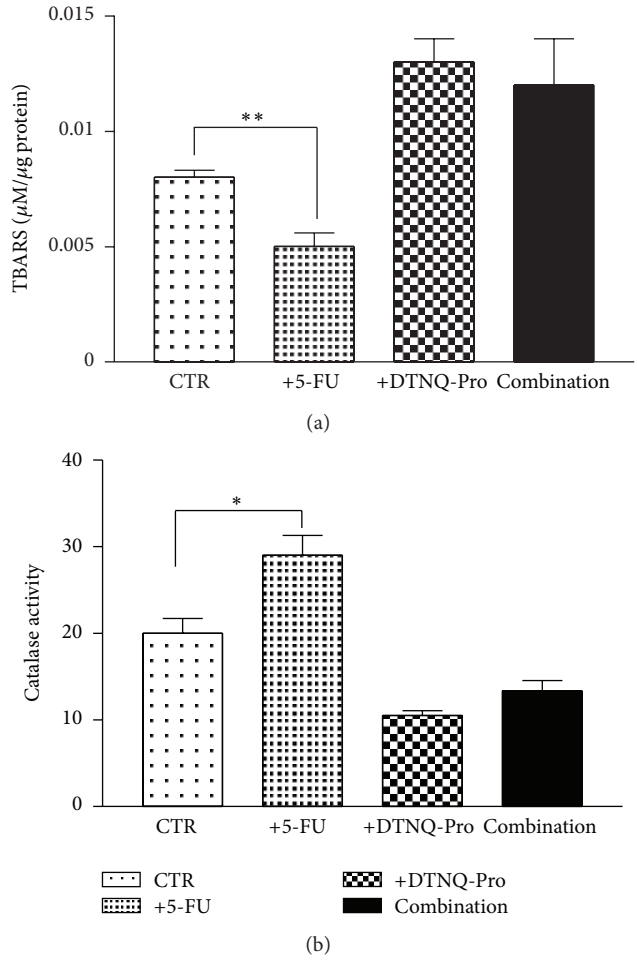

Figure 3: Effect of 5-FU D-Caco-2 treatment on TBARS. The cells were seeded in six multiwell plates at the density of 25×10^4 cells/plate and were incubated for the first 48 h with 500 nM DTNQ-Pro (D-Caco-2) the cells were washed to remove unattached dead cells and were incubated with and without 500 nM of 5-FU for subsequently 48 h. (a) TBARS levels in Caco-2 (CTR) and D-Caco-2 cells after 48 h of incubation without and with 500 nM 5-FU; (b) catalase activity. Catalase activity in Caco-2 (CTR) and D-Caco-2 cells after 48 h of incubation without and with 500 nM 5-FU. The bars represent means ± SEM of three independent experiments. Asterisks indicate significant difference between the D-Caco-2-treated samples compared with control value $^{**}P < 0.003$; $^{*}P < 0.05$; n.s.: not significant.

levels of TBARS and catalase activity were 1.6-fold and 0.5-fold higher, respectively, than those recorded in Caco-2 cells. No changes were observed in both TBARS values and catalase activity when the D-Caco-2 cells were incubated with 500 nM of 5-FU.

3.4. Evaluation of the Expression of Molecular Factors Involved in the Tumour Cell Resistance to 5-FU. We have evaluated, in D-Caco2 cells, the effects of 5-FU treatment on the expression of FOXO-3a, HSP90 and p38 MAPK proteins that are involved in mechanisms of cell resistance to 5-FU. Western blot and densitometric analysis of HSP90, FOXO-3a, and p38 MAPK in Caco2 after DTNQ-Pro treatment is shown in Figure 4. The Caco-2 cells expressed high levels of Hsp90, and this expression was 0.5-fold lower in D-Caco2. Furthermore DTNQ-Pro Caco-2 treatment induced about 0.5-fold decrease of both p38 and FOXO-3a expression. On the other hand, 5-FU induced about 3- and 2-fold increase of Hsp90 levels in Caco-2 and D-Caco-2 cells, respectively; moreover 5-FU weakly increased the expression of FOXO-3a and p38 in D-Caco-2 cells.

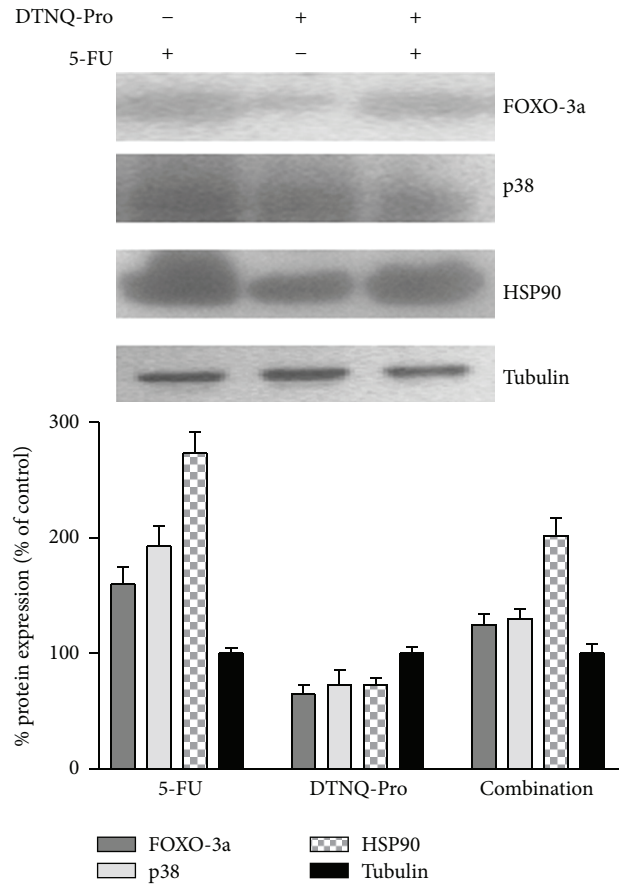

Figure 4: Expression of Foxo3a, p38, and HSP90 in Caco-2 and D-Caco-2 cells treated for 48 h with 5-FU. The cells were incubated with 500 nM of 5-FU, and the protein expression was evaluated by Western blotting. All the experiments were performed at least three times with similar results. The graphs show the summary data (as % of expression in untreated cells), normalized to γ-tubulin expression after 48 h of treatment with 5-FU. Data shown are means ± SEM ($n = 4$; $^{*}P < 0.05$, $^{**}P < 0.003$).

4. Discussion

Previously, we showed that DTNQ-Pro acts on two major targets involved in the resistance of CRC cells to chemotherapy agents: the process of cell differentiation and overexpression of HSP family proteins [26]. We have demonstrated that DTNQ-Pro induced cell membrane modifications by redistribution of HSP27 and vimentin within the cell. Moreover, DTNQ-Pro inhibited the growth by inducing S phase cell cycle arrest and increased cellular differentiation.

In the present study, we show that DTNQ-Pro, a mimetic dipeptide, sensitizes human CRC cells to the conventional chemotherapy agent 5-FU. Exposure of Caco-2 cells to DTNQ-Pro induced a hydrogen peroxide (H_2O_2) increase due to decreased catalase activity. At the same time, an increased rate of lipid peroxidation was recorded as evaluated by TBARS production. Lipid peroxidation occurred together with cell differentiation as demonstrated by the increased ALP activity. The treatment of D-Caco-2 cells with 5-FU caused an additional increase of both ALP activity and cell accumulation in S phase, while no increase of catalase activity or antagonism on TBARS values was recorded. Pretreatment of growing Caco-2 cell lines with 500 nM of DTNQ-pro (D-Caco2) induced also a decrease of FOXO3a protein expression with a consequent downregulation of D-cyclin (data not shown) and an accumulation of Caco-2 cells in the S-phase of the cell cycle. In fact, FOXO transcription factors [33] regulate the expression of antioxidants enzymes such as SOD and Catalase but, in addition to regulation of antioxidants, Foxo is also involved in the transcriptional upregulation of cell cycle inhibitors, including p21, p27, and p130, and downregulation of D-type cyclins. Therefore, our data demonstrate that S phase accumulation occurred together with regulation of transcriptional factors that are involved in the regulation of cell cycle.

5-FU is known to block DNA synthesis by the inhibition of thymidylate synthase (TS), which is regulated by cell cycle proteins controlled by phosphorylation [1]. Increased TS expression in tumors is an underlying mechanism by which tumor cells can escape from the toxic effect of 5-FU and become drug resistant [34]. In fact, the increased expression of the target is a generalized mechanism of resistance of tumour cells to antitumour agents determining an increase of the drug concentration needed to inhibit the molecular target.

DTNQ-Pro induces both cell accumulation in S phase and differentiation, with a probable decrease in the *de novo* DNA synthesis. On the basis of these considerations, we hypothesize that the level of TS expression could be reduced and this reduction may be directly responsible for the increase in sensitivity to 5-FU. Finally, we have found that DTNQ-Pro reduced HSP90 and p38 MAPK proteins. Hsp90 is a ubiquitous cellular protein and its function as a molecular chaperone is vital for cell survival [35] while p38 kinase is a final mediator of stress-induced pathways. We hypothesize that the increased responsiveness to 5-FU of D-Caco-2 could be attributed to (i) block of cell cycle in S phase and differentiation, (ii) decrease of HSP90 and p38 MAPK protein that can, in turn, promote the antiproliferative effects of 5-FU, and (iii) decreased expression of the 5-FU target. Our data provide evidence that DTNQ-pro is a promising chemotherapeutic agent that increases the chemosensitivity of growing adenocarcinoma colon cancer cells to 5-FU treatment.

References

[1] J. G. Kuhn, "Fluorouracil and the new oral fluorinated pyrimidines," *Annals of Pharmacotherapy*, vol. 35, no. 2, pp. 217–227, 2001.

[2] G. Vitale, C. H. J. van Eijck, P. M. van Koetsveld Ing et al., "Type I interferons in the treatment of pancreatic cancer: mechanisms of action and role of related Receptors," *Annals of Surgery*, vol. 246, no. 2, pp. 259–268, 2007.

[3] M. Marra, G. Salzano, C. Leonetti et al., "New self-assembly nanoparticles and stealth liposomes for the delivery of zoledronic acid: a comparative study," *Biotechnology Advances*, vol. 30, no. 1, pp. 302–309, 2011.

[4] M. Caraglia, G. Vitale, M. Marra, A. Budillon, P. Tagliaferri, and A. Abbruzzese, "Alpha-interferon and its effects on signalling pathways within cells," *Current Protein and Peptide Science*, vol. 5, no. 6, pp. 475–485, 2004.

[5] M. Marra, A. Lombardi, E. Agostinelli et al., "Bovine serum amine oxidase and spm potentiate docetaxel and interferon-α effects in inducing apoptosis on human cancer cells through the generation of oxidative stress," *Biochimica et Biophysica Acta*, vol. 1783, no. 12, pp. 2269–2278, 2008.

[6] M. Caraglia, M. Marra, P. Tagliaferri et al., "Emerging strategies to strengthen the anti-tumour activity of type I interferons: overcoming survival pathways," *Current Cancer Drug Targets*, vol. 9, no. 5, pp. 690–704, 2009.

[7] C. Jolly and R. I. Morimoto, "Role of the heat shock response and molecular chaperones in oncogenesis and cell death," *Journal of the National Cancer Institute*, vol. 92, no. 19, pp. 1564–1572, 2000.

[8] S. K. Calderwood, M. A. Khaleque, D. B. Sawyer, and D. R. Ciocca, "Heat shock proteins in cancer: chaperones of tumorigenesis," *Trends in Biochemical Sciences*, vol. 31, no. 3, pp. 164–172, 2006.

[9] C. Garrido, A. Fromentin, B. Bonnotte et al., "Heat shock protein 27 enhances the tumorigenicity of immunogenic rat colon carcinoma cell clones," *Cancer Research*, vol. 58, no. 23, pp. 5495–5499, 1998.

[10] S. Gurbuxani, J. M. Bruey, A. Fromentin et al., "Selective depletion of inducible HSP70 enhances immunogenicity of rat colon cancer cells," *Oncogene*, vol. 20, no. 51, pp. 7478–7485, 2001.

[11] C. De Simone, P. Ferranti, G. Picariello et al., "Peptides from water buffalo cheese whey induced senescence cell death via ceramide secretion in human colon adenocarcinoma cell line," *Molecular Nutrition and Food Research*, vol. 55, no. 2, pp. 229–238, 2011.

[12] R. Hayashi, Y. Ishii, H. Ochiai et al., "Suppression of heat shock protein 27 expression promotes 5-fluorouracil sensitivity in colon cancer cells in a xenograft model," *Oncology Reports*, vol. 28, no. 4, pp. 1269–1274, 2012.

[13] P. Mehlen, A. Mehlen, J. Godet, and A. P. Arrigo, "hsp27 as a switch between differentiation and apoptosis in murine embryonic stem cells," *Journal of Biological Chemistry*, vol. 272, no. 50, pp. 31657–31665, 1997.

[14] D. R. Ciocca, S. Oesterreich, G. C. Chamness, W. L. McGuire, and S. A. W. Fuqua, "Biological and clinical implications of heat shock protein 27 000 (Hsp27): a review," *Journal of the National Cancer Institute*, vol. 85, no. 19, pp. 1558–1570, 1993.

[15] P. Stiuso, G. Giuberti, A. Lombardi et al., "γ-Glutamyl 16-diaminopropane derivative of vasoactive intestinal peptide: a potent anti-oxidative agent for human epidermoid cancer cells," *Amino Acids*, vol. 39, no. 3, pp. 661–670, 2010.

[16] L. Vigh, B. Maresca, and J. L. Harwood, "Does the membrane's physical state control the expression of heat shock and other genes?" *Trends in Biochemical Sciences*, vol. 23, no. 10, pp. 369–374, 1998.

[17] Z. Török, N. M. Tsvetkova, G. Balogh et al., "Heat shock protein coinducers with no effect on protein denaturation specifically modulate the membrane lipid phase," *Proceedings of the National Academy of Sciences of the United States of America*, vol. 100, no. 6, pp. 3131–3136, 2003.

[18] E. Nagy, Z. Balogi, I. Gombos et al., "Hyperfluidization-coupled membrane microdomain reorganization is linked to activation of the heat shock response in a murine melanoma cell line," *Proceedings of the National Academy of Sciences of the United States of America*, vol. 104, no. 19, pp. 7945–7950, 2007.

[19] A. Budillon, F. Bruzzese, E. Di Gennaro, and M. Caraglia, "Multiple-target drugs: Inhibitors of heat shock protein 90 and of histone deacetylase," *Current Drug Targets*, vol. 6, no. 3, pp. 337–351, 2005.

[20] G. Misso, G. Giuberti, A. Lombardi et al., "Pharmacological inhibition of HSP90 and ras activity as a new strategy in the treatment of HNSCC," *Journal of Cellular Physiology*, vol. 228, no. 1, pp. 130–141, 2013.

[21] M. Caraglia, M. Marra, A. Budillon et al., "Chemotherapy regimen GOLF induces apoptosis in colon cancer cells through multi-chaperone complex inactivation and increased Raf-1 ubiquitin-dependent degradation," *Cancer Biology and Therapy*, vol. 4, no. 10, pp. 1159–1167, 2005.

[22] G. Vitale, S. Zappavigna, M. Marra et al., "The PPAR-gamma agonist troglitazone antagonizes survival pathways induced by STAT-3 in recombinant interferon-gamma treated pancreatic cancer cells," *Biotechnology Advances*, vol. 30, no. 1, pp. 169–184, 2012.

[23] G. L. Johnson and R. Lapadat, "Mitogen-activated protein kinase pathways mediated by ERK, JNK, and p38 protein kinases," *Science*, vol. 298, no. 5600, pp. 1911–1912, 2002.

[24] M. G. Wilkinson and J. B. A. Millar, "Control of the eukaryotic cell cycle by MAP kinase signaling pathways," *The FASEB Journal*, vol. 14, no. 14, pp. 2147–2157, 2000.

[25] S.-F. Chen, S. Nieh, S.-W. Jao et al., "Quercetin suppresses drug-resistant spheres via the p38 MAPK-Hsp27 apoptotic pathway in oral cancer cells," *PLoS ONE*, vol. 7, no. 11, Article ID e49275, 2012.

[26] I. Gomez-Monterrey, P. Campiglia, A. Bertamino et al., "A novel quinone-based derivative (DTNQ-Pro) induces apoptotic death via modulation/reduction of hsp expression in a human colon adenocarcinoma cell line," *British Journal of Pharmacology*, vol. 160, no. 4, pp. 931–940, 2010.

[27] C. De Simone, G. Picariello, G. Mamone et al., "Characterisation and cytomodulatory properties of peptides from Mozzarella di Bufala Campana cheese whey," *Journal of Peptide Science*, vol. 15, no. 3, pp. 251–258, 2009.

[28] F. Herz, A. Schermer, M. Halwer, and L. H. Bogart, "Alkaline phosphatase in HT-29, a human colon cancer cell line: Influence of sodium butyrate and hyperosmolality," *Archives of Biochemistry and Biophysics*, vol. 210, no. 2, pp. 581–591, 1981.

[29] M. M. Bradford, "A rapid and sensitive method for the quantitation of microgram quantities of protein utilizing the principle of protein dye binding," *Analytical Biochemistry*, vol. 72, no. 1-2, pp. 248–254, 1976.

[30] Q. M. Ding, T. C. Ko, and B. Mark Evers, "Caco-2 intestinal cell differentiation is associated with G1 arrest and suppression of CDK2 and CDK4," *American Journal of Physiology*, vol. 275, no. 5, pp. C1193–C1200, 1998.

[31] H. Matsumoto, R. H. Erickson, J. R. Gum, M. Yoshioka, E. Gum, and Y. S. Kim, "Biosynthesis of alkaline phosphatase during differentiation of the human colon cancer cell line Caco-2," *Gastroenterology*, vol. 98, no. 5 I, pp. 1199–1207, 1990.

[32] D. A. Wink and J. B. Mitchell, "Chemical biology of nitric oxide: Insights into regulatory, cytotoxic, and cytoprotective mechanisms of nitric oxide," *Free Radical Biology and Medicine*, vol. 25, no. 4-5, pp. 434–456, 1998.

[33] H. Huang and D. J. Tindall, "Dynamic FoxO transcription factors," *Journal of Cell Science*, vol. 120, no. 15, pp. 2479–2487, 2007.

[34] S. Popat, A. Matakidou, and R. S. Houlston, "Thymidylate-synthase expression and prognosis in colorectal cancer: a systematic review and meta-analysis," *Journal of Clinical Oncology*, vol. 22, no. 3, pp. 529–536, 2004.

[35] L. Whitesell and S. L. Lindquist, "HSP90 and the chaperoning of cancer," *Nature Reviews Cancer*, vol. 5, no. 10, pp. 761–772, 2005.

Hindawi Publishing Corporation
Journal of Amino Acids
Volume 2013, Article ID 178381, 12 pages
http://dx.doi.org/10.1155/2013/178381

Research Article

Amino Acid Derivatives as New Zinc Binding Groups for the Design of Selective Matrix Metalloproteinase Inhibitors

Mariateresa Giustiniano,[1] Paolo Tortorella,[2] Mariangela Agamennone,[3] Antonella Di Pizio,[3] Armando Rossello,[4] Elisa Nuti,[4] Isabel Gomez-Monterrey,[1] Ettore Novellino,[1] Pietro Campiglia,[5] Ermelinda Vernieri,[5] Marina Sala,[5] Alessia Bertamino,[5] and Alfonso Carotenuto[1]

[1] *Dipartimento di Chimica Farmaceutica e Tossicologica, Università di Napoli "Federico II," Via D. Montesano 49, 80131 Napoli, Italy*
[2] *Dipartimento di Farmacia, Università degli Studi di Bari "Aldo Moro," Via Orabona 4, 70125 Bari, Italy*
[3] *Dipartimento di Farmacia, Università degli Studi "G. d'Annunzio," Via dei Vestini 31, 66013 Chieti, Italy*
[4] *Dipartimento di Scienze Farmaceutiche, Università di Pisa, Via Bonanno 6, 56126 Pisa, Italy*
[5] *Dipartimento di Scienze Farmaceutiche e Biomediche, Università degli Studi di Salerno, Via Ponte don Melillo, 84084 Fisciano, Italy*

Correspondence should be addressed to Alfonso Carotenuto; alfocaro@unina.it

Received 21 December 2012; Accepted 28 January 2013

Academic Editor: Giuseppe De Rosa

A number of matrix metalloproteinases (MMPs) are important medicinal targets for conditions ranging from rheumatoid arthritis to cardiomyopathy, periodontal disease, liver cirrhosis, multiple sclerosis, and cancer invasion and metastasis, where they showed to have a dual role, inhibiting or promoting important processes involved in the pathology. MMPs contain a zinc (II) ion in the protein active site. Small-molecule inhibitors of these metalloproteins are designed to bind directly to the active site metal ions. In an effort to devise new approaches to selective inhibitors, in this paper, we describe the synthesis and preliminary biological evaluation of amino acid derivatives as new zinc binding groups (ZBGs). The incorporation of selected metal-binding functions in more complex biphenyl sulfonamide moieties allowed the identification of one compound able to interact selectively with different MMP enzymatic isoforms.

1. Introduction

Matrix metalloproteinases (MMPs) are 23-member zinc-dependent endopeptidases family involved in the extracellular matrix turnover [1]. Their aberrant regulation has been implicated in tumoral process, where they showed to have a dual role inhibiting or promoting cell growth and survival, angiogenesis and metastasis [2, 3] differentiation [4], and inflammation and immune surveillance [5]. Moreover, MMPs are overexpressed in a variety of tumor types, and their overexpression is associated with tumor aggressiveness and poor prognosis [6]. The specific alteration of the MMPs in malignant tissues and their participation in some of the major oncogenic mechanisms have both fuelled interest in the design and evaluation of MMP inhibitors (MMPIs) as anticancer agents [7, 8]. Generally, the MMPIs design involves peptide or peptidomimetic backbones containing a zinc-binding group (ZBG) able to interact with both the subpockets surrounding the active site (S_1 and S_1', S_2', and S_3') and the zinc (II) ion present in the catalytic site, respectively [9, 10]. The greater part of MMPIs research has focused on developing the peptide or peptidomimetic containing a hydroxamic acid as chelating group. Although this design has produced potent inhibitors such as Batimastat [11, 12] and Marimastat [13] (Figure 1), none of these MMPIs has successfully completed clinical trials.

The inability of hydroxamates to produce clinically viable compounds has been attributed to low oral availability, poor in vivo stability, and undesirable side effects associated with these compounds [14]. This has prompted the investigation of a limited number of nonhydroxamate-based MMPIs [15–19]. We present herein the results obtained with a small library

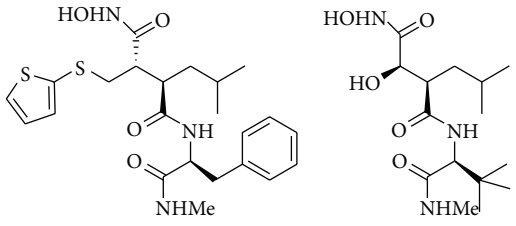

Figure 1: Structures of Batimastat and Marimastat.

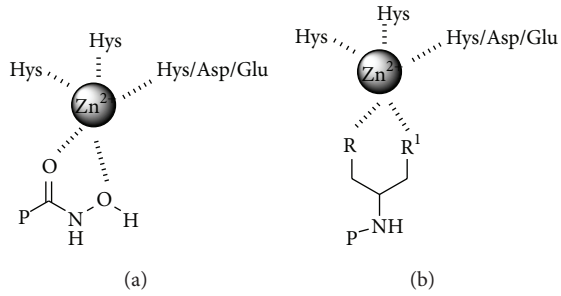

Figure 2: Hypothetical interaction between ZBG and Zn^{2+}.

of compounds synthesized and tested as potential ZBGs. The compounds were selected on the basis of some similarities to hydroxamates, such as the possibility to form five-member chelates (Figure 2), but with potentially enhanced pharmacokinetic properties such as a better hydrolytic stability and/or proposed increased affinity for the MMP zinc (II).

The designed ligands have a general 2-aminopropane-1,3-disubstituted structure which might be visualized as an amino acid derivative with the α carbon atom connected through two β carbons to heteroatoms with lone pairs or simply electron availability (R and R_1). These functional groups are sulfhydryl (SH), alcohol (OH), imidazole, cyano (CN), and azide (N_3) which are able to interact as Lewis-base in the coordination of the catalytic zinc ion. Their symmetric and asymmetric combination gave rise to a small ZBGs library (Table 1). The two β carbons rotational freedom could allow the chelating groups R and R_1 to orient themselves as better as possible in direction of the zinc ion.

According to the preliminary results of enzymatic inhibition activities, we further synthesized, from the most interesting ligands, a small series of sulfonamide derivatives containing a phenoxyphenyl group. This moiety has been widely used in the design of MMPs inhibitors as side chain of choice able to interact with the enzymatic S_1' subsite which plays a pivotal role in the determination of inhibition selectivity [20, 21]. The aims of the current study were to screen a range of nonhydroxamate structures as new ZBGs and to evaluate the enzymatic activity of small molecules designed to interact with the subpocket S_1' and with the zinc (II) ion present in the catalytic site of MMPs.

Table 1: Synthesized ZBGs library.

Compounds		R	R_1
	1a	OH	OH
	1b	CN	CN
	1c	N_3	N_3
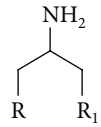	**1d**	SH	OH
	1e	Imidazole	OH
	1f	SH	SH
	1g	Imidazole	SH
	1h	SH	CN
	1i	OH	CN
	1j	SH	N_3
	1k	OH	N_3
	1l	Imidazole	N_3

Scheme 1: Synthesis of symmetric ZBGs **1a**, **1b**, and **1c**.

2. Chemistry

The symmetric ligands were prepared starting from serinol (**1a**) according to synthetic route shown in Scheme 1. After N-Boc-protection, the alcohol groups of **2** were activated as ditosylate derivatives in order to undergo nucleophilic substitution with azide and nitrile salts. Thus, displacement of the OTs group with tetraethylammonium cyanide (TEACN) or sodium azide (NaN_3) in DMF using TEA as base led to **4** and **5**, respectively, with 80%–82% yields. The final symmetric derivatives **1b** and **1c** have been obtained after deprotection of 2-amino group using a solution of 25% TFA in dichloromethane.

The ditosylation reaction was the limiting step in this synthetic strategy, described in the literature using pyridine (py) as solvent [22]. In our case, the treatment of **2** with 4-toluenesulfonyl chloride in pyridine led to ditosylate derivative **3** in only 2% yield. A preliminary study of the influence of solvents, reaction time, and reactive/base concentration ratio on this reaction was performed in order to (a) improve yields and mono/ditosylate adduct ratio; (b) facilitate work-up procedures; (c) use a less toxic solvent.

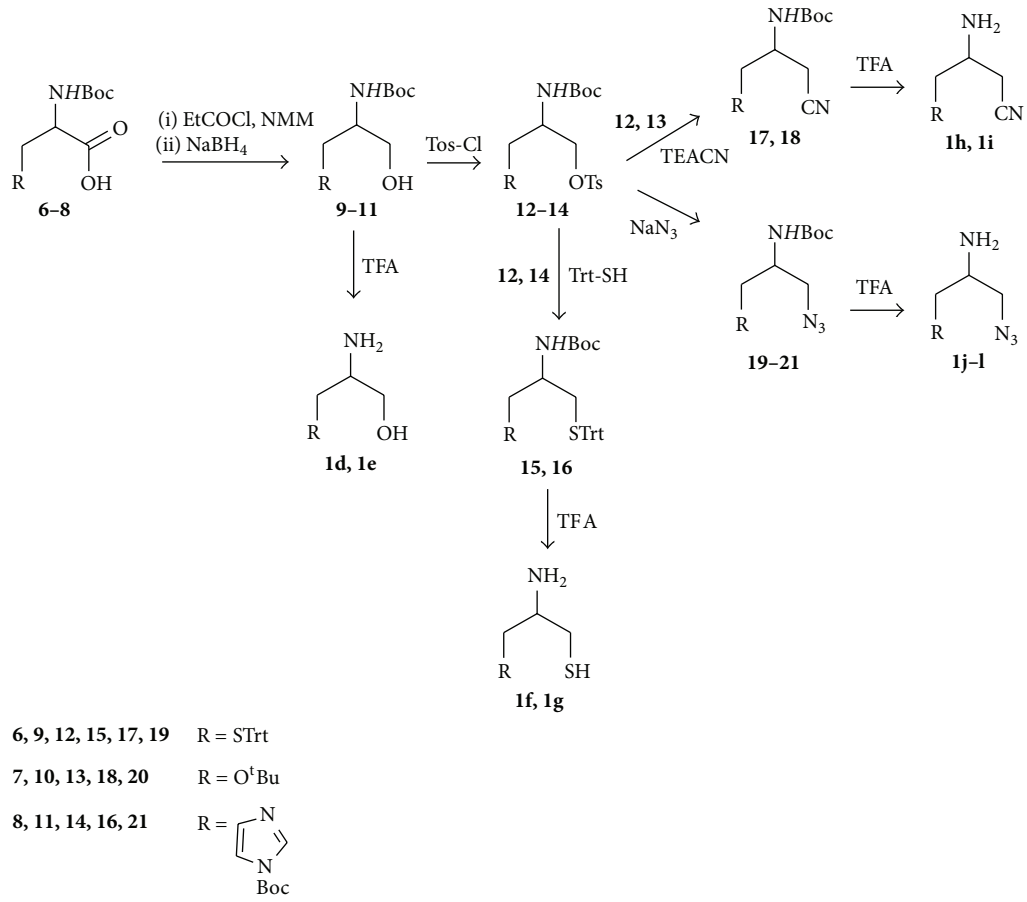

Scheme 2: Synthesis of symmetric (**1f**) and asymmetric (**1d, 1e, 1g–1l**) ZBGs.

Table 2: Study on ditosylation reactionof N-Boc-serinol (**2**).

Entry	Solvents	Reaction time	TsCl : TEA	Yields (%)	Mono/di ratio
1	Py	6 h	2.4 : 3	29	10 : 1
2	Py	10 h	3 : 4	40	10 : 1
3	Py, DMAP cat	6 h	3 : 4	31	10 : 1
4	DCM, Py cat	6 h	2.4 : 3	53	5 : 1
5	DCM, Py cat	10 h	3 : 4	45	5 : 1
6	DCM	6 h	3 : 4	55	1 : 1
7	dry DCM	10 h	3 : 4	68	1 : 2
8	dry DCM	10 h	2.4 : 3	85	1 : 19

As shown in Table 2, treatment of **2** with Tos-Cl and TEA in 2.4 : 3 ratio gave the highest yields (85%) and better selectivity (1 : 19) in the formation of ditosylate derivative **3** using dry dichloromethane as solvent (entry 8). Pyridine or pyridine with dimethylaminopyridine as base catalyst gave low yields with a little percentile of dialkylation product (entries 1, 2, and 3), while DCM as solvent was more effective without base catalyst (entries 6, 7, and 8 versus entries 4 and 5).

The symmetric and asymmetric ligands, **1f** and **1d**, **1e**, and **1g–1l**, respectively, were prepared according to the synthetic route shown in Scheme 2.

Protected amino acids Boc-Cys(Trt)-OH (**6**), Boc-Ser(OtBu)-OH (**7**), and Boc-His(Boc)-OH (**8**) were reduced to corresponding alcohols (**9**–**11**) using sodium borohydride as we previously described [23]. Treatment of hydroxy derivatives **9** and **11** with 20% TFA/DCM gave directly the corresponding final asymmetric ligands **1d** and **1e**. Analogously, reaction of hydroxyl derivatives with Tos-Cl in DCM and TEA led to tosylate intermediates **14**–**16** which were submitted to nucleophilic substitution reaction with azide and nitrile salts in the previously mentioned conditions to give the corresponding cyano (**17**,**18**) and nitrile (**19**–**21**) derivatives. Loss of protective groups after treatment of intermediates **12**–**21** with 50% TFA/DCM solution conduced to final compounds **1f**–**1l**.

Finally, the N-substituted phenoxybenzensulfonamide **25a**, **25d**, and **25e** were prepared according to synthetic route of Scheme 3. The sulfonation of diphenylether **22** with chlorosulfonic acid ($ClSO_3H$) and afterward chlorination with thionyl chloride ($SOCl_2$) afforded the key 4-phenoxybenzensulfonyl chloride **24** with 95% overall yields. The coupling of **24** with **1a**, **1d**, and **1e** in DMF and cesium carbonate (Cs_2CO_3) gave directly the corresponding final compounds in 42%–55% yields.

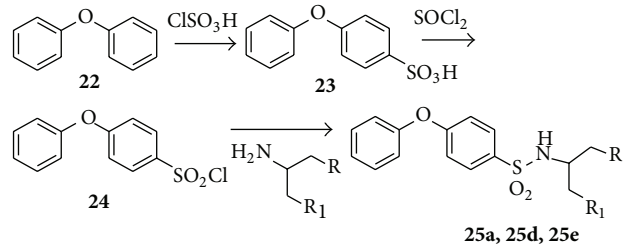

1a, R = R_1 = OH
1d, R = SH, R_1 = OH
1e, R = Imidazole, R_1 = OH

Scheme 3: Synthesis of phenoxybenzensulfonamide derivatives **25a**, **25d**, and **25e**.

Table 3: Enzymatic inhibition of MMP-2 by 2-amino-1,3-disubstituted derivatives **1a–1l**.

Compounds		R	R_1	IC_{50} (μM ± SD)
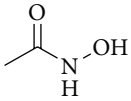 AHA	**AHA**			10000 ± 630
	1a	OH	OH	280 ± 24
	1b	CN	CN	560 ± 52
	1c	N_3	N_3	>1000
	1d	SH	OH	674 ± 88
	1e	Imidazole	OH	450 ± 23
	1f	SH	SH	666 ± 90
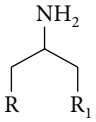 **1a–1l**	**1g**	Imidazole	SH	300 ± 41
	1h	SH	CN	500 ± 49
	1i	OH	CN	807 ± 98
	1j	SH	N_3	520 ± 57
	1k	OH	N_3	520 ± 49
	1l	Imidazole	N_3	480 ± 25

3. Enzymatic Inhibition Assays

The synthesized ZBGs, compounds **1a**–**1l**, were tested against the catalytic domain of MMP-2 in order to evaluate their chelating capability with respect to acetohydroxamic acid (AHA) which was considered a representative of the standard hydroxamate chelator. All the examined compounds exhibited a higher inhibitory activity compared to AHA (Table 3). The enzymatic assays revealed that the most interesting compounds are the serinol **1a** and the asymmetric ligands **1e** and **1g,** containing both an imidazole group and an alcohol or a thiol group, respectively. Surprisingly, the cysteinol **1d**, despite the well-known zinc thiophilicity, showed a lower enzymatic activity with IC_{50} value of 674 μM.

On the basis of these data, we selected the most active ligands **1a** and **1e** to be incorporated as ZBG in a more complex structure. The ligands were linked, through a sulfonamide bind, with a phenoxyphenyl group, described in the literature for its well-validated affinity for the S_1' enzymatic subpocket [10, 24]. A third ligand **1d**, less active, was also chosen in order to evaluate the real influence of ZBG group alone in the enzymatic activity.

Compounds **25a**, **25d**, and **25e** were tested against human recombinants MMP-1, MMP-2, MMP-8, and MMP-9 by a fluorometric assay, and the obtained IC_{50} values are summarized in Table 4. Compound **25a** exhibited an interesting inhibitory activity on MMP-2 and MMP-8, two enzymatic isoforms characterized by an intermediate and a deep S_1' subpocket, respectively [25–28]. This compound showed also a good selectivity over MMP-1 which has a shallow S_1' pocket. The substitution of a hydroxyl with an imidazole group, compound **25e**, caused a loss of both potency (except on MMP-1) and selectivity on the enzymes used in this study. The most interesting results were obtained with compound **25d**. This compound showed a high inhibitory activity on MMP-8 and MMP-9 with IC_{50} values in the micromolar range (10- and 13-fold more potent than **25a**, resp.) and maintained a good selectivity over both MMP-2 and MMP-1.

Table 4: Enzymatic activity of N-substituted phenoxybenzensulfonamide **25a**, **25d**, and **25e** on different MMPs.

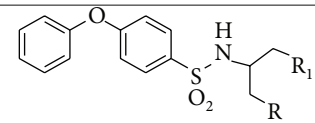

Com.	R	R_1	IC_{50} (μM ± SD)			
			MMP-1	MMP-2	MMP-8	MMP-9
25a	OH	OH	1030 ± 160	71 ± 1.9	98 ± 8.0	160 ± 15
25d	SH	OH	819 ± 116	110 ± 10	9.1 ± 2.3	12 ± 4.0
25e	Imidazole	OH	480 ± 30	190 ± 8.7	330 ± 21	200 ± 15

These preliminary results showed a different behaviour of ZBGs when they are introduced into a more complex structure indicating that, in this case, the modulation of selectivity does not depend only on ZBGs [29].

4. Molecular Modeling

In order to rationalize the observed activity data, docking calculations of the ZBGs and compounds **25a**, **25d**, and **25e** were performed on the MMP-2 catalytic domain. Subsequently, they were submitted to a refinement step, thorough minimization of best poses. The applied protocol allowed to correlate predicted and experimental binding energies. It is well known that docking scores hardly correlate with activity data, and to this aim, more accurate calculations are required such as Free Energy Perturbation or Thermodynamic Integration. Among available approaches, Linear Interaction Energy (LIE) represents a good compromise between accuracy and speed of calculations [30, 31]. In this approach, the binding process is represented as the replacement of water molecules solvating a ligand by the protein, using an implicit water model.

LIE generates a custom scoring function calculating the values of alpha, beta, and gamma coefficients of the following equation:

$$\begin{aligned}\text{Delta } G = {} & \text{alpha} * \left(U \text{ vdw\_}b - U \text{ vdw\_}f\right) \\ & + \text{beta} * \left(U \text{ elec\_}b - U \text{ elec\_}f\right) \\ & + \text{gamma} * \left(U \text{ cav\_}b - U \text{ cav\_}f\right),\end{aligned} \quad (1)$$

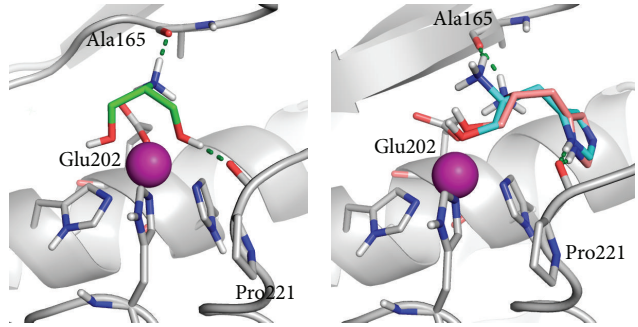

(a) (b)

Figure 3: Docked poses of **1a** (a) and **1e** in both enantiomeric forms (b) into the MMP-2 active site. MMP-2 is represented as a grey cartoon. Ligands and most relevant residues are depicted as sticks. H-bonds are represented as green dashed lines.

Table 5: Predicted and calculated binding energy (kcal) for all compounds toward MMP-2.

Compound	ΔG exp	ΔG calc (R-model)	ΔG calc (S-model)
1a	−4.837	−4.628	−4.484
1b	−4.428	−4.734	−4.619
1c	—[a]	—[a]	—[a]
1d R	−4.319	−4.512	
1d S			−4.492
1e R	−4.565	−4.395	
1e S			−4.614
1f	−4.333	−4.538	−4.592
1g R	−4.796	−4.583	
1g S			−4.739
1h R	−4.497	−4.421	
1h S			−4.303
1i R	−4.210	−4.391	
1i S			−4.379
1j R	−4.469	—[a]	—[a]
1j S			−4.511
1k R	−4.469	−4.237	
1k S			−4.513
1l R	−4.524	−4.624	
1l S			−4.338
25a	−5.655	−5.506	−5.326
25d R	−5.396	−5.349	
25d S			−5.279
25e R	−5.069	5.179	
25e S			−5.378

[a]No suitable docking poses were found.

where Delta G is the calculated binding energy; Uxxx_b is the van der Waals, Coulombic, and Cavity energy terms from the bound state; Uxxx_f is the van der Waals, Coulombic, and Cavity energy terms from the free state.

LIE method applied to our ligands provided a statistically significant correlation between calculated and experimental data, underpinning the validity of predicted docking poses (Table 5).

Table 6: Statistical parameters for LIE R-model and S-model.

Model	R^2	SD	F	P	R^2_{cv}
R-model	0.813	0.218	13.1	0.00125	0.64
S-model	0.751	0.242	10.0	0.00232	0.511

It is worth noting that chiral compounds under study were synthesized and tested as racemic mixture. Consequently, all calculations were carried out for all enantiomers, and quantitative models were generated for both R (R-model) and S forms (S-model) separately. Obtained ΔG values indicate that the R-model works slightly better than the S-model in predicting activity, as demonstrated by statistical correlation values (Table 6); however, the S-model is able to predict the binding energy with acceptable approximation indicating that experimental activity can be due to the contribution of both enantiomers.

This result is confirmed from the analysis of fragments docking poses in fact that no relevant differences can be observed in the binding of enantiomeric forms of chiral compounds, in the MMP-2 active site.

Moreover, differently than expected, just ligand **1a** is able to chelate the zinc ion, providing an explanation of the higher activity observed for this compound. Other fragments give a monodentate binding of the catalytic zinc, and the other electron donating group is usually involved in H-bond interactions with surrounding residues, such as the Pro221 carbonyl oxygen (e.g., **1d**), except for compounds containing the imidazole ring (e.g., **1e**), involved in a π-π stacking with the His201 side chain, which represents one of the main interactions formed by MMPIs in the S_1' pocket (Figure 3). This behavior can be attributed to the strict geometrical requirements, which must be fulfilled by chelating group around the zinc ion in MMPs active site.

The binding of sulfonamide derivatives **25a**, **25d**, and **25e** was studied as well through docking calculation and subsequent refinement as previously described on MMP-1, -8, and -9 (Table 7). No statistical correlations are provided in these cases because of the few available data. Docking results show all ligands occupying the S_1' site, except for MMP-1. This isoform, in fact, is known for having a short S_1' pocket, unable to accommodate the large biphenylether portion of

Table 7: Predicted and calculated binding energy (kcal) for sulfonamide ligands toward MMP-1, -8, and -9.

Compound	MMP-1		MMP-8		MMP-9	
	ΔG exp	ΔG calc	ΔG exp	ΔG calc	ΔG exp	ΔG calc
25a	−4.074	−4.098	−5.460	−5.532	−5.178	−5.168
25d R	−4.224	−4.247	−6.870	−6.504	−6.705	−6.840
25d S		−4.176		−6.870		−6.528
25e R	−4.524	−4.527	−4.740	−4.365	−5.042	−4.970
25e S		−4.522		−5.408		−5.165

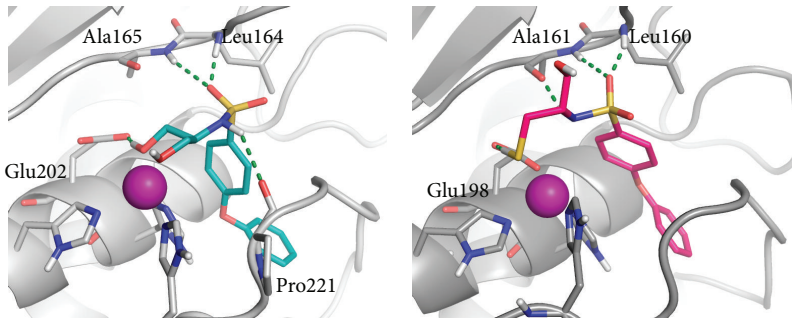

(a) (b)

Figure 4: Docked poses of **25a** into the MMP-2 active site (a) and **25d** into MMP-8 active site (b). MMP-2 and MMP-8 are represented, respectively, as a grey and dark grey cartoons. Ligands and most relevant residues are depicted as sticks. H-bonds are represented as green dashed lines.

these ligands. The imidazole ring of compounds **25e**, the more active towards MMP-1, occupy the hydrophobic pocket of this protein.

Binding mode of sulfonamide derivatives to the other MMPs is well conserved, regardless of chirality: MMP-2, -8, and -9 have a deep S_1' site able to locate the hydrophobic biphenyl ether, whose proximal aromatic ring interacts with the imidazole ring of His201, and the distal ring provides hydrophobic interactions in binding pocket. The sulfonamide moiety provides two H-bonds between a sulfone oxygen and Ala165 and Leu164 NH (MMP-2 numbering) and the sulfonamide NH and the Pro221 CO or alternatively Ala165 CO (Figure 4). Main differences are observed for the binding of the ZBG; in MMP-2, the ZBG of **25a** maintains the ability to chelate the zinc ion.

This chelation, not observed in MMP-8 and -9, can explain the higher activity observed for this ligand in MMP-2.

MMP-8 and -9 zinc ions coordinate all ligands in a monodentate fashion with a similar geometry, similarly to what observed for the ZBG in MMP-2. Therefore, as no chelation is provided by the ZBG in MMP-8 and MMP-9, the zinc thiophilicity seems to play a relevant role in determining activity toward these isoforms.

5. Conclusion

Herein, we described the design, synthesis, inhibitory activity, and molecular modeling studies of new non-hydroxamate-based MMPIs. The adopted synthetic strategy enabled the setting-up of a small ZBGs library through a simple and easily accessible pool of reactions. The biological screening of this library led to the identification of two ZBGs that were incorporated in a more complex structure able to interact with the S_1' enzymatic site. The biological data for compounds **25a** and **25e** confirmed the inhibition trend of the respective ZBGs against MMP-2. Compound **25d**, containing a less potent chelating group (**1d** versus **1a** and **1e**), was equipotent to **25a** against MMP-2 and more potent than **25a** against MMP-8 and MMP-9 (10- and 13-fold, resp.). Molecular modeling studies provided a rationalization of the experimental data, suggesting a putative binding mode of studied ligands in MMPs active site. These preliminary results indicate the importance of testing and selecting firstly compounds containing the minimums structural requirements necessary for a specific biological activity. Furthermore, taking in consideration the complex role of MMPs in the cellular and tumoral homeostasis, the development of selective inhibitors is desirable in order to shed further light on the protein function, signalling pathways, and role in disease of different MMPs [32–34]. Thus, compound **25d** identified in this preliminary study as MMP-8 and MMP-9 inhibitors could be submitted to a rational process of hit optimization with the aim to improve its potency and selectivity of action. The introduction of these new fragments into different peptide structures with the aim to synthesize selective MMPs inhibitors and to explore their structure-activity relationships is currently under study in our laboratory.

6. Experimental

6.1. MMP Inhibition Assays. Pro-MMP-1, pro-MMP-2, pro-MMP-8, and pro-MMP-9 were purchased from Calbiochem.

Proenzymes were activated immediately prior to use with *p*-aminophenylmercuric acetate (APMA 2 mM for 1 h at 37°C for MMP-2 and MMP-8, APMA 2 mM for 2 h at 37°C for MMP-1, and APMA 1 mM for 1 h at 37°C for MMP-9). For assay measurements, the inhibitor stock solutions (10 mM in DMSO) were further diluted, at seven different concentrations (0.01 nM–200 μM) for each MMP in the fluorometric assay buffer (FAB: Tris 50 mM, pH = 7.5, NaCl 150 mM, $CaCl_2$ 10 mM, Brij 35 0.05%, and DMSO 1%). Activated enzyme (final concentration 0.56 nM for MMP-2, 1.3 nM for MMP-9, 1.5 nM for MMP-8, and 2.0 nM for MMP-1) and inhibitor solutions were incubated in the assay buffer for 4 h at 25°C. After the addition of 20 μM solution of the fluorogenic substrate Mca-Lys-Pro-Leu-Gly-Leu-Dap(Dnp)-Ala-Arg-NH_2 (Bachem) for all the enzymes in DMSO (final concentration 2 μM), the hydrolysis was monitored every 15 s for 15 min recording the increase in fluorescence (λex = 325 nm; λem = 395 nm) using a Molecular Devices SpectraMax Gemini XS plate reader. The assays were performed in triplicate in a total volume of 200 μL per well in 96-well microtiter plates (Corning, black, NBS). The MMP inhibition activity was expressed in relative fluorescent units (RFUs). Percent of inhibition was calculated from control reactions without the inhibitor. IC_{50} was determined using the formula: $V_i/V_o = 1/(1 + [I]/IC_{50})$, where V_i is the initial velocity of substrate cleavage in the presence of the inhibitor at concentration [I], and V_o is the initial velocity in the absence of the inhibitor. Results were analyzed using SoftMax Pro software and Origin software.

6.2. General. Reagents, starting materials, and solvents were purchased from commercial suppliers and used as received. Analytical TLC was performed on plates coated with a 0.25 mm layer of silica gel 60 F254 Merck and preparative TLC on 20 cm × 20 cm glass plates coated with a 0.5 mm layer of silica gel PF254Merck. Silica gel 60 (300–400 mesh, Merck) was used for flash chromatography. Melting points were determined by a Kofler apparatus and are uncorrected. ^{1}H NMR and ^{13}C NMR spectra were recorded with a Varian-400 spectrometer, operating at 400 and 100 MHz, respectively. Chemical shifts are reported in δ values (ppm) relative to internal Me_4Si, and J values are reported in hertz (Hz). ESIMS experiments were performed on an Applied Biosystems API 2000 triple-quadrupole spectrometer.

*6.2.1. 2-(tert-Butyloxycarbonyl)-1,3-dihydroxypropane **(2)**.* To a 25 mL round-bottom flask, 2-aminopropane-1,3-diol **1a** (11 mmol) (Sigma-Aldrich, 98%) was added and dissolved in a 1 : 1 mixture water/1,4-dioxan (10 mL). After few minutes, di-tert-butyl dicarbonate (1.2 eq) and KOH until pH 8 were added. The reaction was stirred for 48 h, washed with H_3O^+, dried with Na_2SO_4, and evaporated under reduced pressure (yield: 98%); ^{1}H-NMR (400 MHz, $CDCl_3$) δ 1.34 (s, 9H, Boc); δ 3.59–3.63 (m, 1H, H-2); δ 3.72–3.87 (m, 4H, H-1 and H-3); δ 5.15 (bs, 1H, N*H*Boc)).

*6.2.2. 2-(tert-Butoxycarbonylamino)propane-1,3-diyl bis(4-Methylbenzenesulfonate) **(3)**.* To a 25 mL round-bottom flask, **2** (10 mmol) was added and dissolved in dry DCM (10 mL). After reached 0°C, paratoluensulfonyl chloride (2.4 eq) and TEA (3 eq) were added. The reaction was stirred for 10 h, washed with water, dried with Na_2SO_4, and evaporated under reduced pressure. The crude was then purified by chromatographic column using *n*-hexane/AcOEt 2 : 1 as eluent (yield: 85%); ^{1}H-NMR (400 MHz, $CDCl_3$) δ 1.34 (s, 9H, Boc); 4.00–4.06(m, 5H, H-1, H-2, and H-3); 4.89 (bs, N*H*Boc); 7.31 (d, J = 8 Hz, 4H, aryl); 7.71 (d, 4H, aryl).

7. General Procedure for the Synthesis of Symmetric Ligands 3-Aminopentanedinitrile (1b) and 1,3-Diazidopropan-2-amine (1c)

To a 25 mL round-bottom flask, **3** (5 mmol) was added and dissolved in DMF (10 mL). TEA (3 eq) and TEACN (2.4 eq) or NaN_3 (2.4 eq) were then added, and the reaction was stirred for 10 h at room temperature. The reaction mixtures were washed with water, dried with Na_2SO_4, and evaporated under reduced pressure. The crudes **4** and **5** were purified by chromatographic column using *n*-hexane/AcOEt: 3/1 as eluent. Data for *tert*-butyl 1,3-dicyanopropan-2-ylcarbamate (**4**), Data for *tert*-butyl 1,3-dicyanopropan-2-ylcarbamate (**4**) 1H-NMR(400 MHz, CDCl3): δ 1.41 (s, 9H); 2.73–2.82 (m, 4H,H-2 and H-4); 3.47–3.50 (m, 1H, H-3); 5.06 (bs, 1H, N*H*Boc). Data for *tert*-butyl 1,3-diazidopropan-2-ylcarbamate (**5**) 1H-NMR (400 MHz, CDCl3): δ 1.49 (s, 9H, Boc); 3.40–3.52 (m, 4H, H-1 and H-3); 3.86–3.90 (m,1H, H-2); 4.77 (bs, 1H,N*H*Boc). A solution of derivatives **4** or **5** (1 mmol) in CH_2Cl_2 (10 mL) was treated with trifluoroacetic acid (10 mL) and stirred at room temperature. The reaction was stirred for 2 h at room temperature and evaporated under reduced pressure to yield the corresponding final products as TFA salt.

*7.1. 3-Aminopentanedinitrile Trifluoroacetate **(1b)**.* Yield: 36%. ^{1}H-NMR (400 MHz, CD_3OD) δ 3.00–3.03 (m, 4H, H-2 and H-4); 3.07 (t, 1H, J = 6.0 Hz). ^{13}C-NMR (100 MHz, CD_3OD) δ 20.7 (C-3, C-4), 39.5 (C-3), 114.9 (CN). ESI-MS calc for $C_{15}H_{17}NO_5S$ 323.08, found 323.16.

7.2. 1,3*-Diazidopropan-2-amine Trifluoroacetate **(1c)**.* Yield: 33%. ^{1}H-NMR (400 MHz, CD_3OD) δ 3.46–3.48 (m, 1H, H-2); 3.63–3.77 (m, 4H, H-1, H-3). ^{13}C-NMR (100 MHz, CD_3OD) δ 52.0 (C-2), 59.0 (C-1 and C-3). ESI-MS calc for $C_{15}H_{17}NO_5S$ 323.08, found 323.16.

8. General Procedure for Synthesis of Amino Alcohols Derived from Amino Acids (9–11)

Ethyl chloroformate (1.2 eq) and N-methylmorfoline (1.2 eq) at 0°C were added to a solution of Boc-Cys(Trt)-OH (**6**) or Boc-Ser(OtBu)-OH (**7**) or flask Boc-His(Boc)-OH (**8**) (1 mmol) in THF (4 mL). After 1 h, the reaction was filtered off, and $NaBH_4$ (3 eq) dissolved in 2 mL of water was added. The reaction was then stirred at room temperature for 3 h, washed with H_3O^+, dried with Na_2SO_4, and evaporated

under reduced pressure. Chromatography purification of the corresponding residues using *n*-hexane/AcOEt: 2/1 yielded, in each case, the amino alcohol derivatives.

*8.1. tert-Butyl 1-Hydroxy-3-(tritylthio)propan-2-ylcarbamate **(9)**.* Yield: 73%. ^{1}H-NMR (400 MHz, $CDCl_3$) δ 1.38 (s, 9H, Boc); 2.40–2.42 (m, 2H, H-3); 3.46–3.51 (m, 3H, H-1, H-2); 4.77 (bs, 1H, N*H*Boc); 7.20–7.44 (m, 15H, aryl).

8.2. tert-Butyl 1-(tert-Butoxy)-3-hydroxypropan-2-ylcarbamate (10). Yield: 69%. ^{1}H-NMR (400 MHz, $CDCl_3$) δ 1.08 (s, 9H); 1.41 (s, 9H); 3.12 (m, 1H, H-3); 3.41–3.49 (m, 2H, H-1, H-3); 3.62 (m, 2H, H-1, H-2); 5.12 (s, N*H*Boc).

*8.3. tert-Butyl 1-Hydroxy-3-(1H-imidazol-4-yl)propan-2-ylcarbamate **(11)**.* Yield: 80%. ^{1}H-NMR (400 MHz, $CDCl_3$) δ 1.39 (s, 9H); 1.45 (s, 9H); 2.61–2.72 (m, 2H, H-1); 3.12–3.21 (m, 2H, H-3); 3.62 (m, 1H, H-2); 4.98 (bs, N*H*Boc); 7.00 (s, 1H, imidazole); 8.21(s, 1H, imidazole).

9. General Procedure for Removal of the Boc Protecting Group: Synthesis of Final Ligands 1d and 1e

The compounds **9** or **11** were dissolved in a 1 : 1 mixture DCM/TFA (10 mL), adding triethylsilane (0.1 eq) as scavenger. The reaction was stirred for 2 h at room temperature and evaporated under reduced pressure to yield the title derivatives as TFA salt.

*9.1. 2-Amino-3-mercaptopropan-1-ol Trifluoroacetate **(1d)**.* Amorphous solid (46%). ^{1}H-NMR (400 MHz, D_2O) δ 2.45–2.49 (m, 2H, H-3); 3.15–3.19 (m, 1H, H-2); 3.67–3.71 (m, 2H, H-1). ^{13}C NMR (100 MHz, D_2O) δ 30.2 (C-3) 57.2 (C-2), 63.1 (C-1). ESI-MS calc for $C_5H_{10}F_3NO_3S$ 221.20, found 221.29.

*9.2. 2-Amino-3-(1H-imidazol-4-yl)propan-1-ol Ditrifluoroacetate **(1e)**.* White solid (39%), m.p. 218–220°C. ^{1}H NMR (400 MHz, CD_3OD) δ 2.90–2.93 (m, 2H, H-3); 3.08–3.12 (m, 1H, H-1); 3.66–3.71 (m, 2H, H-1); 7.01 (s, 1H, imidazole); 7.89 (s, 1H, imidazole). ^{13}H-NMR (100 MHz, CD_3OD) δ 29.4 (C-3), 58.2 (C-2), 64.1 (C-1) 118.2, 130.1, 134.7 (imidazole). ESI-MS calc for $C_{10}H_{13}F_6N_3O_5$ 369.22, found 369.16.

10. General Procedure for Synthesis of Tosilated Derivatives 12–14

To a 25 mL round-bottom flask, **9**, **10**, or **11** (1.1 mmol) was added and dissolved in dry DCM (10 mL). After reached 0°C, paratoluensulfonyl chloride (1.2 eq) and TEA (1.5 eq) were added. The reaction is stirred for 10 h, washed with water, dried with Na_2SO_4, and evaporated under reduced pressure. The crudes were then purified by chromatographic column using *n*-hexane/AcOEt: 3/1 as elution system.

*10.1. 2-(tert-Butoxycarbonylamino)-3-(tritylthio)propyl 4-Methylbenzenesulfonate **(12)**.* Yield: 73%. ^{1}H-NMR (400 MHz, $CDCl_3$) δ 1.43 (s, 9H); 2.30 (s, 3H, CH_3); 2.33–2.42 (m, 2H, H-3); 3.55–3.58 (m, 1H, H-1); 3.89–3.93 (m, 3H, H-1, H-2), 4.48 (bs, N*H*Boc); 7.21–7.37 (m, 17 H, aryl); 7.72 (d, J = 8.0 Hz, 2H, aryl).

*10.2. 3-tert-Butoxy-2-(tert-butoxycarbonylamino)propyl 4-Methylbenzenesulfonate **(13)**.* Yield: 77%. ^{1}H-NMR (400 MHz, $CDCl_3$) δ 1.08 (s, 9H); δ 1.43 (s, 9H); 2.31 (s, 3H, CH_3); 3.14–3.23 (m, 2H, H-1, H-3); 3.87–3.91 (m, 2H, H-1, H-3); 4.02–4.08 (m, 1H, H-2); 4.92 (bs, N*H*Boc); 7.16 (d, J = 8.1 Hz, 2H, aryl); 7.89 (d, 2H, aryl).

*10.3. tert-Butyl 4-(2-(tert-Butoxycarbonylamino)-3-(tosyloxy) propyl)-1H-imidazole-1-carboxylate **(14)**.* Yield: 73%. ^{1}H-NMR (400 MHz, $CDCl_3$) δ 1.38 (s, 9H); 1.41 (s, 9H); 2.31 (s, 3H, CH_3); 2.59–2.65 (m, 2H, H-1); 3.53–3.56 (m, 1H, H-3); 3.74–3.82 (m, 1H, H-3); 4.00–4.07 (m, 1H, H-2); δ 5.01 (bs, N*H*Boc); 7.01 (s, 1H, imidazole); 7.19 (d, J = 8.0 Hz, 2H, aryl); 7.80 (d, 2H, aryl); 7.89 (s, 1H, imidazole).

11. General Procedure for the Synthesis of Thio Derivatives 15 and 16

To a 25 mL round-bottom flask, **12** or **14** (1.1 mmol) was added, and dissolved in DMF (10 mL). TEA (1.5 eq) and Trt-SH (1.2 eq) were then added and the reaction was stirred for 10 h at room temperature. The reaction mixture was then washed with water, dried with Na_2SO_4, and evaporated under reduced pressure. The crudes were then purified by chromatographic column using TLC: *n*-hexane/AcOEt: 4/1 as eluent system.

*11.1. tert-Butyl 1,3-bis(Tritylthio)propan-2-ylcarbamate **(15)**.* Yield: 81%. ^{1}H-NMR (400 MHz, $CDCl_3$) δ 1.39 (s, 9H); 2.38–2.41 (m, 4H, H-1, H-3); 4.01–4.05 (m, 1H, H-2); 4.48 (bs, N*H*Boc); 7.08–7.23 (m, 30H, aryl).

*11.2. tert-Butyl 4-(2-(tert-Butoxycarbonylamino)-3-(tritylthio) propyl)-1H-imidazole-1-carboxylate **(16)**.* Yield: 79%. ^{1}H-NMR (400 MHz, $CDCl_3$) δ 1.42 (s, 9H); 2.51–2.64 (m, 4H, H-1, H-3); 4.20–4.26 (m, 1H, H-2); 4.48 (bs, N*H*Boc); 7.08–7.23 (m, 16H, aryl); 7.91 (s, 1H, imidazole).

12. Synthesis of Final Ligands 1f and 1g

The compounds **15** or **16** were dissolved in a 1 : 1 mixture DCM/TFA (10 mL), adding triethylsilane (0.1 eq) as scavenger. The reaction was stirred for 2 h at room temperature and evaporated under reduced pressure to yield the title derivatives as TFA salt.

*12.1. 2-Aminopropane-1,3-dithiol Trifluoroacetate **(1f)**.* Amorphous solid (59%). ^{1}H NMR (400 MHz, D_2O) δ 2.64 (dd, 2H, J = 6.8 and 11.2 Hz, H-1, H-3); 2.74 (dd, J = 5.2 and 6.9 Hz, 2H, H-1, H-3). ^{13}C NMR (100 MHz, D_2O) δ 30.1 (C-1, C-3), 55.0 (C-2). ESI-MS calc for $C_5H_{10}F_3NO_2S_2$: 237.01; found 237.11.

*12.2. 2-Amino-3-(1H-imidazol-2-yl)propane-1-thiol Ditrifluoroacetate **(1g)**.* White solid (61%), m.p. 196–198°C. ^{1}H NMR (400 MHz, CD_3OD) δ 2.79 (dd, 1H, J = 5.7 and 10.1 Hz, H-1);

2.90 (dd, 1H, H-1); 3.18–3.25 (m, 2H, H-3); 3.61–3.70 (m, 1H. H-2). ^{13}H-NMR (100 MHz, CD_3OD) δ 25.8 (C-1); 26.4 (C-3), 52.3 (C-2), 118.2 (imidazole), 134.7 (imidazole). ESI-MS calc for $C_8H_{12}F_3N_3O_2S$: 271.06; found 271.10.

13. General Procedure for the Synthesis of Cyano Derivatives 17 and 18

To a 25 mL round-bottom flask, **12** or **13** (1.1 mmol) was added and dissolved in DMF (10 mL). TEA (1.5 eq) and TEACN (1.2 eq) were added, and the reaction was stirred for 10 h at room temperature. The reaction mixtures were then washed with water, dried with Na_2SO_4, and evaporated under reduced pressure. The crudes were purified by chromatographic column using *n*-hexane/AcOEt: 3/1

*13.1. tert-Butyl 1-Cyano-3-(tritylthio)propan-2-ylcarbamate **(17)***. Yield: 84%. ^{1}H-NMR (400 MHz, $CDCl_3$) δ 1.42 (s, 9H,); 2.29–2.33 (m, 2H, H-3); 2.71–2.86 8 m, 2H, H-1); 3.86–3.91 (m, 1H, C-2); 4.97 (bs, N*H*Boc); δ 7.08–7.45 (m, 15H, aryl).

*13.2. tert-Butyl 1-tert-Butoxy-3-cyanopropan-2-ylcarbamate **(18)***. Yield: 81%. ^{1}H-NMR (400 MHz, $CDCl_3$) δ 1.12 (s, 9H); 1.41 (s, 9H); 2.69 (m, 2H, H-3); 3.23–3.41 (m, 2H, H-1); 3.90–3.94 (m, 1H, H-2); 4.99 (bs, N*H*Boc).

14. Synthesis of Final Ligands 1h and 1i

The intermediates **17** and **18** were dissolved in a 1 : 1 mixture DCM/TFA (10 mL), adding triethylsilane (0.1 eq) as scavenger. The reaction was stirred for 2 h at room temperature and evaporated under reduced pressure to afford the title compounds as TFA salt.

*14.1. 3-Amino-4-mercaptobutanenitrile Trifluoroacetate **(1h)***. Amorphous solid (65%). ^{1}H NMR (400 MHz, CD_3OD) δ 3.09–3.20 (m, 4H, H-2, H-4); 3.87–3.90 (m, 1H, H-3). ^{13}C NMR (100 MHz, CD_3OD) δ 20.3 (C-2), 38.3 (C-4), 46.1 (C-3), 115.4 (C-1). ESI-MS calc for $C_6H_9F_3N_2O_2S$ 230.01, found 230.12.

*14.2. 3-Amino-4-hydroxybutanenitrile Trifluoroacetate **(1i)***. White solid (63%), m.p. 131–133°C. ^{1}H-NMR (400 MHz, CD_3OD) δ 2.41–2.53 (m, 2H, H-2); 3.76–3.89 (m, 3H, H-3, H-4). ^{13}C NMR (100 MHz, CD_3OD) δ 21.1 (C-2), 50.0 (C-3), 61.3 (C-4), 114.7 (C-1) ESI-MS calc for $C_6H_9F_3N_2O_3$ 214.06, found 214.16.

15. General Procedure for the Synthesis of Azido Derivatives 19–21

To a 25 mL round-bottom flask, **12**, **13**, or **14** (1.1 mmol) were added and dissolved in DMF (10 mL). TEA (3 eq) and NaN_3 (2.4 eq) were added, and the reactions were stirred for 10 h at room temperature. The reaction mixtures were washed with water, dried with Na_2SO_4, and evaporated under reduced pressure. The crudes were then purified by chromatographic column using *n*-hexane/AcOEt: 3/1 as eluent system.

*15.1. tert-Butyl 1-Azido-3-(tritylthio)propan-2-ylcarbamate **(19)***. Yield: 75%. ^{1}H-NMR (400 MHz, $CDCl_3$) δ 1.49 (s, 9H); 2.54–2.62 (m, 2H, H-3); 3.29–3.35 (m, 2H, H-1); 3.88–3.90 (m, 1H, H-2); 4.82 (bs, N*H*Boc).

*15.2. tert-Butyl 1-Azido-3-tert-butoxypropan-2-ylcarbamate **(20)***. Yield: 72%. ^{1}H-NMR (400 MHz, $CDCl_3$) δ 1.18 (s, 9H); 1.43 (s, 9H); 3.01–3.23 (m, 2H, H-1); 3.81–3.90 (m, 3H, H-2, H-3); 4.91 (bs, N*H*Boc).

*15.3. tert-Butyl 4-{3-Azido-2-[(tert-butoxycarbonyl)amino] propyl}-1H-imidazole-1-carboxylate **(21)***. Yield: 70%. ^{1}H-NMR (400 MHz, $CDCl_3$) δ 1.39 (s, 9H); 1.59 (s, 9H); 3.21–3.33 (m, 4H, H-1, H-3); 3.98–4.03 (m, 1H, C-2); 4.50 (bs, N*H*Boc).

16. Synthesis of Final Derivatives 1j–1l

The intermediates **19**, **20**, and **21** were dissolved in a 1 : 1 mixture DCM/TFA (10 mL), adding triethylsilane (0.1 eq) as scavenger. The reaction was stirred for 2 h at room temperature and evaporated under reduced pressure to afford the title compounds as TFA salt.

*16.1. 2-Amino-3-azidopropane-1-thiol Trifluoroacetate **(1j)***. Amorphous solid (38%). ^{1}H-NMR (400 MHz, D_2O) δ 2.76–2.82 (m, 2H, H-3); 3.58–3.62 (m, 2H, H-2, H-1); 3.78–3.81 (m, 1H, H-1). ^{13}C NMR (100 MHz, D_2O) δ 30.6 (C-1), 51.8 (C-2), 58.9 (C-3). ESI-MS calc for $C_5H_9F_3N_4O_2S$ 264.04, found 264.12

*16.2. 2-Amino-3-azidopropane-1-ol Trifluoroacetate **(1k)***. Amorphous solid (35%). ^{1}H-NMR (400 MHz, D_2O) δ 3.30–3.33 (m, 1H, H-2); 3.40–3.46 (m, 2H, H-3); 3.53–3.64 (m, 2H, H-1). ^{13}C NMR (100 MHz, D_2O) δ 50.2 (C-3), 52.0 (C-2), 59.1 (C-1). ESI-MS calc for $C_5H_9F_3N_4O_3$ 230.15, found 230.27.

*16.3. 1-Azido-3-(1H-imidazol-4-yl)propan-2-amine Ditrifluoroacetate **(1l)***. Amorphous solid (41%). ^{1}H-NMR (400 MHz, CD_3OD) δ 3.12–3.15 (m, 2H, H-1); 3.62–3.66 (m, 1H, H-2); 3.62–3.66 (m, 1H, H-2); 3.70–3.83 (m, 2H, H-3); 7.48 (s, 1H, imidazole); 8.86 (s, 1H, imidazole). ^{13}C NMR (100 MHz, CD_3OD) δ 25.3 (C-3), 49.7 (C-2), 51.2 (C-1), 118.1, 128.1,134.7(C-imidazole). ESI-MS calc for $C_{10}H_{12}F_6N_6O_4$ 394.23, found 394.31.

*16.4. 4-Phenoxybenzene-1-sulfonyl Chloride **(24)***. In a 25 mL round-bottom flask, **22** (11.75 mmol) was dissolved in dry DCM (10 mL), and chlorosulphonic acid (11.75 mmol.) was added at 0°C. The reaction was stirred for 2 h, evaporated under vacuum, and used for next step without further purification. The reaction mixture was indeed dissolved in thionyl chloride at 0°C and refluxed for 5 h to yield after evaporation product **24** with 95% yield. ^{1}H-NMR (400 MHz,

$CDCl_3$) δ 7.01–7.14 8 m, 5H, aryl); 7.41 (d, J = 8.6 Hz, 2H, aryl); 7.82 (d, 2H, aryl).

*16.5. N-(1,3-Dihydroxypropan-2-yl)-4-phenoxybenzenesulfonamide **(25a)**.* To a 25 mL round-bottom flask, **1a** (3 mmol) was added and dissolved in acetone (10 mL). $NaHCO_3$ (1.5 eq.) and **24** (1.2 eq.) were added, and the reaction was stirred for 24 h at room temperature. The reaction mixture was then washed with water, dried with Na_2SO_4, and evaporated under reduced pressure. The crude was purified by chromatographic column using AcOEt/acetone 9/1 as eluent system. Amorphous solid (55%). ^{1}H-NMR (400 MHz, CD_3OD) δ 3.19–3.21 (m, 1H, H-2); 3.48–3.54 (m, 4H, H-1, H-3); 7.04–7.09 (m, 5H, aryl); 7.40–7.43 (m, 2H, aryl); 7.84–7.89 (m, 2H, aryl). ^{13}C NMR (100 MHz, CD_3OD) δ 56.7 (C-2), 60.9 (C-1, C-3), 117.4, 117.7, 120.0, 121.4, 129.2, 130.1, 132.3, 151.1, 159.2(aryl). ESI-MS calc for $C_{15}H_{17}NO_5S$ 323.08; found 323.16.

*16.6. N-(1-Hydroxy-3-mercaptopropan-2-yl)-4-phenoxybenzenesulfonamide **(25d)**.* To a 25 mL round-bottom flask, 2-amino-3-(tritylthio)propan-1-ol (3 mmol) were added and dissolved in DMF (10 mL). Cs_2CO_3 (1.5 eq.) and **24** (1.2 eq.) were then added, and the reaction was stirred for 24 h at room temperature. The reaction mixtures were washed with water, dried with Na_2SO_4, and evaporated under reduced pressure. The compound N-(1-hydroxy-3-(tritylthio)propan-2-yl)-4-phenoxybenzenesulfonamide was purified by chromatographic column using *n*-hexane/AcOEt: 2/1. Yield: 42%. ^{1}H-NMR (400 MHz, $CDCl_3$) δ 2.34 (d, J = 8.0 Hz, 2H, H-3); 3.18–3.23 (m, 1H, H-2); 3.42–3.49 (m, 2H, H-1); 7.14–7.70 (m, 24H, aryl); 7.74 (d, 2H, aryl). This intermediate was then dissolved in a 1 : 1 mixture DCM/TFA (10 mL), adding triethylsilane (0.1 eq) as scavenger. The reaction was stirred for 2 h at room temperature and evaporated under reduced pressure to afford the title compound as an amorphous solid. Yield: 92%. ^{1}H-NMR (400 MHz, $CDCl_3$) δ 2.65–2.70 (m, 2H, H-3); 3.35–3.40 (m, 1H, H-2); 3.64–3.79 (m, 2H, H-1); 7.03–7.09 (m, 5H, aryl); 7.37 (d, J = 6.8 Hz, 2H, aryl); 7.84 (d, 2H, aryl). ^{13}C NMR (100 MHz, $CDCl_3$) δ 26.6 (C-3), 51.1 (C-1), 62.9 (C-3), 118.0, 121.0, 129.6, 130.5, 138.2, 152.0, 160.1(aryl). ESI-MS calc for $C_{15}H_{17}NO_4S_2$ 339.06; found 339.12.

*16.7. N-(1-Hydroxy-3-(1H-imidazol-4-yl)propan-2-yl)-4-phenoxybenzenesulfonamide Hydrochloride **(25e)**.* To a 25 mL round-bottom flask, **1e** (3 mmol) was added and dissolved in DMF (10 mL). Cs_2CO_3 (1.5 eq.) and **24** (1.2 eq.) were then added, and the reaction was stirred for 24 h at room temperature. The reaction mixture was then washed with water, dried with Na_2SO_4, and evaporated under reduced pressure. The product was precipitated from the crude with dry HCl/eter solution and the filtered washed with Et_2O. White solid (51%) 241–243°C. ^{1}H-NMR (400 MHz, CD_3OD) δ 2.78–2.85 (m, 2H, H-3); 3.47–3.52 (m, 2H, H-1, H-2); 3.68–3.71 (m, 1H, H-1); δ 7.02–7.10 (m, 5H, aryl); 7.39 (d, J = 8.8 Hz, 2H, aryl); 7.48 (s, 1H, imidazole); 7.80 (d, 2H, aryl); 8.85 (s, 1H, imidazole). ^{13}C NMR (100 MHz, CD_3OD) δ 28.4 (C-3), 52.6 (C-1), 63.2 (C-3), 114.0, 117.8, 118.2, 120.10, 121.4, 129.2, 130.1, 133.2, 139.8, 151.1, 159.2 (aryl). ESI-MS calc for $C_{18}H_{20}ClN_3O_4S$ 2409.89, found 409.91.

17. Molecular Modeling

All calculations were performed on a DELL T5500 workstation, equipped with two Intel Xeon E5630 2.53 GHz processors.

All compounds were manually built in Maestro version 9.3.5, [35] exploiting the Built facility and minimized to a derivative convergence of 0.001 kJÅ^{-1} mol^{-1}, using the Truncated Newton Conjugate Gradient (TNCG) minimization algorithm, the OPLS2005 force field, and the GB/SA water solvation model implemented in MacroModel version 9.9 [23].

Conformational searches, applying the mixed torsional/low-mode sampling and the automatic setup protocol, were carried out on all minimized ligand structures to obtain the global minimum geometry of each molecule, to be used as the starting conformation for docking calculations with Glide, version 5.8 [24, 36, 37].

Three-dimensional coordinates of MMP-1, -2, -8, and -9 were downloaded from the Brookhaven Protein Data Bank [38] (PBD ID: 1HFC, 1QIB, 1I76, and 1GKC, resp.). Each 3D structure was submitted to the Protein Preparation routine in Maestro that allows fixing of receptor structures, eliminating water molecules and possible ligands, fixing bond orders, adding hydrogen atoms, and ionizing charged residues. Hydrogen bond network is optimized, and for each structure, a brief relaxation was performed using an all-atom constrained minimization carried out with the Impact Refinement module version 5.8 and the OPLS-2005 force field to reduce steric clashes that may exist in the original PDB structures. The minimization was terminated when the energy converged or the root mean square deviation (RMSD) reached a maximum cut-off of 0.30 Å.

Glide energy grid was generated using the crystallographic ligand of 1I76 as the centre of the grid, after superimposing all MMPs structures under study. The size of the box was determined automatically on the basis of the ligand dimensions. The global minimum geometry of ligands was submitted to docking calculations in the previously prepared proteins. The van der Waals radii for nonpolar ligand atoms were scaled by a factor of 0.8, thereby decreasing penalties for close contacts. Receptor atoms were not scaled. A first docking run was carried out applying the Standard Precision settings of Glide. Ten poses were saved and resubmitted to docking with the Extra Precision (XP) settings; [39] one pose was saved in this second run. The best ranking pose for each ligand in each protein was submitted to Liaison [29] to derive the scoring function applying the LIE method. Ligands and receptors structures were minimized in free and bound states through 1000 TNCG steps, allowing receptor residues 15 A far from the ligand to be freely relaxed. Implicit GB/SA solvent model was applied for solvation energy calculation.

The calculated U_{vdW}, U_{ele}, and U_{cav} parameters were correlated to experimental activity data using Strike [30] and the Multiple Linear Regression method, validating the model through leave-one-out (LOO) cross-validation analysis.

Conflict of Interests

The authors do not have a direct financial relation with the commercial identity mentioned in their submitted paper that might lead to a conflict of interests for any of them.

Acknowledgments

The ESI/MS and NMR spectral data were provided by Centro di Ricerca Interdipartimentale di Analisi Strumentale, Università degli Studi di Napoli "Federico II." The assistance of the staff is gratefully appreciated. This work was supported by grant *from MIUR—PRIN 2005*.

References

[1] M. D. Sternlicht and Z. Werb, "How matrix metalloproteinases regulate cell behavior," *Annual Review of Cell and Developmental Biology*, vol. 17, pp. 463–516, 2001.

[2] H. Nagase and J. F. Woessner Jr, "Matrix metalloproteinases," *The Journal of Biological Chemistry*, vol. 274, no. 31, pp. 21491–21494, 1999.

[3] C. Chang and Z. Werb, "The many faces of metalloproteases: cell growth, invasion, angiogenesis and metastasis," *Trendsin Cell Biology*, vol. 11, pp. S37–S43, 2001.

[4] C. Streuli, "Extracellular matrix remodelling and cellular differentiation," *Current Opinion in Cell Biology*, vol. 11, no. 5, pp. 634–640, 1999.

[5] W. C. Parks, C. L. Wilson, and S. Y. López-Boado, "Matrix metalloproteinases as modulators of inflammation and innate immunity," *Nature Reviews Immunology*, vol. 4, no. 8, pp. 617–629, 2004.

[6] M. Egeblad and Z. Werb, "New functions for the matrix metalloproteinases in cancer progression," *Nature Reviews Cancer*, vol. 2, no. 3, pp. 161–174, 2002.

[7] S. Zucker, C. Jian, and W. T. Chen, "Critical appraisal of the use of matrix metalloproteinase inhibitors in cancer treatment," *Oncogene*, vol. 19, no. 56, pp. 6642–6650, 2000.

[8] C. M. Overall and C. López-Otín, "Strategies for MMP inhibition in cancer: innovations for the post-trial era," *Nature Reviews Cancer*, vol. 2, pp. 657–672, 2002.

[9] M. Hidalgo and S. G. Eckhardt, "Development of matrix mettaloproteinase inhibitors in cancer therapy," *Journalof the National Cancer Institute*, vol. 93, no. 3, pp. 178–193, 2001.

[10] J. F. Fisher and S. Mobashery, "Recent advances in MMP inhibitor design," *Cancer and Metastasis Reviews*, vol. 25, no. 1, pp. 115–136, 2006.

[11] B. Davies, P. D. Brown, N. East, M. J. Crimmin, and F. R. Balkwill, "A synthetic matrix metalloproteinase inhibitor decreases tumor burden and prolongs survival of mice bearing human ovarian carcinoma xenografts," *Cancer Research*, vol. 53, pp. 2087–2091, 1993.

[12] X. Wang, X. Fu, P. D. Brown, M. J. Crimmin, and R. M. Hoffman, "Matrix metalloproteinase inhibitor BB-94 (batimastat) inhibits human colon tumor growth and spread in a patient-like orthotopic model in nude mice," *Cancer Research*, vol. 54, no. 17, pp. 4726–4728, 1994.

[13] A. H. Drummond, P. Beckett, P. D. Brown et al., "Preclinical and clinical studies of MMP inhibitors in cancer," *Annals of the New York Academy of Sciences*, vol. 878, pp. 228–235, 1999.

[14] L. M. Coussens, B. Fingleton, and L. M. Matrisian, "Matrix metalloproteinase inhibitors and cancer: trials and tribulations," *Science*, vol. 295, no. 5564, pp. 2387–2392, 2002.

[15] E. Breuer, J. Frant, and R. Reich, "Recent non-hydroxamate matrix metalloproteinase inhibitors," *Expert Opinion on Therapeutic Patents*, vol. 15, no. 3, pp. 253–269, 2005.

[16] D. T. Puerta and S. M. Cohen, "A bioinorganic perspective on matrix metalloproteinase inhibition," *Current Topics in Medicinal Chemistry*, vol. 4, no. 23, pp. 1551–1573, 2004.

[17] Puerta, D. T. Mongan, J. Ba, L. Tran, J. McCammon, and S. M. Cohen, "Potent, selective pyrone-based inhibitors of stromelysin-1," *Journal of the American Chemical Society*, vol. 127, pp. 14148–14149, 2005.

[18] F. Grams, H. Brandstetter, S. DAlò et al., "Pyrimidine-2,4,6-Triones: a new effective and selective class of matrix metalloproteinase inhibitors," *Biological Chemistry*, vol. 382, pp. 1277–1285, 2001.

[19] M. T. Rubino, M. Agamennone, C. Campestre et al., "Cover picture: biphenyl sulfonylamino methyl bisphosphonic acids as inhibitors of matrix metalloproteinases and bone resorption," *Chemmedchem*, vol. 6, no. 7, p. 1133, 2011.

[20] J. W. Skiles, N. C. Gonnella, and A. Y. Jeng, "The design, structure, and clinical update of small molecular weight matrix metalloproteinase inhibitors," *Current Medicinal Chemistry*, vol. 11, no. 22, pp. 2911–2977, 2004.

[21] M. Whittaker, C. D. Floyd, P. Brown, and A. J. H. Gearing, "Design and therapeutic application of matrix metalloproteinase inhibitors," *ChemicalReviews*, vol. 99, no. 9, pp. 2735–2776, 1999.

[22] G. W. Kabalka, M. Varma, R. S. Varma, P. C. Srivastava, and F. F. Knapp Jr., "Tosylation of alcohols," *Journal of Organic Chemistry*, vol. 51, no. 12, pp. 2386–2388, 1986.

[23] P. Campiglia, I. Gomez-Monterrey, L. Longobardo, T. Lama, E. Novellino, and P. Grieco, "An efficient approach for monosulfide bridge formation in solid-phase peptide synthesis," *Tetrahedron Letters*, vol. 45, no. 7, pp. 1453–1456, 2004.

[24] C. K. Wada, J. H. Holms, M. L. Curtin et al., "Phenoxyphenyl sulfone N-formylhydroxylamines (Retrohydroxamates) as potent, selective, orally bioavailable matrix metalloproteinase inhibitors," *Journal of Medicinal Chemistry*, vol. 45, no. 1, pp. 219–232, 2002.

[25] C. M. Overall and O. Kleifeld, "Towards third generation matrix metalloproteinase inhibitors for cancer therapy," *The British Journal of Cancer*, vol. 94, no. 7, pp. 941–946, 2006.

[26] B. G. Rao, "Recent developments in the design of specific matrix metalloproteinase inhibitors aided by structural and computational studies," *Current Pharmaceutical Design*, vol. 11, no. 3, pp. 295–322, 2005.

[27] F. E. Jacobsen, J. A. Lewis, and S. M. Cohen, "The design of inhibitors for medicinally relevant metalloproteins," *ChemMedChem*, vol. 2, no. 2, pp. 152–171, 2007.

[28] P. Cuniasse, L. Devel, A. Makaritis et al., "Future challenges facing the development of specific active-site-directed synthetic inhibitors of MMPs," *Biochimie*, vol. 87, no. 3-4, pp. 393–402, 2005.

[29] A. Agrawal, D. Romero-Perez, J. A. Jacobsen, F. J. Villarreal, and S. M. Cohen, "Zinc-binding groups modulate selective inhibition of MMPs," *ChemMedChem*, vol. 3, no. 5, pp. 812–820, 2008.

[30] J. Åqvist, C. Medina, and J. E. Samuelsson, "A new method for predicting binding affinity in computer-aided drug design," *Protein Engineering*, vol. 7, no. 3, pp. 385–391, 1994.

[31] T. Hansson and J. Åqvist, "Estimation of binding free energies for HIV proteinase inhibitors by molecular dynamics simulations," *Protein Engineering*, vol. 8, no. 11, pp. 1137–1144, 1995.

[32] C. M. Overall and O. Kleifeld, "Validating matrix metalloproteinases as drug targets and anti-targets for cancer therapy," *Nature Reviews Cancer*, vol. 6, no. 3, pp. 227–239, 2006.

[33] M. D. Martin and L. M. Matrisian, "The other side of MMPs: protective roles in tumor progression," *Cancer and Metastasis Reviews*, vol. 26, pp. 717–724, 2007.

[34] G. S. Butler and C. M. Overall, "Proteomic identification of multitasking proteins in unexpected locations complicates drug targeting," *Nature Reviews Drug Discovery*, vol. 8, no. 12, pp. 935–948, 2009.

[35] *Maestro, Version 9. 3, MacroModel, Version 9. 9, Glide, Version 5. 8, Liaison, Version 5. 8, Strike, Version 2. 1*, Schrödinger LLC, New York, NY, USA, 2012.

[36] T. A. Halgren, R. B. Murphy, R. A. Friesner et al., "Glide: a new approach for rapid, accurate docking and scoring. 2. Enrichment factors in database screening," *Journal of Medicinal Chemistry*, vol. 47, no. 7, pp. 1750–1759, 2004.

[37] R. A. Friesner, J. L. Banks, R. B. Murphy et al., "Glide: a new approach for rapid, accurate docking and scoring. 1. Method and assessment of docking accuracy," *Journal of Medicinal Chemistry*, vol. 47, no. 7, pp. 1739–1749, 2004.

[38] H. M. Berman, J. Westbrook, Z. Feng, G. Gilliland, T. N. Bhat et al., "The protein data bank," *Nucleic Acids Research*, vol. 28, no. 1, pp. 235–242, 2000.

[39] R. A. Friesner, R. B. Murphy, M. P. Repasky et al., "Extra precision glide: docking and scoring incorporating a model of hydrophobic enclosure for protein-ligand complexes," *Journal of Medicinal Chemistry*, vol. 49, no. 21, pp. 6177–6196.

Hindawi Publishing Corporation
Journal of Amino Acids
Volume 2013, Article ID 939804, 7 pages
http://dx.doi.org/10.1155/2013/939804

Review Article

Potential Anticarcinogenic Peptides from Bovine Milk

Giacomo Pepe,[1] Gian Carlo Tenore,[2] Raffaella Mastrocinque,[1] Paola Stusio,[3] and Pietro Campiglia[1]

[1] *Dipartimento di Scienze Farmaceutiche e Biomediche, Università degli Studi di Salerno, Via Ponte Don Melillo, 84084 Fisciano, Italy*
[2] *Dipartimento di Chimica Farmaceutica e Tossicologica, Università di Napoli "Federico II," Via D. Montesano 49, 80131 Napoli, Italy*
[3] *Dipartimento di Biochimica e Biofisica, Seconda Università di Napoli, Via L. De Crecchio 7, 80138 Napoli, Italy*

Correspondence should be addressed to Giacomo Pepe; gipepe@unisa.it

Received 21 December 2012; Accepted 28 January 2013

Academic Editor: Michele Caraglia

Bovine milk possesses a protein system constituted by two major families of proteins: caseins (insoluble) and whey proteins (soluble). Caseins (α_{S1}, α_{S2}, β, and κ) are the predominant phosphoproteins in the milk of ruminants, accounting for about 80% of total protein, while the whey proteins, representing approximately 20% of milk protein fraction, include β-lactoglobulin, α-lactalbumin, immunoglobulins, bovine serum albumin, bovine lactoferrin, and lactoperoxidase, together with other minor components. Different bioactivities have been associated with these proteins. In many cases, caseins and whey proteins act as precursors of bioactive peptides that are released, in the body, by enzymatic proteolysis during gastrointestinal digestion or during food processing. The biologically active peptides are of particular interest in food science and nutrition because they have been shown to play physiological roles, including opioid-like features, as well as immunomodulant, antihypertensive, antimicrobial, antiviral, and antioxidant activities. In recent years, research has focused its attention on the ability of these molecules to provide a prevention against the development of cancer. This paper presents an overview of antitumor activity of caseins and whey proteins and derived peptides.

1. Introduction

Milk proteins can exert a wide range of physiological activities, including enhancement of immune function, defense against pathogenic bacteria, viruses, and yeasts, and development of the gut and its functions [1]. Besides the biologically active proteins naturally occurring in milk, a variety of bioactive peptides are encrypted within the sequence of milk proteins that are released upon suitable hydrolysis of the precursor protein. A large range of bioactivities has been reported for milk protein components, with some showing more than one kind of biological activity [2]. Particularly, the present paper reviews the most important antitumor peptides derived from milk proteins (Table 1).

Peptides derived from casein digestion have demonstrated antimutagenic properties [3]. Animal models for colon and mammary tumorigenesis have generally shown that whey protein is superior to other dietary proteins for suppression of tumour development [4]. This benefit is attributed to its high content of cystine/cysteine and γ-glutamylcyst(e)ine dipeptides, which are efficient substrates for the synthesis of glutathione, an ubiquitous cellular antioxidant that destroys reactive oxygen species and detoxifies carcinogens. Whey protein components, β-lactoglobulin, α-lactalbumin, and serum albumin were studied infrequently, but results suggest they have anticancer potential [2]. The minor component lactoferrin has received the most attention; it inhibits intestinal tumours and perhaps tumours at other sites. Lactoferrin acts by induction of apoptosis, inhibition of angiogenesis, and modulation of carcinogen metabolising enzymes and perhaps acts as an iron scavenger. Supplementing cows with selenium increases the content of selenoproteins in milk, which on isolation inhibited colon tumorigenesis in rats.

Table 1: Anticancer peptide and proteins from bovine milk [5].

Family proteins	Protein precursors		Concentration (g/L)	M.W.†	Peptide fragments	Amino acid sequence
Caseins			24–28		Caseinphosphopeptides	PPPEE$^{\zeta}$
	α_{s1}-casein	α_{s1}-CN	12–15	22.1–23.7	α_{s1}-casein f(90–95)	RYLGYL
					α_{s1}-casein f(90–96)	RYLGYLE
					α_{s1}-casomorphin f(158–162)	YVPFP
	β-casein	β-CN	9–11	23.9–24.1	β-Casomorphins 5 f(60–64)	YPFPG
					β-Casomorphins 7 f(60–66)	YPFPGPI
					Morphiceptin f(60–63)-NH_2	YPFP-NH_2
Whey proteins			5–7			
	β-lactoglobulin	β-lg	2–4	18.3		
	α-lactalbumin	α-la	1–1.5	14.2		
	Bovine serum albumin	BSA	0.1–0.4	66		
	Lactoferrin	Lf	0.1	80	Bovine lactoferricin (LfcinB)	FKCRRWQWRMKK LGAPSITCVRRAF

$^{\zeta}$Characteristic cluster sequence of CPPs.
†Molecular weight expressed in kDa.

2. Caseins

2.1. α- and β-Casomorphins. β-Casomorphins (β-CMs) are a group of exogenous opioid-like peptides derived from the hydrolysis of β-casein and were first isolated from an enzymatic casein digest [6]. Their primary amino acid sequence is NH_2-Tyr-Pro-Phe-Pro-Gly-Pro-Ile-Pro-Asn-Ser-Leu-COOH, located in bovine β-casein at positions 60–70. It was reported that β-CMs may reach significant level in the stomach because they are fairly resistant to proteolysis due to their proline-rich sequence [7].

α-Casomorphins (exorphins) have been isolated from peptic hydrolysates of α-casein fractions. In general, their structures differ considerably from those of β-casomorphins. Active fractions were shown to be a mixture of two separate peptides derived from α_1-casein fragments 90–95 and 90–96 [Arg_{90}-Tyr-Leu-Gly-Tyr-Leu_{95}-(Glu_{96})]. The N-terminal arginine residue was also reported to be essential for opioid activity.

α- and β-Casomorphins may be produced by the enzymatic action of different proteases released from tumor cells [8, 9]. Indeed, Hatzoglou et al. [10] have shown that five different casomorphins, α-casein fragments 90–95 and 90–96 [11], β-Casomorphins 7 (BCM7) fragment 60–66, β-Casomorphins 5 (BCM5) fragment 60–64, and the morphiceptin, the amide of β-Casomorphins 4, have an antiproliferative action on T47D cells, blocking cells in G0/G1 phase.

It is, therefore, possible to make two important considerations: one, on the inhibition that appears to be due to the interaction between the casomorphins and opioid receptors binding sites, decreasing cell proliferation in a dose-dependent manner; another, covering the essential requirements for the interaction of casomorphins with opioid receptors, that are identified by the hydrophobic character of proteins, their high content of proline and the presence of tyrosine at the N-terminal [12]. Also, it appears that, with the exception of morphiceptin whose action is mediated by type II somatostatin receptors, all peptides interact with to δ- and κ-opioid binding sites of T47D cells with different selectivity. It is interesting to note that all casomorphins show a significant interaction with somatostatin receptors in T47D cells, as these peptides may have a major physiological role in breast cancer. Furthermore, the interaction of casomorphins with opioid and somatostatin receptors leads to the inhibition of intracellular levels of cAMP.

Subsequently, Kampa et al. [13] have identified a new casomorphin pentapeptide (α_{s1}-casomorphin), isolated from α_{s1}-casein, with the sequence Tyr-Val-Pro-Phe-Pro (f158–162), capable of inhibiting, in a dose-dependent and reversible manner, the proliferation of T47D human breast cancer cells. Differently from other casomorphins, α_{s1}-casomorphin does not interact with somatostatin receptors in our system.

Recently, De Simone et al. [14] have isolated a partially purified peptide subfraction from buffalo cheese acid whey, called f3, which reduces colon cell proliferation about 30% compared with the control sample represented by H-CaCo2 cells untreated with peptide extract.

The cytomodulatory and antioxidant effects of complex peptide fraction of the buffalo milk waste whey (BWW) in human epithelial colon cancer cells are due at a reduction of mitochondrial superoxide anion level and a subsequent decrease in Hsp 70 and 90 expression. Moreover, a 5-fold decrease was observed in cyclin A expression and cell cycle arrest in G1/G0 phases. These responses were associated with increases in expression of alkaline phosphatase activity, marker of enterocytic differentiation, and senescence-associated (β)-galactosidase.

Moreover, it seems that inhibition effects of f3 on H-CaCo2 cell proliferation may be mediated by secretion of ceramides which resulted in cell cycle arrest, differentiation and in subsequent accelerated senescence.

The structural analyses carried out on f3 showed the presence of peptides β-CN f57–68 and f60–68, precursors of the agonist opioids BCM7 and BCM5 [15]. These peptides could reduce colon cells proliferation by interaction with specific opioid, and somatostatin receptors, present in the intestinal tract of mammals.

2.2. Caseinphosphopeptides. Caseinphosphopeptides (CPPs) are a family of bioactive peptides derived from digestion of casein. Their name is due to their high content of phosphorylated sites, and they are characterized by the ability to bind and solubilize calcium [16]. This property is responsible for their anticancer activity against intestinal tumor HT-29 cells, by modulating cell proliferation and apoptosis.

More recently, it was demonstrated that in HT-29 cells, as well as in a primary human colon cancer cell line (AZ-97), the activation of voltage-activated L-type calcium channels, which mediate the calcium influx according to the depolarization state of the cell, is correlated to apoptosis, and their blockade may promote the growth of colon cancer cells [17]. Perego et al. [18] have demonstrated that CPPs protect differentiated intestinal cells from calcium overload toxicity, prevent their apoptosis favoring proliferation, and at the same time induce apoptosis in undifferentiated tumor cells. Probably, this effect is the result of binding of CPPs with extracellular calcium with a precise dose-response relationship, causing a reduction in the cell proliferation rate and apoptosis. In fact, antagonists of calcium channels abolish the response to CPPs or reduce both percentage of responsive cells and the increase of intracellular calcium concentration.

3. Whey Proteins

3.1. α-Lactoalbumin. α-Lactoalbumin (α-LA) is, quantitatively, the second most important protein in whey, and it contains 123 amino acid residues with a molecular weight of 14,175 kDa and isoelectric point between 4.2 and 4.5 [19]. In aqueous solution, α-LA has a globular structure stabilized by four disulphide bonds, and, actually, three genetic variants (A, B, and C) have already been identified [20]. This globular protein consists in a single polypeptide chain with eight cysteine residues, and it is physiologically important because of its requirements in lactose synthesis.

Some important bioactivities have been reported for α-LA. The best known is the antitumoral activity observed for the complex of bovine α-lactalbumin and oleic acid (BAMLET), the bovine counterpart of HAMLET (human α-lactalbumin and oleic acid), that seems to kill tumor cells via a mechanism involving lysosomal membrane permeabilization. It consists of the calcium depleted apo form of α-LA in the aforementioned molten globule state, which is stabilized by a fatty acid cofactor. It is noteworthy that the α-LA/fatty acid interaction is stereo-specific; it is for this reason that unsaturated *cis*-fatty acids bind to α-LA, and only the C18 : 1 : 9 *cis*-fatty acid (oleic acid), that interacts with α-LA in a compact conformation, is active against tumor cells [21, 22]. BAMLET accumulates rapidly and specifically in the endolysosomal compartment of tumor cells and induces an early leakage of lysosomal cathepsins into the cytosol followed by the activation of the protein Bax, a proapoptotic Bcl-2 family protein.

α-LA can also be a potent calcium concentration-elevating and apoptosis-inducing agent [23]. Multimeric form of α-LA was shown to promote apoptosis in transformed and immature cells while sparing mature epithelial cells. During this process calcium levels are elevated, allowing a connection between calcium levels and apoptosis. Probably, α-LA interacts with cell surface modulators altering calcium transport rates, intracellular calcium, and cell growth rate. High affinity to metal ions is mainly due to junction to subdomains at 79–88 containing five aspartates [24]. Furthermore, this protein possesses antiproliferative effects on colon adenocarcinoma cell lines (CaCo2 or HT-29 monolayers). Low concentrations of α-LA (10–25 μg/mL) stimulate growth during the first 3 to 4 days. After growing for 4 days, proliferation ceases and viable cell numbers decrease dramatically, suggesting a delayed initiation of apoptosis [25].

3.2. β-Lactoglobulin. β-Lactoglobulin (β-Lg) is quantitatively a noncasein protein in bovine milk (58% w/w). It is a small, soluble, and globular protein, but its quaternary structure depends on the medium pH. At pH of 3.0 and above 8.0, β-Lg is a monomer molecule with a molecular weight of 18 kDa, while, at pH between 7.0 and 5.2, it is a stable dimer with molecular mass of about 36.7 kDa; at pH between 5.2 and 3.5 it is an octamer with molecular mass of 140 kDa. β-Lg is composed mainly of β-sheet motifs and consists of 162 aminoacid residues [5].

β-Lg has been implicated in providing protection against development of cancer in animal models when delivered orally. The mechanism of anticancer activity of β-Lg may be related to its sulphur aminoacid content. This suggests a possible role in protecting DNA in methylated form. Indeed, the aminoacid composition of β-Lg plays an important role in preventing oxidative damage. Particularly, β-Lg influences tissue levels of the thiol-glutathione, a multifunctional tripeptide, that binds and eliminates endogenous and exogenous mutagens and carcinogens.

Since the precursors for the synthesis of glutathione, as cysteine and glutamylcysteine, are provided by β-Lg, it is possible to establish a relationship between tripeptide levels and β-Lg [26]. The high nutritional and functional value of β-Lg is widely recognized and has made this protein an ingredient of choice in the formulation of modern foods and beverages [27].

3.3. Bovine Serum Albumin. Bovine serum albumin (BSA) is not synthesized in the mammary gland, but appears in milk following passive leakage from the blood stream. It contains 582 aminoacid residues with a molecular weight of 66,267 kDa; it also possesses 17 intermolecular disulphide bridges and one thiol-group at residue 34 [19]. Because of its size, BSA can bind to free fatty acids and other lipids as well as flavour compounds [28]—a feature that is severely hampered upon denaturation. Its heat-induced gelation at pH 6.5 is initiated by an intermolecular thiol-disulphide interchange, similar to what happens with β-Lg [29].

BSA inhibits the growth of MCF-7 human breast cancer cell line [30]. Inhibition of MCF-7 cell proliferation by BSA is in a concentration-dependent manner. BSA may affect cell proliferation by modulating the activities of autocrine growth regulatory factors.

BSA has also been reported to exhibit strong antiproliferative effects against a Chinese hamster epithelial cell line,

although the mechanisms for this inhibition remain unclear [31].

3.4. Lactoferricin. Lactoferrin, an iron-binding glycoprotein with a molecular weight of about 80 kDa (703-amino acid), is mainly found in external secretions that include breast milk and saliva and in the secretory granules of neutrophils. In addition to its antimicrobial effects, it is well known to possess a variety of biological activities, like regulation of immune response [32, 33], cells transcriptional activation [34], and antiviral activity [35]. The antimicrobial activity of bovine lactoferrin (LF-B) has been attributed to the bovine lactoferricin fragment (LfcinB), which, unlike the parental glycoprotein, displays no iron-binding capacity. In fact, the LfcinB is considered as the active domain responsible for antimicrobial activity of LF-B, against a wide range of microorganisms.

Lactoferricin is a cationic peptide produced by acid-pepsin hydrolysis of mammalian lactoferrin [36], and it consists of 25 aminoacid residues (FKCRRWQWRMKKLGAPSITCVRRAF), including two cysteine residues that create a disulfide bond linking the highly positively charged NH_2-terminal region and the COOH-terminal region of the peptide [37]. LfcinB has a high content of asymmetrically clustered basic aminoacid residues, giving the peptide a net positive charge of 7.84 at pH 7.0.

Its amphipathic property is given by the twisted β-sheet structure that LfcinB assumes in aqueous solution, in which nearly all of the hydrophobic residues are found on one face with the basic aminoacid residues positively charged on the opposing face.

The cytotoxic activity of LfcinB has been demonstrated *in vitro* on many different types of rat and human cancer cell lines, including leukemia, fibrosarcoma, various carcinoma, and neuroblastoma cells [38–41], at concentrations that do not substantially affect the viability of normal fibroblasts, lymphocytes, epithelial cells, endothelial cells, or erythrocytes [40, 42]. The selectivity of action of LfcinB is due to its strongly cationic nature that allows the peptide to target negatively charged cancer cells, whereas healthy untransformed cells are spared because of their net neutral charge due to the high content of zwitterionic phosphatidylcholine in the outer membrane leaflet [43]. The net negative charge that is associated with the outer membrane leaflet of many cancer cells results from differential branching and sialic acid content of N-linked glycans associated with transmembrane glycoproteins [44], as well as elevated expression of anionic molecules such as phosphatidylserine [45, 46] and O-glycosylated mucins [43, 47].

It is this selectivity of action that makes LfcinB unable to bind to PC3 prostate carcinoma cells. Therefore, it seems possible that some cancer cells may be refractory to the cytotoxic effect of LfcinB treatment due to an insufficient net negative charge to promote a strong electrostatic interaction with cationic LfcinB.

Since the cytotoxic activity of LfcinB against cancer cells strongly depends on its structure, amphipathic nature and high net positive charge (+7, if compared to +4 for antimicrobial activity), this activity is, therefore, increased in LfcinB derivatives with clear cationic and hydrophobic moieties, while a glutamic acid-containing homologue of murine lactoferricin lacks the ability to kill cancer cells [48–50].

The activities against fibrosarcoma and neuroblastoma rat cells instead of human cells can be explained by a mechanism that induces the formation of transmembrane pores that allow the peptide to enter the cytoplasmic compartment of the cancer cell and colocalize with negatively charged mitochondria, causing cell death primarily via necrosis by a cell membrane lytic effect. In fact in terms of structural membrane changes, insertion of LfcinB [51] promotes the formation of inverted hexagonal or bicontinuous cubic phases in membrane mimetic systems [52–56]. In contrast, LfcinB kills human T-leukemia and breast cancer cells by triggering caspase-3 activation through the mitochondrial pathway of apoptosis.

According to studies conducted by Yoo et al. [38], LfcinB is able to kill THP-1 human monocytic leukemia cells by the activation of apoptotic pathways. Its apoptosis-inducing activity is associated with the production of intracellular ROS and activation of Ca^{2+}/Mg^{2+}-dependent endonucleases. Treatment of THP-1 cells with LfcinB (100 μg/mL) elicited apoptosis with maximal activity after about 10 h, whereas LF-B did not induce cell death even at a dose of 500 μg/mL. THP-1 cells treated with LfcinB exhibited fragmented DNA in a dose-dependent manner, a time- and dose-dependent progressive reduction in cell membrane integrity that allowed LfcinB to enter the cytoplasmic compartment. However, the membrane-lytic effect of extracellular LfcinB, that does not depend on internalization of the peptide, may also contribute to the LfcinB-induced cytotoxicity. In fact, the addition of Zn^{2+}, an inhibitor of endonucleases, which requires divalent cations for their full activity, inhibited LfcinB-induced cell death. However, LfcinB-induced apoptosis in THP-1 cells was effectively abolished by the addition of antioxidants, such as NAC (N-acetyl-cysteine) and GSH (glutathione), similarly to that induced by H_2O_2.

The capacity of LfcinB to induce apoptosis in cancer cells through a pathway mediated by the production of the intracellular ROS and activation of Ca^{2+}/Mg^{2+}-dependent endonucleases was confirmed by Mader et al. [57], who also documented the mitochondrial pathway of apoptosis for LfcinB. Mader et al. [57] demonstrated that LfcinB-induced apoptosis in human T-leukemia cells was triggered by a sequence of events consisting of LfcinB-mediated permeabilization of the cell membrane, uptake across the damaged cell membrane, colocalization with mitochondria, and depolarization of mitochondria, resulting in cytochrome C release, combination of cytosolic Apaf-1 responsible for recruiting and activating procaspase-9, thereby forming the apoptosome that triggers the caspase cascade and leads to cell death by apoptosis.

Other studies have reported that induction of apoptotic or necrotic cell death is dependent on the concentration of the peptide [41, 58] because the cytotoxic activity of LfcinB is reduced in the presence of high concentrations

of serum. In fact, systemic or intratumoral administration of LfcinB inhibits the *in vivo* growth and/or metastasis of several different tumor types in mice [38, 39, 41]. This inhibitory effect of Lfcin-induced apoptosis is the result of neutralization by anionic serum components rather than proteolytic degradation.

It has been recently shown that LfcinB-induced apoptosis in B-lymphoma cells does not involve the caspase cascade but determines apoptosis via the activation of cathepsin B [59].

Mader et al. [60] have shown that LfcinB may interfere with the interaction of the heparin-binding growth factors bFGF and VEGF with their receptors on the surface of endothelial cells, resulting in decreased endothelial cell proliferation and diminished angiogenesis [61]. Although the exact mechanism by which LfcinB interacts with heparin-like molecules has not been elucidated yet, it was hypothesized that the affinity that LfcinB displays for heparin-like structures is the result of electrostatic interactions between the positive charge of LfcinB and negative charge of heparin and heparan sulfate. This antiangiogenic activity is dependent on the primary structure of the peptide since a scrambled peptide comprised of the same aminoacid residues fails to effectively compete with bFGF or VEGF for heparin-like binding sites on endothelial cells.

However, the main limitation of systemic administration of LfcinB for the antiangiogenic therapy is the susceptibility of the peptide to enzymatic digestion and inactivation through interactions with anionic serum components.

4. Conclusions

Peptides derived from milk protein have been shown to exert beneficial effects on human health. These biological properties may play an important role in the development of medical foods that treat or mitigate the effects of diseases. Bioactive peptide preparations have the potential to be used in the formulation of functional foods and cosmetics and as potent drugs having well-defined pharmacological effects. With the rise of consumer concerns about the deleterious effects of chemical preservatives and the increasing preference for natural components, milk-derived bioactive substances may have value in food preservation and nutraceuticals. Application of enrichment protocols such as membrane processing and chromatographic isolation may also be an area of future interest in the extraction of potent biofunctional peptides from milk and dairy products and their subsequent utilization as functional food ingredients. Molecular studies are required to clarify the mechanisms by which the bioactive peptides exert their activities.

References

[1] I. Lopez-Exposito and I. Recio, "Protective effect of milk peptides: antibacterial and antitumor properties," *Advances in Experimental Medicine and Biology*, vol. 606, pp. 271–293, 2008.

[2] P. W. Parodi, "A role for milk proteins and their peptides in cancer prevention," *Current Pharmaceutical Design*, vol. 13, no. 8, pp. 813–828, 2007.

[3] A. Tellez, M. Corredig, L. Y. Brovko, and M. W. Griffiths, "Characterization of immune-active peptides obtained from milk fermented by Lactobacillus helveticus," *Journal of Dairy Research*, vol. 77, no. 2, pp. 129–136, 2010.

[4] H. Sasaki and H. Kume, "Nutritional and physiological effects of peptides from whey: milk whey proteins/peptides, natural beneficial modulators of inflammation," *Bulletin of the International Dairy Federation*, vol. 417, pp. 43–50, 2007.

[5] L. Sawyer, "β-lactoglobulin," in *Advanced Dairy Chemistry I*, P. F. Fox and P. McSweeney, Eds., pp. 319–386, Kluwer, Amsterdam, The Netherlands, 3rd edition, 2003.

[6] A. Henschen, F. Lottspeich, V. Brantl, and H. Teschemacher, "Novel opioid peptides derived from casein (β-casomorphins). II. Structure of active components from bovine casein peptone," *Hoppe-Seyler's Zeitschrift fur Physiologische Chemie*, vol. 360, no. 9, pp. 1217–1224, 1979.

[7] Z. Sun, Z. Zhang, X. Wang, R. Cade, Z. Elmir, and M. Fregly, "Relation of β-casomorphin to apnea in sudden infant death syndrome," *Peptides*, vol. 24, no. 6, pp. 937–943, 2003.

[8] F. Jänicke, M. Schmitt, L. Pache et al., "Urokinase (uPA) and its inhibitor PAI-1 are strong and independent prognostic factors in node-negative breast cancer," *Breast Cancer Research and Treatment*, vol. 24, no. 3, pp. 195–208, 1992.

[9] A. K. Tandon, G. M. Clark, G. C. Chamness, J. M. Chirgwin, and W. L. McGuire, "Cathepsin D and prognosis in breast cancer," *New England Journal of Medicine*, vol. 322, no. 5, pp. 297–302, 1990.

[10] A. Hatzoglou, E. Bakogeorgou, C. Hatzoglou, P. M. Martin, and E. Castanas, "Antiproliferative and receptor binding properties of α- and β-casomorphins in the T47D human breast cancer cell line," *European Journal of Pharmacology*, vol. 310, no. 2-3, pp. 217–223, 1996.

[11] S. Loukas, D. Varoucha, and C. Zioudrou, "Opioid activities and structures of α-casein-derived exorphins," *Biochemistry*, vol. 22, no. 19, pp. 4567–4573, 1983.

[12] H. Teschemacher, "Opioid receptor ligands derived from food proteins," *Current Pharmaceutical Design*, vol. 9, no. 16, pp. 1331–1344, 2003.

[13] M. Kampa, S. Loukas, A. Hatzoglou, P. Martin, P. M. Martin, and E. Castanas, "Identification of a novel opioid peptide (Tyr-Val-Pro-Phe-Pro) derived from human αs1 casein (αs1-casomorphin, and αs1-casomorphin amide)," *Biochemical Journal*, vol. 319, no. 3, pp. 903–908, 1996.

[14] C. De Simone, P. Ferranti, G. Picariello et al., "Peptides from water buffalo cheese whey induced senescence cell death via ceramide secretion in human colon adenocarcinoma cell line," *Molecular Nutrition and Food Research*, vol. 55, no. 2, pp. 229–238, 2011.

[15] C. De Simone, G. Picariello, G. Mamone et al., "Characterisation and cytomodulatory properties of peptides from Mozzarella di Bufala Campana cheese whey," *Journal of Peptide Science*, vol. 15, no. 3, pp. 251–258, 2009.

[16] R. Berrocal, S. Chanton, M. A. Juillerat, B. Pavillard, J. C. Scherz, and R. Jost, "Tryptic phosphopeptides from whole casein. II. Physicochemical properties related to the solubilization of calcium," *Journal of Dairy Research*, vol. 56, no. 3, pp. 335–341, 1989.

[17] A. Zawadzki, Q. Liu, Y. Wang, A. Melander, B. Jeppsson, and H. Thorlacius, "Verapamil inhibits L-type calcium channel mediated apoptosis in human colon cancer cells," *Diseases of the Colon and Rectum*, vol. 51, no. 11, pp. 1696–1702, 2008.

[18] S. Perego, S. Cosentino, A. Fiorilli, G. Tettamanti, and A. Ferraretto, "Casein phosphopeptides modulate proliferation and apoptosis in HT-29 cell line through their interaction with voltage-operated L-type calcium channels," *The Journal of Nutritional Biochemistry*, vol. 23, no. 7, pp. 808–816, 2012.

[19] K. Brew, F. J. Castellino, T. C. Vanaman, and R. L. Hill, "The complete amino acid sequence of bovine alpha-lactalbumin," *Journal of Biological Chemistry*, vol. 245, no. 17, pp. 4570–4582, 1970.

[20] P. F. Fox, "The milk protein system," in *Developments of Dairy Chemistry-4-Functional Peptides*, P. F. Fox, Ed., pp. 35–45, Elsevier Applied Science Publishers, London, UK, 1989.

[21] J. Fast, A. K. Mossberg, H. Nilsson, C. Svanborg, M. Akke, and S. Linse, "Compact oleic acid in HAMLET," *FEBS Letters*, vol. 579, no. 27, pp. 6095–6100, 2005.

[22] M. Svensson, J. Fast, A. K. Mossberg et al., "α-lactalbumin unfolding is not sufficient to cause apoptosis, but is required for the conversion to HAMLET (human α-lactalbumin made lethal to tumor cells)," *Protein Science*, vol. 12, no. 12, pp. 2794–2804, 2003.

[23] A. Håkansson, B. Zhivotovsky, S. Orrenius, H. Sabharwal, and C. Svanborget, "Apoptosis induced by a human milk protein," *Proceedings of the National Academy of Sciences of the United States of America*, vol. 92, no. 17, pp. 8064–8068, 1995.

[24] E. A. Permyakov and L. J. Berliner, "α-Lactalbumin: structure and function," *FEBS Letters*, vol. 473, no. 3, pp. 269–274, 2000.

[25] L. G. Sternhagen and J. C. Allen, "Growth rates of a human colon adenocarcinoma cell line are regulated by the milk protein alpha-lactalbumin," *Advances in Experimental Medicine and Biology*, vol. 501, pp. 115–120, 2001.

[26] A. S. Goldman, R. M. Goldblum, and L. A. Hanson, "Anti-inflammatory systems in human milk," in *Antioxidant Nutrients and Immune Functions*, A. Bendich, M. Phillips, and R. P. Tengerdy, Eds., pp. 69–76, Plenum Press, New York, NY, USA, 1990.

[27] D. E. W. Chatterton, G. Smithers, P. Roupas, and A. Brodkorb, "Bioactivity of β-lactoglobulin and α-lactalbumin-Technological implications for processing," *International Dairy Journal*, vol. 16, no. 11, pp. 1229–1240, 2006.

[28] J. E. Kinsella and D. M. Whitehead, "Proteins in whey: chemical, physical, and functional properties," *Advances in Food and Nutrition Research*, vol. 33, no. C, pp. 343–438, 1989.

[29] J. N. de Wit, "Functional properties of whey proteins," in *Developments of Dairy Chemistry-4-Functional Peptides*, P. F. Fox, Ed., pp. 285–322, Elsevier Applied Science Publishers, London, UK, 1989.

[30] I. Laursen, P. Briand, and A. E. Lykkesfeldt, "Serum albumin as a modulator on growth of the human breast cancer cell line, MCF-7," *Anticancer Research A*, vol. 10, no. 2, pp. 343–351, 1990.

[31] I. E. M. Bosselaers, P. W. J. R. Caessens, M. A. J. S. Van Boekel, and G. M. Alink, "Differential effects of milk proteins, BSA and soy protein on 4NQO- or MNNG-induced SCEs in V79 cells," *Food and Chemical Toxicology*, vol. 32, no. 10, pp. 905–909, 1994.

[32] J. Hauer, W. Voetsh, and F. A. Anderer, "Identification of a mannose-acetate-specific 87-kDa receptor responsible for human NK and LAK activity," *Immunology Letters*, vol. 42, no. 1-2, pp. 7–12, 1994.

[33] T. Zagulski, P. Lipinski, A. Zagulska, S. Broniek, and Z. Jarzabek, "Lactoferrin can protect mice against a lethal dose of Escherichia coli in experimental infection in vivo," *British Journal of Experimental Pathology*, vol. 70, no. 6, pp. 697–704, 1989.

[34] J. He and P. Furmanski, "Sequence specificity and transcriptional activation in the binding of lactoferrin to DNA," *Nature*, vol. 373, no. 6516, pp. 721–724, 1995.

[35] P. E. Florian, M. Trif, R. W. Evans, and A. Roşeanu, "An overview on the antiviral activity of Lactoferrin," *Romanian Journal of Biochemistry*, vol. 46, no. 2, pp. 187–197, 2009.

[36] M. Tomita, W. Bellamy, M. Takase, K. Yamauchi, H. Wakabayashi, and K. Kawase, "Potent antibacterial peptides generated by pepsin digestion of bovine lactoferrin," *Journal of Dairy Science*, vol. 74, no. 12, pp. 4137–4142, 1991.

[37] W. Bellamy, M. Takase, K. Yamauchi, H. Wakabayashi, K. Kawase, and M. Tomita, "Identification of the bactericidal domain of lactoferrin," *Biochimica et Biophysica Acta*, vol. 1112, no. 1-2, pp. 130–136, 1992.

[38] Y. C. Yoo, R. Watanabe, Y. Koike et al., "Apoptosis in human leukemic cells induced by lactoferricin, a bovine milk protein-devived peptide: involvement of reactive oxygen species," *Biochemical and Biophysical Research Communications*, vol. 237, no. 3, pp. 624–628, 1997.

[39] L. T. Eliassen, G. Berge, B. Sveinbjørnsson, J. S. Svendsen, L. H. Vorland, and Ø. Rekdal, "Evidence for a direct antitumor mechanism of action of bovine lactoferricin," *Anticancer Research*, vol. 22, no. 5, pp. 2703–2710, 2002.

[40] J. S. Mader, J. Salsman, D. M. Conrad, and D. W. Hoskin, "Bovine lactoferricin selectively induces apoptosis in human leukemia and carcinoma cell lines," *Molecular Cancer Therapeutics*, vol. 4, no. 4, pp. 612–624, 2005.

[41] L. T. Eliassen, G. Berge, A. Leknessund et al., "The antimicrobial peptide, Lactoferricin B, is cytotoxic to neuroblastoma cells in vitro and inhibits xenograft growth in vivo," *International Journal of Cancer*, vol. 119, no. 3, pp. 493–500, 2006.

[42] S. J. Furlong, J. S. Mader, and D. W. Hoskin, "Lactoferricin-induced apoptosis in estrogen-nonresponsive MDA-MB-435 breast cancer cells is enhanced by C6 ceramide or tamoxifen," *Oncology reports.*, vol. 15, no. 5, pp. 1385–1390, 2006.

[43] M. D. Burdick, A. Harris, C. J. Reid, T. Iwamura, and M. A. Hollingsworth, "Oligosaccharides expressed on MUC1 by pancreatic and colon tumor cell lines," *Journal of Biological Chemistry*, vol. 272, no. 39, pp. 20202–24198, 1997.

[44] J. W. Dennis, "N-linked oligosaccharide processing and tumor cell biology," *Seminars in Cancer Biology*, vol. 2, no. 6, pp. 411–420, 1991.

[45] T. Utsugi, A. J. Schroit, J. Connor, C. D. Bucana, and I. J. Fidler, "Elevated expression of phosphatidylserine in the outer membrane leaflet of human tumor cells and recognition by activated human blood monocytes," *Cancer Research*, vol. 51, no. 11, pp. 3062–3066, 1991.

[46] I. Dobrzyńska, B. Szachowicz-Petelska, S. Sulkowski, and Z. Figaszewski, "Changes in electric charge and phospholipids composition in human colorectal cancer cells," *Molecular and Cellular Biochemistry*, vol. 276, no. 1-2, pp. 113–119, 2005.

[47] W. H. Yoon, H. D. Park, K. Lim, and B. D. Hwang, "Effect of O-glycosylated mucin on invasion and metastasis of HM7 human colon cancer cells," *Biochemical and Biophysical Research Communications*, vol. 222, no. 3, pp. 694–699, 1996.

[48] L. T. Eliassen, B. E. Haug, G. Berge, and Ø. Rekdal, "Enhanced antitumour activity of 15-residue bovine lactoferricin derivatives containing bulky aromatic amino acids and lipophilic N-terminal modifications," *Journal of Peptide Science*, vol. 9, no. 8, pp. 510–517, 2003.

[49] N. Yang, M. B. Strøm, S. M. Mekonnen, J. S. Svendsen, and Ø. Rekdal, "The effects of shortening lactoferrin derived peptides

against tumour cells, bacteria and normal human cells," *Journal of Peptide Science*, vol. 10, no. 1, pp. 37–46, 2004.

[50] J. L. Gifford, H. N. Hunter, and H. J. Vogel, "Lactoferricin: a lactoferrin-derived peptide with antimicrobial, antiviral, antitumor and immunological properties," *Cellular and Molecular Life Sciences* , vol. 62, no. 22, pp. 2588–2598, 2005.

[51] S. Riedl, B. Rinner, S. Tumer, H. Schaider, K. Lohner, and D. Zweytick, "Targeting the cancer cell membrane specifically with human lactoferricin derivatives," *Annals of Oncology*, vol. 22, pp. 31–34, 2011.

[52] E. Staudegger, E. J. Prenner, M. Kriechbaum et al., "X-ray studies on the interaction of the antimicrobial peptide gramicidin S with microbial lipid extracts: evidence for cubic phase formation," *Biochimica et Biophysica Acta*, vol. 1468, no. 1-2, pp. 213–230, 2000.

[53] R. Willumeit, M. Kumpugdee, S. S. Funari et al., "Structural rearrangement of model membranes by the peptide antibiotic NK-2," *Biochimica et Biophysica Acta*, vol. 1669, no. 2, pp. 125–134, 2005.

[54] A. Hickel, S. Danner-Pongratz, H. Amenitsch et al., "Influence of antimicrobial peptides on the formation of nonlamellar lipid mesophases," *Biochimica et Biophysica Acta*, vol. 1778, no. 10, pp. 2325–2333, 2008.

[55] D. Zweytick, S. Tumer, S. E. Blondelle, and K. Lohner, "Membrane curvature stress and antibacterial activity of lactoferricin derivatives," *Biochemical and Biophysical Research Communications*, vol. 369, no. 2, pp. 395–400, 2008.

[56] D. Zweytick, G. Deutsch, J. Andrä et al., "Studies on Lactoferricin-derived Escherichia coli membrane-active peptides reveal differences in the mechanism of N-acylated versus nonacylated peptides," *Journal of Biological Chemistry*, vol. 286, no. 24, pp. 21266–21276, 2011.

[57] J. S. Mader, A. Richardson, J. Salsman et al., "Bovine lactoferricin causes apoptosis in Jurkat T-leukemia cells by sequential permeabilization of the cell membrane and targeting of mitochondria," *Experimental Cell Research*, vol. 313, no. 12, pp. 2634–2650, 2007.

[58] J. Onishi, M. K. Roy, L. R. Juneja, Y. Watanabe, and Y. Tamai, "A lactoferrin-derived peptide with cationic residues concentrated in a region of its helical structure induces necrotic cell death in a leukemic cell line (HL-60)," *Journal of Peptide Science*, vol. 14, no. 9, pp. 1032–1038, 2008.

[59] S. J. Furlong, J. S. Mader, and D. W. Hoskin, "Bovine lactoferricin induces caspase-independent apoptosis in human B-lymphoma cells and extends the survival of immune-deficient mice bearing B-lymphoma xenografts," *Experimental and Molecular Pathology*, vol. 88, no. 3, pp. 371–375, 2010.

[60] J. S. Mader, D. Smyth, J. Marshall, and D. W. Hoskin, "Bovine lactoferricin inhibits basic fibroblast growth factor- and vascular endothelial growth factor165-induced angiogenesis by competing for heparin-like binding sites on endothelial cells," *American Journal of Pathology*, vol. 169, no. 5, pp. 1753–1766, 2006.

[61] D. W. Hoskin and A. Ramamoorthy, "Studies on anticancer activities of antimicrobial peptides," *Biochimica et Biophysica Acta*, vol. 1778, no. 2, pp. 357–375, 2008.

Hindawi Publishing Corporation
Journal of Amino Acids
Volume 2013, Article ID 606282, 7 pages
http://dx.doi.org/10.1155/2013/606282

Research Article

Design, Synthesis, and Evaluation of New Tripeptides as COX-2 Inhibitors

Ermelinda Vernieri,[1] Isabel Gomez-Monterrey,[2] Ciro Milite,[1] Paolo Grieco,[2] Simona Musella,[3] Alessia Bertamino,[1] Ilaria Scognamiglio,[4] Stefano Alcaro,[5] Anna Artese,[5] Francesco Ortuso,[5] Ettore Novellino,[2] Marina Sala,[1] and Pietro Campiglia[1]

[1] *Dipartimento di Scienze Farmaceutiche e Biomediche, Università degli Studi di Salerno, Via Ponte don Melillo, 84084 Fisciano, Italy*
[2] *Dipartimento di Chimica Farmaceutica e Tossicologica, Università degli Studi di Napoli Federico II, Via D. Montesano 49, 80131 Napoli, Italy*
[3] *Dipartimento Farmaco-Biologico, Università degli Studi di Messina, Viale Annunziata, 98168 Messina, Italy*
[4] *Dipartimento di Biochimica e Biofisica, Seconda Università degli Studi di Napoli, Via L. De Crecchio 7, 80138 Napoli, Italy*
[5] *Dipartimento di Scienze della Salute, Università degli Studi "Magna Grœcia" di Catanzaro, Campus Universitario "S. Venuta", Viale Europa, 88100 Catanzaro, Italy*

Correspondence should be addressed to Marina Sala; msala@unisa.it

Received 21 December 2012; Accepted 17 January 2013

Academic Editor: Michele Caraglia

Cyclooxygenase (COX) is a key enzyme in the biosynthetic pathway leading to the formation of prostaglandins, which are mediators of inflammation. It exists mainly in two isoforms COX-1 and COX-2. The conventional nonsteroidal anti-inflammatory drugs (NSAIDs) have gastrointestinal side effects because they inhibit both isoforms. Recent data demonstrate that the overexpression of these enzymes, and in particular of cyclooxygenases-2, promotes multiple events involved in tumorigenesis; in addition, numerous studies show that the inhibition of cyclooxygenases-2 can delay or prevent certain forms of cancer. Agents that inhibit COX-2 while sparing COX-1 represent a new attractive therapeutic development and offer a new perspective for a further use of COX-2 inhibitors. The present study extends the evaluation of the COX activity to all 20^3 possible natural tripeptide sequences following a rational approach consisting in molecular modeling, synthesis, and biological tests. Based on data obtained from virtual screening, only those peptides with better profile of affinity have been selected and classified into two groups called S and E. Our results suggest that these novel compounds may have potential as structural templates for the design and subsequent development of the new selective COX-2 inhibitors drugs.

1. Introduction

The main cause of the inflammation is the prostaglandins overproduction, which are synthesized by cyclooxygenase enzymes [1].

Prostaglandin-endoperoxide synthase, commonly called cyclooxygenase (COX), is an intracellular enzyme required for the conversion of arachidonic acid to prostaglandins. The two best-known COX isoforms are referred to as COX-1 and COX-2 for the order in which they were discovered [2]. The first isozyme is constitutively expressed in resting cells of most tissues, functions as a housekeeping enzyme, and is responsible for maintaining homeostasis (gastric and renal integrity) and normal production of prostaglandins; *vice versa*, the COX-2 expression is induced by infection and it is responsible for the inflammatory response. Such a difference suggested to report COX-1 as the constitutive form and COX-2 as the inducible one. More recently, the constitutive presence of COX-2 has been highlighted in brain, kidney, and endothelial cells but is virtually absent in most other tissues. In particular, COX-2 expression is significantly upregulated as part of various acute and chronic inflammatory conditions and in neoplastic tissues. The design of a selective inhibitor is difficult as the COX-1 and COX-2 binding sites are almost

identical, and the isoforms show sequence homology of 60–65%. Experimental 3D models of both enzyme structures have shown the complexity of the problem. They suggest that the tertiary conformations of these proteins are very similar, and the substrate binding pocket and catalytic site amino acids are nearly identical in both enzymes. In this case, the only difference is the substitution, at residue position 523, of the COX-1 Ile by the COX-2 Val that, opening an additional pocket, results in an enzyme inducible form binding site larger than the constitutive one. The structural similarities of COX-1 and COX-2 enzymes have made the development of selective inhibitors for COX-2 versus COX-1 a special challenge. Since the discovery of the COX-2 enzyme in the early 1990s, numerous COX-2 selective inhibitors have been proposed (Figure 1).

A common structural feature of these selective COX-2 inhibitors is the presence of two vicinal aryl rings attached to a central five- or six-membered heterocyclic or carbocyclic motif. Typical examples of selective COX-2 inhibitors like celecoxib, rofecoxib, valdecoxib, etoricoxib, and SC57666 demonstrate that a broad variety of five- or six-membered carbo- and heterocycles are acceptable for binding to the cyclooxygenase active site.

Recent reviews on the current status of COX-2 inhibitors further confirm the flexibility of the carbocyclic/heterocyclic core motif for COX-2 binding [3]. Good results were obtained with the coxib family, but their secondary effects, especially affecting the kidney and central nervous system, stimulated the research towards the most powerful substances with a lower isoform selectivity. On the basis of the previously reported information, the present study extends the evaluation of the COX activity to all 20^3 possible natural tripeptide sequences following a rational approach consisting in molecular modeling, synthesis, and biological tests.

2. Materials and Methods

2.1. Molecular Modeling. The PDB entries 1Q4G [4] and 1PXX [5] have been considered as COX-1 and COX-2 receptor models, respectively. The crystallographic resolution, equal to 2.0 Å for 1Q4G and to 2.9 Å for 1PXX, and the kind of cocrystallized ligands, two reversible NSAIDs, have been the choice criterion. The original ligands, α-methyl-4-biphenylacetic acid and diclofenac, respectively, have been removed, and hydrogen atoms, missing into the PDB files, have been added by means of the Maestro GUI [6]. In order to appropriately take into account structural solvent, all cocrystallized water molecules, within 5 Å from the protein atoms, have been included in our preliminary models. Added hydrogen atoms position has been optimized according to MMFFs [7–10] force field implemented in MacroModel ver. 7.2 [11]. The procedure consisted in a preliminary energy minimization computed applying to all nonhydrogen atoms a constant force equal to 200 KJ/mol·Å followed by a further water molecules unconstrained run. Using the same force field and the same constraints, both receptor models final structures have been submitted to 500 ps of molecular dynamics at 300°K, with an integration time step equal to 1.5 fs. In all simulation a distance-dependent dielectric constant equals to 4 has been adopted. Such an approach highlighted the most tightly interacting water molecules that maintained their position, while the other ones have been moved far from the receptor models. In order to achieve a fully relaxed conformation, resulting molecular dynamics structures, containing the tightly interacting solvent molecules only, have been submitted to unconstrained energy minimization producing our COX-1 and COX-2 receptor models.

The 3D tripeptides library was built by an *in-house* PerlMol Chemistry modules-based software. All possible combination of 20 the (*L*)-series natural amino acids have been considered, and the resulting 8000 tripeptide models were energy minimized using the same force field reported for the receptors.

The docking binding site, for both targets, has been defined by means of a regular box centered onto the protein chain A Tyr 385. Its volume was about 390,000 $Å^3$ widely covering COX-1 and -2 binding sites. Glide grid maps have been computed using the standard precision algorithm. Our optimized library has been submitted to flexible Glide docking simulation with respect to both COX receptor models reducing the ligands van der Waals atom radius by a 0.8 factor. Default Glide interaction energies (ECvdW) have been adopted for scoring the tripeptide docking poses.

2.2. Materials. N^{α}-Fmoc-protected amino acids, Wang resin, HOBt, HBTU, DIEA, piperidine, and trifluoroacetic acid were purchased from Iris Biotech (Germany). Peptide synthesis solvents, reagents, and CH_3CN for HPLC were reagent grade and were acquired from commercial sources (Sigma Aldrich, Italy) and used without further purification unless otherwise noted.

2.3. Synthesis. The synthesis of tripeptides (S1–E10) was performed according to the solid phase approach using standard Fmoc methodology in a manual reaction vessel [12]. The first amino acid, N^{α}Fmoc-Xaa-OH, was linked onto the Wang resin (100–200 mesh, 1% DVB, 1.1 mmol/g) and was attached to Wang resin using HOBt/HBTU as an activating agent (3eq.) and a catalytic amount of DMAP.

The following protected amino acids were then added stepwise: N^{α}-Fmoc-Met-OH, N^{α}-Fmoc-Arg(Pbf)-OH, N^{α}-Fmoc-His($N_{(im)}$trityl (Trt))-OH (or N^{α}-Fmoc-Gln(Trt)-OH) N^{α}-Fmoc-Gly-OH, N^{α}-Fmoc-Trp(Boc)-OH, N^{α}-Fmoc-Glu(OtBu-OH, N^{α}-Fmoc-Asp(OtBu)-OH, N^{α}-Fmoc-Phe-OH, N^{α}-Fmoc-Lys(Boc)-OH, N^{α}-Fmoc-Ala-OH, N^{α}-Fmoc-Ser(tBu)-OH, and N^{α}-Fmoc-Ile-OH. Each coupling reaction was accomplished using a 3-fold excess of amino acid with HBTU and HOBt in the presence of DIEA (6 eq.). The N^{α}-Fmoc protecting groups were removed by treating the protected peptide resin with a 25% solution of piperidine in DMF (1 × 5 min and 1 × 25 min). The peptide resin was washed three times with DMF, and the next coupling step was initiated in a stepwise manner. The peptide resin was washed with DCM (3×), DMF (3×), and DCM (3×), and the deprotection protocol was repeated after each coupling step.

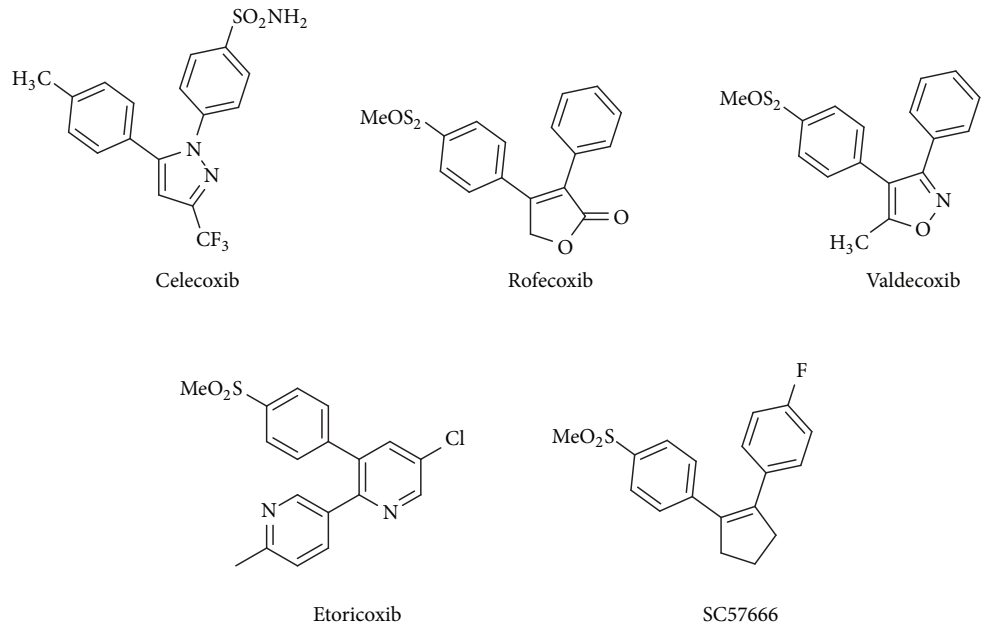

Figure 1: Chemical structures of selective COX-2 inhibitors.

In addition, after each step of deprotection and after each coupling step, Kaiser test was performed to confirm the complete removal of the Fmoc protecting group, respectively, and to verify that complete coupling has occurred on all the free amines on the resin.

The N-terminal Fmoc group was removed as described above, and the peptide was released from the resin with TFA/iPr_3SiH/H_2O (90 : 5 : 5) for 3 h. The resin was removed by filtration, and the crude peptide was recovered by precipitation with cold anhydrous ethyl ether to give a white powder and then lyophilized.

2.4. Purification and Characterization. All crude peptides were purified by RP-HPLC on a semipreparative C18-bonded silica column (Phenomenex, Jupiter, 250 × 10 mm) using a Shimadzu SPD 10A UV/VIS detector, with detection at 215 and 254 nm.

The column was perfused at a flow rate of 3 mL/min with solvent A (10%, v/v, water in 0.1% aqueous TFA), and a linear gradient from 10 to 90% of solvent B (80%, v/v, acetonitrile in 0.1% aqueous TFA) over 40 min was adopted for peptide elution. Analytical purity and retention time (tR) of each peptide were determined using HPLC conditions in the above solvent system (solvents A and B) programmed at a flow rate of 1 mL/min using a linear gradient from 10 to 90% B over 25 min, fitted with C-18 column Phenomenex, Jupiter C-18 column (250 × 4.60 mm; 5 μ).

All analogues showed >97% purity when monitored at 215 nm. Homogeneous fractions, as established using analytical HPLC, were pooled and lyophilized.

Peptides molecular weights were determined by ESI mass spectrometry. ESI-MS analysis in positive ion mode, were made using a Finnigan LCQ ion trap instrument, manufactured by Thermo Finnigan (San Jose, CA, USA), equipped with the Excalibur software for processing the data acquired. The sample was dissolved in a mixture of water and methanol (50/50) and injected directly into the electrospray source, using a syringe pump, which maintains constant flow at 5 μL/min. The temperature of the capillary was set at 220°C (Table 1).

Table 1: Structures and analytical data of tripeptides synthesized.

Peptide	Structure	HPLC	ESI-MS		Yield
		tR	found	calc	
S1	GMD	10.50	322.08	321.10	75%
S2	ERA	9.99	375.3	374.19	80 %
S3	GHE	8.08	342.14	341.13	67%
S4	GER	10.00	361.17	360.18	80%
S5	DRC	9.89	393.20	392.15	62%
S6	ARA	10.46	317.24	316.19	68%
S7	PER	8.87	401.40	400.21	81%
S8	KHI	10.98	397.11	396.25	80%
S9	AER	11.00	375.32	374.19	75%
S10	AGR	9.03	303.34	302.17	79%
E1	SRH	8.95	399.30	398.20	68%
E2	SWE	8.04	421.0	420.16	69%
E3	IRT	8.03	389.3	388.24	76%
E4	SMD	8.00	342.16	351.11	78%
E5	GRN	8.43	346.2	345.18	65%
E6	SHE	8.68	372.17	371.14	76%
E7	SQE	8.45	363.17	362.14	67%
E8	SMH	9.46	374.26	373.14	75%
E9	ARM	8.03	377.6	376.19	77%
E10	AQE	9.97	347.0	346.15	76%

tR: peptide retention time.

2.5. Biological Assay

2.5.1. Preparation of Washed Platelets. Washed human platelets were prepared from blood anticoagulated with citrate-phosphate-dextrose, which was obtained from Centro de Transfusion de Galicia (Santiago de Compostela, Spain).

Bags containing buffy coat from individual donors were diluted with the same volume of washing buffer (NaCl, 120 mM; KCl, 5 mM; trisodium citrate, 12 mM; glucose, 10 mM; sucrose, 12.5 mM; pH 6) and centrifuged at 400 g for 9 min. The upper layer containing platelets (platelet-rich plasma) was removed and centrifuged at 1000 g for 18 min. The resulting platelet pellet was recovered, resuspended with washing buffer, and centrifuged again at 1000 g for 15 min. Finally, the platelet pellet from this step was resuspended in a modified Tyrode-HEPES buffer (HEPES 10 mM; NaCl 140 mM; KCl 3 mM; $MgCl_2$ 0.5 mM; $NaHCO_3$ 5 mM; glucose 10 mM; pH 7.4) to afford a cell density of $3–3.5 \cdot 10^8$ platelet/mL. The calcium concentration in the extracellular medium was 2 mM [13].

2.5.2. hCOX Activity. The potential effects of the test drugs on total hCOX activity (bis-dioxygenase and peroxidase reactions) were investigated by measuring their effects on the oxidation of N,N,N′,N′-tetramethyl-p-phenylenediamine (TMPD) to N,N,N′,N′-tetramethyl-p-phenylenedaimine, using AA as common substrate for both hCOX-1 and hCOX-2, microsomal COX-2 prepared from insect cells (Sf21 cells) infected with recombinant baculovirus containing cDNA inserts for hCOX-2 (Sigma Aldrich Química S.A., Alcobendas, Spain), and COX-1 from human platelet microsomes (obtained as described in the above paragraph since, unlike hCOX-2, hCOX-1 is not available commercially) [14].

3. Results and Discussion

3.1. Design. The purpose of this work consists in the identification of new peptide ligands for COX that show, compared to the current state of the art, a greater power, a lower toxicity, and a high average degree of selectivity.

In particular, the attention has been focused on cyclooxygenase 2 (COX-2) as it has been recently shown to promote multiple events in the tumorigenesis process [15]. Several reports indicate that COXs inhibitors can prevent the development of various human tumors including colon, breast, lung, liver, and gastric neoplasias [16–20].

For several types of cancer, the real risk factor seems to be chronic inflammation that maintains a high level of COX-2 and increases events that promote tumor formation. A tragic example of this mechanism is malignant mesothelioma (MM), a rare tumor of the mesothelial surface of the pleural and peritoneal cavities [21].

The aim of this study is to demonstrate the possibility of modulation of the activity of COX through peptides that may be found in sites in which the inflammatory process is in place.

To achieve this goal, we relied on the data reported in the literature, focused the attention on the structure of COX-2. One of the known potent inhibitors of COX-2 is SC-558 (a dyaril heterocyclic inhibitor) which contains a bromophenyl ring, a pyrazole group, and a phenylsulphonamide moiety. Most of the sulphur containing NSAIDs are selective COX-2 inhibitors, and this sulphur atom reduces the toxicity of the compound.

Using this information, in a recent work, Somvanshi et al. have designed and synthesized several tripeptide sequences containing a hydrophobic amino acid with aromatic ring, a cysteine residue which contains sulphur atom, and a charged residue at the C-terminal end [1]. In particular, 15 tripeptides were screened by ELISA test and the best of them, tripeptide WCS, inhibited more than 85% of the COX-2 activity.

Though the chemical nature of sulphur atom of sulphonamide group in SC-558 and in cysteine residue is different, still similarities in binding constant of peptide with known NSAIDs SC-558 were observed. Thus, preventing the reaction of substrate arachidonic acid with the enzyme supports the possibility of peptide WCS as potent and competitive inhibitor of COX-2. As the phenyl ring of SC-558 interacts with residues in hydrophobic cavity of COX-2 formed by Phe 381, Leu 384, Tyr 385, Trp 387, Phe 518, and Ser 530, it can be assumed that the aromatic ring of tryptophan residue of peptide will also interact with residues in hydrophobic cavity. The free carboxylate group of the peptide can electrostatically interact to Arg 120. WCS can be considered as a potential *lead compound* for developing a new class of COX-2 inhibitors.

Extending the study of Somvanshi et al. [1], we have built a complete tripeptide virtual library containing all possible combinations of the 20 (*L*)-series natural amino acids. The COX-1 and -2 binding pocket recognition, of the 8000 library hits, has been investigated by means of molecular docking techniques, and the resulting complexes stability has been evaluated using the theoretical ligand-enzyme binding energies. The selection of the peptides, for the experimental tests, has been driven by their affinity with respect to both COX isoforms. Such a task has been carried out by computing the ratio between COX-2 and COX-1 peptide interaction energy. The top two COX-2 interacting compounds, still maintaining affinity for the COX-1, and one theoretically inactive peptide have been selected. The first couple corresponds to the sequences Gly-Met-Asp (GMD) and Gly-His-Glu (GHE), while the last one is Tyr-Tyr-Val (YYV). GMD and GHE showed a strong recognition to COX-2 and a weaker interaction to COX-1; YYV was unable to fit into both binding pockets due to its steric hindrance (Table 2).

The graphical inspection of the GMD and GHE COXs complexes revealed, for both peptides, remarkable different recognition of the two enzymes (Figure 2).

In all cases our compounds have occupied the known NSAID binding pocket. Interestingly, the number of enzyme interacting residues, comprise between 21 and 26, is quite similar, but the COX-2 hydrogen bond network is much better than COX-1 and could explain the selectivity of our ligands. COX-2 Ser 530 side chain is involved in hydrogen bond to GMD backbone and, through a water molecule bridge, to the carboxylate groups of both our active peptides.

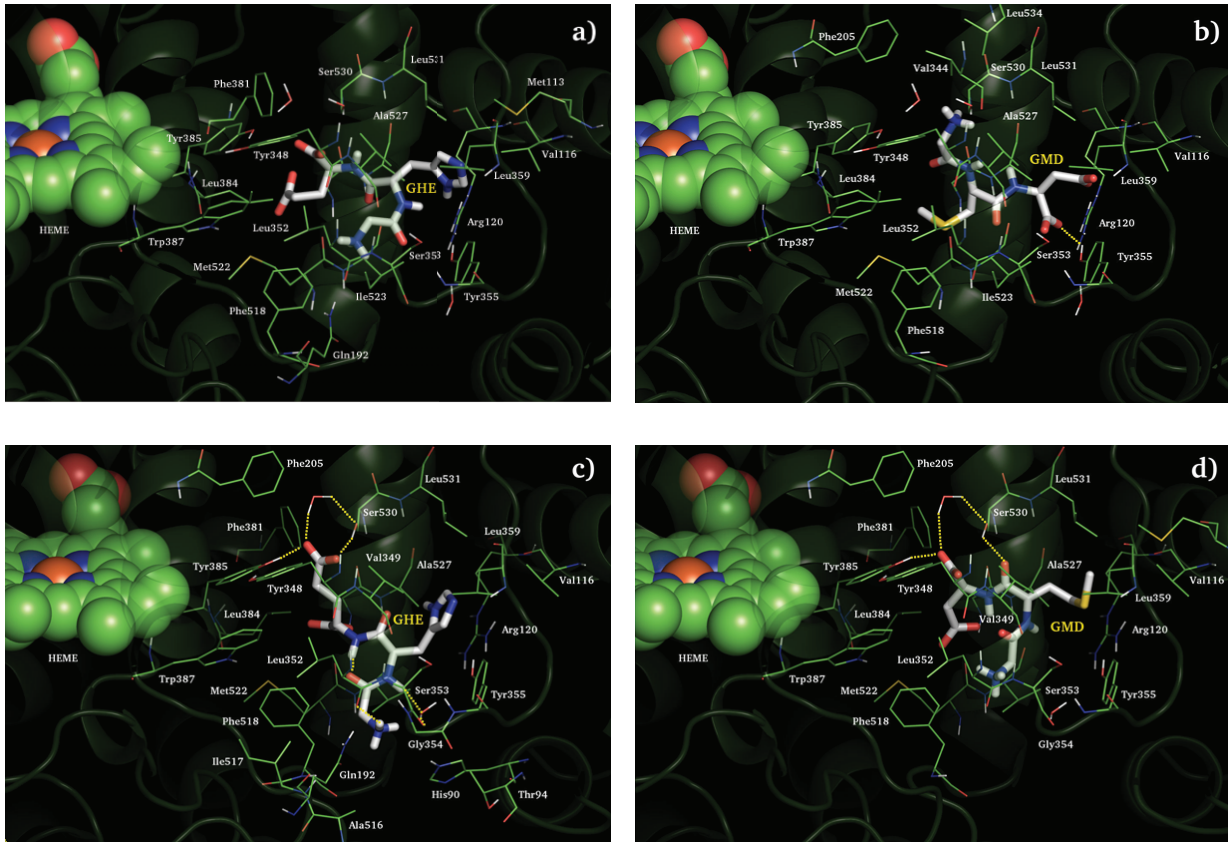

Figure 2: COX-1 (a) and (b) and COX-2 (c) and (d) recognition of GMD and GHE. Tripeptides are depicted in polytube CPK colored notation, interacting enzyme residues in green carbons wireframes, HEME cofactor in green carbons spacefill, and the rest of the enzyme is showed in transparent green cartoon. Yellow dotted lines indicated hydrogen bond interaction.

Table 2: COXs theoretical binding energies (be) in kcal/mol, number of van der Waals interacting enzyme residues (ir), and intermolecular hydrogen bonds (hb).

Peptide	COX-1			COX-2		
	be	ir	hb	be	ir	hb
GMD	−1.20	23	1	−39.87	21	3
GHE	−0.56	25	0	−42.15	26	5
YYV	—	—	—	—	—	—

Tripeptide carboxylate moieties are, also, involved in hydrogen bonds to COX-2 catalytic Tyr 385. GHE still reports such an interaction between its protonated N-terminal and Leu 352 backbone. Even if GMD, through its C-terminal, shows one hydrogen bond to Tyr 355 and favorable electrostatic interaction to COX-1 Arg 120, the steric hindrance of COX-1 Ile 523, bulkier than COX-2 Val, limits the enzyme cleft recognition preventing our compounds, in particular GHE, from establishing hydrogen bonds highlighted in COX-2. The remaining part of contribution to the COXs recognition of our peptides could be addressed an unspecific van der Waals interaction.

At the same time, based on data obtained from virtual screening, only those peptides with better profile of affinity have been selected and classified into two groups called S and E (Table 1). The first group includes 10 sequences capable of interacting with both enzymatic isoform, but with a clear preference towards COX-2. In the second group are placed further 10 tripeptides, which have shown affinity exclusively for COX-2 and no reconnaissance towards COX-1.

3.2. Chemistry. All peptides S1-E10 were synthesized by standard 9-fluorenylmethoxycarbonyl (Fmoc) chemistry using an appropriate orthogonal protection strategy. Peptides were released from the solid support using a cleavage cocktail of 90% TFA, 5% water, and 5% Et_3SiH. All analogues showed >97% purity at HPLC analysis.

3.3. Anti-infiammatory Activity. The biological assays were carried out to evaluate the inhibitory activity against COX-2 by the group of Professor Dr. Francisco Orallo, Department of Pharmacology, Faculty of Pharmacy, University of Santiago de Compostela, Spain.

Results shown in Table 3 are expressed as means ± SEM from five experiments. Means were compared by one-way

Table 3: Inhibitory activity of compounds synthesized and selectivity against COX-2 over COX-1.

	COX-1 (IC_{50})	COX-2 (IC_{50})	Ratio
Indometacina	12.16 ± 1.16 μM	35.20 ± 1.41 μM	2.9
Diclofenac	18.23 ± 1.73 μM	23.62 ± 1.97 μM	1.3
FR122047	93.80 ± 6.55 μM	***	>1.066[a]
Nimesulide	***	231.40 ± 19.84 μM	<0.46[a]
DuP697	22.61 ± 1.56 μM	126.32 ± 7.41 μM	0.0056
S1	150.33 ± 2.34 μM	94.04 ± 2.59 μM	0.6255
S2	143.21 ± 2.57 μM	120.92 ± 2.33 μM	0.8443
S3	152.44 ± 5.18 μM	94.89 ± 2.12 μM	0.6225
S4	99.32 ± 1.14 μM	80.56 ± 2.14 μM	0.8111
S5	161.43 ± 2.57 μM	100.01 ± 2.33 μM	0.6195
S6	102.31 ± 1.14 μM	91.20 ± 2.41 μM	0.8914
S7	100.33 ± 2.19 μM	88.21 ± 3.01 μM	0.8792
S8	122.48 ± 3.78 μM	91.66 ± 2.98 μM	0.7484
S9	221.57 ± 1.04 μM	68.34 ± 5.43 μM	0.308
S10	99.11 ± 1.55 μM	79.20 ± 2.15 μM	0.7991
E1–E10**	—	—	—

Significant differences between the two means ($P < 0.05$ or $P < 0.01$) were determined by one-way analysis of variability (ANOVA) followed by Dunnett's post hoc test.

*** No active at 500 μM (the highest concentration tested).

[a] Value obtained whereas the corresponding IC_{50} to COX-1 or COX-2 is the highest concentration tested.

** Data not shown.

analysis of variance (ANOVA) followed by Dunnett's post-hoc test. The inhibitory effects of the tested compounds are expressed as IC_{50} (concentrations that produce reduction of 50% of the enzymatic activity of COX control isoform) estimated by least-squares linear regression using the program Origin 5.0, with X = log molar concentration of the tested compounds and Y = % of pharmacological response.

This regression was performed using the data obtained with 4–6 different concentrations of each compound assayed, which inhibited the enzymatic activity of COX control isoform between 20 and 80%.

Finally, they were calculated the corresponding indices of selectivity (SI) of COX-1. SI = $[IC_{50}(\text{COX-2})]/[IC_{50}(\text{COX-1})]$.

As demonstrated by the virtual screening, all twenty tripeptides show a greater selectivity against COX-2 over COX-1.

In particular, peptide S9 shows a very interesting profile of both selectivity and inhibitory potency towards COX-2; in fact, the selectivity index between COX-2 and COX-1 is about 0.308, more selective than the nimesulide that has an index of about 0.46; moreover, this peptide also shows an increase in activity compared to the same drug (68.34 ± 5.43 μM S9 activity, 231.40 ± 19.84 μM nimesulide activity).

Analyzing biological data, depending both on the chemical structure that the values of the energies of binding, the peptides S9, S10, S7 and S4 show an analogous biological profile (selectivity and affinity).

However, a complete analysis of the structure-activity relationship of these peptides cannot be performed because of the small number of peptides that limit the goodness of this report. It is possible to highlight two important aspects: the guanidine group of Arg at C-terminal and the carboxyl group in the side chain of the second amino acid are requirements for the interaction with the target, while all peptides that have a carboxyl group in the side chain on the first amino acid show a loss of selectivity that of affinity; the aromatic group present in WCS, peptide lead, is not essential to interact with the target.

In conclusion, previously reported peptides seem to reflect too high potency and selectivity; instead, peptides of series E do not result selective for COX-2 (data not shown). Further studies for the peptides E1–E10 are in progress.

4. Conclusion

There is an increasing interest in the development of new treatments based on cyclooxygenases-2 inhibitors, to prolong survival and even potentially cure various forms of cancer, as malignant mesothelioma.

The present study describes hit identification, synthesis, and biological evaluation of a series of linear tripeptides, most of them are able to selectively inhibit COX-2. Further, other experiments aimed to verify the potentiality of these peptides as anticarcinogenic drugs; as well as the preparation of novel; more potent and selective peptidomimetic derivatives are in progress.

Abbreviations used for amino acids follow the rules of the IUPAC-IUB Commission of Biochemical Nomenclature in J. Biol. Chem. 1972, 247, 977-983. Amino acid symbols denote L-configuration.

Abbreviations

DMAP: 4-dimethylamino-pyridine
TFA: Trifluoroacetic acid
DCM: Dichloromethane
DIPEA: N,N-diisopropylethylamine
DMF: N,N-dimethylformamide
Et_3SiH: Triethylsilane
Fmoc: 9-fluorenyl-methoxycarbonyl
HOBt: N-hydroxy-benzotriazole
HBTU: 2-(1H-benzotriazole-1-yl)-1,1,3,3-tetramethyluronium hexafluoro-phosphate
RP-HPLC: Reversed-phase high performance liquid chromatography
ESI: Electrospray ionization
LC-MS: Liquid chromatography-mass spectrometry
Pbf: 2,2,4,6,7-pentamethyldihydrobenzofuran-5-sulfonyl.

Disclosure

The authors of the paper do not have a direct financial relation with the commercial identity mentioned in thier submitted paper that might lead to a conflict of interests for any of the authors.

Acknowledgments

The assistance of the staff is gratefully appreciated. Dr. Francisco Orallo died unexpectedly on December 9, 2009; The authors dedicate this work to his memory.

References

[1] R. K. Somvanshi, A. Kumar, S. Kant et al., "Surface plasmon resonance studies and biochemical evaluation of a potent peptide inhibitor against cyclooxygenase-2 as an anti-inflammatory agent," *Biochemical and Biophysical Research Communications*, vol. 361, no. 1, pp. 37–42, 2007.

[2] M. E. Turini and R. N. DuBois, "CYCLOOXYGENASE-2: a therapeutic target," *Annual Review of Medicine*, vol. 53, pp. 35–57, 2002.

[3] S. K. Sharma, B. J. Al-Hourani, M. Wuest et al., "Synthesis and evaluation of fluorobenzoylated di- and tripeptides as inhibitors of cyclooxygenase-2 (COX-2)," *Bioorganic & Medicinal Chemistry*, vol. 20, pp. 2221–2226, 2012.

[4] K. Gupta, B. S. Selinsky, C. J. Kaub, A. K. Katz, and P. J. Loll, "The 2.0 Å resolution crystal structure of prostaglandin H 2 synthase-1: structural insights into an unusual peroxidase," *Journal of Molecular Biology*, vol. 335, no. 2, pp. 503–518, 2004.

[5] S. W. Rowlinson, J. R. Kiefer, J. J. Prusakiewicz et al., "A novel mechanism of cyclooxygenase-2 inhibition involving interactions with Ser-530 and Tyr-385," *Journal of Biological Chemistry*, vol. 278, no. 46, pp. 45763–45769, 2003.

[6] Schrödinger, LLC., New York, NY, USA, 2010.

[7] T. A. Halgren, "Merck molecular force field. I. Basis, form, scope, parameterization, and performance of MMFF9," *Journal of Computational Chemistry*, vol. 17, pp. 490–519, 1996.

[8] T. A. Halgren, "Merck molecular force field. II. MMFF94 van der Waals and electrostatic parameters for intermolecular interactions," *Journal of Computational Chemistry*, vol. 17, pp. 520–552, 1996.

[9] T. A. Halgren, "MMFF VI. MMFF94s Option for energy minimization studies," *Journal of Computational Chemistry*, vol. 20, pp. 720–729, 1999.

[10] T. A. Halgren, "MMFF VII. Characterization of MMFF94, MMFF94s, and other widely available force fields for conformational energies and for intermolecular-interaction energies and geometries," *Journal of Computational Chemistry*, vol. 20, pp. 730–748, 1999.

[11] F. Mohamadi, N. G. J. Richards, W. C. Guida et al., "MacroModel-An integrated software system for modeling organic and bioorganic molecules using molecular mechanics," *Journal of Computational Chemistry*, vol. 11, pp. 440–467, 1990.

[12] E. Atherton and R. C. Sheppard, *Solid-Phase Peptide Synthesis: A Practical Approach*, IRL, Oxford, UK, 1989.

[13] S. Vilar, E. Quezada, L. Santana et al., "Design, synthesis, and vasorelaxant and platelet antiaggregatory activities of coumarin-resveratrol hybrids," *Bioorganic and Medicinal Chemistry Letters*, vol. 16, no. 2, pp. 257–261, 2006.

[14] R. Fioravanti, A. Bolasco, F. Manna et al., "Synthesis and biological evaluation of N-substituted-3, 5-diphenyl-2-pyrazoline derivatives as cyclooxygenase (COX-2) inhibitors," *European Journal of Medicinal Chemistry*, vol. 45, pp. e6135–e6138, 2010.

[15] E. P. Spugnini, G. Citro, and A. Baldi, "Cox inhibitors as potential chemotherapic drugs for mesothelioma," *Current Respiratory Medicine Reviews*, vol. 3, no. 1, pp. 15–18, 2007.

[16] F. A. Sinicrope, "Targeting cyclooxygenase-2 for prevention and therapy of colorectal cancer," *Molecular Carcinogenesis*, vol. 45, no. 6, pp. 447–454, 2006.

[17] J. B. Méric, S. Rottey, K. Olaussen et al., "Cyclooxygenase-2 as a target for anticancer drug development," *Critical Reviews in Oncology/Hematology*, vol. 59, no. 1, pp. 51–64, 2006.

[18] D. Mazhar, R. Ang, and J. Waxman, "COX inhibitors and breast cancer," *British Journal of Cancer*, vol. 94, no. 3, pp. 346–350, 2006.

[19] S. Ali, B. F. El-Rayes, F. H. Sarkar, and P. A. Philip, "Simultaneous targeting of the epidermal growth factor receptor and cyclooxygenase-2 pathways for pancreatic cancer therapy," *Molecular Cancer Therapeutics*, vol. 4, no. 12, pp. 1943–1951, 2005.

[20] T. Wu, "Cyclooxygenase-2 in hepatocellular carcinoma," *Cancer Treatment Review*, vol. 32, pp. 28–44, 2006.

[21] I. Cardillo, E. P. Spugnini, A. Verdina, R. Galati, G. Citro, and A. Baldi, "Cox and mesothelioma: an overview," *Histology and Histopathology*, vol. 20, no. 4, pp. 1267–1274, 2005.

Hindawi Publishing Corporation
Journal of Amino Acids
Volume 2013, Article ID 979016, 15 pages
http://dx.doi.org/10.1155/2013/979016

Review Article

Urotensin-II Ligands: An Overview from Peptide to Nonpeptide Structures

Francesco Merlino,[1] Salvatore Di Maro,[1] Ali Munaim Yousif,[1] Michele Caraglia,[2] and Paolo Grieco[1]

[1] *Department of Pharmacy, University of Naples Federico II, 80131 Naples, Italy*
[2] *Department of Biochemistry, Biophysics and General Pathology, Second University of Naples, 80138 Naples, Italy*

Correspondence should be addressed to Paolo Grieco; paolo.grieco@unina.it

Received 2 December 2012; Accepted 14 January 2013

Academic Editor: Giuseppe De Rosa

Urotensin-II was originally isolated from the goby urophysis in the 1960s as a vasoactive peptide with a prominent role in cardiovascular homeostasis. The identification of human isoform of urotensin-II and its specific UT receptor by Ames et al. in 1999 led to investigating the putative role of the interaction U-II/UT receptor in multiple pathophysiological effects in humans. Since urotensin-II is widely expressed in several peripheral tissues including cardiovascular system, the design and development of novel urotensin-II analogues can improve knowledge about structure-activity relationships (SAR). In particular, since the modulation of the U-II system offers a great potential for therapeutic strategies related to the treatment of several diseases, like cardiovascular diseases, the research of selective and potent ligands at UT receptor is more fascinating. In this paper, we review the developments of peptide and nonpeptide U-II structures so far developed in order to contribute also to a more rational and detectable design and synthesis of new molecules with high affinity at the UT receptor.

1. Introduction

Urotensin-II (U-II) belongs to a series of regulatory neuropeptides first isolated from the urophysis of the teleost fish *Gillichthys mirabilis* by Karl Lederis and Howard Bern in the 1960s. This cyclic peptide derived from goby fish, H-Ala-Gly-Thr-Ala-Asp-c[Cys-Phe-Trp-Lys-Tyr-Cys]-Val-OH, was originally characterized on the basis of its interesting smooth muscle contracting and hypertensive effects. It has been long considered that U-II was exclusively produced by the fish urophysis [1]. However, the identification of U-II from the brain of a frog [2, 3] has shown that the cDNA encoding prepro-U-II exists in several species of vertebrates. Moreover, the gene is expressed not only in the caudal portion of the spinal cord but also in brain neurones, from frogs to humans [4]. In fact, urotensin-II isopeptides are present in several species of vertebrates, and although the amino acid sequence in the N-terminus of urotensin-II peptides diverges across species, the cyclic hexapeptide sequence, c[Cys-Phe-Trp-Lys-Tyr-Cys], is conserved in all isoforms (Figure 1, orange residues).

The length of urotensin-II peptides is variable across species and it ranged from 17 amino acid residues in mice to 11 in humans, depending on the proteolytic cleavages that occur in precursors. The N-terminus region of U-II is highly variable among animal species [5], whereas the C-terminal amino acids, organized in a disulphide-linked cyclic array, c[Cys-Phe-Trp-Lys-Tyr-Cys], are continuously conserved from species to species, suggesting their primary role in the biological activity [6]. In addition, the goby isoform of U-II exhibits some structural similarities with somatostatin-14 concerning especially the presence of a disulphide-linked cyclic core at their C-terminus portion containing the biologically active domain Phe-Trp-Lys [7]. Moreover, the characterization of cDNA encoding carp pro-U-II has shown that the U-II and somatostatin-14 precursors

share a common structure organization since the active peptides are both located at the C-terminal portion of the precursors [8]. Later, once the UT receptor was identified as a member of somatostatin receptor family, some somatostatin-like peptides containing a disulphide bridge, such as human melanin-concentrating hormone (MCH), somatostatin-14, cortistatin-14, and octreotide, were screened on UT receptor in order to compare the resulting biological activities with that of the endogenous U-II [9]. By these observations it was established that U-II represented the only endogenous ligand with high affinity for the somatostatin-like receptor named UT receptor.

The human UT-II (hU-II) is a cyclic undecapeptide, H-Glu-Thr-Pro-Asp-c[Cys-Phe-Trp-Lys-Tyr-Cys]-Val-OH, recognized as the natural ligand of an orphan G-protein coupled receptor, first named as a rat receptor with high affinity for U-II, GPR14 [10–12]. Subsequently, a human G-protein coupled receptor showing 75% similarity to the orphan rat receptor was cloned and renamed UT receptor by IUPHAR [13]. The role of UT receptor has been continuously investigated and nowadays it is commonly accepted that it is widely distributed in the CNS and in different peripheral tissues including cardiovascular system [14], kidney, bladder, prostate, and adrenal gland [10, 15–17]. This extensive expression has revealed the multiple pathophysiological effects mediated by the hUT/UT receptor interaction such as cardiovascular disorders (heart failure, cardiac remodelling, and atherosclerosis), smooth muscle cell proliferation, renal disease, diabetes, and tumour growth [18]. Nevertheless, UT receptor is especially expressed in vascular smooth muscle, endothelium, and myocardium and plays a key role in the regulation of the cardiovascular homeostasis. Furthermore, this receptor has much structural homology to members of the somatostatin and receptor family and it could be activated by somatostatin-14 and cortistatin at micromolar doses [10]. The gene coding for the UT receptor has been located in chromosome 17q25.3 [19].

The hU-II binds with high affinity to this receptor, resulting in intracellular calcium mobilization via phospholipase C-dependent increase in inositol phosphates. In isolated rat thoracic aorta fragments hU-II induces contraction mediated by two distinct tonic and phasic components. However, its vasoconstrictor activity is well observed in primate arteries, in which it causes a concentration-dependent contraction of isolated arterial rings with an EC_{50} value less than 1 nM, meaning a 10-fold more potency than endothelin-1. However, the *in vivo* effects can depend on the species, type of blood vessel, concentration of U-II, route of administration, and results of tissue and species in exam, and they can be also contradictory. Accordingly, the peptide also elicits vasodilatory effects on the small arteries of rats and on the resistance arteries of humans, probably due to the release of endothelium-derived hyperpolarizing factor and nitric oxide [20]. In a healthy human, U-II behaves as a chronic regulator of vascular tone rather than influencing tissues in a phasic manner [21]. U-II binds to its receptor in a "pseudo-irreversible" manner, and slow dissociation rate from the UT receptor leads to prolonged activation of the receptor and a functionally silent system [22]. This state of homeostasis is altered since pathogenesis of several cardiovascular disorders provokes an upregulation of UT receptor and of U-II resulting in vasoconstriction.

To date, findings in molecules with high affinity to the urotensin-II system has led to discovering new ligands, peptide, and nonpeptide analogues. This review is aimed at investigating the structure-activity relationship on urotensin-II system by analyzing peptide and nonpeptide structures so far developed in order to contribute also to a more rational and detectable design and synthesis of new molecules with high affinity at the UT receptor.

2. SAR Studies on U-II

The potential therapeutic application of urotensin-II system has continuously stimulated structure-activity relationship studies (SARs), which could elucidate the structural features of this important hormone. On the other hand, the discovery of new analogues acting as agonist or antagonist is extremely important to explore the physiological role of hU-II. First structural studies performed on U-II by nuclear magnetic resonance (NMR) spectroscopy [23–25] have revealed that the peptide adopted a preferential conformation both in DMSO and water solution, which did not show any classical secondary structures. Amino acids in the core region of U-II are identified in a highly compact conformation with the formation of a hydrophobic pocket, in which Ala^4, Phe^7, Trp^8, and Val^{12} are projected on the same side of the molecule being at least in part important residues for the binding site. In contrast, hU-II and some analogues resulted to be fold in defined secondary structure when dissolved in SDS solution, a membrane mimetic environment [26].

Subsequently, with the aim of investigating the role played by the exocyclic region in the receptor interaction, a series of truncated peptides related to hU-II has been investigated. Truncation studies are of prime importance for the detection of the minimal sequence of peptide required to retain the biological activity. The effect of sequential deletion of exocyclic residues from N- or C-termini in hU-II sequence does not appear to be significant in the calcium-mobilizing potency and efficacy, whereas the removal of any residue that belongs to the cyclic region determines reduction or total absence of the biological activity. The shortest and fully potent sequence of U-II was individuated in the octapeptide $U\text{-}II_{(4–11)}$, H-Asp-c[Cys-Phe-Trp-Lys-Tyr-Cys]Val-OH, that preserves the potency at the human UT receptor, showing similarity to somatostatin-14 in which truncation of the segment led to active analogues.

The importance of a free amino group in the N-terminal of the resulted octapeptide $U\text{-}II_{(4–11)}$ was evaluated by its modification in the succinoyl derivative performed in 2002 by Coy et al. [27]. The peptide was extremely potent according to data from the biological activity, $EC_{50} = 0.12 \pm 0.03$ nM, and binding affinity, $K_i = 1.14 \pm 0.01$ nM and $K_i = 1.65 \pm 0.04$ nM, at human and rat UT receptor, respectively. Additional dicarboxylic residues introduced in substitution of Asp^4 have showed similar results. Furthermore, the replacement of this amino acid with the corresponding amidated Asn gives a

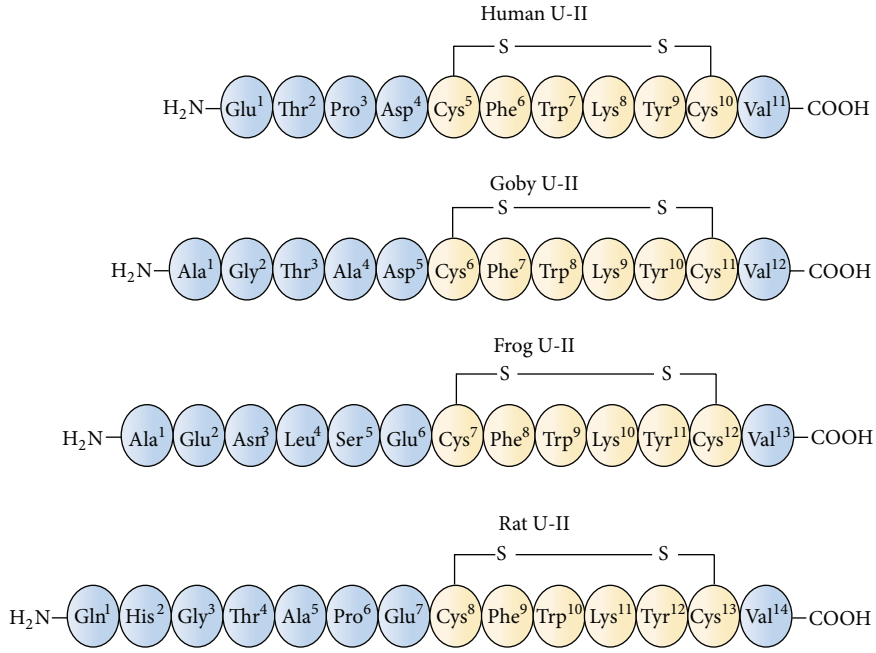

Figure 1: A comparison of urotensin-II (U-II) isopeptides sequences isolated from different species of vertebrates.

Table 1

Name	Peptide sequence
PRL-2903	H-4Fpa-c[Cys-Pal-DTrp-Lys-Tle-Cys]-Nal-NH_2
SB-710411	H-Cpa-c[DCys-Pal-DTrp-Lys-Val-Cys]-Cpa-NH_2
BIM-23127	H-D(2′)Nal-c[Cys-Tyr-DTrp-Orn-Val-Cys]-(2′)Nal-NH_2
BIM-23042	H-DNal-c[Cys-Tyr-DTrp-Lys-Val-Cys]-(2′)Nal-NH_2
[Orn^8]U-II	H-Glu-Thr-Pro-Asp-c[Cys-Phe-Trp-Orn-Tyr-Cys]-Val-OH
P5U	H-Asp-c[Pen-Phe-Trp-Orn-Tyr-Cys]-Val-OH
Urantide	H-Asp-c[Pen-Phe-DTrp-Orn-Tyr-Cys]-Val-OH
UFP-803	H-Asp-c[Pen-Phe-DTrp-Dab-Tyr-Cys]-Val-OH
URP	H-Ala-c[Cys-Phe-Trp-Lys-Tyr-Cys]-Val-OH
Urocontrin	H-Bip-c[Cys-Bip-Trp-Lys-Tyr-Cys]-Val-OH
GSK248451	H-Cin-c[DCys-Pal-DTrp-Orn-Val-Cys]-His-NH_2

compound that retains a full activity in all three assay systems, suggesting that in this position an amino acid negatively charged in the side chain is not required. However, the Nle^4-analogue lacks of potency showing that the $-CH_2COX$ carbonyl group present in both the Asp and Asn side chains is important probably because of its possibility to act as an acceptor for hydrogen bond with the UT receptor. The side chain can also contain an aromatic ring substituted with polar groups such as OH and NO_2, which is of great interest in the development of antagonists based on the previously identified somatostatin antagonist octapeptides.

The cyclic structure is essential for hU-II and McMaster et al. in 1986 [28] reported a lack of biological activity for the corresponding "ring-opened" analogue. In 2002 Grieco et al. considered the replacement of the disulphide bridge by a side-chain-to-side-chain lactam bridge in accordance with observations on several biologically relevant peptides, such as conotoxins, endothelin-1, and somatostatin analogue that gave interesting results by the same modification [29]. Starting from the minimum active fragment $U\text{-}II_{(4-11)}$, introduction of the lactam bridge in an appropriate length led to peptides that maintain bioactivity to the detriment of potency, suggesting that the size of the lactam bridge is a crucial parameter. Peptide analogues synthesized in this study were characterized by ring-closing sequence that ranges from 20 to 24 atoms and, interestingly, the smallest peptide sequence, having the same length as the native peptide containing the disulphide bridge, does not show any biological activity. In contrast, peptide analogue characterized by a larger ring, containing Orn and Asp as residues in the 22 atoms lactam bridge, behaved as a full agonist, but was approximately 100-fold less potent than hU-II. Thus, replacement of the Cys-Cys cyclic motif could be well tolerated by an appropriate longer lactam bridge despite the partial loss of activity, probably

due to the different orientation of the key amino acid side chains. However, in a later work performed by Foister et al. in 2006 [30] a cyclic "cysteine-free" hexapeptide derivative of U-II, in which Tyr^9 was replaced with a β-naphthylalanine residue, [Ala-Phe-Trp-Lys-(2)Nal-Ala], bounds the human UT receptor with higher affinity (K_i = 2.8 nM) than the corresponding disulphide-bridged truncated hexapeptide U-$II_{(5-10)}$ (K_i = 95 nM). Furthermore, modifications of the Cys^5–Cys^{10} disulphide bridge, such as the macrocyclic lactam and the penicillamine-derived disulphide moiety, could chemically stabilize and restrict the conformational flexibility of the biologically active cyclic hexapeptide core sequence. In particular, penicillamine residue in replacement of Cys^5 resulted to be very useful in order to obtain a potent agonist, [Pen^5]hU-$II_{(4-11)}$, subsequently renamed P5U [29]. As potent agonist with reduced conformational flexibility, Lavecchia et al. performed subsequent NMR study in DMSO on this peptide in 2005 [31]. The positions of Lys^8 amino group and Tyr^9 aromatic side chain were in proximity with a distance of 6.2 Å and Trp^7 indole and Lys^8 amine were separated by 5.6 Å. Docking of P5U into a hUT homology model based on the structure of bovine rhodopsin revealed interesting points of interaction. The Lys^8 interacts primarily with Asp^{130}, as well as with residues of Tyr^{100} and Tyr^{305}; Tyr^9 is accommodated in a binding pocket defined by Lys^{212}, Val^{296}, Ala^{281}, and Trp^{277} particularly involved in a π-stacking interaction, and the indole NH of Trp^7 binds to the carbonyl of Tyr^{298}.

In the structure-function study performed by Kinney et al. in 2002 [32], an alanine scan of truncated goby U-II demonstrated that the replacement of Trp, Lys, and Tyr is crucial for the maintenance of biological activity. The sequence Trp-Lys-Tyr within U-II is essential for binding and activation of the receptor, indicating that the hydrophobic side chains of Trp^7 and Tyr^9 and the positive charge of Lys^8 represent pharmacophoric elements. Moreover, NMR studies performed by Flohr et al. in 2002 [24] revealed that the distances between the pharmacophoric points are key elements in the development of SAR. Accordingly, first NMR studies applied to the receptor-unbound hU-II in water were developed in order to provide for a putative agonist pharmacophore. Structural model showed the Lys^8 amino group and Tyr^9 aryl ring being in proximity with a distance of 6.4 Å; the Trp^7 and Tyr^9 were separated by 12.2 Å, and Trp^7 aromatic residue and Lys^8 amino group were separated by 11.3 Å. Later, another agonist pharmacophore model was performed by studying conformation adopted by a less potent analogue without Val residue, that is, Ac-[Cys-Phe-DTrp-Lys-Tyr-Cys]-NH_2 (200-fold less potent than hUT-II). Since this peptide was more closely similar to the receptor-bound conformation, this structural model suggested new distances between pharmacophoric elements of Trp-Lys-Tyr sequence (Lys^8 amino group and Tyr^9 aryl ring at 11.1 Å, Trp^7 and Tyr^9 aryl residues separated by 8.3 Å, and Trp^7 aryl and Lys^8 amino groups separated by 13.7 Å). Flohr et al. also studied the substitution of amino acids in the hexacyclic part of hU-II sequence with the corresponding D isomers. This led to dramatic decrease of the agonist activity, suggesting the importance of the side chains of these amino acids and their spatial orientation for interaction with the UT receptor; surprisingly, stereoinversion of L-Trp in D-Trp does not show a significant change of the EC_{50} value versus the endogenous ligand. The role of Lys^8 was also investigated by replacing it with lipophilic amino acids and hydrophilic nonbasic amino acids that produce inactive peptides [33]. Thus, positive charge represented by primary aliphatic amine of Lys in position 8 is essential for the biological activity. However, reducing the distance of the primary aliphatic amine from the peptide backbone led to a progressive reduction of both potency and efficacy. [Orn^8]U-II analogue showed a weak contraction of rat aorta strips corresponding to about 20% of the U-II maximal effect at micromolar concentrations. In position 9 the –OH group of Tyrosine was proved to be replaced with $–OCH_3$, $–NO_2$, $–CH_3$, –F, –H, and $–NH_2$ obtaining any improvement in potency or efficacy, except for 3-iodo-Tyr residue that produced a full UT receptor agonist, 6-fold more potent than the natural peptide.

A further and useful attempt to alter potency and efficacy versus UT receptor was represented by the introduction of nonnatural amino acids into the sequence [32]. Replacement of the Tyr residue with the bulkier 2-Nal [(2-naphthyl)-L-alanine] in the goby U-II sequence showed similar potency in agonist activity (with a value of EC_{50} = 0.34 ± 0.1 nM than the value for the goby U-II, EC_{50} = 0.17 ± 0.05 nM) in the functional assay and a 6-fold improvement in affinity in the binding assay (K_i = 0.04 ± 0.02 nM), presumably due to enhanced hydrophobic interactions in the tyrosine-binding pocket. In contrast, the Bip residue, [(2-biphenyl)-L-alanine] did not show equal result, confirming that larger groups are not well accommodated. In this work, Kinney et al. also provided for a novel agonist pharmacophore model through the docking of goby UT-II into a rat UT receptor homology model. According to this modelling study, the Lys^8 amino group of the ligand was essential for the interaction with Asp^{130} on transmembrane helix TM3 of UT receptor, with the binding cavity drawn by the extracellular loops that strengthened the accommodation of the ligand. The distances characterized for the pharmacophoric sequence were 11.2 Å between the Lys^8 amino and Tyr^9 aryl groups, 8.4 Å between the indole Trp^7 and Lys^8 amine, and 8.2 Å between the Trp^7 and Tyr^9 aryl groups.

3. Peptide Ligands

As mentioned above, the human U-II is involved in several pathophysiological pathways of disorders especially regarding cardiovascular system along with the observation that the interaction U-II/UT receptor regulates the contractility and growth properties of cardiac and peripheral vascular vessels led to identifying selective ligands. In particular, since the modulation of the U-II system offers a great potential for therapeutic strategies related to the treatment of cardiovascular diseases, the research of selective compounds is more intriguing.

Based on the search for a definitive pathophysiological role for U-II and its receptor in the cardiovascular homeostasis and aetiology of relating disorders, the design of suitable tool compounds of peptide or nonpeptide nature could be of significant utility. New molecules may assist in determining this role by the development of selective UT receptor antagonists.

Therefore, first attempts came out from observations on somatostatin system, due to sharing sequence peculiarities between hU-II and somatostatin. Indeed, some somatostatin analogues such as PRL-2903 Table 1, H-4Fpa-c[Cys-Pal-DTrp-Lys-Tle-Cys]-Nal-NH_2, resulted in the ability to block the hU-II-induced rat aorta ring tone at micromolar concentrations, although it showed low species selectivity [34]. Another peptide somatostatin analogue, described by Coy et al. in 2000, showed moderate affinity for UT receptor. This peptide, named SB-710411, H-Cpa-c[DCys-Pal-DTrp-Lys-Val-Cys]-Cpa-NH_2, was able to inhibit U-II-induced contraction in rat isolated thoracic aorta in a surmountable manner (pK_b = 6.28) [35]. Exposure to 10 μM SB-710411 causes a significant shift in the agonist concentration-response curve with no suppression of the E_{max}, suggesting that it acts as a competitive antagonist. In contrast, SB-710411 did not alter the contractile efficacy of angiotensin-II, phenylephrine, or KCl, although it potentiated the contractile response to endothelin-1 in the isolated rat aorta. However, since little was known about the pharmacology of this ligand in other species, Behm et al. in 2004 [36] reported their observations on the pharmacological effects at the rat and monkey recombinant UT receptor because of the weak homology between rodent and primate UT receptors (~76% of homology than the homology between monkey and human UT receptor that are about 97% identical) [37]. SB-710411 acts as a ligand for both the recombinant rat and monkey UT receptor (30–150 nM affinities, 56- and 87-fold less potent than U-II, resp.). However, functional behaviour of this peptide at these two UT receptor orthologous differs radically. As was reported previously, SB-710411 itself did not promote inositol phosphate formation but inhibited the agonistic actions of U-II in the rat aorta [35]. In contrast to the rat, SB-710411 behaved as a full agonist at the recombinant monkey UT receptor, inducing the maximal response although EC_{50} was approximately 100-fold less potent than U-II. Thus, despite the antagonistic effects of SB-710411 observed at the rat UT receptor, this peptide acts as a full agonist at the monkey UT receptor. These findings suggest that the functional response of UT receptor modulators at the rodent UT receptor does not necessarily predict the functional response at nonrodent UT receptors, and the incoherence could result from alterations in receptor number and/or coupling efficiency as well as Camarda et al. in 2002 [38] proposed for a different UT receptor ligand, [Orn^8]hU-II.

As cyclosomatostatin octapeptide analogue that shares structural similarities with SB-710411, the peptide neuromedin B receptor antagonist BIM-23127, H-D(2′)Nal-c[Cys-Tyr-DTrp-Orn-Val-Cys]-(2′)Nal-NH_2 [39], was investigated by functional activity at recombinant and native UT receptors [40]. The effect of increasing concentration of BIM-23127 on hU-II-induced intracellular calcium mobilization

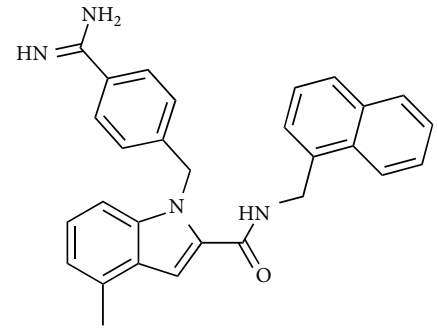

Figure 2: Structure of S7616.

in HEK293 cell lines expressing either the human or rat UT receptor was evaluated by generating hU-II concentration-response curves. These were indeed shifted progressively to the right in a parallel manner with no changes in the maximum response to hU-II, suggesting competitive antagonism. Moreover, BIM-23127 showed about 0.5 log unit lower affinity in competition binding experiments to human or rat UT receptors and inhibition of hU-II-promoted intracellular calcium mobilization producing a significant suppression of the maximum contractile response to hU-II. In contrast of this noncompetitive antagonism of contraction to U-II in isolated rat aorta, BIM-23127 inhibited calcium mobilization in human embryonic kidney 293 cells expressing UT receptors in a competitive manner. A related neuromedin B receptor antagonist, BIM-23042, H-DNal-c[Cys-Tyr-DTrp-Lys-Val-Cys]-(2′)Nal-NH_2, displayed different functional activities at several UT receptor orthologues. It behaved as a full agonist at human and monkey UT receptor, a partial agonist at mouse UT receptor, and a competitive antagonist at rat UT receptor [41].

Among the most potent compounds, Camarda et al. in 2002 [38] identified the hU-II derivative [Orn^8]U-II, that was characterized *in vitro* as a novel peptide ligand for the UT receptor. Modification of Lys^8 to the nonnatural amino acid Orn was suggested by chemical observations that Lys belongs to the most important sequence for the biological activity. This synthetic analogue behaved as a full agonist in the calcium functional assay in HEK293 human and rat UT cells, inducing similar maximal effects as U-II. However, the potency of [Orn^8]U-II at both receptors was 3-fold lower than U-II (pEC_{50} = 7.93 ± 0.16 and 8.06 ± 0.22, resp., whereas U-II increased intracellular calcium levels in HEK293 hUT and rUT cells with similar high potencies, pEC_{50} = 8.51 ± 0.18 and 8.54 ± 0.14, resp.). In contrast, different results were obtained in the rat aorta bioassay, in which the compound behaved as a competitive antagonist, showing only in highest concentrations (10 μM) a weak residual agonist activity (25% compared to the maximal effect of U-II). The variance between results obtained between the cell and tissue assay could be interpreted assuming that [Orn^8]hU-II is a partial agonist.

In 2002 Grieco et al. [29] generated a novel peptide UT receptor agonist by introduction of an unusual amino acid in the disulphide bridge of $hUT\text{-}II_{(4–11)}$, the potent analogue

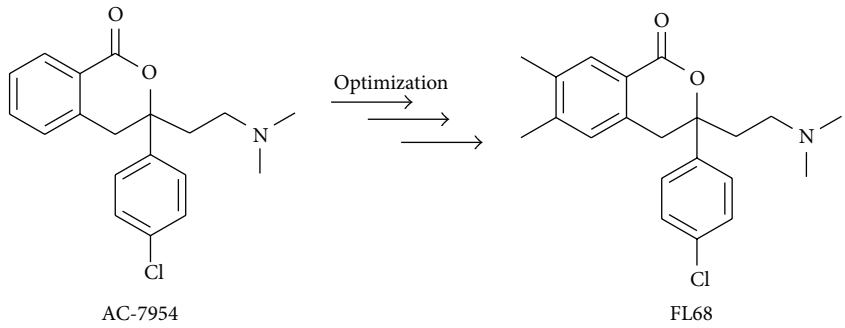

AC-7954 FL68

Figure 3: Structures of AC-7954 and its optimized derivative FL68.

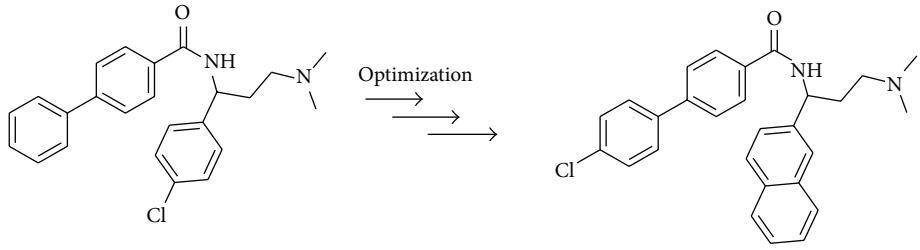

FL-104 Compound 1

Figure 4: Structures of FL-104 and its optimized derivative compound 1.

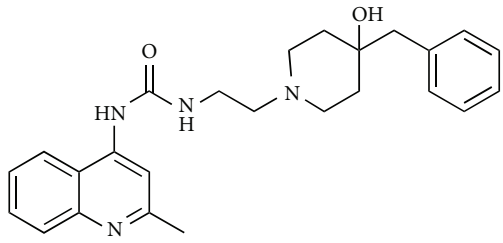

Figure 5: Structure of palosuran (ACT-058362).

[Pen^5]hU-II$_{(4–11)}$, also known as P5U. This β,β-dimethyl-substituted cysteine residue led to higher conformational rigidity in the sequence of hU-II C-terminal octapeptide. Data showed that P5U has a 3-fold higher affinity for the UT receptor than the endogenous ligand as competition experiments witnessed its ability to displace the iodinated radioligand with comparable affinity (iodinated hU-II bound the human UT receptor saturably with high affinity, pK_D = 9.2 ± 0.14, whereas P5U has similar affinity to the unmodified C-terminal octapeptide hU-II$_{(4–11)}$, pK_i = 9.7 ± 0.07). In functional experiments on the rat aorta, P5U was 20-fold more potent than hU-II and 10-fold more potent than hU-II$_{(4–11)}$, being by far the most potent U-II analogue in the rat thoracic aorta bioassay. Interestingly, conformational analysis by [^{1}H] nuclear magnetic resonance (NMR) spectroscopy combined with molecular modelling on this peptide also indicated further details about structure-activity relationships since the putative pharmacophoric Trp-Lys-Tyr sequence into the cyclic portion of this analogue, retained as the most important for full agonist activity, maintains the same spatial orientation as in the native peptide. Thus, the chemical modification brought by the unusual more constrained penicillamine residue mainly influences the proximal Phe^6 position, leaving Trp, Lys, and Tyr residue nearly unaffected. The enhanced pharmacological properties observed in the case of P5U can be assigned to this conformational restriction revealing the importance of the exploration of specific orientations in the three-dimensional space by which amino acid side chains can interact with the receptor.

Since antagonist peptides such as SB-710411, [Orn^8]U-II, BIM-23127 so far described showed weak potency at UT receptors with concomitant antagonist activities to different receptor types and behaved as partial agonist activity at UT, new attempts were challenged in order to develop more potent and selective UT receptor antagonist. Patacchini et al. in 2003 [42] described the pharmacological activities of two compounds: [Pen^5, Orn^8]hU-II$_{(4–11)}$ and [Pen^5, DTrp^7, Orn^8]hU-II$_{(4–11)}$, named urantide (urotensin-II antagonist peptide). Both peptides derived from the hU-II$_{(4–11)}$ fragment, previously reported as the minimal active sequence of hU-II, as well as further replacement of Cys^5 by penicillamine, β,β-dimethylcysteine, were achieved in order to give them conformational rigidity stabilizing the putative bioactive conformation. In functional experiments both peptides showed no agonist effect by cumulative administration in the range 0.1 nM to 10 μM. However, urantide was totally ineffective as an agonist even when administered as a single concentration, that was not shown for [Pen^5, Orn^8]hU-II$_{(4–11)}$, suggesting a sort of desensitization known to affect UT receptor-mediated responses in this preparation. As the most

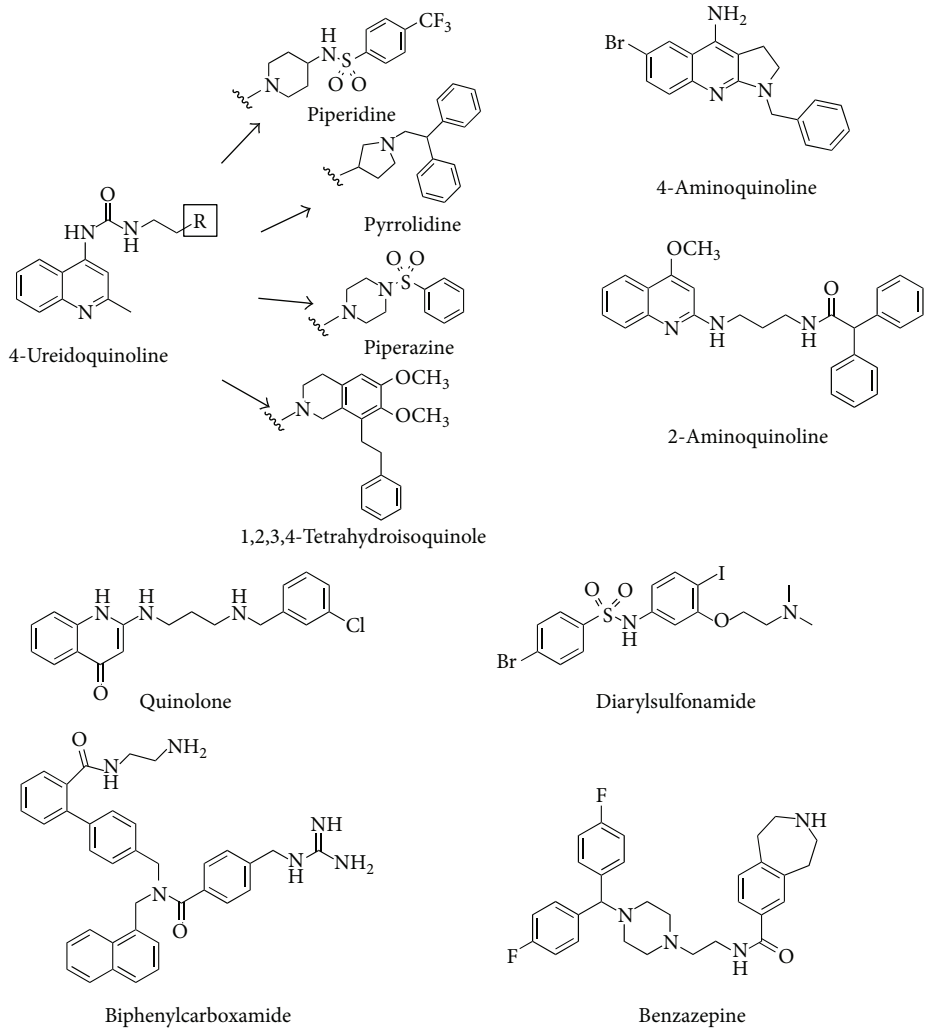

Figure 6: Structures of nonpeptide urotensin-II receptor antagonist reported in the patent literature.

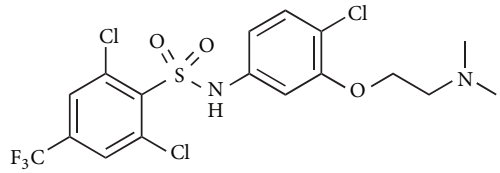

Figure 7: Structure of SB-611812.

potent UT receptor antagonist compound so far reported in the rat isolated aorta, urantide has also high affinity for the human (pK_i = 8.3) and for the rat (pK_i = 8.3) UT receptors. Conformational studies on urantide performed in 2005 by Grieco et al. [43] showed that the distance between Trp^7 and Tyr^9 side chains was 11.5 Å, greater than that observed in peptide agonist P5U (6.1 Å) because of the inversion of L-Trp^7 into the corresponding D isomer in urantide. The feature of inversion of the configuration of the Trp residue in position 7 was suggested by the presence of the same modification in both BIM-23127 and SB-710411. Urantide represented an extremely potent UT receptor antagonist since it was about 50- to 100-fold more potent than any other compounds tested in the rat isolated aorta. Despite of the potent UT receptor antagonist activity in the rat aorta bioassay, urantide showed residual agonist activity at human recombinant assay in a calcium mobilization assay [44]. In order to develop a selective antagonist, chemical modifications led to generating the peptide [Pen^5, $DTrp^7$, Dab^8]U-$II_{(4–11)}$, also known as UFP-803, closely related to the urantide sequence[45]. In the present molecule, the residual agonist activity is less than that of urantide. In the rat aorta bioassay, UFP-803 competitively antagonizes U-II contractile action behaving as a selective UT receptor antagonist.

In 2003 a report from Sugo et al. [46] demonstrated the existence of a paralogue of U-II named U-II related peptide (URP), a novel peptide first isolated from the extract of rat brain and subsequently also proposed as endogenous ligand for UT receptor in the rat, mouse, and possibly in human. The amino acid sequence was determined as H-Ala-c[Cys-Phe-Trp-Lys-Tys-Cys]-Val-OH and it exhibits high

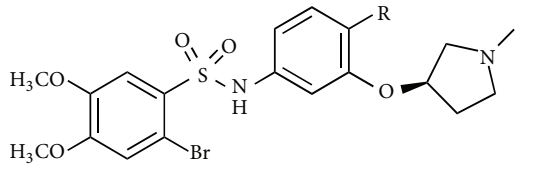

	R
SB-706375	CF_3
SB-657510	Cl

Figure 8: Structure of SB-706375 and SB-657510.

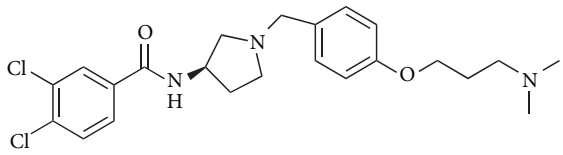

Figure 9: Structure of SB-436811.

binding affinity for human UT receptor in transfected cell lines and high contractile potency in the rat aortic ring assay, suggesting that some physiological effects could be not completely attributed to U-II. In order to evaluate the correct orientation of amino acid side chains belonging to the cyclic region of URP in the activity of the peptide, each amino acid has been replaced with the corresponding stereoisomer in a D-scan analysis [47]. D-isomer substitution within the cyclic portion in replacement of Phe^3, Lys^5, and Tyr^6 reduced binding affinity and contractile activity, confirming the primary role of this portion in receptor recognition. In contrast, the [$DTrp^4$]URP analogue retained important binding affinity, suggesting relative tolerance in the interaction with the receptor by stereoinversion occurring in that position. [$DTrp^4$]URP showed also reduced efficacy appearing to behave as a partial agonist with moderate potency and a full antagonist with low potency, indicating that point substitution of the Trp residue in U-II and URP sequence could lead to the development of antagonists. Therefore, Chatenet et al. in 2012 [48] provided the replacement of the indole moiety in URP in order to obtain promising antagonists. In particular, the introduction of the more hydrophobic uncoded amino acid Bip led to the novel antagonist urocontrin, [Bip^4]URP. The main feature of this peptide was the ability to reduce the efficacy of hU-II but not URP-induced vasoconstriction in a rat aorta assay. Despite the structural homology between U-II and URP and their concurrent expression in several human tissues, recent studies have reported different actions for these two peptides such as cell proliferation [49] and distinctive myocardial contractile activities [50]. Therefore, the identification of more selective ligands should be helpful for the rational design of more selective molecules in order to clarify the role of U-II and URP in the urotensinergic system.

Several peptide UT receptor antagonists such as urantide, [Orn^8]U-II, UFP-803, BIM-23042, and SB-710411 exhibit contradictory actions in selected assay systems since they have showed antagonist properties in rat isolated aorta and partial agonist action by mobilization of intracellular calcium in specific recombinant UT receptor HEK/CHO cell systems. Similar observations upon this residual agonist activity have already been made by Kenakin in 2002 [51] and Camarda et al. in 2002 [38] that have proposed an "assay-dependent" agonism/antagonism resulted from different UT receptor expression and/or signal transduction-coupling efficiency, for example, depending on the receptor density and the efficiency of receptor couplings. For this reason identification of a novel and selective antagonist was achieved by examining ligand-evoked UT receptor agonism under conditions of both low and high receptor density and efficient coupling and amplification. In 2006 Behm et al. [52] described GSK248451, H-Cin-c[DCys-Pal-DTrp-Orn-Val-Cys]-His-NH_2 [53, 54], as a potent UT receptor antagonist in all native mammalian isolated tissues retaining an extremely low level of relative intrinsic activity in recombinant HEK cells (4-5 fold less than observed for urantide). Furthermore, since GSK248451 represents a selective UT receptor antagonist by blocking the systemic vasopressor actions of exogenous U-II it became a suitable tool compound for further investigations concerning the role of U-II in the aetiology of mammalian cardiometabolic diseases.

4. Nonpeptide Ligands

The use of peptides as drugs in a therapeutic approach is often problematic because of their poor oral and tissue absorption, and their low stability due to the rapid proteolytic cleavage by enzymes. The pharmacokinetic limits of peptides can be generally overcome by developing nonpeptide molecules, inspired to the main sequence of the peptide and in particular mimicking the specific secondary structure responsible for the biological activity. Regarding to the design of nonpeptide ligands, the conformation and the size of the peptide backbone is often difficult to mimic by using as scaffold organic molecules and modifications onto hydrophobic, steric, and electronic properties could generate potential active compounds and optimize their affinity and selectivity. Nonpeptide agonists and antagonists at the human UT receptor could be important tool compounds in determining the role of U-II and its derivatives in the urotensin system, and they have been developed in several studies. Specifically, the design and synthesis of selective receptor antagonists should be helpful to clarify the role of human U-II as a multifunctional peptide in mammalian pathophysiological functions. Additionally, a pure nonpeptide antagonist stable on *in vivo* administration could be very helpful to provide an alternative pharmacological strategy in different disease models.

Historically, first approaches for the discovery of new nonpeptide ligands at GPCR receptors were based on high-throughput screening (HTS) studies or knowledge of the 3D structure and secondary conformation adopted by the natural ligand. A virtual screening based on 3D pharmacophores defined from the key residues of U-II was even performed on an Aventis compounds database by Flohr et

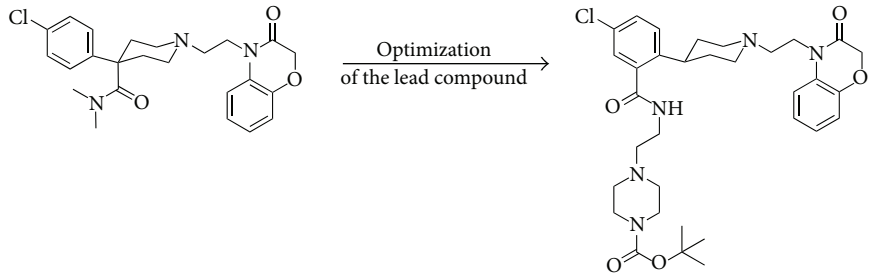

Compound 2 Compound 3

Figure 10: Structures of the lead compound 2 and its analogue compound 3 (piperidine derivatives).

al. in 2002 [24] in order to identify functional antagonists of U-II. The screening was based on their two agonist pharmacophore models: one associated with the human U-II peptide and one associated with Ac-[Cys-Phe-DTrp-Lys-Tyr-Cys]-NH_2. From 500 compounds that matched the U-II pharmacophore, the most notable compound was in S7616, 1-(3-carbamimidoyl-benzyl)-4-methyl-1H-indole-2-carboxylic acid (naphthalene-1-ylmethyl)amide, revealing an IC_{50} of 400 nM (Figure 2).

The phenyl ring of the indole and the naphthalenemethylamine side chain are localized onto the two aromatic features of the pharmacophore. The basic benzamidine group in S6716 was shown to form a charged interaction with Asp^{130} residue within TM3 of the human UT receptor. Here, the basic amino group was considered as crucial feature for all following designed antagonists.

Because of the absence of specific small molecule UT receptor agonists, Croston et al. performed a functional mammalian cell-based R-SAT assay for high-throughput screening in 2002 [55]. In this assay the UT receptor was multiplexed with vectors for the expression of additional receptor targets, such as the muscarinic M3 receptor and some orphan GPCRs, in order to increase the number of drug-target interactions tested without altering the response and sensitivity characteristics of potential ligands. Screening a library of 180000 small diverse organic molecules tested in a multiplexed R-SAT assay, AC-7954, 3-(4-chlorophenyl)-3-(2-(dimethylamino)ethyl)isochroman-1-one, was identified as a novel nonpeptide agonist with a potency of 300 nM at the human UT receptor (Figure 3).

This compound is selective to activate the UT receptor, although the other receptors included in the multiplex screening assay belong to somatostatin and opioid receptor classes that are the closest to UT receptor for genetic sequence homology. Having no significant response when tested at concentrations up to 15 μM on several receptor targets, including dopamine (D1, D2, D5), muscarinic (M1, M3, M5), serotonin (5-HT1A, 5-HT1B, 5-HT1D, 5-HT1E, 5-HT2A, 5-HT2B, 5-HT2C), histamine (H2), β-adrenergic (β-1, β-2), somatostatin (sst-2, sst-3, sst-5), CRF-1, CRF-2a, CRF-2b, κ-opioid, adrenomedullin, and CCK-a receptors, AC-7954 resulted to be a highly selective nonpeptide agonist of the UT receptor. This compound has low molecular weight, drug-like lipophilicity, a basic amino function (pK_a = 8.7), and it exhibits limited conformation flexibility for the presence of the bicyclic isochromane-based ring system. The product was synthesized as racemic mixture ($p\mathrm{EC}_{50}$ = 6.5) that was resolved in order to test enantiomers in R-SAT. Interestingly, the assay revealed that the isomer (+)-AC-7954 is more potent as UT receptor agonist ($p\mathrm{EC}_{50}$ = 6.6), indicating that this activity is highly stereoselective. The mode of interaction of (+)-AC-7954 with human UT receptor was clarified by later docking studies [31]. (+)-AC-7954 binds the human UT receptor through interaction between the basic amino group and Asp^{130} located on TM3 of the receptor as well as the p-chlorophenyl ring located in a hydrophobic pocket, where usually Tyr^{9} residue binds, and the benzo ring interacts with Phe^{118} by an aromatic stacking interaction.

As first nonpeptide agonist the compound named AC-7954 has been considered as a lead compound and a series of analogues of this compound have been developed in order to obtain more potent nonpeptide ligands at the human UT receptor [56]. In accordance with this study the isochromanone core has been kept intact, whereas new bulkier amino groups and introduction of substituents in position 4 or in the aromatic rings were investigated so that the structure-activity relationship study around AC-7954 could complete the knowledge about U-II/UT receptor interaction. These several structural modifications led to both increased and decreased activities, although beneficial effects were obtained when substituents were introduced in the aromatic part of the isochromanone ring system, whereas more sterically demanding amino groups resulted to be damaging to the activity. The 6,7-dimethyl derivative of AC-7954 showed the most potency among the series ($p\mathrm{EC}_{50}$ = 6.87 ± 0.03) and once its racemate has been resolved into the pure enantiomers, it was indicated the (+)-enantiomer, subsequently named FL-68 (Figure 3), as the own potential active stereoisomer ($p\mathrm{EC}_{50}$ = 7.30). From the series of compounds synthesized in this study, FL-68 was found the most interesting since it was very active versus UT receptor and not showing at the same time any activity versus the closely related somatostatin receptors.

Although the isochromanone-based agonists so far described were interesting for their druglikeness properties and their high selectivity for the UT receptor, in 2007 Lehmann et al. [57] chose to obtain new molecules by breaking of C3–C4 bond in the isochromanone scaffold. This synthetic strategy adopting for development of novel urotensin-II agonists was primarily focused to the introduction of

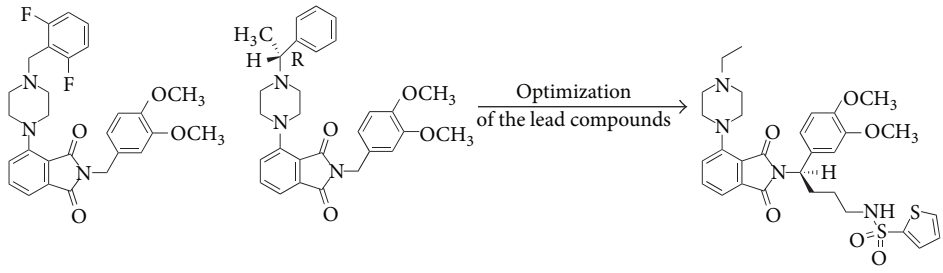

Compound 4 Compound 5 (JNJ-28318706) Compound 6 (JNJ-39319202)

Figure 11: Structures of piperazino-isoindolinone derivatives compound 4 and compound 5 (JNJ-28318706) were optimized into the novel compound 6 (JNJ-39319202).

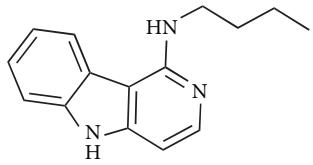

Figure 12: Structure of compound 7.

different linkers between the two aromatic rings. Thus, a series of ether, ester, amide, sulfonamide, carbamate, and urea derivatives were performed. These more flexible compounds led to molecules most retained in activity and efficacy compared to AC-7954 except for ethers and sulfonamide probably due to the absence of conformational effects induced by the pharmacophoric carbonyl group. Interestingly, esters showed lower efficacy than other derivatives, whereas the introduction of larger and lipophilic substituents in the variable aromatic part of the molecule tend generally to increase potency. To investigate the improvement of the efficacy it seems that the introduction of electron-donating groups contributed positively. Furthermore, among benzamide series more lipophilic compounds were approximately 1 order of magnitude more potent than the other amides. Accordingly, the biphenylamide derivative, later known as FL-104, was recognized as a potent agonist ($p\mathrm{EC}_{50}$ = 7.49 ± 0.03) and its racemic mixture was resolved in order to evaluate the main active stereoisomer, identified in (+)-FL-104 isomer ($p\mathrm{EC}_{50}$ = 7.49), considerably more active than (−)-FL-104. The (+)-S-enantiomer of FL-104 was considered as one of the most potent nonpeptide agonists known (Figure 4).

Analogues of FL-104 were designed and synthesized in order to enable comparisons between SAR in the isochromanone and benzamide series of UT agonists [58]. By the evaluation of the distance between the aromatic rings and the dimethylamino group and by the replacement of the dimethylamino group with a piperidine moiety new compounds were obtained and tested for their ability to stimulate the human UT receptor in an R-SAT assay. However, compound 1 was the most interesting among the series (Figure 4). Its racemate mixture was resolved and the (+)-(S)-enantiomer corresponded to the most active nonpeptide agonist compound with a $p\mathrm{EC}_{50}$ value of 7.64 ± 0.23, which is higher than the precursor FL-104.

As pharmacological tool in determining physiological and pathological roles of endogenous U-II in kidney diseases, in 2004 Clozel et al. [59] reported the discovery and characterization of a specific and potent inhibitor of the human UT receptor, the compound palosuran (ACT-058362) (Figure 5).

Results from radioligand binding experiments carried out in membrane preparations from CHO cells expressing the human UT receptor indicated palosuran as potent inhibitor of ^{125}I-U-II, binding at human UT receptor with an IC_{50} of 3.6 ± 0.2 nM, whereas radioligand ^{125}I-U-II was potently inhibited by the unlabeled U-II with an IC_{50} value of 1.2 ± 0.2 nM. On cell lines such as TE-671 and CHO, the inhibitory binding potency of palosuran toward the human UT receptor was lower than on membranes (IC_{50} = 46.2 ± 13 nM on TE-671 cells and IC_{50} = 86 ± 30 nM on recombinant CHO cells). Binding studies showed also that the inhibitory binding potency of palosuran is higher more than 100-fold on human UT receptor compared with the rat UT receptor (IC_{50} = 3.6 nM toward the human receptor, IC_{50} value of 1475 nM for rat receptor). However, palosuran inhibited U-II-induced concentration of rat aortic rings in a potent and concentration-dependent manner and inhibited the maximal contractile response of the rings almost completely at 10^{-4} M suggesting an insurmountable kind of antagonism of contraction induced by U-II. Despite this, in binding studies using membrane preparations expressing human UT receptor, palosuran interacted competitively with its receptor. This controversial mode of inhibition observed between functional assays and receptor binding studies could be linked to the likely noncompetitive antagonism due to the partial internalization of the UT receptor after binding with palosuran. This could reduce the receptor availability on the cell surface in the isolated rat aortic ring system. Functional assays showed that palosuran was a selective antagonist of UT receptor not antagonizing the action of other vasoconstrictor agents such as KCl, endothelin-1, 5-hydroxytryptamine, and norepinephrine. Therefore, palosuran represents an important tool of nonpeptide nature in order to validate the role of endogenous U-II in disease models, in particular in kidney pathologies. For this reason, palosuran was considered as an interesting tool and a novel

and interesting UT receptor antagonist for evaluating the pathophysiological role of endogenous U-II in renal system, since both U-II and UT receptor are highly expressed in the kidney [15]. Endogenous U-II plays a role in mediating the abnormal renal vasoconstriction after ischemia and short-term intravenous administration of palosuran reduced the glomerular and tubular dysfunction and renal tissue injury induced by renal ischemia [59].

Further evidence that the 4-ureido-quinoline core, also shared with the structure of palosuran, could be taken as a promising template for antagonists turned out from several patent applications. In addition, several examples of UT receptor antagonists have appeared in the patent literature but they were less discussed in this paper. Thus, 4-ureido-quinoline derivatives, in which 1,2,3,4-tetrahydroisoquinole, piperidine, piperazine, and pyrrolidine moieties were introduced, were also tested for their ability to displace human [^{125}I]U-II binding to a rhabdomyosarcoma cell line (IC_{50} values ranging from 1 to 1000 nM) [60–62]. Other non-peptide molecules reported in patent applications were based on 4-aminoquinolines [63] and quinolone, such as 2-aminoquinolines and 2-aminoalkylquinolin-4-ones derivatives [64], template (Figure 6).

Researchers at GlaxoSmithKline conducted extensive biological studies leading to the discovery of a series of arylsulfonamide derivatives developed from high-throughput screening. The compound SB-611812 showed potent binding at the rat UT receptor (K_i = 121 nM) and based on its antagonist activity in rat aortic tissue and interesting pharmacokinetic properties such as high bioavailability (~100%) and half-life (~5 h), this compound was proposed as a useful pharmacological tool (Figure 7). Accordingly, a coronary artery ligation study was conducted in rats with this lead UT antagonist since patients with congestive heart failure (CHF) are usually associated with high level of U-II and UT receptor in the heart tissue [65]. In this study, treatment with SB-611812 (30 mg/kg per day) for eight weeks significantly reduced overall mortality, left ventricular end-diastolic pressure, lung edema, right ventricular systolic pressure, central venous pressure, cardiomyocyte hypertrophy, and ventricular dilatation, underlying the importance of hUT-II in this disorder.

The identification and characterization of compound SB-706375 was originally described by Douglas et al. in 2005 [66] (Figure 8). This compound was identified as novel UT receptor antagonist, acting in a surmountable, reversible manner with high affinity across species (binding K_i = 4.7–20.7 nM) and good selectivity. The potent antagonist activity was demonstrated by its ability to inhibit [^{125}I]hU-II binding to both mammalian recombinant and "native" UT receptors with a reversible mode of action (K_i = 4.7 ± 1.5 to 20.7 ± 3.6 nM at rodent, feline, and primate recombinant UT receptors; K_i = 5.4 ± 0.4 nM at the endogenous UT receptor in SJRH30 cells). The antagonist activity was also validated in a number of assays such as the inhibition of contraction of the rat isolated aorta (pK_b = 7.47) and the inhibition of intracellular calcium mobilization in HEK293 cells expressing UT receptor (pK_b = 7.29–8.00). SB-706375 was a selective U-II antagonist for the human UT receptor (≥100-fold) compared to 86 distinct receptors including ion channels, enzymes, transporters, and nuclear hormones (K_i/IC_{50} > 1 μM). The contractile responses induced in isolated aortae by KCl, phenylephrine, angiotensin-II, and endothelin-1 were unaltered by SB-706375 (at 1 μM concentration).

The very closely related compound SB-657510 [67] was also indicated as potent antagonist in isolated arteries from rats, cats, monkeys, and hUT-transgenic mice (Figure 8). The characterization of this compound led to the first nonpeptide UT receptor radiolabel, namely, the tritiated radiotracer [^{3}H]SB-657510 [66].

Substituted diarylsulfonamides, reported in other patent applications, possessed significant affinity for UT receptors (K_i ~ 1 μM). They were designed as UT receptor antagonists and CCR-9 antagonists for the treatment of congestive heart failure, stroke, ischemic heart disease, and so forth [68].

Other UT antagonist series was represented by aminoalkoxy benzyl pyrrolidine derivatives even reported by GlaxoSmithKline. Based on an HTS protocol involving hU-II-mediated calcium mobilization in hUT-expressing HEK293 cells, the lead compound SB-436811 was identified for its moderate potency (K_i = 200 nM) binding to human UT receptor but weak potency in rat hUT binding (K_i = 3.2 μM) [69] (Figure 9). As group linker between the substituted-phenyl moiety and the heterocyclic ring, the sulfonamide group was replaced with an alkyl group.

Biphenylcarboxamide and benzazepine scaffolds were also reported in patent applications since these derivatives demonstrated highly potent UT receptor antagonism [70]. In particular, most structurally different from other UT receptor antagonists, benzazepines represented one of the most potent antagonists at the human UT receptor so far described (IC_{50} ~ 2 nM).

With the aim to identify a compound with low nanomolar potency toward both rat and human UT receptor, as research tool for evaluating the role of U-II/UT receptor interaction in disease models, Luci et al. in 2007 [71] developed new series of small organic molecules. New lead structures were obtained by executing an HTS protocol involving a functional assay based on cells transfected with rat UT receptor, a fluorometric imaging plate reader (FLIPR) to measure intracellular calcium flux, and the potent peptide UT agonist Ac-c[Cys-Phe-Trp-Lys-(2′)Nal-Cys]-NH_2 [32]. By the application of this assay to a large compound library, various 4-phenylpiperidine-benzoxazin-3-ones derivatives were identified. Compound 2, which contained a 4-(4-chlorophenyl)piperidine subunit, was identified as moderately potent compound (IC_{50} = 7.1 μM). On the basis of this lead compound more analogues were elaborated and compound 3 (Figure 10) that, containing an aryl-substituted piperidine subunit, was found to be a more potent antagonist toward both rat and human UT receptor (IC_{50} = 10 nM at rat UT receptor and K_i = 65 nM at human UT receptor). For this reason, this compound was selected for *in vivo* evaluation and its efficacy was shown in reversing the ear-flush response induced by U-II in rats.

Other classes of compound that turned out from this screening were represented by piperazino-phtalimide and piperazino-isoindolinone derivatives, very different structural type of UT receptor antagonists from those previously reported in literature. Thus, Lawson and coworkers in 2009 [72] realized these novel series starting from the identification of the compound 4 (rat FLIPR EC_{50} = 0.54 nM, rat UT binding K_i = 0.12 nM) and the strictly related compound 5, also known as JNJ-28318706. The latter had improved metabolic stability and improved potency (rat FLIPR IC_{50} = 84 nM), and (R)-enantiomer exhibited also good oral bioavailability in pharmacokinetics experiments. However, as piperazino-isoindolinone derivative (Figure 11), the compound 6 (JNJ-39319202) showed single-digit nanomolar potencies in the rat FLIPR assay (IC_{50} = 1.0 nM) and in the human UT receptor binding assay (K_i = 4.0 nM). This compound also exhibited potent antagonism in the human calcium flux assay (IC_{50} = 8.0 nM). Moreover, a recent study reported a facile alkylation-cyclization reaction performed on isoindolinone core of JNJ-39319202 that yielded to novel tricyclic derivatives with retained potency in antagonism activity [73].

Aminomethylpiperazines derivatives were also drawn out from the structure belonging to κ-opioid receptor agonists [74]. In accordance with this study, optimization of the piperazine moiety provided high affinity urotensin-II receptor antagonists (more than 100-fold selectivity over the κ-opioid receptor) and, among this series, specific compounds inhibited urotensin-induced vasoconstriction in isolated rat aortic ring.

Other 2-aminomethyl piperidine derivatives had moderate hUT binding affinity (K_i = 400 nM) and hUT functional activity (FLIPR IC_{50} = 600 nM) [75]. However, these series were correlated to problems such as cytochrome P450 inhibition and low oral bioavailability. Therefore, some improvements were obtained by using a piperazine core in such promising compounds. Subsequently, removal of the piperidine and piperazine linker groups led to a series of potent biphenylmethyl derivatives.

Wang et al. in 2008 [76] described a series of N-alkyl-5H-pyrido[4,3-*b*]-indol-1-amines as UT receptor antagonists since the tricyclic compound 7 was identified in an HTS as a lead compound due to its binding affinity (pK_i = 8.1) and submicromolar antagonist activity ($p\mathrm{IC}_{50}$ = 6.3) at human UT receptor (Figure 12).

5. Conclusion

Despite of the large number of studies performed on U-II system, less knowledge even belongs to the issue regarding the pathophysiological role of urotensin-II/UT receptor interaction. Accordingly, several studies have reported contradictory activities resulting from the injection of exogenous U-II in the bloodstream. Vasoconstriction induced by exogenous U-II is indeed subjected to significant species and/or regional differences. Thus, from our point of view, the investigation of structure-activity relationships of U-II system represents the keystone that could address the unsolved question regarding the putative role of U-II in several disorders and physiological effects. The synthesis of U-II analogues has been performed adopting two main strategies based on the design and development of peptide or nonpeptide derivatives. Both the approaches present several advantages and disadvantages. Although peptides offer several advantages as therapeutic tools over small organic molecules, when they are composed of natural amino acids they are not very good drug candidates because of their intrinsic physicochemical and pharmacokinetic properties such as low bioavailability and biodistribution. On the other hand, as drug candidates in a therapeutic strategy, peptides offer greater efficacy, selectivity and specificity, and lower toxicity than small organic molecules since they represent the smallest functional part of a protein. However, the introduction of pharmacophoric elements in small organic structures is fascinating and favourable in the treatment of some diseases. Thereby, organic compounds represent the key for obtaining promising drug candidates by reaching easily a compromise between stability and selectivity.

The research of the best therapeutic tools in disorders produced by U-II could be achieved by chemical optimization strategies for urotensin-II derivatives, peptides or nonpeptide analogues. The best knowledge of structure-activity relationships may provide useful chemical requirements in order to improve pharmacodynamic and pharmacokinetic properties such as bioavailability, reduction of elimination and biodegradation by proteolytic enzymes activity, low toxicity, reduced drug-drug interactions, and short half-life values avoiding accumulation of metabolites in tissues. As for urotensin peptides, substitution of natural amino acid residues by unnatural amino acid such as D-stereoisomer, nonproteogenic constrained amino acid or β-amino acid has represented strategic chemical approach resulting in the increase of stability and/or affinity for the UT receptor. At least, development of nonpeptide antagonists at the UT receptor is an attractive alternative as pharmacological tool in the identification of the role of endogenous U-II in several pathophysiological effects.

References

[1] H. A. Bern, D. Pearson, B. A. Larson, and R. S. Nishioka, "Neurohormones from fish tails: the caudal neurosecretory system. I. "Urophysiology" and the caudal neurosecretory system of fishes," *Recent Progress in Hormone Research*, vol. 41, pp. 533–552, 1985.

[2] J. M. Conlon, F. O'Harte, D. D. Smith, M. C. Tonon, and H. Vaudry, "Isolation and primary structure of urotensin II from the brain of a tetrapod, the frog Rana ridibunda," *Biochemical and Biophysical Research Communications*, vol. 188, no. 2, pp. 578–583, 1992.

[3] J. M. Conlon, N. Chartrel, J. Leprince, C. Suaudeau, J. Costentin, and H. Vaudry, "A proenkephalin A-derived peptide analogous to bovine adrenal peptide E from frog brain: purification, synthesis, and behavioral effects," *Peptides*, vol. 17, no. 8, pp. 1291–1296, 1996.

[4] H. Tostivint, I. Lihrmann, C. Bucharles et al., "A second somatostatin gene is expressed in the brain of the frog Rana ridibunda," *Annals of the New York Academy of Sciences*, vol. 839, no. 1, pp. 496–497, 1998.

[5] J. M. Conlon, K. Yano, D. Waugh, and N. Hazon, "Distribution and molecular forms of urotensin II and its role in cardiovascular regulation in vertebrates," *Journal of Experimental Zoology*, vol. 275, no. 2-3, pp. 226–238, 1996.

[6] A. L. Colton, "Effective thermal parameters for a heterogenous land surface," *Remote Sensing of Environment*, vol. 57, no. 3, pp. 143–160, 1996.

[7] P. Brazeau, W. Vale, R. Burgus et al., "Hypothalamic polypeptide that inhibits the secretion of immunoreactive pituitary growth hormone," *Science*, vol. 179, no. 4068, pp. 77–79, 1973.

[8] S. Ohsako, I. Ishida, T. Ichikawa, and T. Deguchi, "Cloning and sequence analysis of cDNAs encoding precursors of urotensin II-α and -γ," *Journal of Neuroscience*, vol. 6, no. 9, pp. 2730–2735, 1986.

[9] D. Pearson, J. E. Shively, B. R. Clark et al., "Urotensin II: a somatostatin-like peptide in the caudal neurosecretory system of fishes," *Proceedings of the National Academy of Sciences of the United States of America*, vol. 77, no. 8, pp. 5021–5024, 1980.

[10] R. S. Ames, H. M. Sarau, J. K. Chambers et al., "Human urotensin-II is a potent vasoconstrictor and agonist for the orphan receptor GPR14," *Nature*, vol. 401, pp. 282–286, 1999.

[11] H. P. Nothacker, Z. Wang, A. M. McNeill et al., "Identification of the natural ligand of an orphan G-protein-coupled receptor involved in the regulation of vasoconstriction," *Nature Cell Biology*, vol. 1, no. 6, pp. 383–385, 1999.

[12] K. Mori, H. Nagao, and Y. Yoshihara, "The olfactory bulb: coding and processing of odor molecule information," *Science*, vol. 286, no. 5440, pp. 711–715, 1999.

[13] S. A. Douglas and E. H. Ohlstein, "Human urotensin-II, the most potent mammalian vasoconstrictor identified to date, as a therapeutic target for the management of cardiovascular disease," *Trends in Cardiovascular Medicine*, vol. 10, no. 6, pp. 229–237, 2000.

[14] J. J. Maguire, R. E. Kuc, and A. P. Davenport, "Orphan-receptor ligand human urotensin II: receptor localization human tissues and comparison of vasoconstrictor responses with endothelin-1," *British Journal of Pharmacology*, vol. 131, no. 3, pp. 441–446, 2000.

[15] M. Matsushita, M. Shichiri, T. Imai et al., "Co-expression of urotensin II and its receptor (GPR14) in human cardiovascular and renal tissues," *Journal of Hypertension*, vol. 19, no. 12, pp. 2185–2190, 2001.

[16] J. J. Maguire and A. P. Davenport, "Is urotensin-II the new endothelin?" *British Journal of Pharmacology*, vol. 137, no. 5, pp. 579–588, 2002.

[17] Y. C. Zhu, Y. Z. Zhu, and P. K. Moore, "The role of urotensin II in cardiovascular and renal physiology and diseases," *British Journal of Pharmacology*, vol. 148, pp. 884–901, 2006.

[18] S. Suzuki, Z. Wenyi, M. Hirai et al., "Genetic variations at urotensin II and urotensin II receptor genes and risk of type 2 diabetes mellitus in Japanese," *Peptides*, vol. 25, no. 10, pp. 1803–1808, 2004.

[19] O. V. Muravenko, R. Z. Gizatullin, A. N. Al-Amin et al., "Human ALY/BEF gene map position 17q25.3," *Chromosome Research*, vol. 8, no. 6, p. 562, 2000.

[20] R. d'Emmanuele di Villa Bianca, E. Mitidieri, F. Fusco et al., "Endogenous urotensin II selectively modulates erectile function through eNOS," *PLoS One*, vol. 7, no. 2, Article ID e31019, 2012.

[21] S. A. Douglas and E. H. Ohlstein, "Human urotensin-II, the most potent mammalian vasoconstrictor identified To date, as a therapeutic target for the management of cardiovascular disease," *Trends in Cardiovascular Medicine*, vol. 10, no. 6, pp. 229–237, 2000.

[22] S. A. Douglas, D. Naselsky, Z. Ao et al., "Identification and pharmacological characterization of native, functional human urotensin-II receptors in rhabdomyosarcoma cell lines," *British Journal of Pharmacology*, vol. 142, no. 6, pp. 921–932, 2004.

[23] R. Bhaskaran and C. Yu, "NMR spectra and restrained molecular dynamics of the mushroom toxin viroisin," *International Journal of Peptide and Protein Research*, vol. 43, no. 4, pp. 393–401, 1994.

[24] S. Flohr, M. Kurz, E. Kostenis, A. Brkovich, A. Fournier, and T. Klabunde, "Identification of nonpeptidic urotensin II receptor antagonists by virtual screening based on a pharmacophore model derived from structure-activity relationships and nuclear magnetic resonance studies on urotensin II," *Journal of Medicinal Chemistry*, vol. 45, no. 9, pp. 1799–1805, 2002.

[25] P. Grieco, A. Carotenuto, R. Patacchini, C. A. Maggi, E. Novellino, and P. Rovero, "Design, synthesis, conformational analysis, and biological studies of urotensin-II lactam analogues," *Bioorganic and Medicinal Chemistry*, vol. 10, no. 12, pp. 3731–3739, 2002.

[26] A. Carotenuto, P. Grieco, P. Campiglia, E. Novellino, and P. Rovero, "Unraveling the active conformation of urotensin II," *Journal of Medicinal Chemistry*, vol. 47, no. 7, pp. 1652–1661, 2004.

[27] D. H. Coy, W. J. Rossowski, B. L. Cheng, and J. E. Taylor, "Structural requirements at the N-terminus of urotensin II octapeptides," *Peptides*, vol. 23, pp. 2259–2264, 2002.

[28] D. McMaster, Y. Kobayashi, J. Rivier, and K. Lederis, "Characterization of the biologically and antigenically important regions of urotensin II," *Proceedings of the Western Pharmacology Society*, vol. 29, pp. 205–208, 1986.

[29] P. Grieco, A. Carotenuto, P. Campiglia et al., "A new, potent urotensin II receptor peptide agonist containing a Pen residue at the disulfide bridge," *Journal of Medicinal Chemistry*, vol. 45, no. 20, pp. 4391–4394, 2002.

[30] S. Foister, L. L. Taylor, J. J. Feng et al., "Design and synthesis of potent cystine-free cyclic hexapeptide agonists at the human urotensin receptor," *Organic Letters*, vol. 8, no. 9, pp. 1799–1802, 2006.

[31] A. Lavecchia, S. Cosconati, and E. Novellino, "Architecture of the human urotensin II receptor: comparison of the binding domains of peptide and non-peptide urotensin II agonists," *Journal of Medicinal Chemistry*, vol. 48, no. 7, pp. 2480–2492, 2005.

[32] W. A. Kinney, H. R. Almond Jr., J. Qi et al., "Structure-function analysis of urotensin II and its use in the construction of a ligand-receptor working model," *Angewandte Chemie—International Edition*, vol. 41, no. 16, pp. 2940–2944, 2002.

[33] R. Guerrini, V. Camarda, E. Marzola et al., "Structure-activity relationship study on human urotensin II," *Journal of Peptide Science*, vol. 11, no. 2, pp. 85–90, 2005.

[34] A. Carotenuto, P. Grieco, P. Rovero, and E. Novellino, "Urotensin-II receptor antagonists," *Current Medicinal Chemistry*, vol. 13, no. 3, pp. 267–275, 2006.

[35] D. J. Behm, C. L. Herold, E. H. Ohlstein, S. D. Knight, D. Dhanak, and S. A. Douglas, "Pharmacological characterization of SB-710411 (Cpa-c[D-Cys-Pal-D-Trp-Lys-Val-Cys]-Cpa-amide), a novel peptidic urotensin-II receptor antagonist," *British Journal of Pharmacology*, vol. 137, no. 4, pp. 449–458, 2002.

[36] D. J. Behm, C. L. Herold, V. Camarda, N. V. Aiyar, and S. A. Douglas, "Differential agonistic and antagonistic effects of the urotensin-II ligand SB-710411 at rodent and primate UT receptors," *European Journal of Pharmacology*, vol. 492, no. 2-3, pp. 113–116, 2004.

[37] N. A. Elshourbagy, S. A. Douglas, U. Shabon et al., "Molecular and pharmacological characterization of genes encoding urotensin-II peptides and their cognate G-protein-coupled receptors from the mouse and monkey," *British Journal of Pharmacology*, vol. 136, no. 1, pp. 9–22, 2002.

[38] V. Camarda, R. Guerrini, E. Kostenis et al., "A new ligand for the urotensin II receptor," *British Journal of Pharmacology*, vol. 137, no. 3, pp. 311–314, 2002.

[39] M. Orbuch, J. E. Taylor, D. H. Coy et al., "Discovery of a novel class of neuromedin B receptor antagonists, substituted somatostatin analogues," *Molecular Pharmacology*, vol. 44, no. 4, pp. 841–850, 1993.

[40] C. L. Herold, D. J. Behm, P. T. Buckley et al., "The neuromedin B receptor antagonist, BIM-23127, is a potent antagonist at human and rat urotensin-II receptors," *British Journal of Pharmacology*, vol. 139, no. 2, pp. 203–207, 2003.

[41] C. L. Herold, D. J. Behm, P. T. Buckely, J. J. Foley, and S. A. Douglas, "The peptidic somatostatin analogs lanreotide, BIM-23127 and BIM-23042 are urotensin-II receptor ligands," *Pharmacologist*, vol. 44, pp. 170–171, 2002.

[42] R. Patacchini, P. Santicioli, S. Giuliani et al., "Urantide: an ultrapotent urotensin II antagonist peptide in the rat aorta," *British Journal of Pharmacology*, vol. 140, no. 7, pp. 1155–1158, 2003.

[43] P. Grieco, A. Carotenuto, P. Campiglia et al., "Urotensin-II receptor ligands. From agonist to antagonist activity," *Journal of Medicinal Chemistry*, vol. 48, no. 23, pp. 7290–7297, 2005.

[44] V. Camarda, W. Song, E. Marzola et al., "Urantide mimics urotensin-II induced calcium release in cells expressing recombinant UT receptors," *European Journal of Pharmacology*, vol. 498, no. 1–3, pp. 83–86, 2004.

[45] V. Camarda, M. Spagnol, W. Song et al., "In vitro and in vivo pharmacological characterization of the novel UT receptor ligand [Pen^5,DTrp^7,Dab^8]urotensin II(4-11) (UFP-803)," *British Journal of Pharmacology*, vol. 147, no. 1, pp. 92–100, 2006.

[46] T. Sugo, Y. Murakami, Y. Shimomura et al., "Identification of urotensin II-related peptide as the urotensin II-immunoreactive molecule in the rat brain," *Biochemical and Biophysical Research Communications*, vol. 310, no. 3, pp. 860–868, 2003.

[47] D. Chatenet, C. Dubessy, J. Leprince et al., "Structure-activity relationships and structural conformation of a novel urotensin II-related peptide," *Peptides*, vol. 25, no. 10, pp. 1819–1830, 2004.

[48] D. Chatenet, Q. T. Nguyen, M. Létourneau, J. Dupuis, and A. Fournier, "Urocontrin, a novel UT receptor ligand with a unique pharmacological profile," *Biochemical Pharmacology*, vol. 83, no. 5, pp. 608–615, 2012.

[49] M. Jarry, M. Diallo, C. Lecointre et al., "The vasoactive peptides urotensin II and urotensin II-related peptide regulate astrocyte activity through common and distinct mechanisms: involvement in cell proliferation," *Biochemical Journal*, vol. 428, no. 1, pp. 113–124, 2010.

[50] H. C. G. Prosser, J. Leprince, H. Vaudry, A. M. Richards, M. E. Forster, and C. J. Pemberton, "Cardiovascular effects of native and non-native urotensin II and urotensin II-related peptide on rat and salmon hearts," *Peptides*, vol. 27, no. 12, pp. 3261–3268, 2006.

[51] T. Kenakin, "Drug efficacy at G protein-coupled receptors," *Annual Review of Pharmacology and Toxicology*, vol. 42, pp. 349–379, 2002.

[52] D. J. Behm, G. Stankus, C. P. A. Doe et al., "The peptidic urotensin-II receptor ligand GSK248451 possesses less intrinsic activity than the low-efficacy partial agonists SB-710411 and urantide in native mammalian tissues and recombinant cell systems," *British Journal of Pharmacology*, vol. 148, no. 2, pp. 173–190, 2006.

[53] D. H. Coy, W. J. Rossowski, B. L. Cheng, and J. E. Taylor, "Highly potent heptapeptide antagonists of the vasoactive peptide urotensin II," in *Proceedings of the 225th ACS National Meeting*, American Chemical Society, New Orleans, La, USA, March 2003.

[54] N. Aiyar, D. G. Johns, Z. Ao et al., "Cloning and pharmacological characterization of the cat urotensin-II receptor (UT)," *Biochemical Pharmacology*, vol. 69, no. 7, pp. 1069–1079, 2005.

[55] G. E. Croston, R. Olsson, E. A. Currier et al., "Discovery of the first nonpeptide agonist of the GPR14/Urotensin-II receptor: 3-(4-chlorophenyl)-3-(2-(dimethylamino)ethyl)isochroman-1-one (AC-7954)," *Journal of Medicinal Chemistry*, vol. 45, no. 23, pp. 4950–4953, 2002.

[56] F. Lehmann, E. A. Currier, R. Olsson, U. Hacksell, and K. Luthman, "Isochromanone-based urotensin-II receptor agonists," *Bioorganic and Medicinal Chemistry*, vol. 13, no. 8, pp. 3057–3068, 2005.

[57] F. Lehmann, L. Lake, E. A. Currier, R. Olsson, U. Hacksell, and K. Luthman, "Design, parallel synthesis and SAR of novel urotensin II receptor agonists," *European Journal of Medicinal Chemistry*, vol. 42, no. 2, pp. 276–285, 2007.

[58] F. Lehmann, E. A. Currier, B. Clemons et al., "Novel and potent small-molecule urotensin II receptor agonists," *Bioorganic and Medicinal Chemistry*, vol. 17, no. 13, pp. 4657–4665, 2009.

[59] M. Clozel, C. Binkert, M. Birker-Robaczewska et al., "Pharmacology of the urotensin-II receptor antagonist palosuran (ACT-058362; 1-[2-(4-benzyl-4-hydroxy-piperidin-1-yl)-ethyl]-3-(2-methyl-quinolin-4-yl)-urea sulfate salt): first demonstration of a pathophysiological role of the urotensin system," *Journal of Pharmacology and Experimental Therapeutics*, vol. 311, no. 1, pp. 204–212, 2004.

[60] H. Aissaoui, C. Binkert, M. Clozel et al., "Preparation of 1-(piperazinylalkyl)-3-quinolinylurea derivatives as urotensin II antagonists," Actelion Pharmaceuticals Ltd., PCT International Application no. WO2004099179, 2004.

[61] H. Aissaoui, C. Binkert, M. Clozel et al., "Preparation of novel piperidine derivatives as urotensin II antagonists," Actelion Pharmaceutical Ltd., PCT International Application no. WO2004099180, 2004.

[62] H. Aissoui, C. Binkert, M. Clozel et al., "Preparation of 1, 2, 3, 4-tetrahydroisoquinolinyl ureas and related derivatives as urotensin II receptor antagonists," Actelion Pharmaceuticals Ltd., PCT International Application no. WO2002076979, 2002.

[63] N. Tarui, T. Santo, M. Mori, and H. Watanabe, "Quinoline derivatives as vasoactive agents exhibiting orphanr eceptor GPR14 protein antagonism," Takeda Chemical Industries, PCT International Application no. WO2001066143, 2001.

[64] D. Dhanak and S. D. Knight, "Preparation of quinolones as urotensin-II receptor antagonists," Smithkline Beecham Corporation, PCT International Application no. WO2002047456, 2002.

[65] N. Bousette, J. Pottinger, W. Ramli et al., "Urotensin-II receptor blockade with SB-611812 attenuates cardiac remodeling in

experimental ischemic heart disease," *Peptides*, vol. 27, no. 11, pp. 2919–2926, 2006.

[66] S. A. Douglas, D. J. Behm, N. V. Aiyar et al., "Nonpeptidic urotensin-II receptor antagonists I: *in vitro* pharmacological characterization of SB-706375," *British Journal of Pharmacology*, vol. 145, no. 5, pp. 620–635, 2005.

[67] D. J. Behm, J. J. McAtee, J. W. Dodson et al., "Palosuran inhibits binding to primate UT receptors in cell membranes but demonstrates differential activity in intact cells and vascular tissues," *British Journal of Pharmacology*, vol. 155, no. 3, pp. 374–386, 2008.

[68] C. Wu, D. Gao, R. Biediger, J. Chen, and R. V. Market, "Phenylenediamine urotensin-II receptor antagonists and CCR-9 antagonists," Encysive Pharmaceuticals, Inc., US patent no. 7,288,538 B2, 2007.

[69] J. Jin, D. Dhanak, S. D. Knight et al., "Aminoalkoxybenzyl pyrrolidines as novel human urotensin-II receptor antagonists," *Bioorganic and Medicinal Chemistry Letters*, vol. 15, no. 13, pp. 3229–3232, 2005.

[70] N. Tarui, T. Santo, H. Watanabe, K. Aso, T. Miwa, and S. Takekawa, "Preparation of biphenylcarboxamide compounds as GPR14 antagonists or somatostatin receptor regulators," Takeda Chemical Industries, PCT International Application no. WO2002000606, 2002.

[71] D. K. Luci, S. Ghosh, C. E. Smith et al., "Phenylpiperidine-benzoxazinones as urotensin-II receptor antagonists: synthesis, SAR, and in vivo assessment," *Bioorganic and Medicinal Chemistry Letters*, vol. 17, no. 23, pp. 6489–6492, 2007.

[72] E. C. Lawson, D. K. Luci, S. Ghosh et al., "Nonpeptide urotensin-II receptor antagonists: a new ligand class based on piperazino-phthalimide and piperazino-isoindolinone subunits," *Journal of Medicinal Chemistry*, vol. 52, no. 23, pp. 7432–7445, 2009.

[73] D. K. Luci, E. C. Lawson, S. Ghosh et al., "Generation of novel, potent urotensin-II receptor antagonists by alkylation-cyclization of isoindolinone C3-carbanions," *Tetrahedron Letters*, vol. 50, no. 35, pp. 4958–4961, 2009.

[74] M. A. Hilfiker, D. Zhang, S. E. Dowdell et al., "Aminomethylpiperazines as selective urotensin antagonists," *Bioorganic and Medicinal Chemistry Letters*, vol. 18, no. 16, pp. 4470–4473, 2008.

[75] J. Jin, Y. Wang, F. Wang et al., "2-aminomethyl piperidines as novel urotensin-II receptor antagonists," *Bioorganic and Medicinal Chemistry Letters*, vol. 18, no. 9, pp. 2860–2864, 2008.

[76] Y. Wang, Z. Wu, B. F. Guida et al., "N-alkyl-5*H*-pyrido[4,3-*b*]indol-1-amines and derivatives as novel urotensin-II receptor antagonists," *Bioorganic and Medicinal Chemistry Letters*, vol. 18, no. 18, pp. 4936–4939, 2008.

Hindawi Publishing Corporation
Journal of Amino Acids
Volume 2013, Article ID 251398, 13 pages
http://dx.doi.org/10.1155/2013/251398

Research Article

The Antitumor Peptide CIGB-552 Increases COMMD1 and Inhibits Growth of Human Lung Cancer Cells

Julio R. Fernández Massó,[1] Brizaida Oliva Argüelles,[2] Yelaine Tejeda,[1] Soledad Astrada,[3] Hilda Garay,[4] Osvaldo Reyes,[4] Livan Delgado-Roche,[5] Mariela Bollati-Fogolín,[3] and Maribel G. Vallespí[2]

[1] *Department of Genomic, Center for Genetic Engineering and Biotechnology, Cubanacan, P.O. Box 6162, 10600 Havana, Cuba*
[2] *Pharmaceutical Department, Laboratory of Cancer Biology, Center for Genetic Engineering and Biotechnology, Cubanacan, P.O. Box 6162, 10600 Havana, Cuba*
[3] *Cell Biology Unit, Institute Pasteur of Montevideo, Mataojo 2020, 11400 Montevideo, Uruguay*
[4] *Synthetic Peptide Group, Physical Chemistry Department, Center for Genetic Engineering and Biotechnology, Cubanacan, P.O. Box 6162, 10600 Havana, Cuba*
[5] *Center of Studies for Research and Biological Evaluations, Pharmacy and Food Sciences College, University of Havana, 19250 Havana, Cuba*

Correspondence should be addressed to Maribel G. Vallespí; maribel.guerra@cigb.edu.cu

Received 18 October 2012; Revised 12 December 2012; Accepted 12 December 2012

Academic Editor: Michele Caraglia

We have demonstrated that the peptide L-2 designed from an alanine scanning of the *Limulus*-derived LALF32-51 region is a potential candidate for the anticancer therapy and its cell-penetrating capacity is an associated useful property. By the modification in the primary structure of L-2, a second-generation peptide (CIGB-552) was developed. However, the molecular mechanism underlying its cytotoxic activity remains partially unknown. In this study, it was shown that CIGB-552 increases the levels of COMMD1, a protein involved in copper homeostasis, sodium transport, and the NF-κB signaling pathway. We found that CIGB-552 induces ubiquitination of RelA and inhibits the antiapoptotic activity regulated by NF-κB, whereas the knockdown of COMMD1 blocks this effect. We also found that CIGB-552 decreases the antioxidant capacity and induces the peroxidation of proteins and lipids in the tumor cells. Altogether, this study provides new insights into the mechanism of action of the peptide CIGB-552, which could be relevant in the design of future anticancer therapies.

1. Introduction

In previous work, a peptide-based approach was used to identify peptides devoid of LPS-binding capacity from LALF residues 32–51. Two peptides (L-2 and L-20) lost their ability to bind LPS and exhibited a differential cytotoxic activity, although a similar cell penetrating capacity was demonstrated for both peptides [1]. We introduced a chemical modification in the primary structure of the peptide L-2 to improve the biological activity and specificity. The chemical modification included the substitution of a natural amino acid residue by an unnatural amino acid (D-configuration) and blocked N-terminal by acylation. This modification led to the development of a second-generation peptide (CIGB-552) with increased cytotoxic activity on murine and human tumor cells [2]. Although the antitumor effects of the peptides involve an increase in the apoptosis and a negative regulation of cell-cycle progression, little is known regarding this mechanism of action.

In this study, two complementary approaches were used: a yeast two-hybrid search for molecules that specifically interact with the peptides and a pull-down technique to

validate the interaction. COMMD1 was identified as a peptide-binding protein. Furthermore, the specificity peptide/COMMD1 complexes were corroborated by related synthetic peptides with a differential cytotoxic activity (L-2, L-20, and CIGB-552) in cells expressing endogenous COMMD1.

COMM domain—containing 1 (COMMD1), the first COMMD family member to be identified, is a pleiotropic factor that participates in multiple processes, including copper metabolism, sodium excretion, inflammatory responses, and adaptation to hypoxia [3–6]. A growing body of data suggests that COMMD1 is associated with a multimeric E3 ubiquitin ligase complex and regulates the stability of proteins such as NF-κB subunits, ATP7B, and HIF-1-α [7–11]. In addition to its physiological roles, HIF participates in the pathophysiology of several disorders, including cancer, in which enhanced HIF activity is associated with tumor growth, neovascularization, local invasion, metastatic disease, and poor clinical outcomes [12]. While under physiological conditions NF-κB plays critical roles in inflammatory responses and cellular survival to stress, the activation of NF-κB has also a frequent occurrence in cancer. In particular, the ability of NF-κB to promote the expression of various antiapoptotic factors is thought to play a major role in the survival of cancer cells [11].

Consistent with the notion that COMMD1 functions in multiple cellular pathways involved in the survival of cancer cells, it has been demonstrated that the decreased COMMD1 expression in human cancer correlates with a more invasive tumor phenotype [13]. It is reported in this study that CIGB-552 increases the levels of the protein COMMD1 and negatively regulates the anti-apoptotic activity of NF-κB. Furthermore, CIGB-552 induces an imbalance in the antioxidant/prooxidant balance in cancer cells that promotes the peroxidation of proteins and lipids. These findings have relevance for the design of anticancer agents that act by targeting COMMD1 to inhibit NF-κB activity.

2. Materials and Methods

2.1. Peptides Synthesis. Peptides were synthesized on a solid phase and purified by reverse-phase-high-performance liquid chromatography to >95% purity on an acetonitrile/H_2O-trifluoracetic acid gradient and confirmed by ion-spray mass spectrometry (Micromass, Manchester, UK). Lyophilized peptides were reconstituted in phosphate-buffered saline (PBS) for experiments *in vitro*. The sequences of peptides used were L-2: HARIKPTFRRLKWKYKGKFW; L-20: HYRIKPTFRRLKWKYKGKFA and CIGB-552 second-generation peptide Ac-HARIK**p**TFRR**I**KWKYKGKFW where proline and leucine were substituted by D-amino acid; and N-terminal blocked by acylation.

2.2. Yeast Two-Hybrid Screening. Oligonucleotides with the sequences corresponding to peptides L-2 and L-20 were synthesized and cloned in-frame into pGBKT7 yeast two-hybrid vector (Table 1). The recombinant clones pGBKT7-L2 and pGBKT7-L20 were verified by DNA sequence and subsequently transformed into yeast strain AH109.

A matchmaker pretransformed liver cDNA library in Y187 (Clontech) was used to identify the protein interactions of L-2. Briefly, 5×10^8 AH109 cells containing the plasmid pGBKT7-L2 were grown and matted with 5×10^8 Y187 cells containing the cDNA library from human liver and transferred to minimal medium plates SD-Trp-Leu-His-Ade and grown at 30°C 7 days. The positive colonies were grown in Trp-Leu medium and the plasmids recovered and transformed into DH10B cells. Each individual clone was transformed in Y187 strain and the interaction verified by matting with the strain AH109 transformed with the plasmids pGBKT7, pGBKT7-L2, and pGBKT7-L20. The positive clones were sequenced and their sequences were analyzed using BLAST [14].

COMMD1 subclones N-terminus containing 6–110 amino acids and C-terminus containing 111–190 amino acids (nucleotides 18–332 and 333–570, resp.) were cloned in-frame into a two-hybrid yeast vector containing the GAL4 activation domain (pGADT7). Each COMMD1 subclone was transformed into Y187 strain and the interaction verified by matting with the AH109 strain transformed with the plasmids pGBKT7, pGBKT7-L-2, and pGBKT7-L-20.

2.3. Chemicals Reagents. The following chemicals and reagents used were from the indicated companies: RPMI 1640 (Gibco BRL, NY, USA); fetal bovine serum (FBS) and PBS 1X (from PAA, Canada); gentamicin, hydrogen peroxide (H_2O_2), MG132, propidium iodide, Nonidet P-40 (NP-40), dithiothreitol (DTT), Protease Inhibitor Cocktail and Albumin (BSA) (all from Sigma); and RNase A, (Boehringer Mannheim) and absolute ethanol from Merck.

2.4. Cell Fractioning. H460 (ATCC, HTB-117) cells were seeded in Flasks T-75, and were kept at 37°C and 5% CO_2 in RPMI 1640 medium supplemented with 10% (v/v) FBS, L-glutamine plus 50 μg/mL of gentamicin. The cells' fractioning was performed as described previously [15]. Briefly, the pelleted cells were resuspended in 300 μL of hypotonic buffer (10 mM Hepes, pH 7.5, 10 mM KCl, 3 mM NaCl, 3 mM $MgCl_2$, 1 mM EDTA, and 2 mM DTT) containing a protease inhibitor mixture from Sigma (P-8340), used at 60 μL/5 $\times$ 10^6 cells. After 15 min incubation on ice, 0,05 volumes of 10% NP-40 were added, the cells were mixed for 10 s and immediately centrifuged at 500 g for 10 min at 4°C. The supernatants were collected, labeled as cytoplasmic extracts, aliquoted, and stored at −80°C. The pelleted nuclei were resuspended in 50 μL of the ice-cold nuclear buffer (20 mM Hepes, pH 7.5; 25% glycerol, 0.8 m KCl, 1 mM $MgCl_2$, 1% NP-40, 0.5 mM EDTA, 2 mM DTT) containing the protease and phosphatase inhibitors as described above. Following a 20 min incubation on ice with occasional stirring, the samples were centrifuged (14,000 g, 15 min, 4°C) and the resulting supernatants were aliquoted and stored at −80°C.

2.5. Western Blot and Immunoprecipitation Analysis. 40 μg of total protein extract was applied on 7.5% to 12.5% SDS polyacrylamide gels and Western blot conducted by standard procedures [16]. The primary antibodies used

Table 1: Oligonucleotides sequences corresponding to L-2 and L-20.

Name	Sequence
L-2	CATGCACGCTAGAATCAAGCCAACCTTCAGAAGATTGAAGTGGAAGTACAAGGGTAAGTTCTGGTAA
L-2C	GATCTTACCAGAACTTACCCTTGTACTTCCACTTCAATCTTCTGAAGGTTGGCTTGATTCTAGCGTG
L-20	ATGCACTACAGAATCAAGCCAACCTTCAGAAGATTGAAGTGGAAGTACAAGGGTAAGTTCGCTTAA
L-20C	GATCTTAAGCGAACTTACCCTTGTACTTCCACTTCAATCTTCTGAAGGTTGGCTTGATTCTGTAGTG

were COMMD1 monoclonal (2A12), beta-actin monoclonal (AC15), heterogeneous nuclear ribonucleoproteins (hnRNP) monoclonal (4F4), anti-caspase 3, active (C8487) (all from Sigma); Bcl-2 polyclonal (C21) and Bax antibody (Santa Cruz Biotechnology), monoclonal RelA (ab95020) and polyclonal ubiquitin (ab19247) Abcam; and PARP antibody (9542) from Cell Signaling Technology. For immunoprecipitation assays, the cells were lysed in RIPA lysis buffer (1% Nonidet P40, 0.5% sodium deoxycholate, 0.1% SDS, and 0.5% BSA in PBS). The buffer was supplemented with Protease Inhibitor Cocktail and 2 mM of DTT. Immunoprecipitation assays were done using 200 μg of whole-cell lysate. Rabbit polyclonal anti-RelA (ADI-KAS-TF-110) (Abcam) was used to immunoprecipitate the appropriate protein and monoclonal IgG (A-1949) (Sigma) was used as a negative control. Complexes were separated by SDS-PAGE and then analyzed by Western blot analysis.

2.6. Immunofluorescence Detection of COMMD1. HT-29 (ATCC, HTB38) and MCF-7 (ATCC, HTB22) cells were seeded in 12 well plates containing cover slips (5×10^4 cell/well) and were cultured in D-MEM-Glutamax, 10% fetal bovine serum, at 37°C for 24 h. Subsequently, CIGB-552 peptide was added to a final concentration of 60 and 20 μM in HT-29 and MCF-7, respectively. Cells were incubated at 37°C for 5 h, then cover slips were washed with PBS, and the cells were fixed in 4% paraformaldehyde for 15 min and permeabilized in Tween 20 solution (0.2% in PBS). Blocking was performed with 3% bovine serum albumin in PBS (BSA-PBS) for 1 h. Anti-COMMD1 monoclonal antibody (2A12) (Abnova) was diluted 1 : 500 in BSA-PBS and the secondary antibody Cy3 goat anti-mouse IgG (Invitrogen) was used at 1 : 1000 dilution. All images were taken using laser confocal microscope Leica TCS SP5 and a 63x oil objective. In order to make comparable data, fluorescence images were taken using the same microscope settings (laser power, photomultiplier voltage, and offset). Four optical sections scanned at intervals of 0.3 μm were taken per sample projected using Maximum Intensity Model and colored with predefined Lut (spectrum) provided in the LASAF Lite 2.6.0v software.

2.7. Precipitation of COMMD1 in Pull-Down Assay. For COMMD1 precipitation, H460 (ATCC, HTB-117) cells were lysed in Triton lysis buffer (1% Triton X-100, 25 mM Hepes, 100 mM NaCl, 1 mM EDTA, and 10% glycerol) supplemented with Protease Inhibitor Cocktail and 2 mM of dithiothreitol. Pull-down assays were done using 500 μg of whole-cell lysates. The biotinylated peptides L-2, L-20, and CIGB-552 (300 μg) were independently incubated with 50 μL of the resin streptavidin sepharose (GE Healthcare) for 1 h. Resin of streptavidin sepharose without peptides was used as a negative control. The resins were washed extensively with PBS containing 1 mM DTT. Proteins remaining bound to the resins were resuspended in 25 μL of SDS sample loading buffer and separated by SDS-PAGE. COMMD1 detection was performed by Western blot using an anti-COMMD1 monoclonal antibody. The quantification of signals was carried out using ImageJ program 1.41 [17].

2.8. Quantitative PCR Analysis of COMMD1 Gene. H460 cells were seeded at confluence and treated with 25 μM of CIGB-552 for 30 min, 2 h, and 5 h. Cells were harvested and total RNA was extracted using the AllPrep DNA/RNA/Protein mini kit (Quiagen, Valencia). cDNA synthesis from RNA using 500 ng of total RNA was done with the Quantitect Reverse Transcription kit (Quiagen, Valencia). cDNA was diluted 20-fold and 5 μL was used in each quantitative PCR reaction (qPCR). Reactions were conducted in Rotor Gene 6000 equipment using ABsolute SYBR GreenQPCR kit (Abgene, Epsom). Primers sequences for reference genes: B2M, GAPDH, HMBS, ACTB, DDX5 and gene of interest COMMD1 were selected from http://primerdepot.nci.nih.gov/ database [18]. The gene expression of selected genes was conducted following MIQE recommendations [19]. Specificity of all products was verified by melting curve analysis. Reference genes were selected using GeNorm software [20]. Quantification was carried out using the $\Delta\Delta$ CT method. A statistical analysis was conducted using REST software [21].

2.9. Measurement of Oxidative Stress Variables. All biochemical parameters of oxidative stress were determined by spectrophotometric methods using a Pharmacia 1000 Spectrophotometer (Pharmacia LKB, Uppsala, Sweden). Total protein levels were determined using the method described by Bradford with bovine serum albumin as standard [22]. SOD activity was determined using RANSOD kit (Randox Labs, Crumlin), where xanthine and xanthine oxidase were used to generate superoxide anion radicals ($O_2^{\bullet -}$), which react with 2-(4-iodophenyl)-3-(4-nitrophenol)-5-phenyltetrazolium chloride (INT) to form a red formazan dye. SOD activity was measured by the inhibition degree of this reaction [23]. The advanced oxidation protein products (AOPP) were measured as described previously [24]. Briefly, 1 mL of samples in PBS was treated with 50 μL of 1.16 M potassium iodide followed by the addition of 100 μL of glacial acetic acid. The absorbance was immediately read at 340 nm. AOPP concentration was expressed as μM of chloramines-T. The

concentration of malondialdehyde (MDA) was determined using the LPO-586 kit obtained from Calbiochem (La Jolla, CA, USA). In the assay, the production of a stable chromophore was read at 586 nm after 40 min of incubation at 45°C [25]. Freshly prepared solutions of MDA bisdimethyl acetal (Sigma St Louis, MO, USA) were employed to generate standard curves. Ferric reducing ability of plasma (FRAP) was assayed through the reduction of Fe^{3+} to Fe^{2+} by cell lysates or ascorbic acid as reference. The Fe^{2+}-2,4,6-tripiridil-s-triazine complex was detected at 593 nm [26]. All results shown are the mean of duplicates of at least three independent experiments with SE.

2.10. Generation of Stable H460 COMMD1 Knockdown Cell. Plasmids encoding a short hairpin control (shControl) and plasmid encoding a short hairpin targeting COMMD1 mRNA sequence (shCOMMD1) were obtained from Genecopeia (USA). Generation of H460 stable cell lines was performed with *Lentivirus* infection with the addition of 4 μg/mL polybrene (Sigma). The selection was done in RPMI 1640 supplemented with 1 μg/mL puromycin (Sigma) according to the manufacturer's instructions. The knockdown level of COMMD1 was determined by Western blot analysis using mouse monoclonal anti-COMMD1. Determination of the IC_{50} values was performed as described previously [1].

2.11. Cell Cycle Assay. Cells were seeded on 6 well plates during 24 h and then treated with 25 μM of CIGB-552 for 24 h. The harvested cells were fixed gently by putting 100% ice-cold ethanol in freezer for 2 h. Subsequently, cells were resuspended in 300 μL of PBS containing 40 μg/mL of propidium iodide and 10 μg/mL DNase-free RNase and incubated for 20 min at 37°C. After gating out cellular aggregates, the cell cycle distribution analysis was done on FACSCalibur flow cytometer using CellQuest software (Becton Dickinson). For each sample, at least 20,000 cells were counted and plotted on a single parameter histogram.

2.12. Detection of Apoptosis. Cells in early and late stages of apoptosis were detected with an Annexin V-FITC apoptosis detection kit from Sigma (041M4083). Cells were treated with CIGB-552 (25 μM) and incubated for 24 h and 48 h prior to analysis. Briefly, 2.5×10^5 cells were washed with PBS and adjusted in 1 × binding buffer to a concentration of 1×10^6/mL. To 100 μL of cell suspension, 5 μL of Annexin V-FITC and 10 μL propidium iodide (PI) were added and incubated for 10 min at room temperature prior to analysis. Samples were analyzed (20,000 events) using a Becton Dickinson FACSCalibur instrument. Cells that were positive for Annexin V-FITC alone (early apoptosis) and Annexin V-FITC and PI (late apoptosis) were counted.

2.13. Statistical Analysis. The quantitative data in this paper are represented as means ± SD. Statistical evaluation was made using the Mann-Whitney test. Differences were considered to be significant at $P < 0.05$.

3. Results

3.1. Identification of Proteins That Interact with Peptides Derived from $LALF_{32-51}$ Region. To identify proteins that interact with the antitumor peptides L-2 and L-20, a yeast two-hybrid screening was performed. As the peptide L-2 has shown the major antitumor activity, the plasmid pGBKT7-L-2 was selected as bait in the yeast two-hybrid screening of a human liver cDNA library to identify peptide-binding partners. A total of 10^7 diploids were screened. Eighty-seven different positive clones were obtained. The interaction of each positive clone was verified by matting with pGBKT7 as a negative control and with constructions pGBKT7 L-2 and pGBKT7 L-20. From the initial number of clones thirty-eight positive interactions were confirmed. All positive clones were sequenced and their sequences analyzed using BLAST. Among them, a plasmid containing the sequence of COMMD1 (from amino acids 6 to 190) was identified. Interestingly, the diploid of COMMD1 with the L-20 peptide on selection plate showed a lower growth indicating a lower strength of this interaction compared with L-2 (Figure 1(a)). A second GAL-4-based yeast two-hybrid screening identified the region containing the amino acids 111–190 of COMMD1 as the potential interaction site for the peptides Figure 1(a), (bottom of the figure).

The proteolytic stability of natural peptides is one of the principal limitations for their use as drug candidates. In this study, the substitution of proline (Pro6) and leucine (Leu11) by an unnatural amino acid and blocking N-terminal ends by N-acylation from L-2 resulted in a second generation peptide named CIGB-552, which showed an increased antitumor activity *in vitro* and *in vivo* [2]. This finding suggests that the incorporation of unnatural amino acids in the sequence could improve the metabolic stability of the peptide.

To elucidate the functional significance of this chemical modification, the interaction between COMMD1 and the peptides was examined. The interaction between COMMD1 and the synthetic peptides L-2, L-20, and CIGB-552 was evaluated by pull-down analysis in human lung cancer cells H460, following Western blot with specific COMMD1 antibody. As shown in Figure 1(b), COMMD1 was detected in the peptides-pull-down precipitation confirming the existence of specific COMMD1/peptide complexes in cells that express endogenously COMMD1. Quantification of the complexes COMMD1/peptides (RI) inversely correlates with the cytotoxic activity of the peptides expressed by its inhibitory concentration (IC_{50}), Table 2. The complex CIGB-552/COMMD1 increases in respect to the complex's L-2 and L-20/COMMD1 indicating that modifications done in the primary structure of the peptides increased the affinity to COMMD1 and this correlates with the increased cytotoxic activity. The results of two hybrid and pull-down experiments indicate that the interaction between the peptides and COMMD1 is specific and that the strength of this interaction may be relevant for the antitumor effect of the peptides. In addition, the interaction between CIGB-552 and COMMD1 was also confirmed in whole-cell lysates of human cancer cells of different histological origins (data not shown).

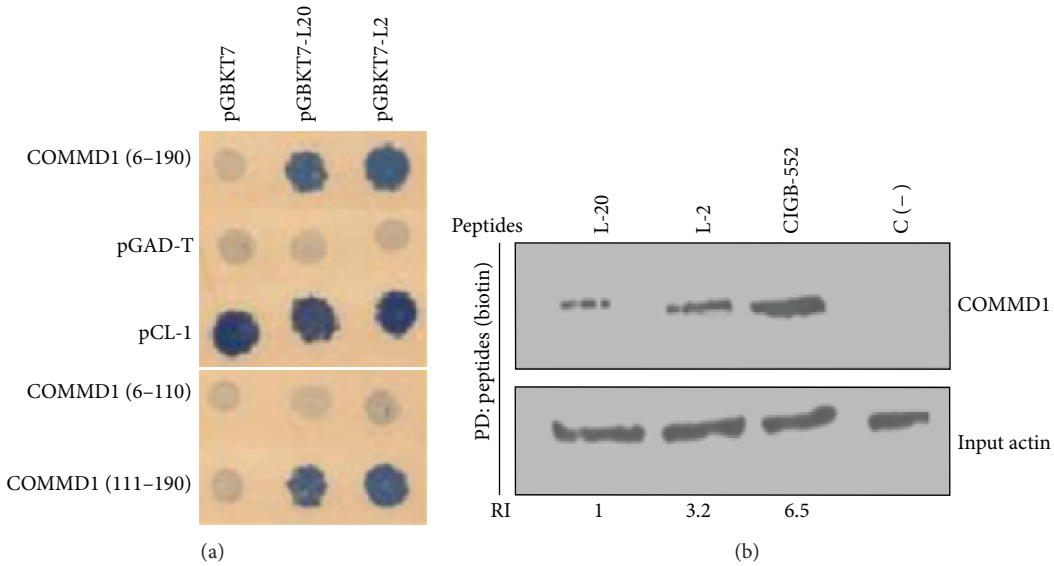

Figure 1: Peptides and COMMD1 interact in mammalian cells. (a) Yeast two hybrids showing interactions between full length COMMD1 and COMMD1 (111–190) prey fusions and the indicated L-2 and L-20 peptides as baits tested by interaction mating using SD Leu/Trp/His/Ade plates. pCL1 was used as a positive control of growth and the interaction between empty bait vector pGBKT7 and empty prey pGAD-T was used as a negative control. Interactions between pGBKT7 and preys constructions and pGAD-T and baits were used as a control of the interaction specificity. (b) Pull-down assay demonstrating specific COMMD1/peptides complex in H460 cells. Endogenous COMMD1 was precipitated from H460 cell lysates. The biotinylated peptides bond to streptavidin sepharose was used as bait and cell lysates as prey. The precipitated material was analysis by Western blot using antibodies directed against endogenous COMMD1. C (−) indicates streptavidin sepharose without peptide. Actin was used as input housekeeping. Relative levels of precipitated COMMD1 were determined by densitometry and normalized to actin. Ratios were depicted under each lane (RI) relative to COMMD1 levels immuprecipitated with peptide L-20. ImajeJ was used for quantification.

3.2. CIGB-552 Accumulates COMMD1 in Human Cancer Cells. Given that COMMD1 was identified as a protein that associates to the above-mentioned antitumor peptides, we studied the role of COMMD1 in the mechanism of action of CIGB-552. First, the cellular expression of COMMD1 in whole-cell lysates of human cancer cells of different histological origin was determined using Western blot analysis, and the proteasome inhibitor MG132 which induces the accumulation of COMMD1 was used as a positive control [27]. These experiments revealed an increase in the levels of COMMD1 after 5 h of treatment with the peptide. Treatment with MG132 led to the increase of COMMD1 but not at a greater extent than CIGB-552 (Figure 2(a)). The cellular accumulation of COMMD1 was also found *in situ* immunofluorescence in human cancer cells. Both cell lines assayed, MCF7 and HT29, showed the accumulation of COMMD1 after 5 h of treatment with the peptide similar to the obtained results by Western blot (Figure 2(b)). Talking together these data confirm that the peptide CIGB-552 induces the accumulation of COMMD1.

COMMD1 undergoes constitutive nucleocytoplasmic transport and its nuclear localization is needed for negative regulation of NF-κB signaling [28]. Since our interest in this study is focused on the human lung cancer, the levels of the protein COMMD1 in the cytoplasm and nucleus of the H460 cells treated with CIGB-552 were evaluated by Western blot. We found a low expression of COMMD1 in untreated cells. However, in response to CIGB-552, COMMD1 was increased in the cytoplasm and nucleus of cells at 40 min following treatment, and, most interestingly, this increment remained until up to 5 h after treatment (Figure 2(c)). To examine whether the increase of COMMD1 levels is due to an increase in the RNA expression, a qPCR experiment was performed. The results showed that increased levels of COMMD1 were not accompanied by significant changes in mRNA expression of the protein (Figure 2(d)), suggesting a posttranscriptional effect of CIGB-552 on COMMD1.

3.3. CIGB-552 Promotes the Ubiquitination of RelA Subunit of NF-κB. It has been known that overexpression of COMMD1 accelerates the ubiquitination and degradation of the RelA subunit of NF-κB and decreases the activation of anti-apoptotic genes [29]. Taking into account the above data, the second question to elucidate in this study was the effect of CIGB-552 on the NF-κB signaling in human lung cancer cells. The effect of CIGB-552 on the endogenous levels of ubiquitinated RelA was investigated. Immunoprecipitation of endogenous RelA using a mouse anti-RelA followed by antiubiquitin Western blot confirmed the increased amounts of ubiquitinated RelA in response to the peptide as early as 2 h after treatment, and the increment remained for 12 h after treatment (Figure 3(a)). Immunoprecipitation using a rabbit anti-IgG as negative control did not result in the recovery of ubiquitinated RelA, indicating the specificity of the recovered material. As shown in Figure 3(a), CIGB-552 as

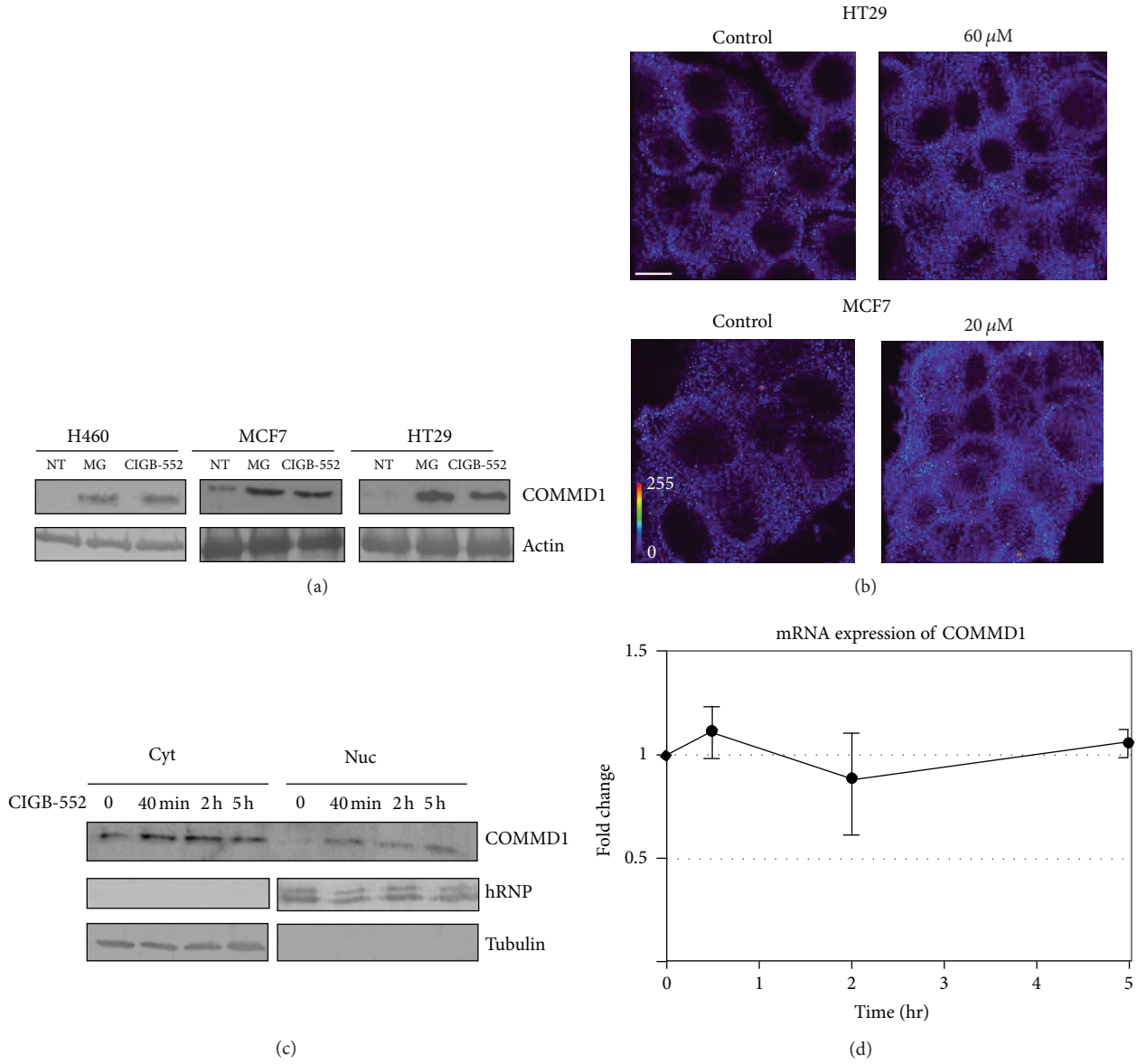

Figure 2: CIGB-552 promotes accumulation of endogenous COMMD1. (a) The cell lines H460, HT-29, and MCF-7 were treated with CIGB-552 (25, 60, and 20 μM, resp.) or MG132 (25 μmol/L) during 5 h. The levels of COMMD1 were determined by Western blot analysis of whole-cell lysates. NT untreated cells. Actin was used as a control for protein loading. (b) Cellular distribution of COMMD1 in HT-29 and MCF-7 cells following CIGB-552 treatment. Representative confocal micrographs of the duplicate samples are shown (scale bar = 5 μm). Color bar (bottom left of the figure) indicate the signal strength. (c) In H460 cells, the localization of endogenous COMMD1 in the presence of CIGB-552 (25 μM) at the indicated times was determined by cell fractionation followed by immunoblotting using antibodies directed against endogenous COMMD1. The protein expression of human ribonucleoprotein (hRNP) and tubulin were used as loading controls and markers for nuclear and cytosolic fractions. Nuc indicates nuclear fraction and cyt indicates cytosolic fractions. (d) COMMD1 mRNA expression determined after CIGB-552 treatment in H460 cells. mRNA expression was normalized to an expression on time point zero and shown as the mean fold induction ± SEM of three biological replicates. No differences were found at any time in the levels of COMMD1 mRNA.

well as MG132 (used as a positive control) increased the ubiquitinated forms of RelA. To investigate whether the CIGB-552 induces ubiquitination and subsequent degradation of RelA through a proteasome-dependent process, the effect of MG132 and CIGB552 on the basal levels of the protein was tested. Treatment with CIGB-552 led to a decrease in basal levels of RelA, while protein levels were accumulated in the presence of MG132 treatment and CIGB-552. This result suggests that CIGB-552 induces ubiquitination of RelA and promotes its proteasomal degradation (Figure 3(b)).

3.4. CIGB-552 Regulates Apoptosis-Related Proteins in H460 Cells. Further, we assess whether CIGB-552 could modulate the expression of proteins involved in the intracellular apoptosis signaling. As shown in Figure 3(c), proapoptotic

Table 2: Effect of L-2 and CIGB-552 on the cell viability in different tumor cell lines.

Tumor cell line	Origin	L-2 IC_{50} (μM)*	CIGB-552 IC_{50} (μM)*
H460	Human nonsmall-cell lung cancer	57 ± 6	23 ± 8
H-125	Human nonsmall-cell lung cancer	75 ± 9	42 ± 6
H-82	Human small-cell lung cancer	50 ± 6	15 ± 3
LS174T	Human colon adenocarcinoma	56 ± 3	22 ± 4
MDA-231	Human breast adenocarcinoma	125 ± 3	40 ± 9
PBMC	Human mononuclear cells	234 ± 9	249 ± 6

The peptides were added to 10,000 cells in a range of concentrations from 0 to 200 μM. After 48 hours of incubation, cell viability was determined by SRB (sulforhodamine B, sodium salt) assay. Finally, absorbance was measured at 492 nm, and the IC_{50} values were calculated from the growth curves.
*Mean ± SD of three determinations. Data were obtained from two different experiments.

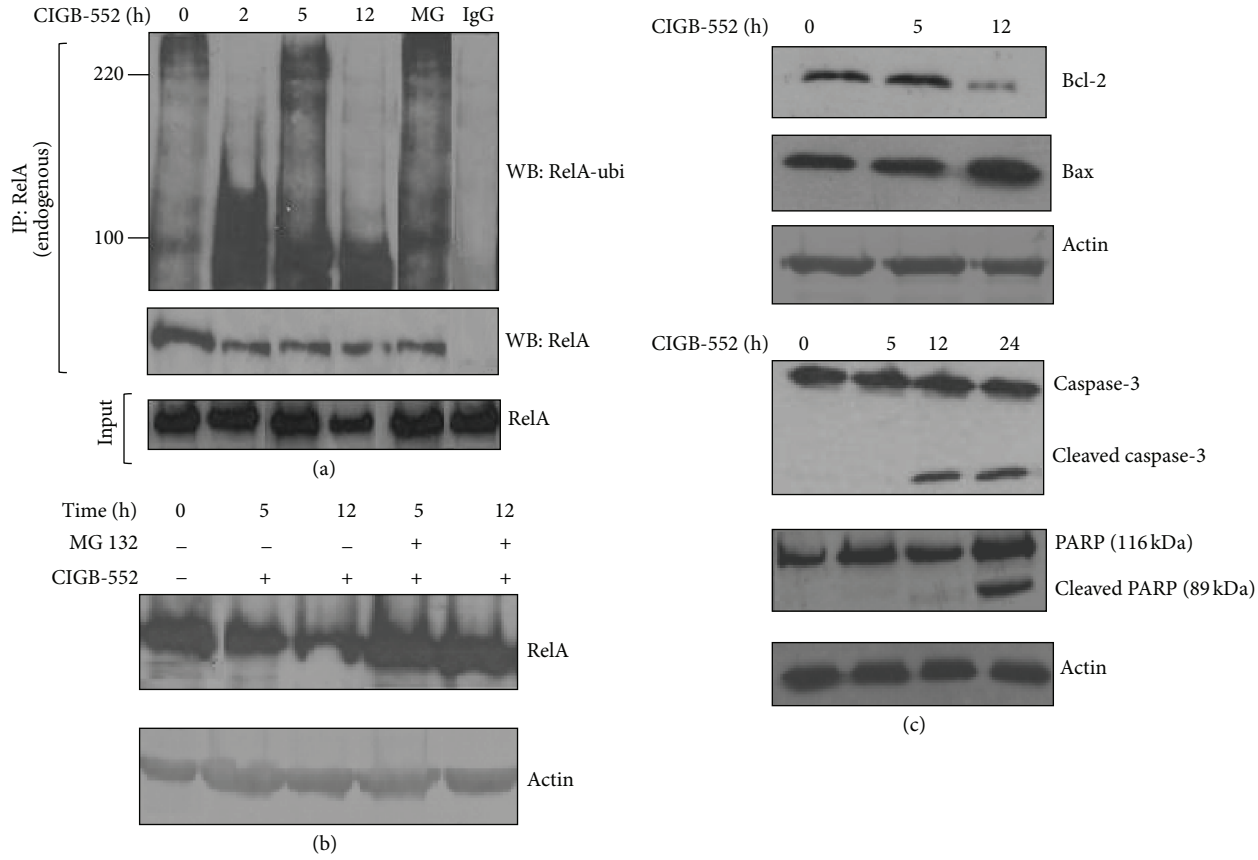

Figure 3: CIGB-552 induces ubiquitination and proteasomal degradation of RelA. (a) H460 cells were treated with CIGB-552 (25 μM) for the times specified or MG132 (25 μmol/L) for 5 h. Immunoprecipitation (IP) of ubiquitinated protein following antiubiquitin Western blot analysis (WB) show an increase of ubiquitinated forms of RelA 2 h after CIGB-552 treatment. The control of immunoprecipitation was done with anti-rabbit IgG. RelA in input samples is shown. MG indicates MG132 (positive control). (b) H460 cells were treated with either CIGB-552 (25 μM) and MG132 (25 μmol/L) for the indicated times. Anti-RelA immunoblot shows native protein in whole-cell extracts. The levels of RelA were increased in cells treated with CIGB-552 and MG132 with respect to the cells treated alone with CIGB-552, indicative of proteasomal degradation of RelA after CIGB-552 treatment. Actin was used as a control for protein loading. (c) H460 cells were treated with CIGB-552 (25 μM) for the times indicated and Bcl-2, Bax, caspase-3, and PARP proteins were determined by Western blot analysis. Actin was used as a control for protein loading.

protein Bax was markedly induced, whereas Bcl-2 was significantly inhibited after 12 h of treatment with the peptide, indicating that the apoptotic effect of CIGB-552 is partly caused by upregulating the Bax/Bcl-2 protein ratio, which is a critical determinant of apoptosis. Additionally, Western immunoblotting showed a significant appearance of cleaved caspase-3 and PARP in H460 cells after 24 h of treatment with CIGB-552 (Figure 3(c)). A downstream event in the activation of the caspase-3 is the PARP cleavage. PARP helps cells to maintain their viability; the cleavage of PARP

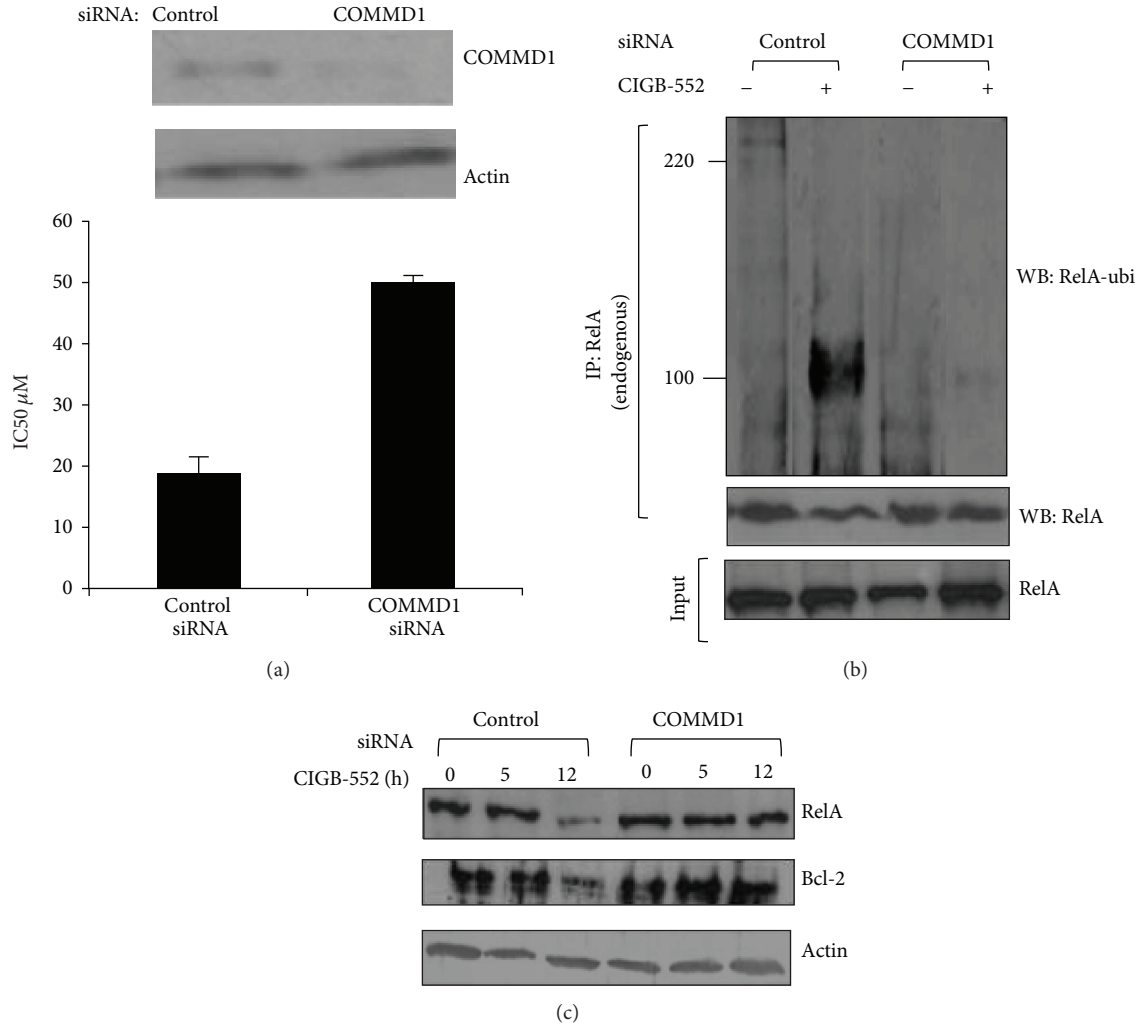

Figure 4: COMMD1 is involved in the antitumor activity of CIGB-552. (a) H460 cells were transfected with control or COMMD1 siRNA and then the IC_{50} values were determined using a logarithmic regression of the growth curves obtained from SRB (sulforhodamine B, sodium salt). Mean ± SD of three determinations are shown. Data were obtained from two different experiments. Top, Western blot demonstrating stable shRNA mediated repression of COMMD1 in H460 cells. Actin was used as a control for protein loading. H460 cells were transfected with control or COMMD1 siRNA and then treated with CIGB-552 (25 μM) from 0 to 12 h. (b) Ubiquitination of RelA is greatly impaired in COMMD1 deficiency cells treated with CIGB-552. Anti-RelA immunoblot shows levels of ubiquitinated RelA after 5 h of treatment. (c) Repression of the levels of proteins RelA and Bcl-2 are impaired in COMMD1 deficiency treated with CIGB-552. Bcl-2 and RelA proteins levels were determined by Western blot analysis. Actin was used as a control for protein loading.

facilitates cellular disassembly and serves as a marker of cells undergoing apoptosis. Our results provide molecular evidence of apoptosis induction by CIGB-552 treatment.

The kinetics of responses to CIGB-552 was examined. We found that RelA ubiquitination occurred within 2 h of treatment (Figure 3(a)) and was associated with a nuclear accumulation of COMMD1 (Figure 2(c)). These early events had no effect on the levels of apoptotic-related proteins (Figure 3(c)). Based on our observations so far, the accumulation of COMMD1 and ubiquitination of RelA are events that precede a repression of the antiapoptotic activity of NF-κB.

3.5. COMMD1 Deficiency Alters Degradation of RelA Mediated by CIGB-552. To assess if COMMD1 has a functional role in the antitumor activity of CIGB-552, knockdown of COMMD1 by siRNA was generated in H460 cell line and the cytotoxic effect of the peptide was determined. As shown in Figure 4(a), the cytotoxic activity of CIGB-552 in knockdown cells decreased in comparison to control cells. To confirm that the observed reduction in the antitumor effect of CIGB-552 in knockdown cells was not an artifact, the levels of protein were determined by Western blot. As shown in Figure 4(a), COMMD1 expression decreased in respect to control cells (top of the figure). However, the cytotoxic activity of the peptide was not completely blocked in knockdown cells. This result might be explained by the efficiency of knockdown but we do not discard that other factors could be involved in the cytotoxic activity of the peptide.

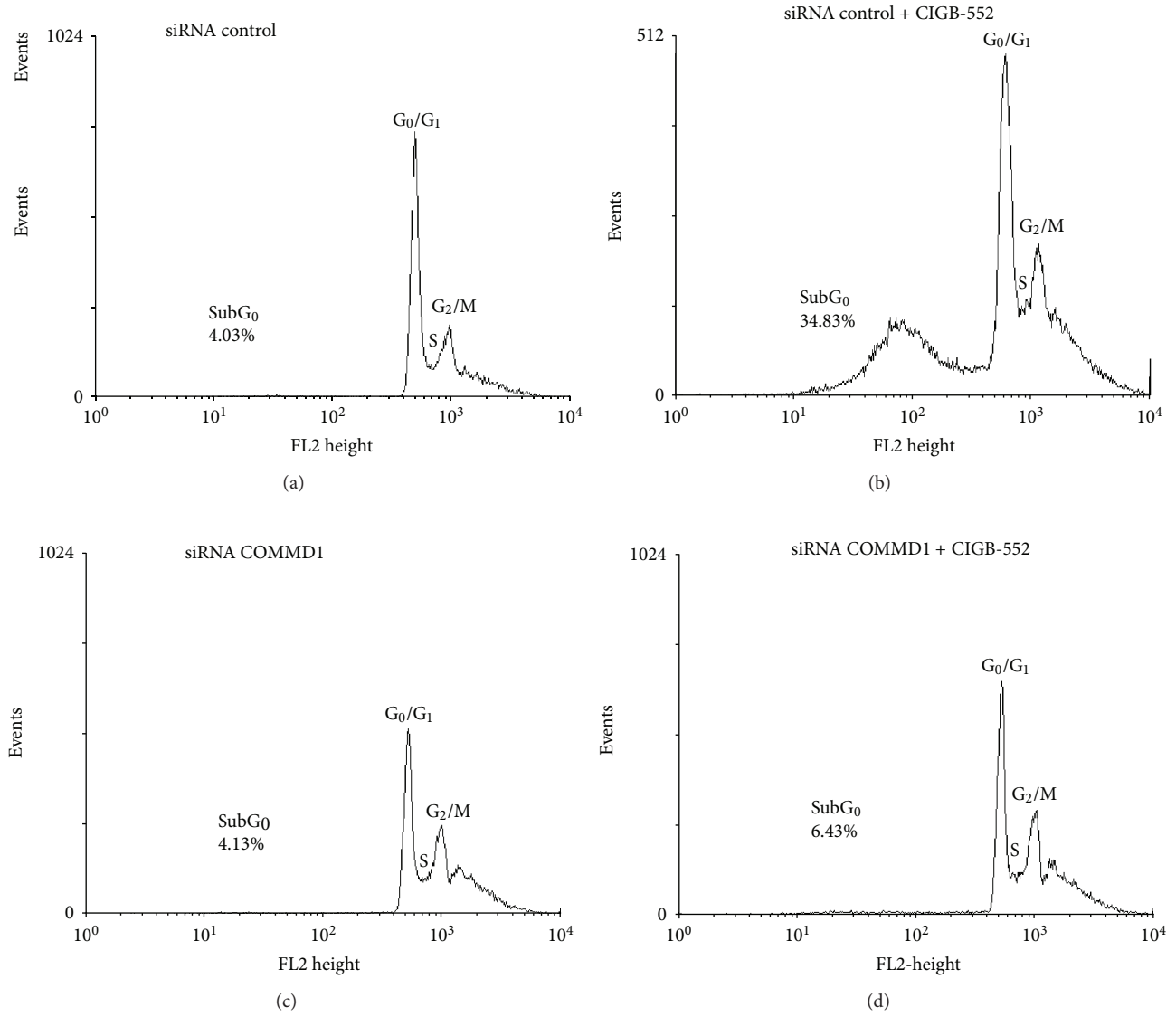

Figure 5: COMMD1 is involved in the apoptosis induced by CIGB-552. H460 cells were transfected with control or COMMD1 siRNA and then treated with CIGB-552 (25 μM) for 24 h. The cell cycle distribution analysis was done on FACSCalibur flow cytometer using CellQuest software (Becton Dickinson). The percentage of apoptotic cells (sub-G_0 peak) within the total cell population was calculated. Data shown here are from a representative experiment repeated two times with similar results.

The reduced cytotoxic activity of the peptide in COMMD1 knockdown cells could be associated with decreased RelA ubiquitination and degradation. To study this possibility, the endogenous ubiquitination of the RelA levels in control and COMMD1 knockdown cells treated with the peptide was examined. As shown in Figure 4(b), COMMD1 deficiency cells resulted in lesser levels of ubiquitinated RelA when treated with the CIGB-552 in respect to the control cells. Next, we examined the levels of endogenous RelA and Bcl-2 in cytosolic extracts of control and COMMD1 deficiency cells using Western blot. As shown in Figure 4(c), COMMD1 knockdown cells showed greater levels of RelA and Bcl-2 proteins when treated with the CIGB-552 in respect to the control cells.

We have previously reported that the cytotoxic effect of the L-2 peptide involved cell cycle arrest followed by cell death [1]. Therefore, the possibility that COMMD1 might be involved in the cell death induced by CIGB-552 was explored. To elucidate this, the alteration of the cell division cycle in control and COMMD1 knockdown cells was analyzed by flow cytometry. As shown in Figure 5, control cells undergoing apoptosis after 24 h of treatment showed a significant increase in the sub-G_0 peak. In contrast, the apoptosis induced by the CIGB-552 was blocked in COMMD1 knockdown cells. Apoptosis can be assessed by using several characteristic features of programmed cell death. One variable of apoptosis is phosphatidylserine externalization, which can be measured by Annexin V staining.

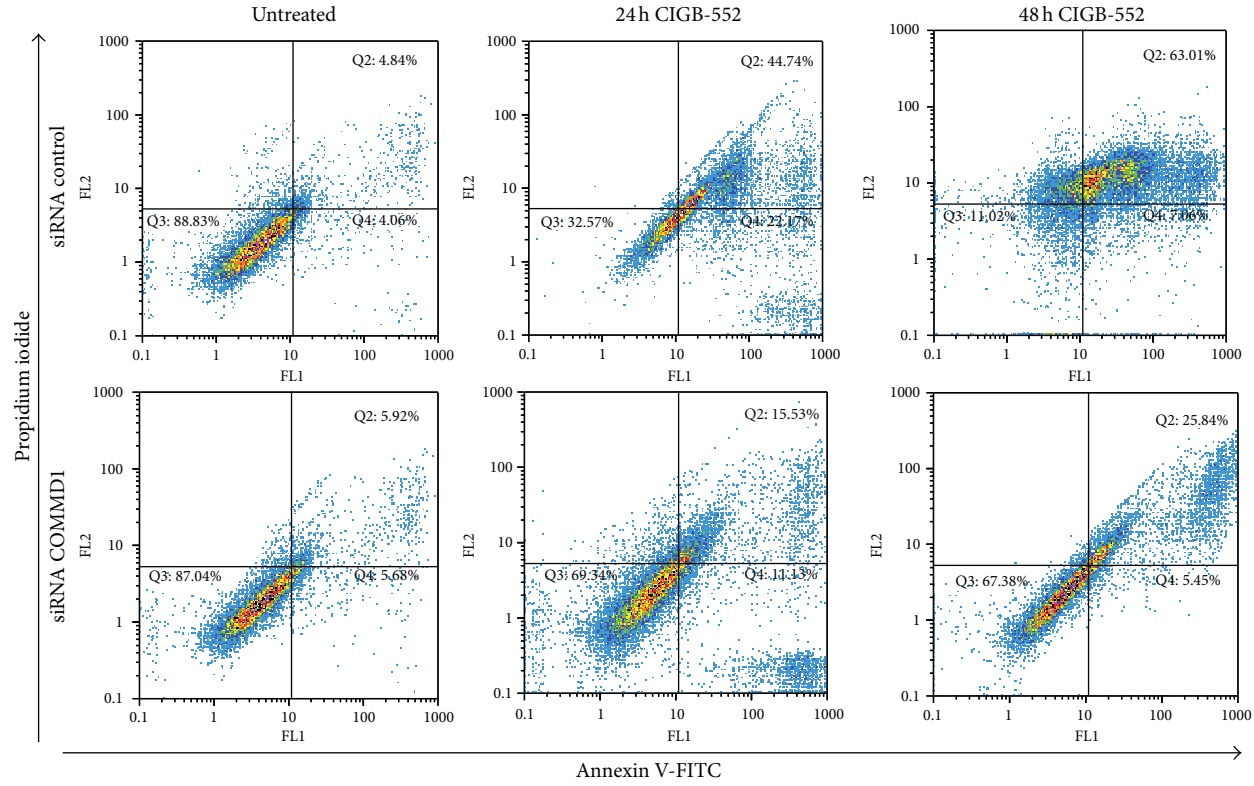

Figure 6: Annexin V/PI double-staining assay. Control or COMMD1 siRNA cells were treated with CIGB-552 (25 μM) for 24 h and 48 h and apoptosis was examined with flow cytometry after Annexin V/propidium iodine double staining. The data shown are representative of three independent experiments with similar findings.

The effect of the CIGB-552 on Annexin V staining was determined after 24 h and 48 h of treatment. As shown in Figure 6, control cells treated with CIGB-552 showed a significant increase in Annexin V positive cells compared with COMMD1 knockdown cells.

Altogether, these results support the hypothesis of the effect of COMMD1 on the apoptosis induced by CIGB-552.

3.6. Altered Redox Status of H460 Treated with CIGB-552. The maturation and activation of the antioxidant superoxide dismutase (SOD1) are highly regulated processes that require several posttranslational modifications. Recently, it has been described that COMMD1 is a novel interaction partner of SOD1. COMMD1 impairs SOD1 activity by reducing the expression levels of enzymatically active SOD1 homodimers late in the posttranslational maturation process of SOD1 [30].

Our previous results demonstrated that CIGB-552 induces the accumulation of COMMD1 in the cytosol. Next, we considered it important to determine the relevance of this accumulation in the enzymatic activity of SOD1, and the antioxidant capacity of the lung cancer cells. The activity of the superoxide dismutase SOD1 was measured and the total antioxidant capacity was evaluated by FRAP. Consistent with our expectation, the activity of SOD1 in knockdown cells is markedly increased compared to H460 cells after 8 h of treatment with CIGB-552 (Figure 7(a)). In line with Vonk's report [30], we also found that endogenous COMMD1 modulates SOD1 activity. As shown in Figure 7(b), the total antioxidant capacity was significantly diminished after 8 h of treatment. Next, we examined the levels of protein and lipid peroxidation, as a sign of oxidative stress damage by the formation of MDA (malondialdehyde) and AOPP (advance oxidation protein products) [31]. Concordantly, the levels of MDA and AOPP markedly increased after 8 h of treatment, likely in response to an imbalance in the antioxidant capacity Figure 7(c). Altogether, these data demonstrate that CIGB-552 might promote cell cycle arrest and apoptosis by inducing damage to proteins and lipids in lung cancer cells.

4. Discussion

Our previous studies showed that the substitution of alanine in specific amino acids of the region $LALF_{32-51}$ led to the design of peptides that lost the ability to bind LPS and exhibit a differential cytotoxic activity (L-2 and L-20). In this study, we developed the peptide CIGB-552 from the chemical optimization in the primary structure of the peptide L-2 with the purpose of reducing the elimination and biodegradation of the peptide and increasing selectivity or affinity to its potential target [32].

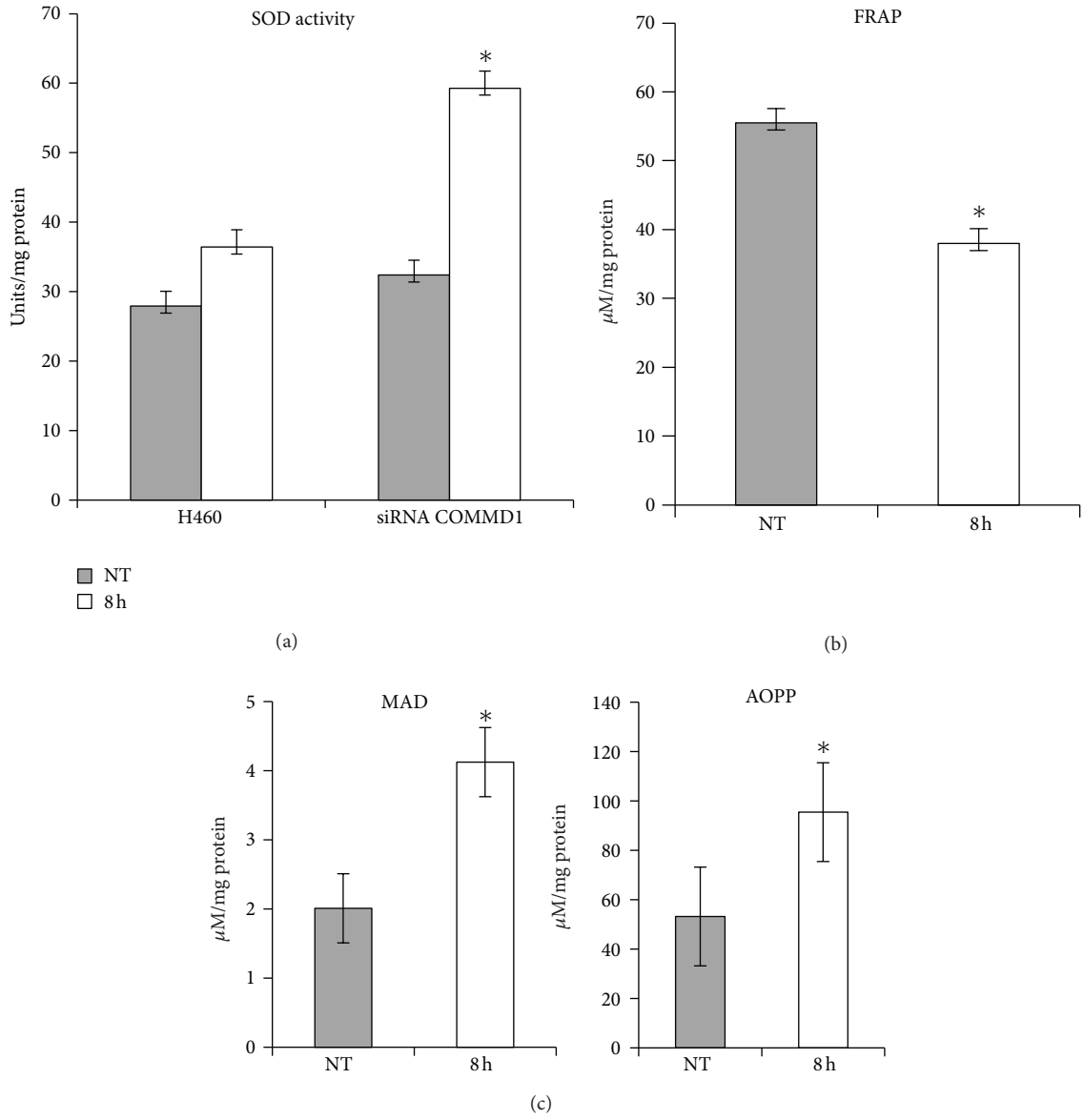

Figure 7: CIGB-552 modifies the redox status in lung cancer cells. H460 cells were treated with CIGB-552 (25 μM) for the indicated times. (a) Activity of SOD1, H460 siRNA was used as a control of the experiment. (b) Total antioxidant capacity measured by FRAP. (c) Levels of proteins and lipids peroxidation measured by concentration of malondialdeyde (MDA) and advanced oxidative protein products (AOPP). Means ± SD ($n = 6$). $^*P < 0.05$ statistically significant. NT indicates untreated cells.

First we confirmed that the peptides L-2 and L-20 bound the region 111–190 of COMMD1 protein. Particularly a higher capacity of binding was shown by the peptide L-2 and this correlated with its higher cytotoxic activity [1]. Interestingly, our subsequent studies using the pull-down technique demonstrated that modifications in the primary structure of the peptides increased the affinity to associate COMMD1 and this correlated with increased antitumor activity. For the first time, our results identified COMMD1 as a potential target of the anticancer peptide CIGB-552 and indicated that targeting of a protein-peptide interaction may be a strategy to increase the specificity and biological activity of novel anticancer peptides derived from $LALF_{32–51}$ region.

Recently, it has been reported that a decreased expression of COMMD1 is frequently observed in a variety of cancers and that this correlates with tumor invasion as well as with the overall patient survival. This suggests that decreased COMMD1 expression might represent a novel mechanism that confers cancer cells with invasion potential and proliferating capacity [13]. CIGB-552 was undoubtedly found to accumulate COMMD1 in cancer cells and this accumulation was not accompanied by changes in the mRNA expression. These data suggested the outstanding possibility that CIGB-552 may stabilize COMMD1 through posttranscriptional events. The basal levels of COMMD1 expression are tightly regulated by XIAP (X-linked inhibitor of apoptosis). The

interaction between COMMD1 and XIAP have been mapped to the COMM domain and identified leucine repetitions within the COMM domain are required for ubiquitination and proteasomal degradation of COMMD1 [33]. Interestingly, the peptides derived from $LALF_{32-51}$ region were found to bind COMM domain (amino acids 119–190) and, more important, our results provide the first indication that CIGB-552 could regulate the levels of COMMD1 to induce the cell death in cancer cells. The mechanism by which CIGB-552 induces the stabilization of COMMD1 is currently the issue of ongoing researches in our lab.

A central function of NF-κB, in particular of RelA subunit, is the regulation of cellular growth and apoptosis [11]. Besides, the persistent activation of NF-κB is a recognized contributory factor in a number of carcinomas and may provide the cancer cells with a survival advantage [34]. Recently, it has been demonstrated that ubiquitination and the degradation of RelA subunit by COMMD1-containing ubiquitin ligase is a critical mechanism of regulation of the antiapoptotic activity of NF-κB and this event has considerable relevance to cancer prevention and therapy, as well as the postinduction regulation of RelA/NF-κB [7, 35].

It was found in this study that the treatment of lung cancer cells with CIGB-552 increased the levels of the protein COMMD1 in the cytoplasm and nucleus. This observation, along with the fact that COMMD1 can repress NF-κB activation, suggests a significant role for CIGB-552 in the regulation of RelA/NF-κB in lung cancer cells. Our results demonstrated that CIGB-552 induces the ubiquitination of the RelA subunit of NF-κB and our data also indicated that this effect promotes its proteasomal degradation. The stabilization and nuclear accumulation of COMMD1 mediated by CIGB-552 could be an attractive mechanism for the regulation of the constitutive activity of the transcription factor NF-κB in cancer cells.

Consistently, our studies showed a role for COMMD1 in the cytotoxic effect of CIGB-552. H460 knockdown of COMMD1 was more resistant to the cytotoxic effect of the peptide, and this COMMD1 deficiency correlates with reduced levels of ubiquitinated RelA and apoptosis.

Oxidative stress, involved in the etiology of cancer, results from an imbalance in the production of reactive oxygen species (ROS) and the cells' own antioxidant defenses. High levels of oxidative stress have been observed in various types of cancer cells. Accordingly, there is an aberrant regulation of redox homeostasis and stress adaptation in cancer cells and this event is associated with drug resistance [36, 37]. Here, we found that the treatment of the lung cancer cells with CIGB-552 impaired the SOD1 activity and it could be associated with the accumulation of COMMD1. Moreover, the CIGB-552 induced a failure of the antioxidant defenses and this effect was accompanied by damage to proteins and lipids. These observations suggest that CIGB-552 plays a significant role in the regulation of the redox status of cancer cells.

5. Conclusions

Altogether, our results demonstrate that CIGB-552 could regulate the anti-apoptotic activity of NF-κB and the oxidative stress in lung cancer cells, two biological processes involved in the survival and growth of tumor cells.

Conflict of Interests

No potential conflict of interests was disclosed.

Acknowledgments

The authors thank the laboratories of Dr. Iduna Fitchtner for kindly evaluating the antitumor activity of CIGB-552. They also thank Jeovanis Gil for the experimental assistance. They thank Daniel Palenzuela Gardon, Isabel Guillén Perez, Dania Vázquez Blomquist, and Lidia Ines for the generation of microarray data helpful for the comprehension of possible mechanisms of the antitumor activity. They thank Amelia Rodriguez Ruiz for his critical reading of the paper.

References

[1] M. G. Vallespi, J. R. Fernandez, I. Torrens et al., "Identification of a novel antitumor peptide based on the screening of an Ala-library derived from the LALF32-51 region," *Journal of Peptide Science*, vol. 16, no. 1, pp. 40–47, 2010.

[2] M. Guerra Vallespi, J. R. Fernandez Masso, A. Musacchio Lasa, J. Gil Valdez, O. Reyes Acosta, and B. Oliva Arguellez, "Cancer Therapy method," WO/2011/150897, 2011.

[3] P. de Bie, B. van de Sluis, L. Klomp, and C. Wijmenga, "The many faces of the copper metabolism protein MURR1/COMMD1," *Journal of Heredity*, vol. 96, no. 7, pp. 803–811, 2005.

[4] T. Chang, Y. Ke, K. Ly, and F. J. McDonald, "COMMD1 regulates the delta epithelial sodium channel (δENaC) through trafficking and ubiquitination," *Biochemical and Biophysical Research Communications*, vol. 411, no. 3, pp. 506–511, 2011.

[5] P. de Bie, B. van de Sluis, E. Burstein et al., "Characterization of COMMD protein-protein interactions in NF-κB signalling," *Biochemical Journal*, vol. 398, no. 1, pp. 63–71, 2006.

[6] B. van de Sluis, P. Muller, K. Duran et al., "Increased activity of hypoxia-inducible factor 1 is associated with early embryonic lethality in Commd1 null mice," *Molecular and Cellular Biology*, vol. 27, no. 11, pp. 4142–4156, 2007.

[7] H. Geng, T. Wittwer, O. Dittrich-Breiholz, M. Kracht, and M. L. Schmitz, "Phosphorylation of NF-κB p65 at Ser468 controls its COMMD1-dependent ubiquitination and target gene-specific proteasomal elimination," *EMBO Reports*, vol. 10, no. 4, pp. 381–386, 2009.

[8] G. N. Maine, X. Mao, C. M. Komarck, and E. Burstein, "COMMD1 promotes the ubiquitination of NF-κB subunits through a cullin-containing ubiquitin ligase," *The EMBO Journal*, vol. 26, no. 2, pp. 436–447, 2007.

[9] S. Materia, M. A. Cater, L. W. Klomp, J. F. Mercer, and S. la Fontaine, "Clusterin and COMMD1 independently regulate degradation of the mammalian copper ATPases ATP7A and ATP7B," *The Journal of Biological Chemistry*, vol. 287, no. 4, pp. 2485–2499, 2012.

[10] B. van de Sluis, A. J. Groot, J. Vermeulen et al., "COMMD1 promotes pVHL and O_2-independent proteolysis of HIF-1α via HSP90/70," *PLoS One*, vol. 4, no. 10, Article ID e7332, 2009.

[11] G. Xiao and J. Fu, "NF-κB and cancer: a paradigm of Yin-Yang," *American Journal of Cancer Research*, vol. 1, no. 2, pp. 192–221, 2011.

[12] E. Poon, A. L. Harris, and M. Ashcroft, "Targeting the hypoxia-inducible factor (HIF) pathway in cancer," *Expert Reviews in Molecular Medicine*, vol. 11, p. e26, 2009.

[13] B. van de Sluis, X. Mao, Y. Zhai et al., "COMMD1 disrupts HIF-1α/β dimerization and inhibits human tumor cell invasion," *Journal of Clinical Investigation*, vol. 120, no. 6, pp. 2119–2130, 2010.

[14] C. Camacho, G. Coulouris, V. Avagyan et al., "BLAST+: Architecture and applications," *BMC Bioinformatics*, vol. 10, article 421, 2009.

[15] I. Vancurova, V. Miskolci, and D. Davidson, "NF-κB activation in tumor necrosis factor α-stimulated neutrophils is mediated by protein kinase Cδ. Correlation to nuclear IκBα," *Journal of Biological Chemistry*, vol. 276, no. 23, pp. 19746–19752, 2001.

[16] H. Towbin and J. Gordon, "Immunoblotting and dot immunobinding. Current status and outlook," *Journal of Immunological Methods*, vol. 72, no. 2, pp. 313–340, 1984.

[17] C. A. Schneider, W. S. Rasband, and K. W. Eliceiri, "NIH Image to ImageJ: 25 years of image analysis," *Nature Methods*, vol. 9, no. 7, pp. 671–675, 2012.

[18] W. Cui, D. D. Taub, and K. Gardner, "qPrimerDepot: a primer database for quantitative real time PCR," *Nucleic Acids Research*, vol. 35, no. 1, pp. D805–D809, 2007.

[19] S. A. Bustin, J. F. Beaulieu, J. Huggett et al., "MIQE précis: practical implementation of minimum standard guidelines for fluorescence-based quantitative real-time PCR experiments," *BMC Molecular Biology*, vol. 11, article 74, 2010.

[20] J. Vandesompele, K. de Preter, F. Pattyn et al., "Accurate normalization of real-time quantitative RT-PCR data by geometric averaging of multiple internal control genes," *Genome biology*, vol. 3, no. 7, p. RESEARCH0034, 2002.

[21] M. W. Pfaffl, G. W. Horgan, and L. Dempfle, "Relative expression software tool (REST) for group-wise comparison and statistical analysis of relative expression results in real-time PCR," *Nucleic Acids Research*, vol. 30, no. 9, p. e36, 2002.

[22] M. M. Bradford, "A rapid and sensitive method for the quantitation of microgram quantities of protein utilizing the principle of protein dye binding," *Analytical Biochemistry*, vol. 72, no. 1-2, pp. 248–254, 1976.

[23] H. Ukeda, S. Maeda, T. Ishii, and M. Sawamura, "Spectrophotometric assay for superoxide dismutase based on tetrazolium salt 3′-{1-[(phenylamino)-carbonyl]-3,4-tetrazolium}-bis(4-methoxy-6-nitro)benzenesulfonic acid hydrate reduction by xanthine-xanthine oxidase," *Analytical Biochemistry*, vol. 251, no. 2, pp. 206–209, 1997.

[24] V. Witko-Sarsat, M. Friedlander, T. N. Khoa et al., "Advanced oxidation protein products as novel mediators of inflammation and monocyte activation in chronic renal failure," *Journal of Immunology*, vol. 161, no. 5, pp. 2524–2532, 1998.

[25] I. Erdelmeier, D. Gérard-Monnier, J. C. Yadan, and J. Chaudière, "Reactions of N-methyl-2-phenylindole with malondialdehyde and 4-hydroxyalkenals. Mechanistic aspects of the colorimetric assay of lipid peroxidation," *Chemical Research in Toxicology*, vol. 11, no. 10, pp. 1184–1194, 1998.

[26] I. F. F. Benzie and J. J. Strain, "The ferric reducing ability of plasma (FRAP) as a measure of "antioxidant power": the FRAP assay," *Analytical Biochemistry*, vol. 239, no. 1, pp. 70–76, 1996.

[27] A. Zoubeidi, S. Ettinger, E. Beraldi et al., "Clusterin facilitates COMMD1 and I-κB degradation to enhance NF-κB activity in prostate cancer cells," *Molecular Cancer Research*, vol. 8, no. 1, pp. 119–130, 2010.

[28] P. A. J. Muller, B. V. de Sluis, A. J. Groot et al., "Nuclear-cytosolic transport of COMMD1 regulates NF-κB and HIF-1 activity," *Traffic*, vol. 10, no. 5, pp. 514–527, 2009.

[29] H. C. Thoms, C. J. Loveridge, J. Simpson et al., "Nucleolar targeting of RelA(p65) is regulated by COMMD1-dependent ubiquitination," *Cancer Research*, vol. 70, no. 1, pp. 139–149, 2010.

[30] W. I. M. Vonk, C. Wijmenga, R. Berger, B. van de Sluis, and L. W. J. Klomp, "Cu,Zn superoxide dismutase maturation and activity are regulated by COMMD1," *Journal of Biological Chemistry*, vol. 285, no. 37, pp. 28991–29000, 2010.

[31] B. Halliwell, "Oxidative stress and cancer: have we moved forward?" *Biochemical Journal*, vol. 401, no. 1, pp. 1–11, 2007.

[32] P. Vlieghe, V. Lisowski, J. Martinez, and M. Khrestchatisky, "Synthetic therapeutic peptides: science and market," *Drug Discovery Today*, vol. 15, no. 1-2, pp. 40–56, 2010.

[33] G. N. Maine, X. Mao, P. A. Muller, C. M. Komarck, L. W. J. Klomp, and E. Burstein, "COMMD1 expression is controlled by critical residues that determine XIAP binding," *Biochemical Journal*, vol. 417, no. 2, pp. 601–609, 2009.

[34] Y. Ben-Neriah and M. Karin, "Inflammation meets cancer, with NF-κB as the matchmaker," *Nature Immunology*, vol. 12, no. 8, pp. 715–723, 2011.

[35] G. N. Maine and E. Burstein, "COMMD proteins and the control of the NFκB pathway," *Cell Cycle*, vol. 6, no. 6, pp. 672–676, 2007.

[36] H. Pelicano, D. Carney, and P. Huang, "ROS stress in cancer cells and therapeutic implications," *Drug Resistance Updates*, vol. 7, no. 2, pp. 97–110, 2004.

[37] A. A. Dayem, H. Y. Choi, J. H. Kim, and S. G. Cho, "Role of oxidative stress in stem, cancer, and cancer stem cells," *Cancers*, vol. 2, no. 2, pp. 859–884, 2010.

Hindawi Publishing Corporation
Journal of Amino Acids
Volume 2012, Article ID 967347, 13 pages
doi:10.1155/2012/967347

Review Article

Cancer Treatment Using Peptides: Current Therapies and Future Prospects

Jyothi Thundimadathil

American Peptide Company Inc., Sunnyvale, CA 94086, USA

Correspondence should be addressed to Jyothi Thundimadathil, jyothitm@yahoo.com

Received 30 October 2012; Accepted 7 December 2012

Academic Editor: Michele Caraglia

This paper discusses the role of peptides in cancer therapy with special emphasis on peptide drugs which are already approved and those in clinical trials. The potential of peptides in cancer treatment is evident from a variety of different strategies that are available to address the progression of tumor growth and propagation of the disease. Use of peptides that can directly target cancer cells without affecting normal cells (targeted therapy) is evolving as an alternate strategy to conventional chemotherapy. Peptide can be utilized directly as a cytotoxic agent through various mechanisms or can act as a carrier of cytotoxic agents and radioisotopes by specifically targeting cancer cells. Peptide-based hormonal therapy has been extensively studied and utilized for the treatment of breast and prostate cancers. Tremendous amount of clinical data is currently available attesting to the efficiency of peptide-based cancer vaccines. Combination therapy is emerging as an important strategy to achieve synergistic effects in fighting cancer as a single method alone may not be efficient enough to yield positive results. Combining immunotherapy with conventional therapies such as radiation and chemotherapy or combining an anticancer peptide with a nonpeptidic cytotoxic drug is an example of this emerging field.

1. Introduction

Mortality from cancer is about to surpass that from cardiovascular diseases in near future. About 7 million people die from cancer-related cases per year, and it is estimated that there will be more than 16 million new cancer cases every year by 2020 [1, 2]. Cancer is characterized by uncontrolled division of cells and the ability of these cells to invade other tissues leading to the formation of tumor mass, vascularization, and metastasis (spread of cancer to other parts of the body) [3]. Though angiogenesis (growth of new blood vessels from preexisting vessels) is a normal and vital process in growth and development, it is also a fundamental step in the transition of tumors from a dormant state to a malignant one [4]. Chemotherapy is one of the major approaches to treat cancer by delivering a cytotoxic agent to the cancer cells. The main problem with the conventional chemotherapy is the inability to deliver the correct amount of drug directly to cancer cells without affecting normal cells [5]. Drug resistance, altered biodistribution, biotransformation, and drug clearance are also common problems [5]. Targeted chemotherapy and drug delivery techniques are emerging as a powerful method to circumvent such problems [6–10]. This will allow the selective and effective localization of drugs at predefined targets (e.g., overexpressed receptors in cancer) while restricting its access to normal cell thus maximizing therapeutic index and reducing toxicity.

Discovery of several protein/peptide receptors and tumor-related peptides and proteins is expected to create a "new wave" of more effective and selective anticancer drugs in the future, capturing the large share of the cancer therapeutic market [6, 8, 11]. The "biologics" treatment option against cancer includes the use of proteins, monoclonal antibodies, and peptides. The monoclonal antibodies (mAbs) and large protein ligands have two major limitations compared to peptides: poor delivery to tumors due to their large size and dose-limiting toxicity to the liver and bone marrow due to nonspecific uptake into the reticuloendothelial system. The use of such macromolecules has therefore been restricted to either vascular targets present on the luminal side of tumor vessel endothelium or hematological malignancies [12–17]. Peptides possess many advantages,

such as small size, ease of synthesis and modification, tumor-penetrating ability, and good biocompatibility [18, 19]. Peptide degradation by proteolysis can be prevented by chemical modifications such as incorporation of D-amino acids or cyclization [18].

Over the years peptides have been evolved as promising therapeutic agents in the treatment of cancer, diabetes, and cardiovascular diseases, and application of peptides in a variety of other therapeutic areas is growing rapidly. Currently there are about 60 approved peptide drugs in the market generating an annual sale of more than $13 billion [18]. Out of four peptide drugs in the market which have reached global sales over $1 billion, three peptides are used in treating cancer directly or in the treatment of episodes associated with certain tumors (leuprolide, goserelin, and octreotide). The number of peptide drugs entering clinical trials is increasing steadily; it was 1.2 per year in the 1970s, 4.6 per year in the 1980s, 9.7 per year in the 1990s, and 16.8 per in 2000s [19]. There are several hundred peptide candidates in the clinic and preclinic development. From 2000 onwards, peptides entering clinical study were most frequently for indications of cancer (18%) and metabolic disorders (17%) [20].

This paper focuses on different strategies of employing peptides in cancer treatment and management. A special emphasis is given to current peptide drugs available in the market for treating cancer and also peptide candidates in clinical and preclinical stages of development. Peptides can be utilized in a number of different ways in treating cancer [8–10, 19]. This includes using peptides directly as drugs (e.g., as angiogenesis inhibitors), tumor targeting agents that carry cytotoxic drugs and radionuclides (targeted chemotherapy and radiation therapy), hormones, and vaccines. Different possible cancer treatment options using peptides are summarized in Figure 1. Due to the ability to bind to different receptors and also being part of several biochemical pathways, peptides act as potential diagnostic tool and biomarkers in cancer progression. Out of these different possibilities, peptide drugs currently available in the market come from peptide hormone therapy and tumor targeting agents carrying radionuclides (peptide-receptor radio nuclide therapy and imaging). Exceptions to these are two short chain peptide-related drugs, bortezomib and mifamurtide [21, 22]. There is a tremendous progress in other areas such as peptide-vaccine development and peptide angiogenesis inhibitors, and several clinical trials are underway which is expected to bear fruit in near future providing better options to millions of cancer patients.

2. Peptide Hormones: LHRH Agonists and Antagonists

The best classical example of the application of peptides in cancer treatment is the use of LHRH (luteinizing hormone-releasing hormone) agonists introduced by Schally et al. as a therapy for prostate cancer [23–25]. Since then, depot formulations of LHRH agonists such as buserelin, leuprolide, goserelin, and triptorelin have been developed for more

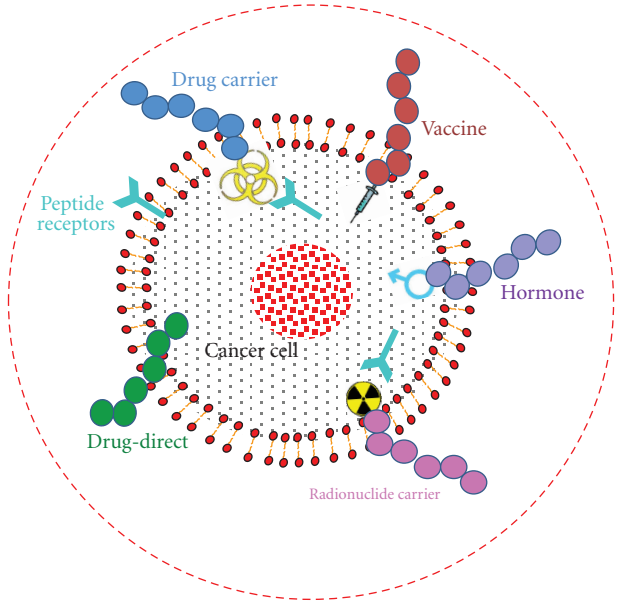

Figure 1: Different possible treatment options of cancer using peptides. Peptides can be used as anticancer drug, cytotoxic drug carrier, vaccine, hormones, and radionuclide carrier.

efficacious and more convenient treatment of patients with prostate cancer [26–28]. Administration of these peptides causes downregulation of LHRH receptors in the pituitary, leading to an inhibition of follicle-stimulating hormone (FSH) and LH release, and a concomitant decrease in testosterone production. This offered a new method for androgen deprivation therapy in prostate cancer patients. Discovery of LHRH antagonists resulted in therapeutic improvement over agonists as they cause an immediate and dose-related inhibition of LH and FSH by competitive blockade of the LHRH receptors. To date, many potent LHRH antagonists are available for the clinical use in patients. Cetrorelix was the first LHRH antagonist given marketing approval and, thus, became the first LHRH antagonist available clinically [29]. Subsequently new generation LHRH antagonists such as abarelix and degarelix have been approved for human use [30, 31]. A list of LHRH agonists and antagonists available in the market is shown in Table 1.

3. Peptide as Radionuclide Carrier: Somatostatin Analogues in Cancer Therapy and Peptide Receptor Radionuclide Therapy (PRRT)

Apart from the use of peptide-based LHRH agonists and antagonists for treating cancer, somatostatin analogues are the only approved cancer therapeutic peptides in the market [32]. Potent analogues of somatostatin (peptide hormone consisting of 14 amino acids, found in δ cells of the pancreas as well as in hypothalamic and other gastrointestinal cells) including octreotide (sandostatin) have been developed for the treatment of acromegaly, gigantism, thyrotropinoma, diarrhea and flushing episodes associated with carcinoid

Table 1: LHRH agonists and new generation antagonists available in the market.

Peptide	Sequence comparison	Indications
Agonists		
Buserelin	Pyr-His-Trp-Ser-Tyr-D-Ser(OtBu)-Leu-Arg-Pro-NHEt	Prostate cancer
Gonadorelin	Pyr-His-Trp-Ser-Tyr-Gly-Leu-Arg-Pro-Gly-NH_2	Cystic ovarian disease, agent for evaluating hypothalamic-pituitary gonadotropic function
Goserelin	Pyr-His-Trp-Ser-Tyr-D-Ser(OtBu)-Leu-Arg-Pro-AzGly-NH_2	Prostate cancer; breast cancer
Histrelin	Pyr-His-Trp-Ser-Tyr-D-His(N-benzyl)-Leu-Arg-Pro-NHEt	Prostate cancer; breast cancer
Leuprolide	Pyr-His-Trp-Ser-Tyr-D-Leu-Leu-Arg-Pro-NHEt	Prostate cancer; breast cancer
Nafarelin	Pyr-His-Trp-Ser-Tyr-2Nal-Leu-Arg-Pro-Gly-NH_2	Treat symptoms of endometriosis, central precocious puberty
Triptorelin	Pyr-His-Trp-Ser-Tyr-D-Trp-Leu-Arg-Pro-Gly-NH_2	Prostate cancer; breast cancer
Antagonists		
Abarelix	Ac-D-2Nal-D-4-chloroPhe-D-3-(3′-pyridyl) Ala-Ser-(N-Me)Tyr-D-Asn-Leu-isopropylLys-Pro-DAla-NH_2	Prostate cancer
Cetrorelix	Ac-D-2Nal-D-4-chloroPhe-D-3-(3′-pyridyl) Ala-Ser-Tyr-D-Cit-Leu-Arg-Pro-D-Ala-NH_2	Prostate cancer; breast cancer
Degarelix	Ac-D-2Nal-D-4-chloroPhe-D-3-(3′-pyridyl) Ala-Ser-4-aminoPhe(L-hydroorotyl)- D-4-aminoPhe(carbamoyl)-Leu-isopropylLys-Pro-D-Ala-NH_2	Prostate cancer
Ganirelix	Ac-D-2Nal-D-4-chloroPhe-D-3-(3′-pyridyl) Ala-Ser-Tyr-D-(N9, N10-diethyl)-homoArg-Leu-(N9, N10-diethyl)-homoArg-Pro-D-Ala-NH_2	Fertility treatment

syndrome, and diarrhea in patients with vasoactive intestinal peptide-secreting tumors (VIPomas) [33]. Similarly, another long-acting analogue of somatostatin, lanreotide (somatuline), is used in the management of acromegaly and symptoms caused by neuroendocrine tumors, most notably carcinoid syndrome and VIPomas [34].

Most neuroendocrine tumors (NETs) feature a strong overexpression of somatostatin receptors, mainly of subtype 2 (sst2). Currently five somatostatin receptor subtypes (sst) are known (sst1-5) [32, 35]. The density of these receptors is vastly higher than on nontumor tissues. Therefore, somatostatin receptors are attractive targets for delivery of radioactivity via radiolabeled somatostatin analogs. The sst2 has been shown to internalize into the cell in a fast, efficient, and reversible manner after specific binding of a receptor agonist. This molecular process is likely to be responsible for the high and long-lasting uptake of radioactivity in the target cell after binding of the radiolabeled somatostatin analog. Introduced in the late 1980s, [111In-DTPA]-octreotide (Octreoscan), the first available radiolabeled somatostatin analog, rapidly became the gold standard for diagnosis of sst-positive NETs [36, 37]. Numerous peptide-based tracers targeting somatostatin receptors have been developed over the past decade [36, 37]. Octreoscan and NeoTect (tc-99m depreotide) are the only radiopeptide tracers on the market approved by the Food and Drug Administration [37, 38]. An octreotide scan or octreoscan is a type of scintigraphy used to find carcinoid and other types of tumors and to localize sarcoidosis. Octreotide, a drug similar to somatostatin, is radiolabeled with indium-111 and is injected into a vein and travels through the bloodstream. The radioactive octreotide attaches to tumor cells that have receptors for somatostatin. A radiation-measuring device detects the radioactive octreotide and makes pictures showing where the tumor cells are in the body. NeoTect is a radioactive imaging test used to evaluate certain lung lesions in patients who test positive for lung lesions using other imaging tests (e.g., CT or MRI) and have been diagnosed with cancer or have a strong likelihood of cancer. NeoTect identifies certain cells that may be associated with lung cancer and sometimes with other conditions [38].

Peptide receptor radionuclide therapy (PRRT) combines octreotide (or other somatostatin analogs) with a radionuclide (a radioactive substance) to form highly specialized molecules called radiolabeled somatostatin analogues or radiopeptides [39–48]. Radiolabeled somatostatin analogs generally comprise three main parts: a cyclic octapeptide (e.g., octreotide), a chelator (e.g., DTPA or DOTA), and a radioactive element (111In, 90Y, or 177Lu). These radiopeptides can be injected into a patient and will travel throughout the body binding to carcinoid tumor cells that have receptors for them. Once bound, these radiopeptides emit radiation and kill the tumor cells they are bound to (Figure 2). PRRT using [111In-DTPA]-octreotide (where DTPA is diethylenetriamine pentaacetic acid) is feasible because, besides gamma radiation, 111In emits both therapeutic Auger and internal conversion electrons having tissue penetration ability [39, 40]. However, studies have shown that 111In-coupled peptides are not efficient for PRRT, as the short distance traveled by Auger electrons after emission means that decay of 111In has to occur close to the cell nucleus to be tumoricidal [39, 40]. It was found that replacement of phenylalanine by tyrosine as the third amino acid in the octapeptide leads to an increased affinity for somatostatin-receptor subtype 2.

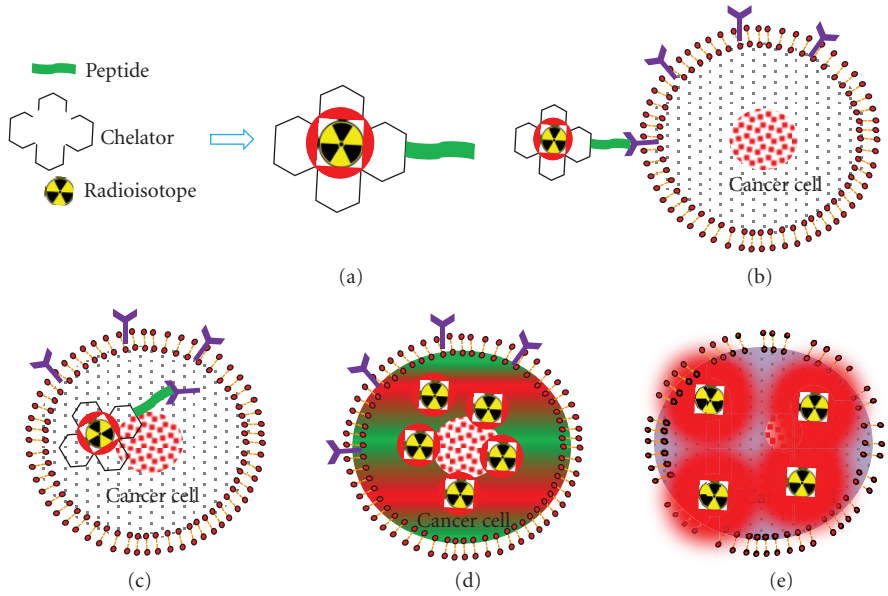

Figure 2: Peptide receptor radionuclide therapy (PRRT); radiolabeled somatostatin analogs generally comprise three main parts: a cyclic octapeptide (e.g., Tyr3-octreotide or Tyr3-octreotate), a chelator (e.g., DTPA or DOTA), and a radioactive element. Radioisotopes commonly used in PRRT are 111In, 90Y, and 177Lu.

This resulted in the development of next generation therapy using 90Y-DOTA, Tyr3-octreotide [41–44]. This compound has DOTA (tetraazacyclododecane tetraacetic acid) instead of DTPA as the chelator, which allows stable binding of 90Y, a β-emitting radionuclide. Various clinical trials around the world showed that it is better than [111In-DTPA]-octreotide in treating gastroenteropancreatic neuroendocrine tumors (GEPNETs). A third generation of somatostatin-receptor-targeted radionuclide therapies was introduced using 177Lu-DOTA, Tyr3-octreotate [49, 50]. The only difference between DOTA, Tyr3-octreotate and DOTA, Tyr3-octreotide is that the C-terminal threoninol of DOTA, Tyr3-octreotide is replaced with the amino acid, threonine. As a result, DOTA, Tyr3-octreotate displays improved binding to somatostatin-receptor-positive tissues when compared with DOTA, Tyr3-octreotide [49]. Gastroenteropancreatic tumors predominantly express subtype 2 of the somatostatin receptor, and DOTA, Tyr3-octreotate has a sixfold to ninefold increased affinity for this receptor subtype *in vitro* compared with DOTA, Tyr3-octreotide [43, 49, 50]. 177Lu-octreotate was very successful in terms of tumor regression and survival in an experimental model in rats. 177Lu-labeled somatostatin analogs have an important practical advantage over their 90Y-labeled counterparts: 177Lu is not a pure β emitter, but also emits low-energy γ rays, which allows direct posttherapy imaging and dosimetry. Treatment with 177Lu-octreotate resulted in a survival benefit of several years and markedly improved quality of life. PRRT might soon become the therapy of choice for patients with metastatic or inoperable GEPNETs. Nowadays, different somatostatin analogs are available not only for therapeutic purposes but also when labeled with b1-emitters (e.g., 68Ga and 64Cu) for tumor imaging with integrated PET/CT scanners [51, 52]. The PET/CT technology provides a highly valuable combination of physiologic and anatomic information and has been shown to impact significantly on the patient's management.

Tumor imaging and PRRT have been extended to many other receptors such as Gastrin-releasing peptide/bombesin (GRP) and Cholecystokinin (CCK) in recent years [53, 54]. Radiolabelled receptor antagonists are also emerging as alternatives in this area [55, 56].

4. Peptide Vaccines

Active immunization seems to be one of the promising strategies to treat cancer though many approaches based on the employment of immune cells or immune molecules have been studied [57, 58]. In the last decade, this idea of vaccinations against cancer has transformed into clinical studies aiming to optimally deliver vaccines based on defined antigens to induce anticancer immunity. This method of treating cancerous cells relies on vaccines consisting of peptides derived from the protein sequence of candidate tumor-associated or specific antigens [57]. Tumor cells express antigens known as tumor-associated antigens (TAAs) that can be recognized by the host's immune system (T cells). Many TAAs have already been identified and molecularly characterized [59, 60]. These TAAs can be injected into cancer patients in an attempt to induce a systemic immune response that may result in the destruction of the cancer growing in different body tissues. This procedure is defined as active immunotherapy or vaccination as the host's immune system is either activated de novo or restimulated to mount an effective, tumor-specific immune reaction that may ultimately lead to tumor regression (Figure 3). Any protein/peptide produced in a tumor cell that has an abnormal structure due to mutation can act as a tumor antigen. Such abnormal proteins are produced due to mutation of

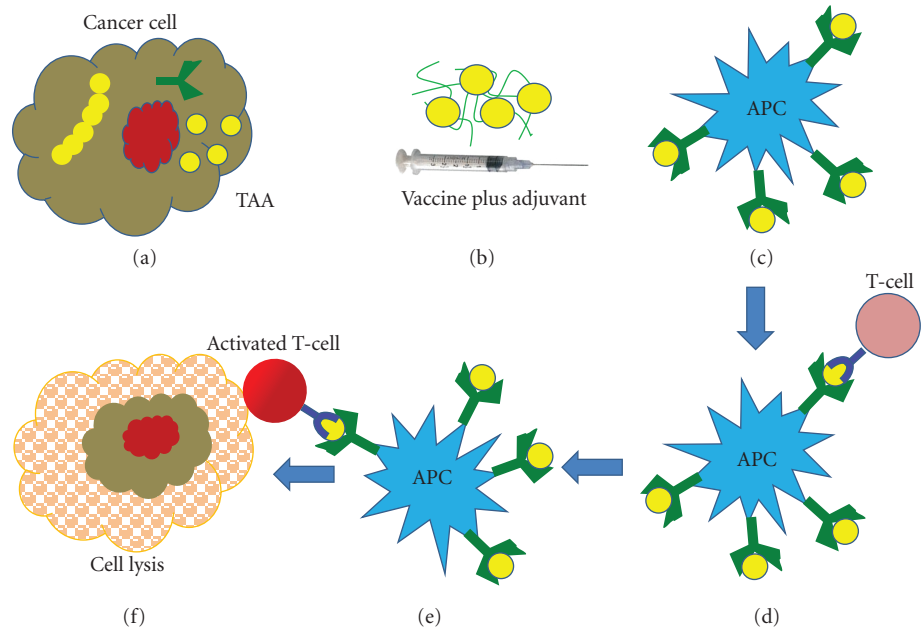

Figure 3: Peptide-based cancer vaccines: tumor cells express antigens known as tumor-associated antigens (TAAs) that can be recognized by the host's immune system (a). These TAAs mixed with an adjuvant can be injected into cancer patients in an attempt to induce a systemic immune response (b). The antigen presenting cell (APC) presents the antigen to T cell ((c) and (d)), thereby the T cell is activated (e) which results in the destruction of the cancer cell (f).

the concerned gene. Various clinical studies focus on the therapeutic potential of active immunization or vaccination with TAA peptides in patients with metastatic cancer [61–63].

Most known TAAs are CTL (cytotoxic T lymphocyte also known as CD8+ T-cells or killer T cell) epitopes [64]. Peptide antigens are usually 8–10 amino acids long with 2-3 primary anchor residues that interact with MHC class 1-molecules and 2-3 residues which bind to T-cell receptor [64, 65]. CTLs directed against peptides presented by MHC class 1 molecules constitute powerful effectors of the immune system against tumor cells. The T-cell antigen receptor (TCR) on T cells recognizes the complex of a small peptide located in the antigen-binding groove of an MHC molecule [66]. MHC molecules (also called human leukocyte antigens (HLAs) in humans) are subdivided into class I molecules, which are found on all nucleated cells and class II molecules, which are found on specialized antigen-presenting cells (APCs) such as dendritic cells, macrophages, B cells, and selected activated endothelial or epithelial cells. CD4+ T cells recognize antigens bound to MHC class II molecules, and, as noted, class II molecules are expressed on APCs that possess the capability of antigen capture through phagocytosis or binding to surface antibody [67, 68].

Several of the peptide vaccines have undergone phase I and II clinical trials and have shown promising results in immunological as well as clinical responses. The notable peptide vaccines that have undergone phase I/II/III clinical trials include HER-2/neu immunodominant peptide (lung, breast, or ovarian cancer) [69–71], Mucin-1 (MUC-1, Stimuvax), peptide (breast or colon cancer) [72, 73], Carcinoembryonic antigen (colorectal, gastric, breast, pancreatic and non-small-cell lung cancers) [74, 75], Prostate-specific membrane antigen (prostate cancer) [76–78], HPV-16 E7 peptide (cervical cancer) [79], Ras oncoprotein peptide (colorectal and pancreatic carcinomas) [80–82], and Melanoma antigens (Melanoma) [62, 68, 83–85]. Another vaccine known as GV-1001 is under development, which is an injectable formulation of a promiscuous MHC class II peptide derived from the telomerase reverse transcriptase catalytic subunit (hTERT). GV-1001 is currently undergoing phase II clinical trials for liver cancer and NSCLC (non-small-cell lung cancer) as well as a phase III trial for pancreatic cancer [86].

The peptide vaccines are relatively less expensive, easy to manufacture and manipulate, are of defined structure, and being synthetic in nature do not have a problem of batch-to-batch variation. The major disadvantage of the peptide vaccines is their weak immunogenicity. Several strategies such as epitope enhancement, use of various T-cell epitopes, adjuvants, incorporation of costimulatory molecules, *ex vivo* loading into antigen presenting cells are being explored to enhance the immunogenicity and efficacy of the peptide vaccines [73–86].

5. Peptide as Cytotoxic Drug Carrier

Several peptide receptors are known which can be used as potential drug targets in cancer therapy [53–56, 87, 88]. The role of somatostatin receptors has already been discussed in the previous section for peptide receptor radionuclide therapy (PRRT). Similarly, a peptide can be conjugated to a cytotoxic drug to deliver it to a cancer cell expressing the corresponding peptide receptor. Such peptides are known

as cell targeting peptides as they can specifically target a cell expressing its receptor. Cytotoxic compounds linked to analogs of hormonal peptides like LHRH, bombesin, and somatostatin can be targeted to certain tumors possessing receptors for those peptides and therefore are more selective for killing cancer cells [89, 90]. For example, a potential drug candidate, AEZS-108, couples a peptide LHRH with the chemotherapeutic agent doxorubicin to directly target cells that express LH-RH receptors, specifically prostate cancer cells [91, 92]. A list of different peptide receptors, their subtypes, tumors in which these receptors are expressed, and some of the targeting agents used are depicted in Table 2 [93]. Most of the studies so far are in the area of radionuclide therapy and imaging though a few studies examined the transport of cytotoxic drugs such as AN-201 and doxorubicin [94]. Nevertheless, these receptors provide good platform for the cell-specific delivery of chemotherapeutic agents.

Apart from peptides that can selectively bind to the previous peptide receptors, many other peptides which are relevant to cancer treatment were discovered in recent years. These peptides obtained by *in vivo* phage display technology are known as homing peptides as they home very specifically to various normal organs or diseased tissues [95–97]. The RGD (Arg-Gly-Asp) and NGR (Asn-Gly-Arg) peptides represent the first generation of homing peptides [95]. Tumor homing of the RGD and NGR peptides appears to be independent of the tumor type, demonstrating that the receptors for these peptides are upregulated during angiogenesis. The RGD motif was originally discovered in peptides that bind to different integrins. The RGD peptide was shown to home to malignant melanoma, breast carcinoma xenografts, and rheumatoid arthritis model indicating that they recognize angiogenic vessels in general. The RGD peptides have high affinity towards the α_v integrin receptors in the angiogenic vasculature. The NGR motif was identified in an *in vivo* screen on human breast carcinoma xenografts [96]. It was originally identified as a cell adhesion motif, and it homes selectively to tumor blood vessels and other types of angiogenic vessels. The receptor for the NGR peptide is a peptidase, aminopeptidase N (APN), expression of which is upregulated in the angiogenic blood vessels. Several other peptides such as TAASGVRSMH and LTLRWVGLMS (chondroitin sulfate proteoglycan NG2 receptor) and F3 peptide (31 amino acid peptide that binds to cell surface-expressed nucleolin receptor) were identified thereafter [98, 99]. Recently, homing peptides with cell-penetrating ability were discovered [99–101]. Cell-penetrating peptides (CPPs) are small peptides, generally less than 30 amino acids long, that internalize very efficiently into all cells they come into contact with [102]. These internalizing homing peptides are similar to the classic cell-penetrating peptides, such as the transcription-transactivating (Tat) protein of HIV-1, and penetrating with an important exception: the internalization of the homing peptides is cell-type-specific. Both the F3 and LyP-1 (CGNKRTRGC) peptides are cell-type-specific CPPs [99–101]. They are able to internalize tumor cells and blood (F3) or lymphatic (LyP-1) endothelial cells in the tumors they home to.

Homing peptides have been successfully used as delivery vehicles to target imaging agents, drug molecules, oligonucleotides, liposomes, and inorganic nanoparticles to tumors and other tissues [97, 103, 104]. One drug that has been delivered using RGD and NGR peptides is the tumor necrosis factor-α (TNF-α) that has potent antitumor activity [98, 105]. The clinical use of TNF-α itself as an anticancer drug is limited to local treatments due to its dose-limiting systemic toxicity. RGD and NRG peptide-targeted TNF-α treatment decreased tumor growth with smaller doses than free TNF-α. The antitumor activity of NGR-TNF-α was also studied in combination with various chemotherapeutic drugs: doxorubicin and melphalan as well as cisplatin, paclitaxel, and gemcitabine and compared to the efficacy of the chemotherapeutic drugs alone in various murine tumor models [105]. The results showed that targeted delivery of low doses of NGR-TNF-α to tumor vasculature increased the efficacy of various drugs acting via different mechanisms. Moreover, transgenic mice with androgen-independent prostate carcinoma (TRAMP-C1) were treated with repeated cycles of doxorubicin, administered either alone or following NGR-TNF-α administration. Pretreatment with NGR-TNF-α significantly expanded the therapeutic index of doxorubicin and significantly delayed tumor growth without increasing drug-related toxicity. The RGD homing peptide has also been conjugated to doxorubicin [97, 106]. This treatment inhibited tumor growth and prolonged the lifespan of tumor-bearing animals. Again the doxorubicin-RGD conjugate was less toxic than doxorubicin alone or doxorubicin conjugated to a control peptide. Conjugation of IL-12 (Interleukin-12) to the CDCRGDCFC (RGD-4C) peptide, a specific ligand for $\alpha_v\beta 3$ integrin, targets IL-12 directly to tumor neovasculature [107]. This fusion protein stimulated interferon-γ production *in vitro* and *in vivo*, suggesting biological activity consistent with IL-12. Localization of IL-12 to the angiogenic vasculature significantly enhanced the antiangiogenic effect in corneal angiogenesis assay, augmented antitumor activity in a neuroblastoma model, and decreased toxicity of the IL-12.

A number of clinical trials based on RGD and NGR targeted drug delivery are currently ongoing or recruiting patients [108–110]. For example, a phase Ib study was conducted to verify the safety of NGR peptide-targeted hTNF in combination with doxorubicin in treatment of refractory/resistant solid tumors [108]. Fifteen patients received various doses of a combination of NGR-targeted hTNF and doxorubicin intravenously. One partial response (7%) and ten stable diseases (66%) lasting for a median duration of 5.6 months were observed. These results prompted plans for the phase II development (http://clinicaltrials.gov/). In addition, a phase III trial on newly diagnosed glioblastoma has been started [97]. A recently identified peptide called iRGD is able to specifically recognize and penetrate cancerous tumors but not normal tissues [111]. Chlorotoxin (a 36 amino acid peptide derived from scorpion venom) binds preferentially to glioma cells compared with nonneoplastic cells or normal brain has allowed the development of new methods for the treatment and diagnosis of cancer [112].

Table 2: Peptide receptors which have potential in cancer therapy.

Peptide receptors	Receptor subtypes	Expressing tumor type	Targeting agents
Somatostatin	sst1, sst2, sst3, sst4, and sst5	GH-producing pituitary adenoma, paraganglioma, nonfunctioning pituitary adenoma, pheochromocytomas	Radioisotopes, AN-201 (a potent cytotoxic radical 2-pyrrolinodoxorubicin), doxorubicin
Pituitary adenylate cyclase activating peptide (PACAP)	PAC1	Pheochromocytomas and paragangliomas	Radioisotopes, doxorubicin
Vasoactive intestinal peptide (VIP/PACAP)	VPAC1, VPAC2	Cancers of lung stomach, colon, rectum, breast, prostate, pancreatic ducts, liver, and urinary bladder	Radioisotopes, camptothecin
Cholecystokinin (CCK)	CCK1 (formerly CCK-A) and CCK2	Small cell lung cancers, medullary thyroid carcinomas, astrocytomas, and ovarian cancers	Radioisotopes, cisplatin
Bombesin/gastrin-releasing peptide (GRP)	BB1, GRP receptor subtype (BB2), the BB3 and BB4	Renal cell, breast, and prostate carcinomas	Doxorubicin, 2-pyrrolinodoxorubicin
Neurotensin	NTR1, NTR2, NTR3	Small cell lung cancer, neuroblastoma, pancreatic and colonic cancer	Radioisotopes
Substance P	NK1 receptor	Glial tumors	Radioisotopes
Neuropeptide Y	Y1–Y6	Breast carcinomas	Radioisotopes

6. Anticancer Peptides

Direct use of peptide as a therapeutic agent to treat cancer is gaining momentum in the recent years. Anticancer activity of different peptides is attributed to a variety of mechanisms that restrict tumor growth. The mechanism involves the inhibition of angiogenesis, protein-protein interactions, enzymes, proteins, signal transduction pathways, or gene expression [113–120]. Another category of anti-cancer peptides is peptide antagonists which can preferentially bind to a known receptor [121, 122]. Moreover "pro-apoptotic" peptides mediate significant induction of apoptosis (programmed cell death) in tumors [123–125].

Angiogenesis involves the migration, growth, and differentiation of endothelial cells, which line the inside wall of blood vessels. There is a tremendous effort to discover angiogenesis inhibitors, based on peptides as the safest and least toxic therapy for diseases associated with abnormal angiogenesis [113]. Angiogenesis requires the binding of signaling molecules, such as vascular endothelial growth factor (VEGF), to receptors on the surface of normal endothelial cells. When VEGF and other endothelial growth factors bind to their receptors on endothelial cells, signals within these cells are initiated that promote the growth and survival of new blood vessels. Angiogenesis inhibitors interfere with various steps in this process. A number of ongoing clinical trials in this area focus on peptides derived from extracellular matrix proteins, growth factors and growth factor receptors, coagulation cascade proteins, chemokines, and type I Thrombospondin domain containing proteins and serpins [113, 114]. Recently it was found that angiotensin-(1–7) can stop lung cancer tumor growth in mice by inhibiting blood vessel formation [126]. The antiangiogenic agent cilengitide (Merck) is a derivative of the RGD peptide [127–130]. It is the inner salt of a cyclized RGD pentapeptide (cyclo-[Arg-Gly-Asp-DPhe-(NMeVal)]) that is selective for αv integrins, which are important in angiogenesis. It is currently under phase II trial for the treatment of glioblastoma and refractory brain tumors in children. Another peptide, ATN-161 (Ac-PHSCN-NH2), is in early phase II trials for cancer [120]. It binds to and inhibits integrins involved in tumor progression (a5ß1, avß3, and avß5), while not inhibiting adhesion as it is not based on the RGD sequence [131]. A dipeptide, L-glutamine L-tryptophan (IM862) that is made normally in the thymus gland, has shown antiangiogenic properties. Though it was shown recently to be ineffective against AIDS-Kaposi's sarcoma in a phase III trial, it still holds promise for other forms of cancer [132, 133].

BN/GRP (bombesin/gastrin-releasing peptide) peptides were shown to bind selectively to the G-protein-coupled receptors on the cell surface, stimulating the growth of various malignancies in murine and human cancer models [134, 135]. Thus, it has been proposed that the secretion of BN/GRP by neuroendocrine cells might be responsible for the development and progression of prostate cancer to androgen independence. GRP is widely distributed in lung and gastrointestinal tracts. It is produced in small cell lung cancer (SCLC), breast, prostatic, and pancreatic cancer and functions as a growth factor. The involvement of bombesin-like peptides in the pathogenesis of a wide range of human tumors, their function as autocrine/paracrine tumoural growth factors, and the high incidence of BN/GRP receptors in various human cancers prompted the design and synthesis of BN/GRP receptor (GRPR) antagonists such as RC-3095, RC-3940-II, and RC-3950 [136–138]. Recently, many researchers are focusing on the development of GHRH (growth hormone releasing hormone—a hypothalamic polypeptide) antagonists as potential anticancer therapeutics since the GHRH is produced by various

human tumors, including prostate cancer, and seems to exert an autocrine/paracrine stimulatory effect on tumors [139, 140].

Recently, scientists have designed peptides to target the protein-protein interface of a key enzyme in DNA synthesis crucial for cancer growth [141]. The peptides act by a novel inhibitory mechanism and curb cancer cell growth in drug-resistant ovarian cancer cells. These octapeptides specifically target the protein-protein interface of thymidylate synthase. Thymidylate synthase is composed of two identical polypeptide chains; that is, it is a homodimer. The peptides stabilize the inactive form of the enzyme, show a novel mechanism of inhibition for homodimeric enzymes, and inhibit cell growth in drug sensitive and resistant cancer cell lines [141].

Cisplatin, cisplatinum, or *cis*-diamminedichloroplatinum(II) is the first member of a class of platinum-containing anti-cancer drugs. These platinum complexes react *in vivo*, binding to and causing crosslinking of DNA, which ultimately triggers apoptosis (programmed cell death). Recently, Pt (IV)-peptide conjugates were found to be good inhibitors of cellular proliferation when compared to a nontargeting platinum(IV) parent compound, showing that its relatively low cytotoxicity is greatly improved by addition of the peptides [142]. (KLAKLAK)2 is an antimicrobial apoptosis-inducing peptide that upon internalization causes mitochondrial swelling and disruption of the mitochondrial membrane leading to apoptosis [123, 124, 143]. The RGD-(KLAKLAK)2 and NGR-(KLAKLAK)2 were especially toxic to angiogenic endothelial cells leading to reduced tumor growth and metastases as well as prolonged survival. LyP-1 is unique among the tumor homing peptides since it has cytotoxic activity on its own [144]. When injected into the tail vein of mice with MDA-MB-435 breast cancer xenografts, LyP-1 peptide by itself inhibited tumor growth and reduced the number of lymphatic vessels, thus demonstrating a cytotoxic activity of the peptide.

7. Other Anticancer Drugs Closely Related to Peptides

Bortezomib is the first therapeutic proteasome inhibitor to be tested in humans [21, 145, 146]. It is approved in the USA for treating relapsed multiple myeloma and mantle cell lymphoma (2003). In multiple myeloma, complete clinical responses have been obtained in patients with otherwise refractory or rapidly advancing disease. The drug is an N-protected dipeptide and can be written as Pyz-Phe-boroLeu, which stands for pyrazinoic acid, phenylalanine, and leucine with a boronic acid instead of a carboxylic acid. Mifamurtide (Mepact) is a drug against osteosarcoma, which is lethal in about a third of cases [147]. The drug was approved in Europe in March 2009 and is not currently approved in the USA. Mifamurtide is a fully synthetic derivative of muramyl dipeptide (MDP) the smallest naturally occurring immune stimulatory component of cell walls from *Mycobacterium* species. The side chains of the molecule give it a longer elimination half-life than the natural substance. Being a phospholipid, it accumulates in the lipid bilayer of the liposomes in the infusion. It recognizes muramyl dipeptide and simulates a bacterial infection by binding to NOD2 (NOD2 is a pattern recognition receptor which is found in several kinds of white blood cells, mainly monocytes and macrophages) activating white cells [148]. This results in an increased production of TNF-α, interleukin 1, interleukin 6, interleukin 8, interleukin 12, and other cytokines, as well as ICAM-1. The activated white cells attack cancer cells, but not other cells. Brentuximab Vedotin, an antibody drug conjugate (ADS) approved in 2011, is a chimeric monoclonal antibody, brentuximab (which targets the cell-membrane protein CD30) linked to three to five units of the antimitotic agent monomethyl auristatin E. The linker here is a valine-citrulline dipeptide which is cleaved by cathepsin once the conjugate has entered a tumor cell. The antimitotic agent monomethyl auristatin E can be considered as a peptidomimetic [149, 150].

8. Conclusion

In conclusion, peptides are poised to make a huge impact in near future in the area of cancer treatment and diagnosis. Targeted chemotherapy and drug delivery techniques are emerging as an excellent tool in minimizing problems with the conventional chemotherapy. Along with different peptide-based cancer therapeutics already available for patients, a number of peptide-based therapies such as cancer vaccines, tumor targeting with cytotoxic drugs and radioisotopes, and anti-angiogenic peptides are currently on clinical trials and are expected to yield positive results. Stimuvax (palmitoylated peptide vaccine against nonsmall lung cancer, Merck), Primovax (peptide cancer vaccine, Pharmexa), Melanotan (precancerous actinic keratosis, Clinuvel), and Cilengitide (Glioblastoma, Merck) are some examples of potential peptides in late clinical trials. Due to the tremendous advancement in the large scale synthesis of peptides it will be possible to make peptide-based anti-cancer drugs more affordable to patients. In recent years combination therapy is emerging as an important strategy to fight cancer as just one method may not be efficient enough to cure the disease completely or prevent recurrence [151]. In the hope of achieving synergistic effects, combinations of antiangiogenesis with traditional chemotherapy are currently being pursued in clinical trials [151–155]. For example, cilengitide was used in a phase I/IIa combination trial, which combined cilengitide with radiotherapy and temozolomide for newly diagnosed Glioblastoma patients resulting in better overall survival (OS) rates [152]. ATN-161 enhances the activity of radiation and chemotherapy and is progressing to a phase II trial for head and neck cancer [153]. Encouraging data are emerging that strongly support the notion that combining immunotherapy with conventional therapies, for example, radiation and chemotherapy, may improve efficacy [154] in cancer treatment and management.

References

[1] A. Jemal, F. Bray, M. M. Center, J. Ferlay, E. Ward, and D. Forman, "Global cancer statistics," *CA Cancer Journal for Clinicians*, vol. 61, no. 2, pp. 69–90, 2011.

[2] "Global cancer facts & figures," 2nd edition, American Cancer Society, http://www.cancer.org/.
[3] B. Vogelstein and K. W. Kinzler, "Cancer genes and the pathways they control," *Nature Medicine*, vol. 10, no. 8, pp. 789–799, 2004.
[4] J. Folkman, "Angiogenesis in cancer, vascular, rheumatoid and other disease," *Nature Medicine*, vol. 1, no. 1, pp. 27–31, 1995.
[5] D. Kakde, D. Jain, V. Shrivastava, R. Kakde, and A. T. Patil, "Cancer therapeutics—opportunities, challenges and advances in drug delivery," *Journal of Applied Pharmaceutical Science*, vol. 1, no. 9, pp. 1–10, 2011.
[6] J. Enbäck and P. Laakkonen, "Tumour-homing peptides: tools for targeting, imaging and destruction," *Biochemical Society Transactions*, vol. 35, no. 4, pp. 780–783, 2007.
[7] R. T. Dorsam and J. S. Gutkind, "G-protein-coupled receptors and cancer," *Nature Reviews Cancer*, vol. 7, no. 2, pp. 79–94, 2007.
[8] O. H. Aina, T. C. Sroka, M. L. Chen, and K. S. Lam, "Therapeutic cancer targeting peptides," *Biopolymers*, vol. 66, no. 3, pp. 184–199, 2002.
[9] L. Meng, L. Yang, X. Zhao, L. Zhang, H. Zhu et al., "Targeted delivery of chemotherapy agents using a liver cancer-specific aptamer," *PLoS One*, vol. 7, no. 4, Article ID e33434, 2012.
[10] X. X. Zhang, H. S. Eden, and X. Chen, "Peptides in cancer nanomedicine: drug carriers, targeting ligands and protease substrates," *Journal of Controlled Release*, vol. 159, pp. 2–13, 2012.
[11] P. Vlieghe, V. Lisowski, J. Martinez, and M. Khrestchatisky, "Synthetic therapeutic peptides: science and market," *Drug Discovery Today*, vol. 15, no. 1-2, pp. 40–56, 2010.
[12] X. Q. Qiu, H. Wang, B. Cai, L. L. Wang, and S. T. Yue, "Small antibody mimetics comprising two complementarity-determining regions and a framework region for tumor targeting," *Nature Biotechnology*, vol. 25, no. 8, pp. 921–929, 2007.
[13] T. M. Allen, "Ligand-targeted therapeutics in anticancer therapy," *Nature Reviews Cancer*, vol. 2, pp. 750–763, 2002.
[14] I. Pastan, R. Hassan, D. J. Fitzgerald, and R. J. Kreitman, "Immunotoxin therapy of cancer," *Nature Reviews Cancer*, vol. 6, pp. 559–565, 2006.
[15] P. E. Thorpe, "Vascular targeting agents as cancer therapeutics," *Cancer Research*, vol. 10, pp. 415–427, 2004.
[16] T. Mori, "Cancer-specific ligands identified from screening of peptide-display libraries," *Current Pharmaceutical Design*, vol. 10, no. 19, pp. 2335–2343, 2004.
[17] M. E. Reff, K. Hariharan, and G. Braslawsky, "Future of monoclonal antibodies in the treatment of hematologic malignancies," *Cancer Control*, vol. 9, no. 2, pp. 152–166, 2002.
[18] A. M. Thayer, "Improving peptides," *Chemical and Engineering News*, vol. 89, pp. 13–20, 2011.
[19] C. Borghouts, C. Kunz, and B. Groner, "Current strategies for the development of peptide-based anti-cancer therapeutics," *Journal of Peptide Science*, vol. 11, no. 11, pp. 713–726, 2005.
[20] Peptide Therapeutics Foundation, "Development trends for peptide therapeutics," Tech. Rep., San Diego, Calif, USA, 2010.
[21] J. Adams and M. Kauffman, "Development of the proteasome inhibitor Velcade (Bortezomib)," *Cancer Investigation*, vol. 22, no. 2, pp. 304–311, 2004.
[22] P. A. Meyers, C. L. Schwartz, M. Krailo et al., "Osteosarcoma: a randomized, prospective trial of the addition of ifosfamide and/or muramyl tripeptide to cisplatin, doxorubicin, and high-dose methotrexate," *Journal of Clinical Oncology*, vol. 23, no. 9, pp. 2004–2011, 2005.
[23] W. R. Miller, W. N. Scott, and R. Morris, "Growth of human breast cancer cells inhibited by a luteinizing hormone-releasing hormone agonist," *Nature*, vol. 313, no. 5999, pp. 231–233, 1985.
[24] A. V. Schally, A. M. Comaru-Schally, A. Plonowski, A. Nagy, G. Halmos, and Z. Rekasi, "Peptide analogues in the therapy of prostate cancer," *Prostate*, vol. 5, no. 2, pp. 158–166, 2000.
[25] E. D. Crawford, "Hormonal therapy in prostate cancer: historical approaches," *Reviews in Urology*, vol. 6, no. 7, pp. S3–S11, 2004.
[26] J. B. Engel and A. V. Schally, "Drug insight: clinical use of agonists and antagonists of luteinizing-hormone-releasing hormone," *Nature Clinical Practice Endocrinology and Metabolism*, vol. 3, no. 2, pp. 157–167, 2007.
[27] P. C. Sogani and W. R. Fair, "Treatment of advanced prostatic cancer," *Urologic Clinics of North America*, vol. 14, no. 2, pp. 353–371, 1987.
[28] M. Wirth and M. Froehner, "A review of studies of hormonal adjuvant therapy in prostate cancer," *European Urology*, vol. 36, no. 2, pp. 14–19, 1999.
[29] T. H. Lee, Y. H. Lin, K. M. Seow, J. L. Hwang, C. R. Tzeng, and Y. S. Yang, "Effectiveness of cetrorelix for the prevention of premature luteinizing hormone surge during controlled ovarian stimulation using letrozole and gonadotropins: a randomized trial," *Fertility and Sterility*, vol. 90, no. 1, pp. 113–120, 2008.
[30] F. Debruyne, G. Bhat, and M. B. Garnick, "Abarelix for injectable suspension: first-in-class gonadotropin-releasing hormone antagonist for prostate cancer," *Future Oncology*, vol. 2, no. 6, pp. 677–696, 2006.
[31] P. Broqua, P. J. M. Riviere, P. Michael Conn, J. E. Rivier, M. L. Aubert, and J. L. Junien, "Pharmacological profile of a new, potent, and long-acting gonadotropin-releasing hormone antagonist: Degarelix," *Journal of Pharmacology and Experimental Therapeutics*, vol. 301, no. 1, pp. 95–102, 2002.
[32] M. Z. Strowski and A. D. Blake, "Function and expression of somatostatin receptors of the endocrine pancreas," *Molecular and Cellular Endocrinology*, vol. 286, no. 1-2, pp. 169–179, 2008.
[33] L. Saltz, B. Trochanowski, M. Buckley et al., "Octreotide as an antineoplastic agent in the treatment of functional and nonfunctional neuroendocrine tumors," *Cancer*, vol. 72, no. 1, pp. 244–248, 1993.
[34] S. Faiss, U. F. Pape, M. Böhmig et al., "Prospective, randomized, multicenter trial on the antiproliferative effect of lanreotide, interferon alfa, and their combination for therapy of metastatic neuroendocrine gastroenteropancreatic tumors—the International Lanreotide and Interferon Alfa Study Group," *Journal of Clinical Oncology*, vol. 21, no. 14, pp. 2689–2696, 2003.
[35] D. Hoyer, G. I. Bell, M. Berelowitz et al., "Classification and nomenclature of somatostatin receptors," *Trends in Pharmacological Sciences*, vol. 16, no. 3, pp. 86–88, 1995.
[36] V. Rufini, M. L. Calcagni, and R. P. Baum, "Imaging of neuroendocrine tumors," *Seminars in Nuclear Medicine*, vol. 36, no. 3, pp. 228–247, 2006.
[37] I. Virgolini, T. Traub, C. Novotny et al., "Experience with Indium-111 and Yttrium-90-labeled somatostatin analogs," *Current Pharmaceutical Design*, vol. 8, no. 20, pp. 1781–1807, 2002.

[38] D. L. Bushnell, Y. Menda, M. T. Madsen et al., "99mTc-depreotide tumour uptake in patients with non-Hodgkin's lymphoma," *Nuclear Medicine Communications*, vol. 25, no. 8, pp. 839–843, 2004.

[39] D. Kwekkeboom, E. P. Krenning, and M. de Jong, "Peptide receptor imaging and therapy," *Journal of Nuclear Medicine*, vol. 41, pp. 1704–1713, 2000.

[40] E. P. Krenning, M. de Jong, P. P. Kooij et al., "Radiolabelled somatostatin analogue(s) for peptide receptor scintigraphy and radionuclide therapy," *Annals of Oncology*, vol. 10, no. 2, pp. 23–29, 1999.

[41] D. J. Kwekkeboom, J. J. Teunissen, W. H. Bakker et al., "Radiolabeled somatostatin analog [177Lu-DOTA0, Tyr3]octreotate in patients with endocrine gastroenteropancreatic tumors," *Journal of Clinical Oncology*, vol. 23, no. 12, pp. 2754–2762, 2005.

[42] S. Pauwels, R. Barone, S. Walrand et al., "Practical dosimetry of peptide receptor radionuclide therapy with 90Y-labeled somatostatin analogs," *Journal of Nuclear Medicine*, vol. 46, no. 1, pp. S92–S98, 2005.

[43] J. P. Esser, E. P. Krenning, J. J. M. Teunissen et al., "Comparison of [177Lu-DOTA0,Tyr3]octreotate and [177Lu-DOTA0,Tyr3]octreotide: ehich peptide is preferable for PRRT?" *European Journal of Nuclear Medicine and Molecular Imaging*, vol. 33, no. 11, pp. 1346–1351, 2006.

[44] A. Otte, E. Jermann, M. Behe et al., "DOTATOC: a powerful new tool for receptormediated radionuclide therapy," *European Journal of Nuclear Medicine*, vol. 24, pp. 792–795, 1997.

[45] M. De Jong, R. Valkema, F. Jamar et al., "Somatostatin receptor-targeted radionuclide therapy of tumors: preclinical and clinical findings," *Seminars in Nuclear Medicine*, vol. 32, no. 2, pp. 133–140, 2002.

[46] G. Nicolas, G. Giovacchini, J. Müller-Brand, and F. Forrer, "Targeted radiotherapy with radiolabeled somatostatin analogs," *Endocrinology and Metabolism Clinics of North America*, vol. 40, no. 1, pp. 187–204, 2011.

[47] S. Grozinsky-Glasberg, I. Shimon, M. Korbonits, and A. B. Grossman, "Somatostatin analogues in the control of neuroendocrine tumours: efficacy and mechanisms," *Endocrine-Related Cancer*, vol. 15, no. 3, pp. 701–720, 2008.

[48] D. Wild, H. R. Mäcke, B. Waser et al., "68Ga-DOTANOC: a first compound for PET imaging with high affinity for somatostatin receptor subtypes 2 and 5," *European Journal of Nuclear Medicine and Molecular Imaging*, vol. 32, no. 6, p. 724, 2005.

[49] D. J. Kwekkeboom, W. W. De Herder, B. L. Kam et al., "Treatment with the radiolabeled somatostatin analog [177Lu- DOTA0,Tyr3]octreotate: toxicity, efficacy, and survival," *Journal of Clinical Oncology*, vol. 26, no. 13, pp. 2124–2130, 2008.

[50] M. Van Essen, E. P. Krenning, P. P. Kooij et al., "Effects of therapy with [177Lu-DOTA0, Tyr 3]octreotate in patients with paraganglioma, meningioma, small cell lung carcinoma, and melanoma," *Journal of Nuclear Medicine*, vol. 47, no. 10, pp. 1599–1606, 2006.

[51] R. P. Baum, V. Prasad, M. Hommann, and D. Hörsch, "Receptor PET/CT imaging of neuroendocrine tumors," *Cancer Research*, vol. 170, pp. 225–242, 2008.

[52] I. Buchmann, M. Henze, S. Engelbrecht et al., "Comparison of 68Ga-DOTATOC PET and 111In-DTPAOC (Octreoscan) SPECT in patients with neuroendocrine tumours," *European Journal of Nuclear Medicine and Molecular Imaging*, vol. 34, no. 10, pp. 1617–1626, 2007.

[53] C. Van De Wiele, P. Phonteyne, P. Pauwels et al., "Gastrin-releasing peptide receptor imaging in human breast carcinoma versus immunohistochemistry," *Journal of Nuclear Medicine*, vol. 49, no. 2, pp. 260–264, 2008.

[54] H. Zhang, J. Chen, C. Waldherr et al., "Synthesis and evaluation of bombesin derivatives on the basis of pan-bombesin peptides labeled with Indium-111, Lutetium-177, and Yttrium-90 for targeting bombesin receptor-expressing tumors," *Cancer Research*, vol. 64, no. 18, pp. 6707–6715, 2004.

[55] M. Ginj, H. Zhang, B. Waser et al., "Radiolabeled somatostatin receptor antagonists are preferable to agonists for in vivo peptide receptor targeting of tumors," *Proceedings of the National Academy of Sciences*, vol. 103, pp. 16436–16441, 2006.

[56] D. Wild, M. Fani, M. Behe, I. Brink, J. E. Rivier, J. C. Reubi et al., "First clinical evidence that imaging with somatostatin receptor antagonists is feasible," *Journal of Nuclear Medicine*, vol. 52, pp. 1412–14217, 2011.

[57] R. A. Henderson, S. Mossman, N. Nairn, and M. A. Cheever, "Cancer vaccines and immunotherapies: emerging perspectives," *Vaccine*, vol. 23, pp. 2359–2362, 2005.

[58] J. A. Berzoksky, J. D. Ahlers, and I. M. Belyakov, "Strategies for designing and optimizing new generation vaccines," *Nature*, vol. 1, pp. 209–219, 2001.

[59] M. Hareuveni, C. Gautier, M. P. Kieny, D. Wreschner, P. Chambon, and R. Lathe, "Vaccination against tumor cells expressing breast cancer epithelial tumor antigen," *Proceedings of the National Academy of Sciences of the United States of America*, vol. 87, no. 23, pp. 9498–9502, 1990.

[60] P. G. Coulie, T. Hanagiri, and M. Takenoyama, "From tumor antigens to immunotherapy," *International Journal of Clinical Oncology*, vol. 6, no. 4, pp. 163–170, 2001.

[61] L. Eisenbach, E. Bar-Haim, and K. El-Shami, "Antitumor vaccination using peptide based vaccines," *Immunology Letters*, vol. 74, no. 1, pp. 27–34, 2000.

[62] G. Parmiani, C. Castelli, P. Dalerba et al., "Cancer immunotherapy with peptide-based vaccines: what have we achieved? Where are we going?" *Journal of the National Cancer Institute*, vol. 94, no. 11, pp. 805–818, 2002.

[63] A. Beck, C. Klinguer-Hamour, M. C. Bussat et al., "Peptides as tools and drugs for immunotherapies," *Journal of Peptide Science*, vol. 13, no. 9, pp. 588–602, 2007.

[64] G. F. Gao and B. K. Jakobsen, "Molecular interactions of coreceptor CD8 and MHC class I: the molecular basis for functional coordination with the T-cell receptor," *Immunology Today*, vol. 21, no. 12, pp. 630–636, 2000.

[65] H. I. Cho and E. Celis, "Optimized peptide vaccines eliciting extensive CD8 T-cell responses with therapeutic antitumor effects," *Cancer Research*, vol. 69, no. 23, pp. 9012–9019, 2009.

[66] V. Apanius, D. Penn, P. R. Slev, L. R. Ruff, and W. K. Potts, "The nature of selection on the major histocompatibility complex," *Critical Reviews in Immunology*, vol. 17, no. 2, pp. 179–224, 1997.

[67] M. Oshima, P. Deitiker, T. Ashizawa, and M. Z. Atassi, "Vaccination with a MHC class II peptide attenuates cellular and humoral responses against tAChR and suppresses clinical EAMG," *Autoimmunity*, vol. 35, no. 3, pp. 183–190, 2002.

[68] J. Banchereau, A. K. Palucka, M. Dhodapkar et al., "Immune and clinical responses in patients with metastatic melanoma to $CD34^+$ progenitor-derived dendritic cell vaccine," *Cancer Research*, vol. 61, no. 17, pp. 6451–6458, 2001.

[69] K. L. Knutson, K. Schiffman, and M. L. Disis, "Immunization with a HER-2/neu helper peptide vaccine generates HER-2/neu CD8 T-cell immunity in cancer patients," *Journal of Clinical Investigation*, vol. 107, no. 4, pp. 477–484, 2001.

[70] K. Sole, "HER-2/neu peptide vaccine for the prevention of prostate cancer recurrence," *Nature Reviews Urology*, vol. 3, p. 6, 2006.

[71] M. T. Hueman, Z. A. Dehqanzada, T. E. Novak et al., "Phase I clinical trial of a HER-2/neu peptide (E75) vaccine for the prevention of prostate-specific antigen recurrence in high-risk prostate cancer patients," *Clinical Cancer Research*, vol. 11, no. 20, pp. 7470–7479, 2005.

[72] R. K. Ramanathan, K. M. Lee, J. McKolanis et al., "Phase I study of a MUC1 vaccine composed of different doses of MUC1 peptide with SB-AS2 adjuvant in resected and locally advanced pancreatic cancer," *Cancer Immunology, Immunotherapy*, vol. 54, no. 3, pp. 254–264, 2005.

[73] K. Yamamoto, T. Ueno, T. Kawaoka et al., "MUC1 peptide vaccination in patients with advanced pancreas or biliary tract cancer," *Anticancer Research*, vol. 25, no. 5, pp. 3575–3579, 2005.

[74] Y. Ma, Z. H. Zhu, D. R. Situ, Y. Hu, T. H. Rong, and J. Wang, "Expression and prognostic relevance of tumor carcino-embryonic antigen in stage IB non-small cell lung cancer," *Journal of Thoracic Disease*, vol. 4, no. 5, pp. 490–496, 2012.

[75] M. Grunnet and J. B. Sorensen, "Carcinoembryonic antigen (CEA) as tumor marker in lung cancer," *Lung Cancer*, vol. 76, no. 2, pp. 138–143, 2012.

[76] J. S. Weber, N. J. Vogelzang, M. S. Ernstoff et al., "A phase 1 study of a vaccine targeting preferentially expressed antigen in melanoma and prostate-specific membrane antigen in patients with advanced solid tumors," *Journal of Immunotherapy*, vol. 34, no. 7, pp. 556–567, 2011.

[77] S. Garetto, F. Sizzano, D. Brusa, A. Tizzani, F. Malavasi, and L. Matera, "Binding of prostate-specific membrane antigen to dendritic cells: a critical step in vaccine preparation," *Cytotherapy*, vol. 11, no. 8, pp. 1090–1100, 2009.

[78] N. H. Akhtar, O. Pail, A. Saran, L. Tyrell, and S. T. Tagawa, "Prostate-specific membrane antigen-based therapeutics," *Advances in Urology*, vol. 2012, Article ID 973820, 9 pages, 2012.

[79] L. Muderspach, S. Wilczynski, L. Roman et al., "A phase I trial of a human papillomavirus (HPV) peptide vaccine for women with high-grade cervical and vulvar intraepithelial neoplasia who are HPV 16 positive," *Clinical Cancer Research*, vol. 6, no. 9, pp. 3406–3416, 2000.

[80] S. N. Khleif, S. I. Abrams, J. M. Hamilton et al., "A phase I vaccine trial with peptides reflecting ras oncogene mutations of solid tumors," *Journal of Immunotherapy*, vol. 22, no. 2, pp. 155–165, 1999.

[81] M. K. Gjertsen and G. Gaudernack, "Mutated ras peptides as vaccines in immunotherapy of cancer," *Vox Sanguinis*, vol. 74, no. 2, pp. 489–495, 1998.

[82] S. I. Abrams, P. H. Hand, K. Y. Tsang, and J. Schlom, "Mutant ras epitopes as targets for cancer vaccines," *Seminars in Oncology*, vol. 23, no. 1, pp. 118–134, 1996.

[83] H. L. Kaufman, "Vaccines for melanoma and renal cell carcinoma," *Seminars in Oncology*, vol. 39, no. 3, pp. 263–275, 2012.

[84] S. Markowicz, Z. I. Nowecki, P. Rutkowski et al., "Adjuvant vaccination with melanoma antigen-pulsed dendritic cells in stage III melanoma patients," *Medical Oncology*, vol. 29, pp. 2966–2977, 2012.

[85] J. C. Yang, "Melanoma vaccines," *Cancer Journal*, vol. 17, no. 5, pp. 277–282, 2011.

[86] P. Nava-Parada and L. A. Emens, "GV-1001, an injectable telomerase peptide vaccine for the treatment of solid cancers," *Current Opinion in Molecular Therapeutics*, vol. 9, no. 5, pp. 490–497, 2007.

[87] M. Gotthardt, M. P. Béhé, J. Grass et al., "Added value of gastrin receptor scintigraphy in comparison to somatostatin receptor scintigraphy in patients with carcinoids and other neuroendocrine tumours," *Endocrine-Related Cancer*, vol. 13, no. 4, pp. 1203–1211, 2006.

[88] J. C. Reubi, "Targeting CCK receptors in human cancers," *Current Topics in Medicinal Chemistry*, vol. 7, pp. 1239–1242, 2007.

[89] A. V. Schally and A. Nagy, "Cancer chemotherapy based on targeting of cytotoxic peptide conjugates to their receptors on tumors," *European Journal of Endocrinology*, vol. 141, no. 1, pp. 1–14, 1999.

[90] A. V. Schally and A. Nagy, "Chemotherapy targeted to cancers through tumoral hormone receptors," *Trends in Endocrinology and Metabolism*, vol. 15, no. 7, pp. 300–310, 2004.

[91] A. V. Schally, J. B. Engel, G. Emons, N. L. Block, and J. Pinski, "Use of analogs of peptide hormones conjugated to cytotoxic radicals for chemotherapy targeted to receptors on tumors," *Current Drug Delivery*, vol. 8, no. 1, pp. 11–25, 2011.

[92] G. Emons, S. Tomov, P. Harter et al., "Phase II study of AEZS-108 (AN-152), a targeted cytotoxic LHRH analog, in patients with LHRH receptor-positive platinum resistant ovarian cancer," *Journal of Clinical Oncology*, vol. 28, no. 15, 2010.

[93] J. C. Reubi, "Peptide receptors as molecular targets for cancer diagnosis and therapy," *Endocrine Reviews*, vol. 24, no. 4, pp. 389–427, 2003.

[94] K. Szepeshazi, A. V. Schally, G. Halmos et al., "Targeting of cytotoxic somatostatin analog AN-238 to somatostatin receptor subtypes 5 and/or 3 in experimental pancreatic cancers," *Clinical Cancer Research*, vol. 7, no. 9, pp. 2854–2861, 2001.

[95] S. Zitzmann, V. Ehemann, and M. Schwab, "Arginine-glycine-aspartic acid (RGD)-peptide binds to both tumor and tumor-endothelial cells in vivo," *Cancer Research*, vol. 62, no. 18, pp. 5139–5143, 2002.

[96] K. Temminga, R. M. Schiffelers, G. Molemad, and R. J. Kok, "RGD-based strategies for selective delivery of therapeutics and imaging agents to the tumour vasculature," *Drug Resistance Updates*, vol. 8, pp. 381–402, 2005.

[97] P. Laakkonen and K. Vuorinen, "Homing peptides as targeted delivery vehicles," *Integrative Biology*, vol. 2, no. 7-8, pp. 326–337, 2010.

[98] M. A. Burg, R. Pasqualini, W. Arap, E. Ruoslahti, and W. B. Stallcup, "NG2 proteoglycan-binding peptides target tumor neovasculature," *Cancer Research*, vol. 59, no. 12, pp. 2869–2874, 1999.

[99] K. Porkka, P. Laakkonen, J. A. Hoffman, M. Bernasconi, and E. Ruoslahti, "A fragment of the HMGN2 protein homes to the nuclei of tumor cells and tumor endothelial cells in vivo," *Proceedings of the National Academy of Sciences of the United States of America*, vol. 99, no. 11, pp. 7444–7449, 2002.

[100] L. Zhang, E. Giraudo, J. A. Hoffman, D. Hanahan, and E. Ruoslahti, "Lymphatic zip codes in premalignant lesions and tumors," *Cancer Research*, vol. 66, no. 11, pp. 5696–5706, 2006.

[101] P. Laakkonen, K. Porkka, J. A. Hoffman, and E. Ruoslahti, "A tumor-homing peptide with a targeting specificity related to lymphatic vessels," *Nature Medicine*, vol. 8, no. 7, pp. 751–755, 2002.

[102] K. M. Wagstaff and D. A. Jans, "Protein transduction: cell penetrating peptides and their therapeutic applications," *Current Medicinal Chemistry*, vol. 13, no. 12, pp. 1371–1387, 2006.

[103] K. Chen and X. Chen, "Integrin targeted delivery of chemotherapeutics," *Theranostics*, vol. 1, pp. 189–200, 2011.

[104] E. Garanger, D. Boturyn, and P. Dumy, "Tumor targeting with RGD peptide ligands-design of new molecular conjugates for imaging and therapy of cancers," *Anti-Cancer Agents in Medicinal Chemistry*, vol. 7, no. 5, pp. 552–558, 2007.

[105] A. Sacchi, A. Gasparri, C. Gallo-Stampino, S. Toma, F. Curnis, and A. Corti, "Synergistic antitumor activity of cisplatin, paclitaxel, and gemcitabine with tumor vasculature-targeted tumor necrosis factor-α," *Clinical Cancer Research*, vol. 12, no. 1, pp. 175–182, 2006.

[106] E. Ruoslahti, S. N. Bhatia, and M. J. Sailor, "Targeting of drugs and nanoparticles to tumors," *Journal of Cell Biology*, vol. 188, no. 6, pp. 759–768, 2010.

[107] E. B. Dickerson, N. Akhtar, H. Steinberg et al., "Enhancement of the antiangiogenic activity of interleukin-12 by peptide targeted delivery of the cytokine to $\alpha v\beta 3$ integrin," *Molecular Cancer Research*, vol. 2, no. 12, pp. 663–673, 2004.

[108] V. Gregorc, A. Santoro, E. Bennicelli et al., "Phase Ib study of NGR-hTNF, a selective vascular targeting agent, administered at low doses in combination with doxorubicin to patients with advanced solid tumours," *British Journal of Cancer*, vol. 101, no. 2, pp. 219–224, 2009.

[109] V. Gregorc, F. G. De Braud, T. M. De Pas et al., "Phase I study of NGR-hTNF, a selective vascular targeting agent, in combination with cisplatin in refractory solid tumors," *Clinical Cancer Research*, vol. 17, no. 7, pp. 1964–1972, 2011.

[110] A. Santoro, L. Rimassa, A. F. Sobrero et al., "Phase II study of NGR-hTNF, a selective vascular targeting agent, in patients with metastatic colorectal cancer after failure of standard therapy," *European Journal of Cancer*, vol. 46, no. 15, pp. 2746–2752, 2010.

[111] Z. J. Li and C. H. Cho, "Peptides as targeting probes against tumor vasculature for diagnosis and drug delivery," *Journal of Translational Medicine*, vol. 10, supplement 1, p. S1, 2012.

[112] L. Soroceanu, Y. Gillespie, M. B. Khazaeli, and H. Sontheimer, "Use of chlorotoxin for targeting of primary brain tumors," *Cancer Research*, vol. 58, no. 21, pp. 4871–4879, 1998.

[113] E. V. Rosca, J. E. Koskimaki, C. G. Rivera, N. B. Pandey, A. P. Tamiz, and A. S. Popel, "Anti-angiogenic peptides for cancer therapeutics," *Current Pharmaceutical Biotechnology*, vol. 12, no. 8, pp. 1101–1116, 2011.

[114] E. D. Karagiannis and A. S. Popel, "Novel anti-angiogenic peptides derived from ELR-containing CXC chemokines," *Journal of Cellular Biochemistry*, vol. 104, no. 4, pp. 1356–1363, 2008.

[115] J. A. Kritzer, O. M. Stephens, D. A. Guarracino, S. K. Reznika, and A. Schepartza, "β-Peptides as inhibitors of protein-protein interactions," *Bioorganic & Medicinal Chemistry*, vol. 13, pp. 11–16, 2005.

[116] D. Mochly-Rosen and N. Qvit, "Peptide inhibitors of protein-protein interactions: from rational design to the clinic," *Chimica Oggi*, vol. 28, no. 1, pp. 14–16, 2010.

[117] H. Eldar-Finkelman and M. Eisenstein, "Peptide inhibitors targeting protein kinases," *Current Pharmaceutical Design*, vol. 15, no. 21, pp. 2463–2470, 2009.

[118] R. Tonelli, S. Purgato, C. Camerin et al., "Antigene peptide nucleic acid specifically inhibits MYCN expression in human neuroblastoma cells leading to cell growth inhibition and apoptosis," *Molecular Cancer Therapeutics*, vol. 4, no. 5, pp. 779–786, 2005.

[119] D. Kakde, D. Jain, V. Shrivastava, R. Kakde, and A. T. Patil, "Cancer therapeutics-opportunities, challenges and advances in drug delivery," *Journal of Applied Pharmaceutical Science*, vol. 1, no. 9, pp. 1–10, 2011.

[120] L. Zheng, Y. Wang, J. Sheng et al., "Antitumor peptides from marine organisms," *Marine Drugs*, vol. 9, pp. 1840–1859, 2011.

[121] D. B. Cornelio, R. Roesler, and G. Schwartsmann, "Gastrin-releasing peptide receptor as a molecular target in experimental anticancer therapy," *Annals of Oncology*, vol. 18, no. 9, pp. 1457–1466, 2007.

[122] S. Sotomayor, L. Muñoz-Moreno, M. J. Carmena et al., "Regulation of HER expression and transactivation in human prostate cancer cells by a targeted cytotoxic bombesin analog (AN-215) and a bombesin antagonist (RC-3095)," *International Journal of Cancer*, vol. 127, no. 8, pp. 1813–1822, 2010.

[123] R. Smolarczyk, T. Cichoń, K. Graja, J. Hucz, A. Sochanik, and S. Szala, "Antitumor effect of RGD-4C-GG-D(KLAKLAK)2 peptide in mouse B16(F10) melanoma model," *Acta Biochimica Polonica*, vol. 53, no. 4, pp. 801–805, 2006.

[124] H. M. Ellerby, W. Arap, L. M. Ellerby et al., "Anti-cancer activity of targeted pro-apoptotic peptides," *Nature Medicine*, vol. 5, no. 9, pp. 1032–1038, 1999.

[125] L. D. Walensky, A. L. Kung, I. Escher et al., "Activation of apoptosis in vivo by a hydrocarbon-stapled BH3 helix," *Science*, vol. 305, no. 5689, pp. 1466–1470, 2004.

[126] D. R. Soto-Pantoja, J. Menon, P. E. Gallagher, and E. A. Tallant, "Angiotensin-(1-7) inhibits tumor angiogenesis in human lung cancer xenografts with a reduction in vascular endothelial growth factor," *Molecular Cancer Therapeutics*, vol. 8, no. 6, pp. 1676–1683, 2009.

[127] G. C. Alghisi, L. Ponsonnet, and C. Rüegg, "The integrin antagonist cilengitide activates $\alpha V\beta 3$, disrupts VE-cadherin localization at cell junctions and enhances permeability in endothelial cells," *PLoS One*, vol. 4, no. 2, Article ID e4449, 2009.

[128] S. Hariharan, D. Gustafson, S. Holden et al., "Assessment of the biological and pharmacological effects of the $\alpha v\beta 3$ and $\alpha v\beta 5$ integrin receptor antagonist, cilengitide (EMD 121974), in patients with advanced solid tumors," *Annals of Oncology*, vol. 18, no. 8, pp. 1400–1407, 2007.

[129] D. A. Reardon, K. L. Fink, T. Mikkelsen et al., "Randomized phase II study of cilengitide, an integrin-targeting arginine-glycine-aspartic acid peptide, in recurrent glioblastoma multiforme," *Journal of Clinical Oncology*, vol. 26, no. 34, pp. 5610–5617, 2008.

[130] K. Park, Y. S. Kim, G. Y. Lee et al., "Tumor endothelial cell targeted cyclic RGD-modified heparin derivative: inhibition of angiogenesis and tumor growth," *Pharmaceutical Research*, vol. 25, no. 12, pp. 2786–2798, 2008.

[131] P. Khalili, A. Arakelian, G. Chen et al., "A non-RGD-based integrin binding peptide (ATN-161) blocks breast cancer growth and metastasis in vivo," *Molecular Cancer Therapeutics*, vol. 5, no. 9, pp. 2271–2280, 2006.

[132] A. Noy, D. T. Scadden, J. Lee et al., "Angiogenesis inhibitor IM862 is ineffective against AIDS-Kaposi's sarcoma in a phase III trial, but demonstrates sustained, potent effect of highly active antiretroviral therapy: from the AIDS malignancy consortium and IM862 study team," *Journal of Clinical Oncology*, vol. 23, no. 5, pp. 990–998, 2005.

[133] G. Deplanque, S. Madhusudan, P. H. Jones et al., "Phase II trial of the antiangiogenic agent IM862 in metastatic renal cell carcinoma," *British Journal of Cancer*, vol. 91, no. 9, pp. 1645–1650, 2004.

[134] A. Stangelberger, A. V. Schally, and B. Djavan, "New treatment approaches for prostate cancer based on peptide analogues," *European Urology*, vol. 53, no. 5, pp. 890–900, 2008.

[135] R. Cescato, T. Maina, B. Nock et al., "Bombesin receptor antagonists may be preferable to agonists for tumor targeting," *Journal of Nuclear Medicine*, vol. 49, no. 2, pp. 318–326, 2008.

[136] A. M. Bajo, A. V. Schally, M. Krupa, F. Hebert, K. Groot, and K. Szepeshazi, "Bombesin antagonists inhibit growth of MDA-MB-435 estrogen-independent breast cancers and decrease the expression of the ErbB-2/HER-2 oncoprotein and c-jun and c-fos oncogenes," *Proceedings of the National Academy of Sciences of the United States of America*, vol. 99, no. 6, pp. 3836–3841, 2002.

[137] R. Z. Cai, Y. Qin, T. Ertl, and A. V. Schally, "New pseudononapeptide bombesin antagonists with C-terminal LeuΨ(CH2N)Tac-NH2 show high binding affinity to bombesin/GRP receptors on CFPAC-1 human pancreatic cancer cells," *International Journal of Oncology*, vol. 6, no. 6, pp. 1165–1172, 1995.

[138] V. J. Hruby, "Designing peptide receptor agonists and antagonists," *Nature Reviews Drug Discovery*, vol. 1, pp. 847–858, 2002.

[139] M. Letsch, A. V. Schally, R. Busto, A. M. Bajo, and J. L. Varga, "Growth hormone-releasing hormone (GHRH) antagonists inhibit the proliferation of androgen-dependent and -independent prostate cancers," *Proceedings of the National Academy of Sciences of the United States of America*, vol. 100, no. 3, pp. 1250–1255, 2003.

[140] F. Hohla, S. Buchholz, A. V. Schally et al., "GHRH antagonist causes DNA damage leading to p21 mediated cell cycle arrest and apoptosis in human colon cancer cells," *Cell Cycle*, vol. 8, no. 19, pp. 3149–3156, 2009.

[141] D. Cardinale, G. Guaitoli, D. Tondi et al., "Protein-protein interface-binding peptides inhibit the cancer therapy target human thymidylate synthase," *Proceedings of the National Academy of Sciences*, vol. 108, no. 34, pp. 542–549, 2011.

[142] L. Gaviglio, A. Gross, N. Metzler-Nolte, and M. Ravera, "Synthesis and in vitro cytotoxicity of cis, cis, trans-diamminedichloridodisuccinatoplatinum(IV)-peptide bioconjugates," *Metallomics*, vol. 4, no. 3, pp. 260–266, 2012.

[143] J. C. Mai, Z. Mi, S. H. Kim, B. Ng, and P. D. Robbins, "A proapoptotic peptide for the treatment of solid tumors," *Cancer Research*, vol. 61, no. 21, pp. 7709–7712, 2001.

[144] P. Laakkonen, M. E. Åkerman, H. Biliran et al., "Antitumor activity of a homing peptide that targets tumor lymphatics and tumor cells," *Proceedings of the National Academy of Sciences of the United States of America*, vol. 101, no. 25, pp. 9381–9386, 2004.

[145] S. T. Nawrocki, J. S. Carew, M. S. Pino et al., "Bortezomib sensitizes pancreatic cancer cells to endoplasmic reticulum stress-mediated apoptosis," *Cancer Research*, vol. 65, no. 24, pp. 11658–11666, 2005.

[146] D. Chen, M. Frezza, S. Schmitt, J. Kanwar, and Q. P. Dou, "Bortezomib as the first proteasome inhibitor anticancer drug: current status and future perspectives," *Current Cancer Drug Targets*, vol. 11, no. 3, pp. 239–253, 2011.

[147] P. A. Meyers, "Muramyl tripeptide (mifamurtide) for the treatment of osteosarcoma," *Expert Review of Anticancer Therapy*, vol. 9, no. 8, pp. 1035–1049, 2009.

[148] N. Inohara, Y. Ogura, A. Fontalba et al., "Host recognition of bacterial muramyl dipeptide mediated through NOD2: implications for Crohn's disease," *Journal of Biological Chemistry*, vol. 278, no. 8, pp. 5509–5512, 2003.

[149] J. A. Francisco, C. G. Cerveny, D. L. Meyer et al., "cAC10-vcMMAE, an anti-CD30-monomethyl auristatin E conjugate with potent and selective antitumor activity," *Blood*, vol. 102, no. 4, pp. 1458–1465, 2003.

[150] P. D. Senter, "The discovery and development of brentuximab vedotin for use in relapsed Hodgkin lymphoma and systemic anaplastic large cell lymphoma," *Nature Biotechnology*, vol. 30, pp. 631–637, 2012.

[151] K. C. Foy, M. J. Miller, N. Moldovan, W. E. Carson III, and P. T. Kaumaya, "Combined vaccination with HER-2 peptide followed by therapy with VEGF peptide mimics exerts effective anti-tumor and anti-angiogenic effects in vitro and in vivo," *OncoImmunology*, vol. 1, pp. 1048–1060, 2012.

[152] R. Stupp, M. E. Hegi, B. Neyns et al., "Phase I/IIa study of cilengitide and temozolomide with concomitant radiotherapy followed by cilengitide and temozolomide maintenance therapy in patients with newly diagnosed glioblastoma," *Journal of Clinical Oncology*, vol. 28, no. 16, pp. 2712–2718, 2010.

[153] A. S. Retter, W. D. Figg, and W. L. Dahut, "The combination of antiangiogenic and cytotoxic agents in the treatment of prostate cancer," *Clinical Prostate Cancer*, vol. 2, no. 3, pp. 153–159, 2003.

[154] M. H. Andersen, N. Junker, E. Ellebaek, I. M. Svane, and P. T. Straten, "Therapeutic cancer vaccines in combination with conventional therapy," *Journal of Biomedicine and Biotechnology*, vol. 2010, Article ID 237623, 10 pages, 2010.

[155] F. G. Rick, S. Buchholz, A. V. Schally et al., "Combination of gastrin-releasing peptide antagonist with cytotoxic agents produces synergistic inhibition of growth of human experimental colon cancers," *Cell Cycle*, vol. 11, no. 13, pp. 2518–2525, 2012.